Geological mapping of the inner shelf off Cape Town's Atlantic Seaboard, South Africa

Frederik Wilhelm van Zyl

Department of Geological Sciences

University of Cape Town

Submitted for the fulfilment of the academic requirements for the degree of Master of Science in the Department of Geological Sciences, University of Cape Town.

February 2018

Abstract

The Atlantic Seaboard is an 18 km stretch of coastline located on the Cape Peninsula, South Africa, roughly between the Cape Town suburbs of Mouille Point in the north and Hout Bay in the south. It borders heavy shipping traffic and contains a mix of urban and natural environments including up-market seaside neighbourhoods and is part of the Table Mountain National Park. The predominantly rocky coastline has a northeast–southwest orientation with interspersed sandy pocket beaches. A narrow, low-lying coastal plain (marine terrace) in the north merges with coastal cliffs further south. The geomorphology and sedimentology of the coast are closely linked to the underlying geology, influencing the shape of coastal embayments and promontories, as well as the composition and distribution of sediment. Hydrographic, geophysical and sedimentological techniques were used to collect high-resolution bathymetry, seafloor geology and sediment distribution data to better understand modern coastal processes. The results indicate a low-relief seafloor consisting of Malmesbury Group rocks in the north. To the south the seafloor consists of high-relief Cape Granite reefs interspersed with fine to medium grain sand and bioclastic (shelly) gravel. Sediment transport is generally northward by longshore drift. In the south, the high-relief granite reef and headlands form sediment traps resulting in several large pocket beaches and offshore sediment deposits. In the north, the low-relief Malmesbury bedrock is largely free of sediment, except within narrow erosional gullies. Most sediment rapidly passes through to the north resulting in a sediment-starved rocky seafloor. The three principal sources of beach sand are aeolian fine sand transported by the Karbonkelberg headlands bypass dune entering the sea at Sandy Bay, biogenic carbonate production along the coast, and weathering of Table Mountain Group sandstone and granite bedrock. A fourth source is sediment entering the system via longshore drift from the south of Duiker Point. The water depth around the Duiker Point headland is presently too deep for sediment to be transported easily through longshore drift, other than during large storm events, but during past sea-level low stands this would have played an important part in supplying sediment to the coast. Changes in sea level play an important part in shaping the geomorphology of the coastline. Beach deposits, both sandy and boulder beaches have been left at various elevations along the coast, both offshore and onshore. Although today the Sea Point area is protected by sea walls and man-made structures, a higher sea level

was responsible for shaping the narrow coastal plain. Increasing rates of global sea-level change are becoming an important issue all over the world and the Atlantic Seaboard coast is not immune to the effects of sea-level rise. The frequency and magnitude of storm events that breach the sea defences erode beaches and sea cliffs and cause damage to private and public property are likely to increase in the future.

Acknowledgements

The work detailed in this study was carried out as collaboration between the Marine Geoscience Unit (MGU) of the Council for Geoscience (CGS) and the Department of Geological Sciences of the University of Cape Town, under the supervision of Prof John Compton. The project later became part of the CGS's South African Near-shore Mapping Programme (SANMAP) with funding supplied by the Council for Geoscience.

I would like to thank my family; Marista, Morné, Albert and Christiaan for putting up with the time and effort that went into this project. My colleagues at the MGU, Michael Machutchon for his survey experience and ideas, Hayley Cawthra for proof reading and many insightful suggestions, Willem Kupido for putting his back out pulling dozens of grab samples by hand, Leslee Salzmann for assisting with running settling tube tests and Coenie de Beer for assisting with the geological legend.

The following people contributed with interviews and discussions: Andre Theron (CSIR), Peter Holmes and Dr Alan Boyd (DEA Oceans and Coast) for permission to use the Coastal Vulnerability Assessment report by the CSIR.

Plagiarism Statement

I know the meaning of plagiarism and declare that all of the works in this dissertation save for that which is properly acknowledged, is my own and has not been submitted in any form for a degree at any other tertiary institution.

Name: Frederik Wilhelm van Zyl

Signed by candidate

Date: 5 February 2018

Contents

1 Introduction

1.1 The coastal zone

The coastal zone is a complex, dynamic zone where land and sea meet (Woodroffe, 2002). Various definitions and legal acts have different ideas about the extent of the coastal zone, but generally it is the geomorphologic area where marine and terrestrial processes interact and can include river deltas, coastal plains, wetlands, beaches and dunes, offshore reefs, mangrove forests, lagoons and other features (Rust, 1991). The coastal zone experiences continuous adjustments of form and process (morphodynamics) in response to geomorphological and oceanographic factors (Wong et al., 2014). The geomorphology (shape) and geology (composition) form the base on which a host of other natural oceanographic processes, for example wind, tides, ocean swell, currents and sea level play a role. Human activity plays a role that often overshadows natural processes (Wong et al., 2014). Modifying coastal dunes and coastal geomorphology without understanding the sediment dynamics of the system can cause serious erosional problems further down the line (McLachlan et al., 1994; Holmes and Luger, 1996; Louw and Van Eeden, 2013). A prime example of this can be seen in Hout Bay, where the natural movement of sand through the Karbonkelberg sediment bypass cordon has been modified to such an extent that it is no longer functioning (Holmes and Luger, 1996).

Figure 1: Rocky coastline of the Atlantic Seaboard looking south towards Llandudno.

Understanding the morphodynamics and sediment dynamics of the coastal zone is important for coastal engineering and coastal zone management strategies. This is not only from an environmental point of view but also from the desire to protect coastal infrastructure from damage by sand migration, erosion and storm surges. Sea-level rise due to climate change or geological processes can have a detrimental effect on coastal infrastructure. Storms, such as on June 7 2017 (Figure 2), which caused extensive damage around the Sea Point area, will become more frequent in future (Cai et al., 2014; Trenberth et al., 2015). Detailed bathymetry and seabed geology are needed to produce setback lines and plan breakwater protection. Bathymetry, together with coastal topography or elevation, is used in numerical modelling to calculate wave run-up and coastal inundation of low-lying areas.

Figure 2: June 7 2017, storm surge hitting the breakwater at Sea Point and Three Anchor Bay (Photo credit Jacaranda FM).

Geological baseline mapping together with seabed bathymetry are two important components in reef habitat mapping for conservation, marine biodiversity and fisheries management. These thematic maps provide a baseline to assess environmental change in reef systems, changes in sediment distribution and reef health. Geological mapping and bathymetry can also play a role in shipping for safe passage at sea. During May of 2012 a 50 m long fishing trawler, the *Eihatsu Maru* ran aground on Clifton First Beach (Figure 3).

The vessel was towed off the beach a week later (IOL 2012). Detailed mapping of the seabed (from this study), which indicated potential hazards in the form of submerge reef was supplied to the City of Cape Town Disaster Management to assist in the salvage operation.

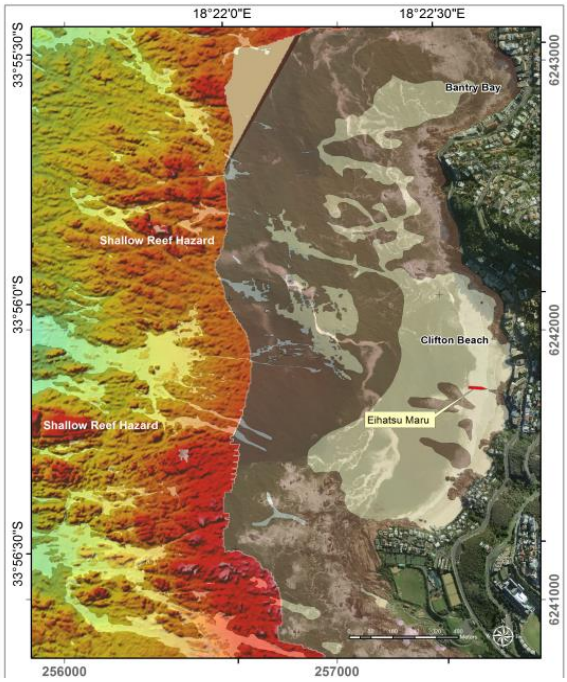

Figure 3: Stranding of the Eihatsu Maru on Clifton First Beach. Detailed Geological mapping of the area assisted in the salvage operation. (Photo credit SApeople 2012). Unpublished chart supplied to City of Cape Town disaster Management by the CGS. The chart is a combination of high-resolution bathymetry and side scan sonar data, showing the location of reef structures.

With an increase in usage of the coastal zone due to population growth there has been an increase in user conflicts across space and time (Collie et al., 2013). In recent years marine spatial planning has become a more popular field of study to try and manage these conflicts by following an ecosystem-based approach. Baseline geology and bathymetry are some of the input datasets required for effective marine spatial planning. The coastal zone and the nearshore environment along the Cape Peninsula is a major economic asset to the City of Cape Town. Tourism and recreation, which generated R 15.3 billion in direct spend during 2014 (City of Cape Town, 2015), residential area development, economic and employment opportunities, as well as industrial and commercial services are all focus areas that benefit from a healthy coastal environment. It is important to understand the natural processes that influence the distribution and movement of sediment along this coastline in order to improve management of these areas.

1.2 Coastal features

Coastal zone processes and features have been described by many authors and summarised in Figure 4 (USACE - CERC, 1984; Komar, 1998; Nichols, 2009; Mangor et al., 2017). The coastal zone can be divided into three sub zones; the nearshore or shoreface, beach and the coast. Inland of the coastal zone is the coastal hinterland and on the sea ward side of the coastal zone is the offshore zone.

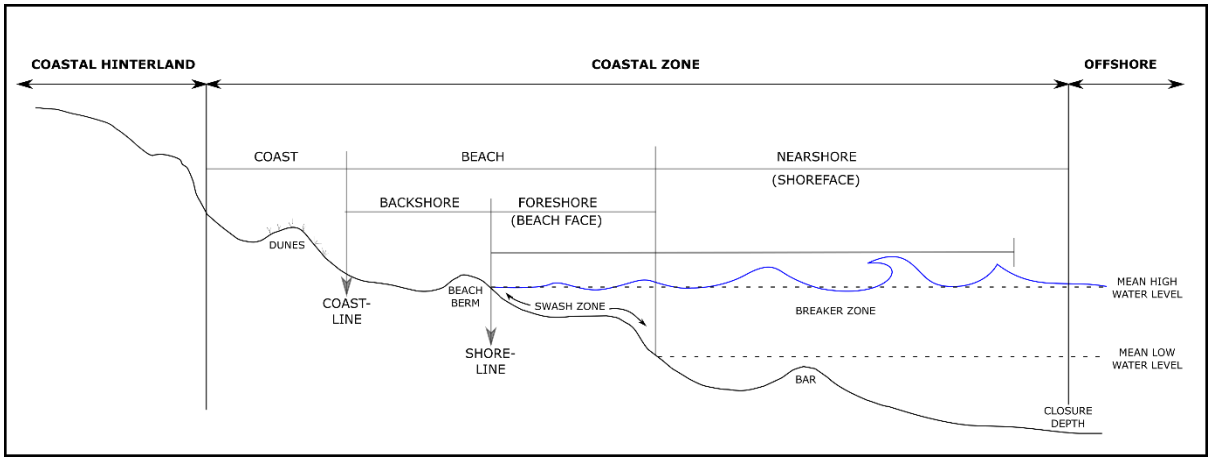

Figure 4: Diagram of a beach profile with processes shown (modified from the USACE - CERC Shore Protection Manual, 1984 and Komar, 1998).

The nearshore (also called the shoreface) is the zone which stretches from closure depth up to the mean low water level (MLWL). Closure depth is the offshore depth where wave action no longer has a significant impact on sediment movement. A breaker zone can be found within the shoreface zone. The breaker zone is highly variable and depends on the wave conditions, but generally starts inshore of the closure depth and can extend up onto the foreshore or beach face. Inshore of the shoreface between the MLWL and the coastline is the beach or shore. The beach can be further subdivided into the foreshore (or beach face) and the backshore. The foreshore is the area between the MLWL and the mean high water level (MHWL) and is generally inundated by tidal and wave action on a regular basis. MHWL is also known as the shoreline. The backshore extends between the shoreline (or MHWL) to the coastline and is generally only inundated during extreme high tide and storm surges. The coast is a narrow strip of land which extends from the coastline inland to the first major change in morphology. Features in this zone include dunes, coastal cliffs and coastal plains. Other features located in the coastal zone include beach berms, offshore bars and blinders. A beach berm is a shore parallel ridge formed by the change in slope of the

foreshore (beachface) and backshore. During storm events the berm often shifts higher up the beach towards the backshore. A bar is a submerged, shore parallel sediment deposit forming in the breaker zone. There can be several rows of bars which can be constantly changing location in the breaker zone. Bars tend to move towards the offshore during storm wave conditions and towards the inshore during calm conditions. A blinder is a partially submerged rocky outcrop that is normally located just below the water surface but can be exposed during low tide. Larger waves will tend to form breakers around blinders.

1.3 Beaches

A beach is a section of coastline between the low water mark and the high water mark. It can consist of sand, pebbles, boulders and mud. Beaches are often found in bays between rocky headlands where the wave energy is less, resulting in beach formation by constructive waves (Woodroffe, 2002). Beaches are also found on long open stretches of coast where they are influenced by longshore drift.

1.4 Rocky coasts

Along rocky shorelines, the presence of rocky headlands separating pocket beaches disrupts longshore sand transport in the surf zone caused by wave action. For sediment to be transported past the rocky headlands from one pocket beach to the next, there needs to be either a cross shore component, such as a dune sediment bypass, or the sediment needs to be transported outside of the surf zone to bypass the rocky headlands (Storlazzi and Field, 2000). Headland bypass dunes are often formed between beaches separated by headlands (Tinley, 1985; Boeyinga et al., 2010). Where the bypass meets opposing hillslopes a climbing-falling dune will be formed (Tinley, 1985). The climbing dune forms on the windward slope, while finer sand is blown over the hill crest to form the falling part of the dune on the lee side. Additionally, sediment can be transported offshore and past the headland. For this to happen storm events are generally required to move sediment offshore and past headlands (Tait, 1995; Storlazzi and Field, 2000).

1.5 Sediment dynamics

"Sediment dynamics is the process of entrainment, transport and deposition of sediment in the marine or coastal environment" (Hopley, 2011). In the coastal zone there are several ways in which sediment can be transported, such as aeolian or wind transport, fluvial transport in rivers or by marine processes such as waves and currents. When a fluid increases velocity near a sediment bed, some particles start to move by sliding and rolling. A fluid can mean air, water or ice. With a further increase in velocity uneven bed forms start to appear, forming wave ripples or current ripples. The ripples cause uneven flow conditions, smaller particles may be entrained for short distances before falling to the seabed again (saltation), while others may stay in suspension or even solution for longer periods (Figure 5). The source and composition of the sediment plays an important role in the dynamics of the system. Potential sources can be terrigenous material from rivers, headland-bypass dune fields, longshore drift and biogenic carbonate production in offshore reefs (Illenberger, 1993).

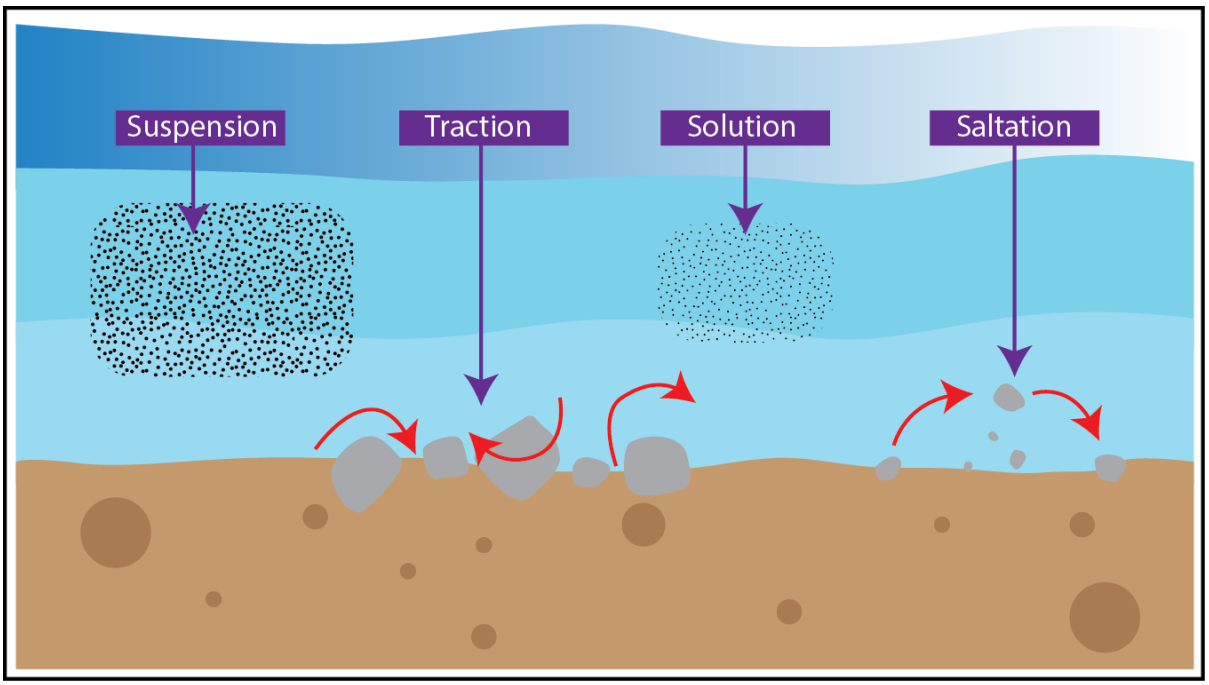

Figure 5: Ways in which sediment is transported on the seabed (modified from BBC 2017).

1.6 Waves

The wave regime of the coastline plays a critical role in the movement of sediments and the erosion of coastal cliffs. Coupled with wind, waves generate nearshore surf zone currents which shape the coastline by eroding, transporting and depositing sediments (Tinley, 1985). Deep-water ocean waves can be formed hundreds of kilometres offshore. The wave height is determined by the strength, duration and fetch of wind blowing out at sea. As waves moves across the continental shelf towards the coastline, their strength and height are influenced by attenuation, refraction and reflection (Short and Hesp, 1982). Friction against the seabed causes the wave to slow as it reaches the coast. When the wave moves across the beach it changes shape, wave length and amplitude causing the wave to eventually break and form a bore (Galvin, 1972). Wave refraction is the process whereby waves bend towards the coastline as the water depth decreases. The wave energy is therefore focused on headlands and dissipates in embayments (Figure 6). Waves reaching a beach can be classified as constructive waves or destructive waves. Constructive waves have less energy and longer periods and result in material being deposited on the beach. Destructive waves are created during storm events with high energy and shorter wave period. Destructive waves cause erosion of the beach and moves sediment offshore (Galvin, 1972).

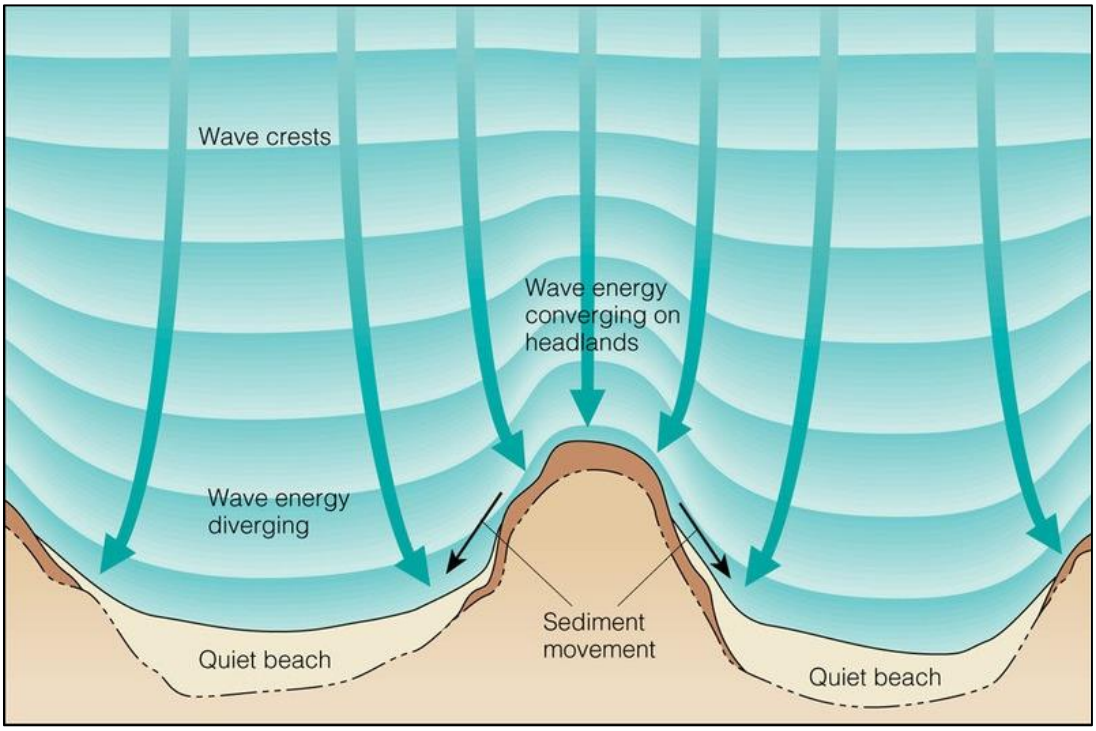

Figure 6: Wave refraction focusing wave energy on the headlands and dissipating energy on sandy beaches (Garrison, 2005).

1.7 Wave-induced nearshore currents

Waves produce two types of current in the nearshore; shore parallel longshore currents and offshore-directed shore perpendicular rip currents (Reading, 1991). Longshore drift is the process whereby sediment is transported in the littoral and surf zone. Two mechanisms can result in longshore drift occurring along a coastline. The first more widely accepted mechanism is when a wave brakes obliquely on a coastline. The sediment is carried onto the beach face at an angle by the wave. When the water recedes the sediment is transported straight down the beach face back to the sea (Komar and Inman, 1970). This result in a zig zag pattern of sediment transport developing (Figure 7).

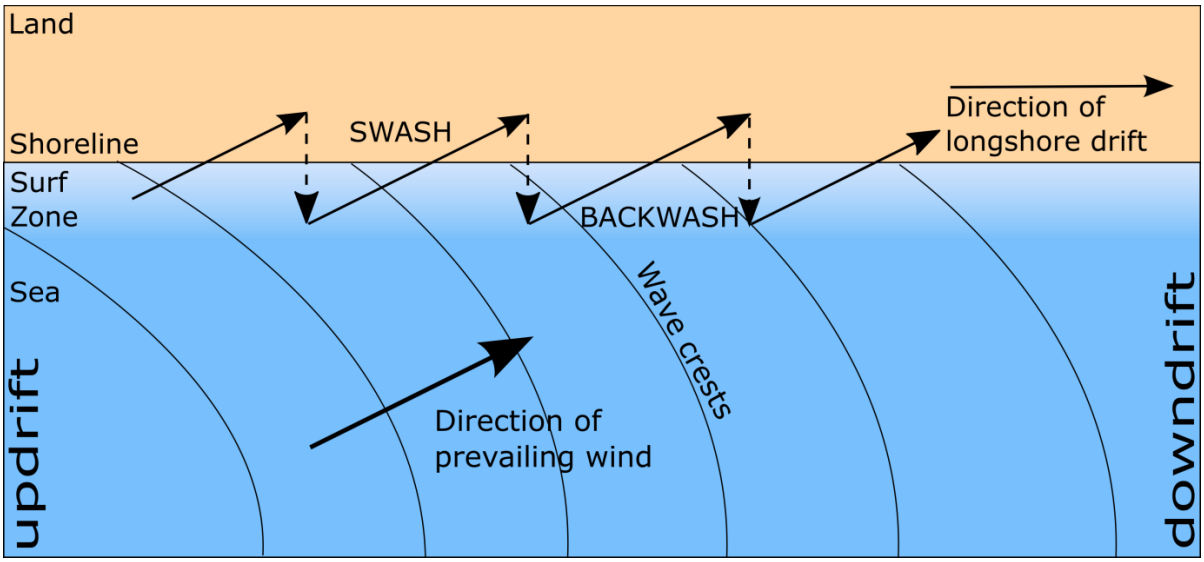

Figure 7: Longshore drift on sandy beaches.

In the second mechanism energy from breaking waves places sediment into suspension in the surf zone (Smith and Mocke, 2002). For the suspended sediment to be transported in a net direction the presence of a current is required (Bagnold, 1973). The current can be caused by waves hitting the coast-line at an oblique angle, tidal currents or wind driven. Suspended sediment is believed to be the dominant mode of transport of sediment in the near shore along a rocky coast (Bayram et al., 2007). Rip-currents occur in conjunction with longshore currents. Waves approaching the shore and longshore currents cause variations in water level, or set-up, along the shore line (Komar and Inman, 1970). The longshore currents flow away from the set-up cells and turn into rip-currents which transport the excess water offshore (Figure 8). Rip-currents often erode channels in the shoreface, which

then subsequently confine the currents (Reading, 1991). Rip-currents are most active during storm events when they can transport a considerable amount of sediment towards the offshore.

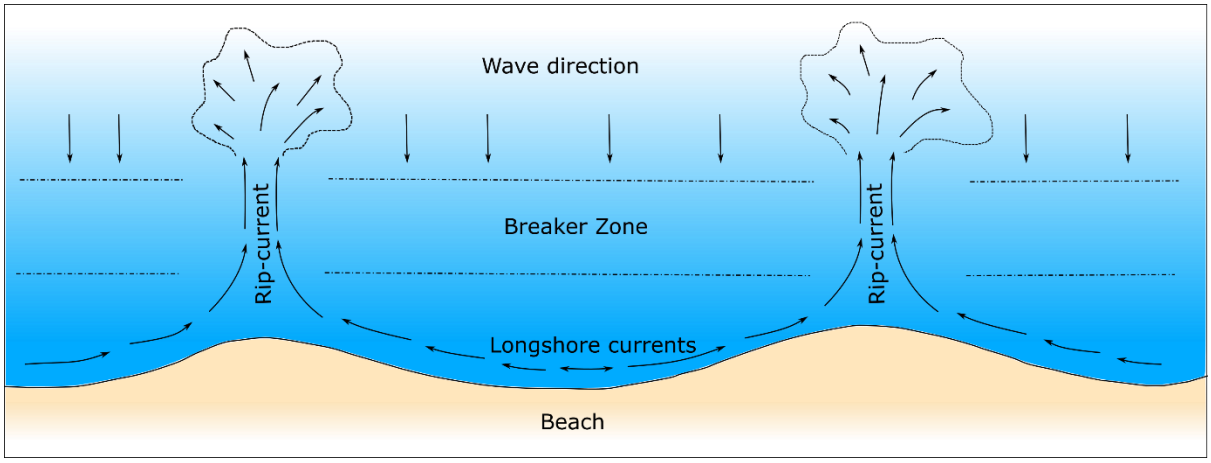

Figure 8: Wave-induced nearshore currents showing longshore currents and offshore-directed rip-currents (Reading, 1991).

1.8 Human Impact

Development and utilization of the coastal zone is expanding at a rapid rate, much more so than inland areas (Neumann et al., 2015). The rapid growth in population and development are important factors affecting and changing the coastal zone and place pressure on the management of coastal zone environments. The geomorphology of the coastal zone cannot be studied in isolation from human impact and development. Development in one area can bring about changes in the coastal geomorphology further along the coast. Unintended interference with coastal sediment transport can have far reaching effects further down the line, for example, erosion of popular beaches or silting up of harbours (Woodroffe, 2002). Erosion of coastal dunes or cliffs can have disastrous effect on infrastructure. To protect infrastructure susceptible to severe storm damage, such as during the 2007 storm on the KwaZulu Natal coast, coastal engineering solutions may be required. There are several methods generally used to protect infrastructure in the coastal zone. Beach nourishment is a technique used worldwide where dredged sediment is deposited on the beach to shift the wave run-up further from infrastructure (Corbella and Stretch, 2012). Other methods include building groynes (piers), retaining walls or placing geotextile sand-filled containers. A South African invention called a dolos, is a large 20 ton, tetrapod shaped, concreate block

used to protect harbor walls and other structures. Dolos work by interlocking and dissipating the wave energy instead of reflecting or blocking the wave energy. Unfortunately, all these solutions can have unintended outcomes further along the coast. Beach nourishment is not always successful. The predominant wave conditions will determine the equilibrium profile of the beach and the additional sand could simply be moved offshore.

1.9 Sea-level Change

Sea-level change pose a real threat across the world as 11% of the world's population lives in low-lying areas within the coastal zone. Low-lying coastal areas are defined as being below 10 m above mean sea level (AMSL) (Neumann et al., 2015). The latest estimates puts global sea-level rise between 1.7 ± 0.3 mm yr^{-1} (Church and White, 2006) and 3.3 ± 0.3 mm yr^{-1} (Chen et al., 2017). Rising sea level has several detrimental effects on the coastal zone, especially in developed areas. Rising sea level causes inundation of low-lying areas, increased flooding though storm surges and tsunamis and re-distribution of sediment along sandy coastlines (FitzGerald et al., 2008). With sea-level rise storms of the same magnitude reach higher elevations, inundating larger areas and causes more damage. Long-term effects include migration of barrier islands towards the shoreline through sediment transport. On a geological time-scale, changes in sea level can also affect sediment transport along the coastline. During lower sea level for example, long coastal beaches may be exposed, which would facilitate sediment transport through longshore drift. During higher sea level the coastline might consist of rocky coastlines and headlands which would restrict sediment transport.

1.10 The Cape Peninsula

The Cape Peninsula of the Western Cape, South Africa comprises a combination of a sprawling urban area of the greater City of Cape Town and the wilderness areas of the Table Mountain National Park, which includes Cape Point and Table Mountain. The Atlantic Ocean is located to the west of the peninsula, False Bay is on the eastern shore of the Cape Peninsula and Table Bay bounds it to the north (Figure 9). The coastline consists of a mix of

rocky shorelines, sandy shores and pocket beaches (Tinley, 1985). The western peninsula is dominated by rocky coastline consisting of steep plunging cliffs, which in combination with the high-energy wave conditions, make sediment deposition along this coast relatively minor (Brown, 1971). The exception is Noordhoek Beach, with its 3.6 km beach to the south of Hout Bay. In contrast, Table Bay and False Bay have long unbroken stretches of sandy beaches. Historically, before urban development of Cape Town and surrounds, the coastal zone contained extensive coastal dune systems. Today, most of these dune systems have been stabilised by planting of alien vegetation, which has effectively stopped dune functioning.

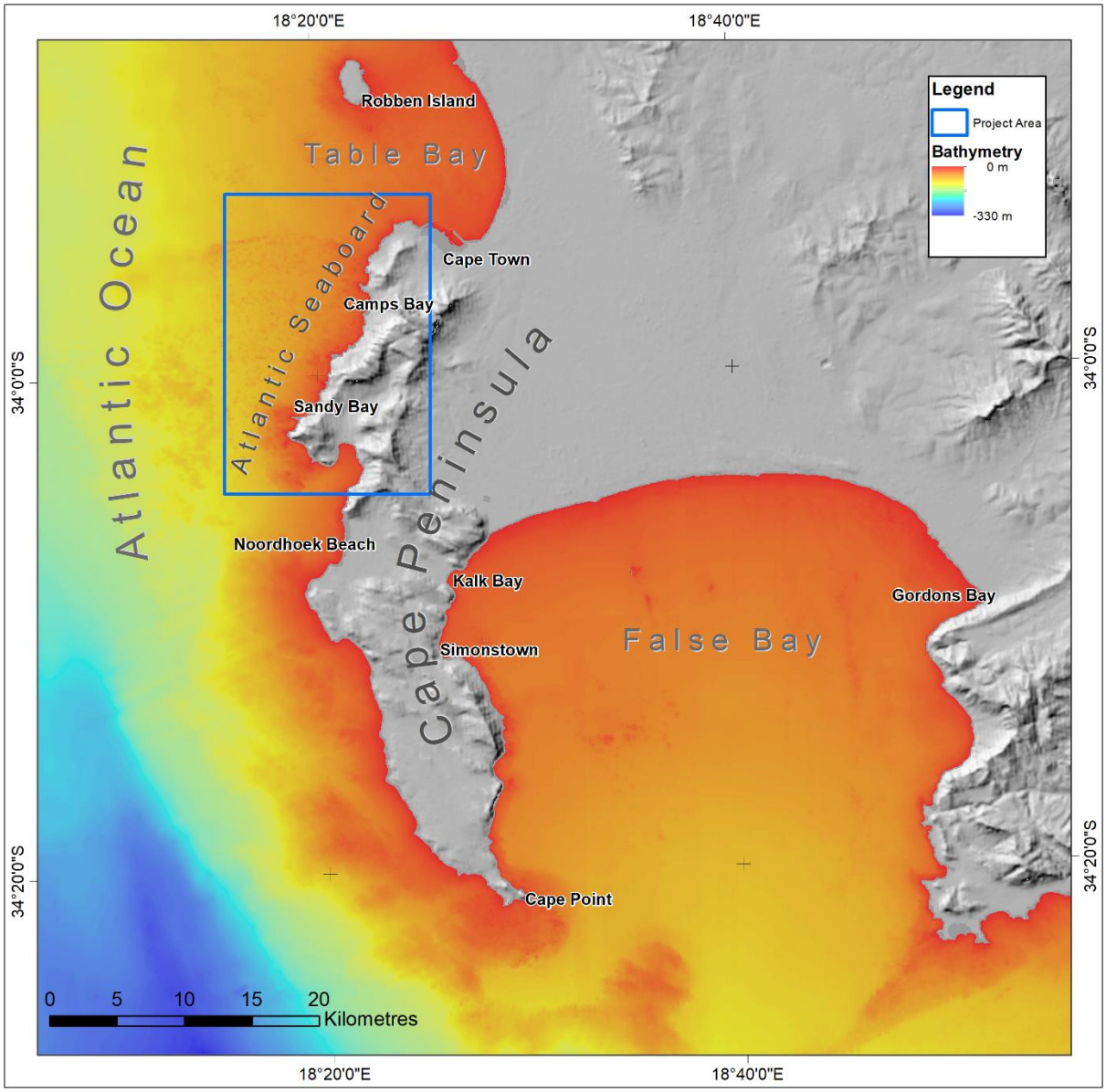

Figure 9: The Atlantic Seaboard study area (blue outline), located on the north western coast of the Cape Peninsula on the south-western tip of South Africa.

1.11 The Atlantic Seaboard

The study area for this project, locally known as the Atlantic Seaboard, is located between Hout Bay in the south and Mouille Point near the entrance to Table Bay in the north (Figure 10).

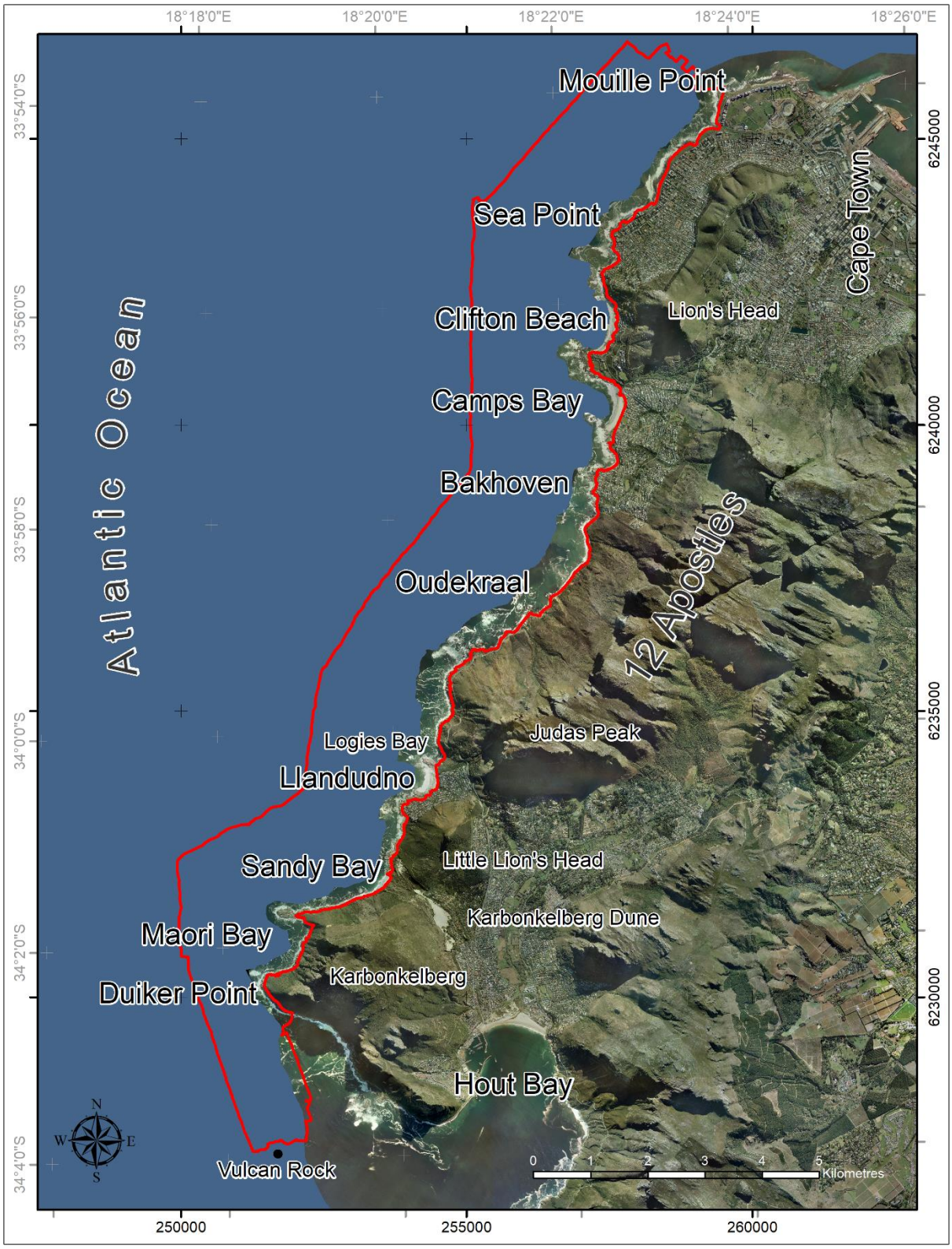

Figure 10: The Atlantic Seaboard study area, with the survey area indicated in red outline.

This stretch of coastline is considered to be a sediment-starved coastline and generally consists of a rocky shoreline and steeply plunging cliffs interrupted by several small sandy bays, or pocket beaches. The pocket beaches are generally flanked by large rocky headlands which act as energy barriers that allow sediment accumulation on their leeward side (Tait, 1995). To the north between Sea Point and Mouille Point, a narrow coastal plain lies beneath Lion's Head and Signal Hill. The coastal plain is a remnant marine terrace formed during times of higher sea level. The width of the coastal plain varies between 800 m and 1200 m. Five major pocket beaches are located in the study area, namely Clifton (Clifton 1st to 4th beach), Camps Bay, Llandudno, Sandy Bay and Hout Bay, which was studied in detail by MacHutchon (2013). Several smaller patches of sediment occur, but these are mostly above the high water mark or protected by shallow reef in the surf zone and not influenced by waves on a regular basis. The Karbonkelberg sediment bypass is a dune or sediment bypass corridor which extends from Hout Bay in the southeast to Sandy Bay on the Atlantic Seaboard to the northwest. The only other notable sandy beach in the region is Noordhoek Beach which is located south of the study area (Figure 9). This beach is important nonetheless as it could be considered an important source of sediment for the Atlantic Seaboard.

1.12 Objective

The objective of this study is to integrate high-resolution bathymetry, side scan sonar, seismic profiles, beach profiles and the distribution and sedimentology of unconsolidated offshore sediment to construct a geological map of the inner shelf out to 70 m water depth between Vulcan Rock and Table Bay. This geological map provides the basis for understanding the sediment dynamics of a high-energy, predominantly rocky coast in terms of seabed morphology, source and movement of sediment, and the role changes in sealevel, together with anthropogenic structures, plays in the sediment budget.

2 Regional Setting

2.1 Geological Overview

Deposition and deformation of sediments and rocks of the south western continental margin were the result of various tectonic cycles of supercontinent formation and break-up (Tankard et al., 1982). The oldest rocks found in the region were deposited during the Late Proterozoic during the formation of the Saldania orogenic belt. The Saldania Belt is one of several deformation belts that formed during the closure of the Adamastor Ocean during the assembly of the super-continent Gondwana. During deformation of the Saldania Belt a deepening basin formed into which sediments were deposited and subsequently deformed and folded by low grade metamorphism to form the Malmesbury Group (Rozendaal et al., 1999). The age of the Malmesbury Group is between 980 Ma and 560 Ma with the volcanic rocks of the Blouberg strand member dated at 555 ±5 Ma, using zircon ages (Belcher and Kisters, 2003; Kisters et al., 2015). The Malmesbury Group was intruded by the Cape Granite Suite during several phase between 555 and 515 Ma (Scheepers and Schoch, 2006). The Malmesbury and Granite uplifted, eroded to form a peneplain which then subsided. Deposition and deformation of the Cape Supergroup sediments occurred between 500 – 330 Ma during a period of internal rifting and extension of Gondwana (Dingle et al., 1983). This was followed by the deposition of the Karoo Supergroup sediments which were deposited in a retro-arc foreland basin setting between 310 – 182. Both the Cape Supergroup and the edges of the lower Karoo Supergroup underwent intense thrusting and folding to form the Cape Fold Belt during the early Permian (280 – 230 Ma). The initial breakup started with lithospheric stretching and minor rifting, between 183 - 175 Ma. Initial rifting was associated with extensive Karoo flood-basalt volcanism, which terminated the Karoo sedimentary succession (Partridge and Maud, 1987). Rifting continued between 175 – 135 Ma with the activation of the Agulhas-Falkland Fracture Zone. The South American and African plates started separating between 135 – 115 Ma, to form the South Atlantic Ocean and Mid-Atlantic Ridge (Rust, 1973). Along the African margin depositional basins formed in response to the final stages of Gondwana break-up (Shone, 2006). These basins are characterised by graben and half-graben structures. The earliest deposits in these basins which are associated with synrifting are fluvial and lacustrine in origin, with associated volcanics and volcaniclastics. Subsequent deposits consist of deltaic and shallow marine

deposits. The Drift phase deposits consist of deep-marine argillaceous sediments. Repeated episodes of uplift, tilting and down-faulting occurred during the late Cretaceous which resulted in major erosion inland on the African continent. This resulted in large deposits of terrigenous sediments to be deposited in the offshore basins during the Cenozoic (Dingle et al., 1983; Partridge and Maud, 1987).

2.1.1 Cape Town Geology

In the Cape Town area, the Cape Fold Belt underwent extensive erosion to form the landscape seen today. Erosion exposed Malmesbury and Granite basement over large parts of Cape Town, the Cape Flats and West Coast, leaving Table Mountain with its resistant sandstone as an outlier covering the basement rocks on the Cape Peninsula (Figure 11).

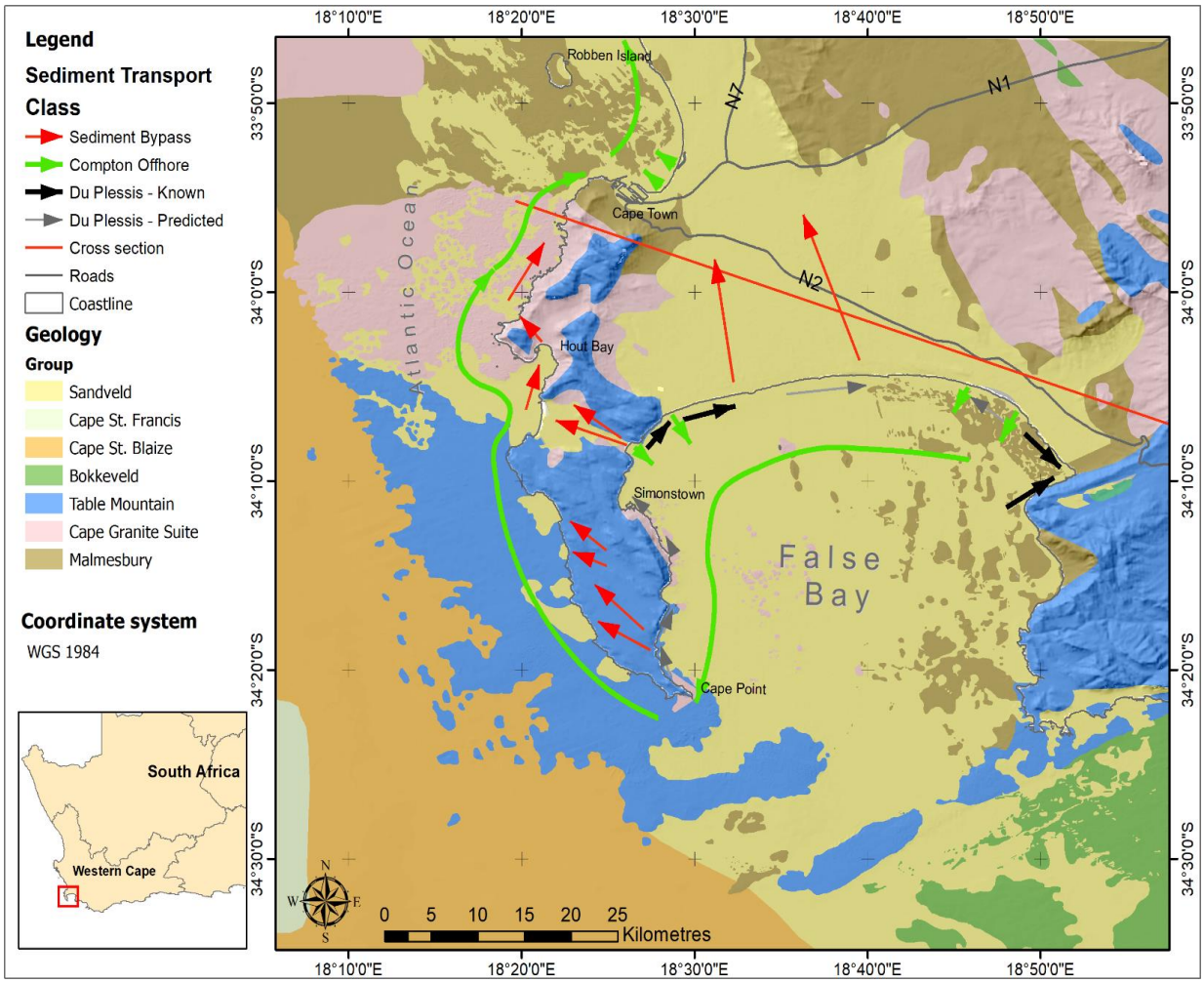

Figure 11: On-offshore Geology of the South Western Cape. Offshore geology data from unpublished Marine Geoscience data, onshore geology data simplified from CGS 1:250 000 map series. Offshore sediment transport pathways (Compton, 2004), Inshore sediment pathways (Du Plessis and Glass, 1991) and Sediment bypass systems (Tinley, 1985).

The Malmesbury, which weathers more readily, generally forms flat, low-lying areas, except for the Tygerberg Hills and Lion's Head. These hills are formed by more resistant Malmesbury horfeslic slates and greywakes which metamorphosed along the contact auriole of the underlying Cape Peninsula Pluton. The Table Mountain outlier formed part of a synclinal trough of a large regional fold (Figure 12). Once the anticlinal limb of the fold was eroded, and the Malmesbury underneath was exposed, the Malmesbury eroded at a much higher rate than the Table Mountain Group sandstone which remained (Compton, 2004).

2.1.2 Malmesbury Group

The regional basement of the Cape Peninsula consists of the Malmesbury Group. The Malmesbury Group is comprised of greenschist facies metavolcanic and metasedimentary rocks of Neoproterozoic age. The sediments were deposited during the Saldanian orogeny in the late-Precambrian between 980 Ma and 560 Ma (Hartnady et al., 1974; Belcher and Kisters, 2003; Rowe et al., 2010). The Malmesbury Group is represented by the Tygerberg Formation within the study area and consists mainly of metamorphosed greywacke sandstones and shales. The rocks are well exposed along the coast between Mouille Point and Sea Point where it goes through a transition zone into the Cape Granite Suite which intruded into the Malmesbury Group at the Sea Point Contact (Von Veh, 1983). The greywacke sandstones are of greenish-grey color and medium to fined grained rocks. Sedimentary features found in the deposits include cross-bedding, ripple cross-lamination, and graded bedding. Rowe et al. (2010) concluded that rocks from the Tygerberg Formation on Robben Island were deposited in a high-energy environment with a high deposition rate and tectonically deepening basin. To the north of the study area at Bloubergstrand, the Bloubergstrand Member of the Tygerberg Formation contains minor andesitic lavas and tuffs (Belcher and Kisters, 2003). Detrital zircon ages from this formation range between 1200 and 560 Ma. The youngest zircon ages indicate that the deposition of Malmesbury sediments continued until at least 560 Ma (Kisters et al., 2015). The large-scale structural pattern of the Tygerberg Formation appears to consist of a succession of tight to open, upright folds with a NW strike and axial planar cleavage (Belcher and Kisters, 2003). Bedding varies by dipping between 60˚ and 90˚. The strata have subsequently been weathered down to a plain situated roughly at current sea level (Von Veh, 1983).

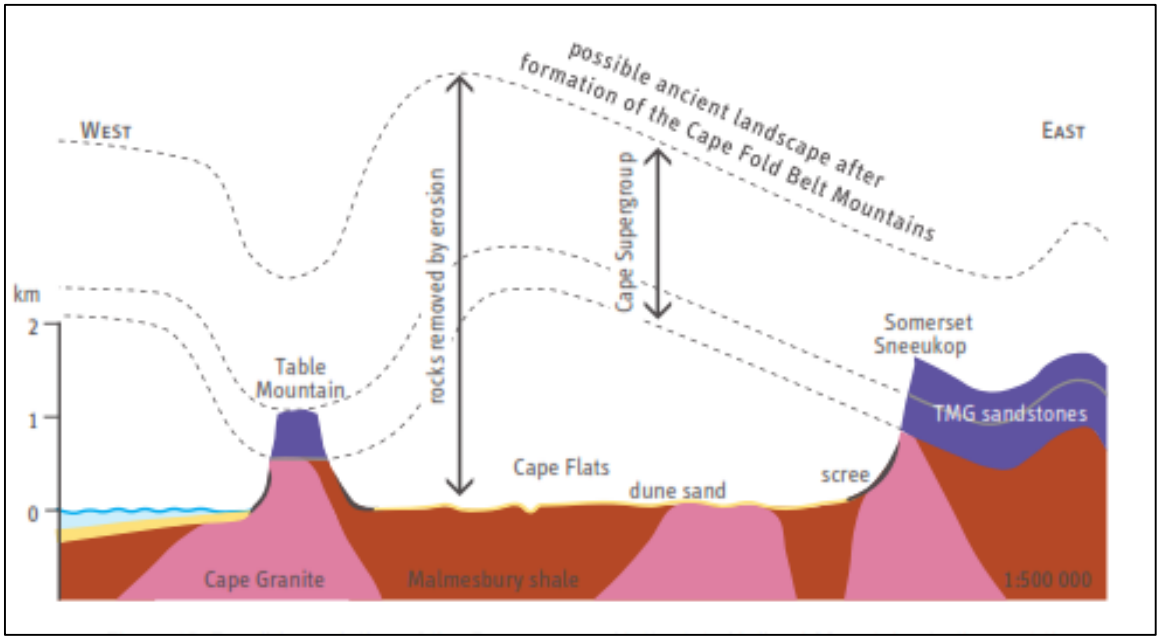

Figure 12: Geological cross section between Cape Town, roughly along the N2 highway to Sir Lowry's Pass (see Figure 11, Compton, 2004).

From side scan sonar work conducted by the National Research Institute for Oceanology of the sea bed between Sea Point and Bloubergstrand, the area has been described as consisting mostly of exposed Malmesbury bedrock covered in places by a thin veneer of coarse shelly sediment (Woodborne, 1983).

2.1.3 Cape Granite Suite

The Cape Granite Suite is composed of late Precambrian granitoids which intruded into the Precambrian Malmesbury Group (Belcher and Kisters, 2003). This intrusion occurred during several major phases during the late Proterozoic and early Cambrian between 550 and 510 Ma (Scheepers and Schoch, 2006). Based on their petrological and geochemical composition the Cape Granite intrusions can be classified into three types, namely S, I and A, each with its own sub-types. Each type is associated with a specific phase and is only found in a specific part of the Saldania Belt. The Cape Peninsula Pluton which intruded into the Tygerberg Formation of the Malmesbury Group is one of the oldest intrusions in the region and occurred during Phase I of the intrusion between 555 and 540 Ma (Scheepers, 1995). Phase 1 intrusions consist of S-type prealuminous and metaluminous assemblages, which were emplaced in at least eighteen individual major intrusive phases. Between Sea Point and Maori Bay, the pluton belongs to Sa_1 type, with rock types consisting of granodiorite,

biotite granite and granite. Large twinned orthoclase feldspar phenocrysts are characteristic of Sa_1 plutons (Horn, 2009). Microcline perthite is the dominant feldspar with oligoclase and andesite lamellae. Secondary muscovite is common with garnet, monazite, apatite, zircon, tourmaline, clinozoisite and uraninite as additional secondary minerals (Scheepers and Schoch, 2006).

2.1.4 Sea Point Contact

The Sea Point contact which is situated towards the northern part of the study area exposes the contact relationship between the low grade metamorphic rocks of the Malmesbury Group and the intrusive rocks of the Cape Granite suite. The Sea Point Contact was first described by Playfair and Hall, (1813) from observations made by Hall at Platteklip Gorge during 1812. Clark Able was the first author who in 1818 described the granite-schist contact at Sea Point. Observations by these authors strengthened the theory of Huttonian Plutonism and the intrusive nature of granites vs Wernerian Neptunism, which proposed that granites (and all other igneous rocks) crystalized or precipitated from the primordial oceans (Master, 2012). The contact was later visited and made famous by Charles Darwin in 1836 on his voyage around the world on the HMS *Beagle*. The Sea Point Contact was instrumental in arguing for the magmatic origin of granite, which then intruded into older metasedimentary rocks. Von Veh (1983) carried out a study of the structural evolution of the Tygerberg Terrane around Sea Point. He described the granitic pluton as a migmatite containing granitic lithosomes and hornfelsic palaeosomes. The contact zone has a unique preferred planar fabric which is defined by the orientation of orthoclase phenocrysts in the lithosomes (granite) and by slaty cleavage in the palaeosomes (Malmesbury). Horn (2009) revisited the Sea Point Contact and refuted the migmatic nature of the intrusion. Migmatic intrusions are defined as a mixture of igneous material of granitic composition within a high grade metamorphic host rock with a banded or veined appearance. The metasediments of Malmesbury Group have only been metamorphosed to low grade and temperatures were therefore not high enough to cause partial melting of the rocks. Horn (2009), therefore, regards the Sea Point Contact as an intrusive or injection contact. Increasing effects of the contact metamorphism resulting from the Granite intrusion can be observed from Granger Bay towards Sea Point. Indicators include specks of cordierite and chlorite porphoblasts in the pelitic layers and massive bluish-grey hornfels close to the contact (Von Veh, 1983).

2.1.5 Table Mountain Group

After an extended period of uplift and weathering, the Cape Supergroup sediments were deposited unconformably on top of the Malmesbury Group and Cape Granite Suite. The siliciclastic sediments were deposited after the Saldanian Orogeny ended, from the Cambrian to the early Carboniferous between ~500 Ma and ~ 330 Ma. Deposition occurred in a passive margin setting and up to 10 km of strata are preserved even though they were subsequently deformed during the Cape Orogeny (Thamm and Johnson, 2006). Two formations from the Table Mountain Group (TMG) are present near the study area, namely the Graafwater Formation and the Peninsula Formation. The Graafwater Formation consists of maroon sandstone, siltstone and mudstone layers, which occur in upward-fining cycles. Sedimentary structures such as lenticular and flysch type bedding, ripple marks, stream lineations, desiccation cracks, ball-and-pillow structures and clay-pellet conglomerates are abundant. The formation reaches a thickness of 65 m at Llandudno and Karbonkelberg (Theron et al., 1992). The sedimentary structures of the Graafwater Formation are indicative of a nearshore tidal and tidal flat environment. Alternative hypotheses points to sediments being deposited in fluvial channels draining low relief coastal floodplain (Turner, 1990).

The majority of the TMG on the Cape Peninsula consists of the Peninsula Formation sandstone. The formation consists of clean, uniformly light–grey, medium to coarse grained, well-bedded quartz arenite sandstone with minor interlayers. Well-rounded quartz pebbles are found in lenses or thin conglomerate layers. The Peninsula Formation has been regarded as a shallow-marine shelf deposit close to a transgressive barrier, tidal and beach environments (Rust, 1973). More recently it has been suggested that the formation was deposited in a fluvial braid-plain (Fuller, 1985; Turner, 1990). The Peninsula Formation reaches a thickness of 575 m in the Table Mountain area. The absence of muddy and other fine grained layers indicate a high-energy environment on a shallow continental shelf (Theron et al., 1992).

2.1.6 False Bay Dolerite Swarm

The dolerite dykes found around the Cape Peninsula form part of a dolerite dyke swarm which intruded into the Malmesbury Group, the Cape Granite Suite and the lower formations of the Table Mountain Group (Reid et al., 1991). The False Bay dyke swarm is the southernmost occurrence of a series of dyke swarms, central complexes and continental flood basalts which formed along the southwest African margin during the Cretaceous (Figure 13).

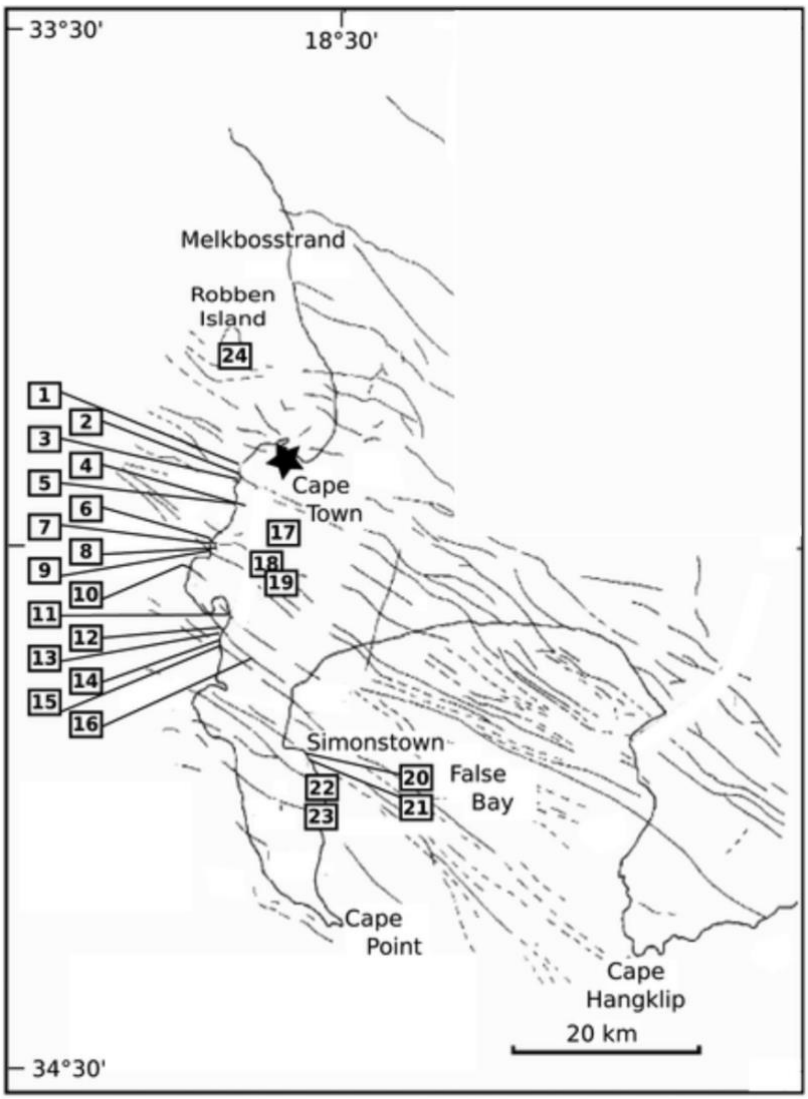

Figure 13: False Bay Dolerite Swarm (modified from Day, 1986 and Backeberg et al., 2011). Solid lines indicate positive magnetic anomalies and dotted lines indicate negative magnetic anomalies. The number dykes corresponds to dykes sampled by Reid *et al.* (1991).

The dykes intruded during several events between 130 and 132 Ma during the initial breakup of Gondwana and formation of the South Atlantic Ocean. Some dykes intrude into the Graafwater Formation, but generally do not penetrate the Peninsula Formation (Walker, 1956). Backeberg (2012) suggested that the thick massive quartz arenite bedding planes of the Peninsula Formation prevented further penetration of the dykes into the TMG. Alternatively, the dolerite dyke material did penetrate into the TMG, but has since weathered out. The gap left by the weathered dyke has subsequently closed due to compressional forces. Some of the older dykes display deformation related to the formation of the Cape Fold Belt, while others cut across folds and displacements (Theron et al., 1992). The dyke swarm generally follows a NW-SE trend. Several intrusions have been mapped along the Atlantic Seaboard by Day (1986). Most dykes are between 1 – 2 m wide, except for the dyke at Logies Bay which is more than 40 m wide in places (Reid et al., 1991). Most dykes are fine- to medium-grained, dark-grey, melanocratic rocks, which consist of augite and plagioclase minerals. Some olivine, biotite, quartz, ilmenite and magnetite can also be present (Theron et al., 1992).

2.1.7 Cenozoic Deposits

Extensive Cenozoic deposits are found along the South African coast. These deposits are generally thin in the coastal setting, but can be very thick in the offshore environment where they have been deposited in extensional rift basins and sedimentary cones at major river outflows (Roberts et al., 2006). Older Cenozoic deposits can be found offshore of the study area and can be divided in to the Paleogene deposits of the Cape St Blaize Formation and the Neogene deposits of the Cape St Francis Formation. Most of the Cenozoic deposits are Paleogene in age. The boundary between the Paleogene and the Neogene is characterised by a hiatus in deposition and an unconformity that can be seen on seismic records (Dingle et al., 1983). On the continental shelf Paleogene sediments consist mostly of clays and terrigenous quartz. The clays are generally rich in zeolites and fish remains. The sequence thickens towards the coastline. Much lower deposition rates occurred during the Neogene and in some cases Neogene deposits are missing with Quaternary deposits lying directly over the Paleogene deposits (Dingle et al., 1983).

In the study area the Quaternary deposits are represented by the Sandveld Group which consists of fluvial, aeolian and shallow marine deposits. The Sandveld Group unconformably overlies a variety of pre-Mesozoic basement rocks, such as the Malmesbury Group and the Cape Granite Suite and extends from Cape Hangklip to Elands Bay. The Atlantic Seaboard is covered by the bioclastic-siliciclastic sands of the Witzand Formation. This formation was formed by aeolian activity during the most recent phase of the Sandveld Group. The Holocene Witzand Formation consists of white to greyish sand with a high biogenic carbonate content of between 20 and 85% derived mainly from shell, spicules and foraminifera (Roberts et al., 2006). The formation occurs intermittently along the coast forming sandy beaches and coastal dunes. The deposition of the formation was controlled by repeated cycles of marine transgressions and regressions during the late Neogene (Roberts, 2006). Pleistocene sediments along the south and west coast generally occur as cemented dune deposits or beach rocks. Some Pleistocene deposits are known to occur in the study area onshore between Sandy Bay and Llandudno at about 6 m above current sea level (McMillan, 1990). These deposits have been identified and dated from the foraminifera assemblages they contain.

2.2 Coastal Geomorphology

The coastal geomorphology is mainly influenced by the geological evolution and to some degree by the climate and ocean processes described in the following sections. The regional fabric, with its NW-SE orientation was already in existence during deformation of the Malmesbury Group. Subsequent events generally followed the same orientation by reactivating existing zones of weakness, as can be seen in the orientation of the dolerite dyke swarm. The shape and orientation of the coastline is also influenced by weathering of the underlying geology along joints and fractures (Theron, 1984). Hard, more resistant rock types, such as the Cape Granite and the TMG sandstone form topographic highs and major headlands. This can be seen at the Cape Peninsula and Cape Columbine with its mountain ranges and rocky coastlines (Figure 14). In between are the more weathered rocks of the Malmesbury Group forming embayments such as Table Bay and False Bay (Rust, 1991).

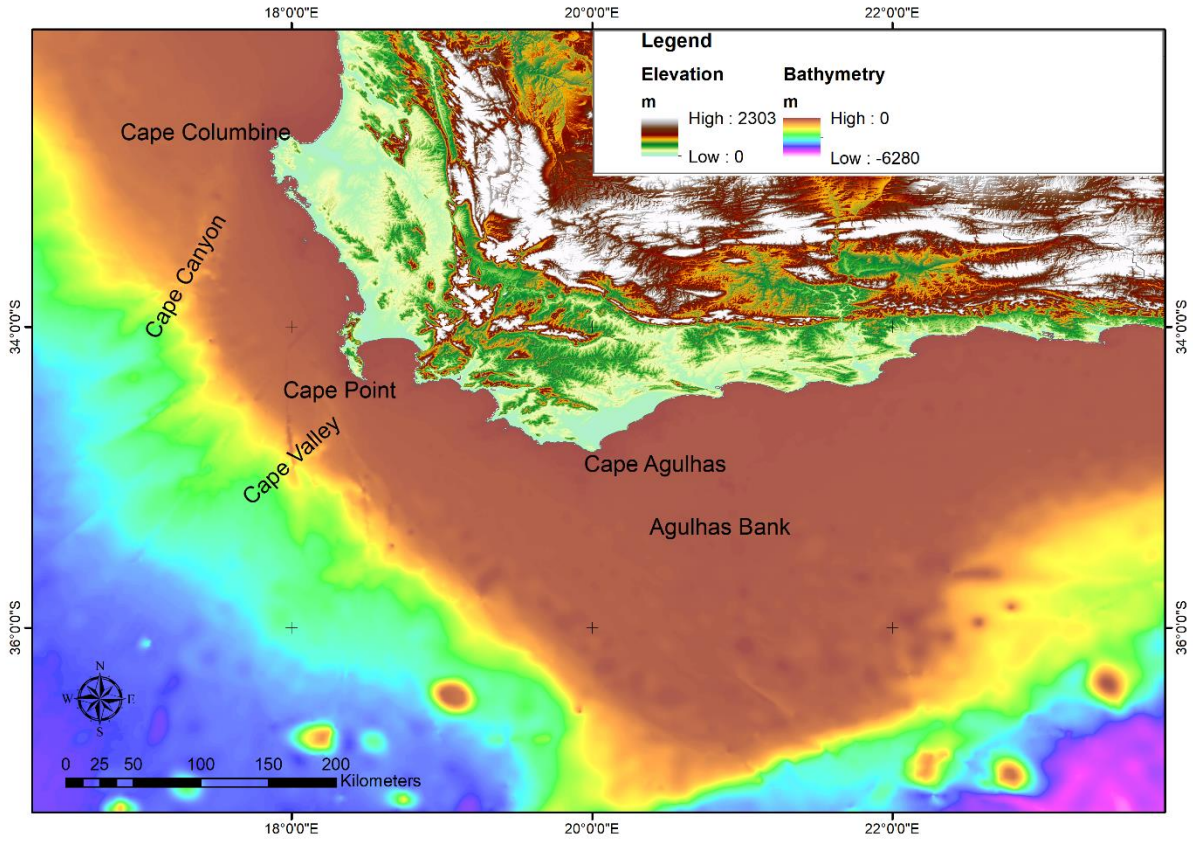

Figure 14: Regional Geomorphology showing a general NW – SE orientation of the coastline between Cape Columbine and Cape Agulhas (Elevation from 30m SRTM data, Bathymetry from GEBCO).

The Agulhas Arch is a major north west orientated, regional feature consisting of a buoyant high between Cape Columbine and Cape Agulhas. It is believed to have been formed by a buoyant intrusive granitic body below the basement rocks of the Malmesbury and TMG (Dingle et al., 1983). Although the general orientation of the West Coast of South Africa is in a NW-SE orientation, the Atlantic Seaboard is the only significant stretch of coastline with a mostly NE-SW orientation (Harris, 1978).

2.3 Quaternary Sea-Level Fluctuations

Sea-level change plays an important role in the shaping of the geomorphology of the coastline. During prolonged sea-level still stands ocean processes will contribute to coastal erosion at that specific elevation, often leaving wave cut terraces, nick points or coastal cliffs (Zecchin et al., 2011). A series of nick points have been identified along the South African continental shelf at various depths; ~40 m, 55 – 50 m, 80 – 75 m and 105 – 100 m below mean sea level (BMSL) (Martin and Flemming, 1986). These terraces have been extensively

studied along the South African West coast north of the Olifants River where they play important role in the deposition of diamond bearing gravel (De Decker, 1987).

During the Quaternary global sea-level fluctuations consisted of several rapid sea-level rises with long periods of sea-level regressions (Figure 15). These cycles were the result of northern hemisphere ice sheets melting and forming (Waelbroeck et al., 2002; Miller, 2005). When the ice sheets are larger, more water is stored in the ice, resulting in lower sea levels, while melting of ice sheets results in a rapid rise of sea level (Compton, 2001). Sea level was at its lowest during the last two glacial maximums at 20 ka and 136 ka during which time sea level drop to below 120 m. Sea level was highest 124 ka ago during the Pleistocene, when it rose to between 6 and 9 m above present (Figure 15).

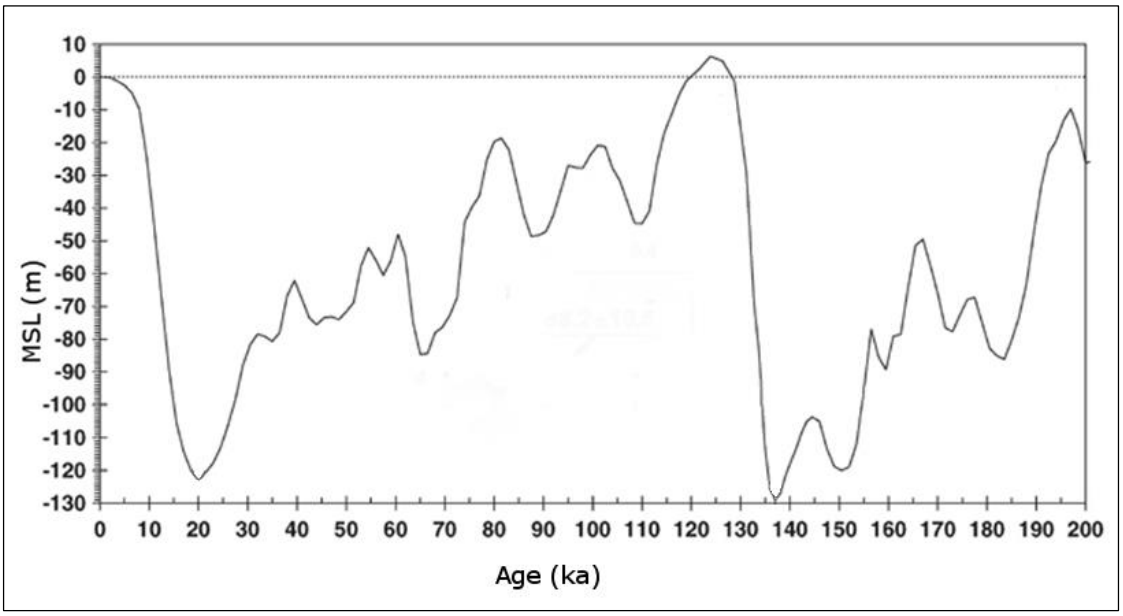

Figure 15: Holocene and Pleistocene sea-level curve (Waelbroeck et al., 2002).

In the South African context local Quaternary and Holocene sea-level curves have been developed by Ramsay (1996) and Ramsay and Cooper (2002), based on dating of beachrocks and potholes in submerged aeolianites. A Holocene highstand of 3.5 m AMSL at 3880 yr B.P. was based on ^{14}C dating. On the west coast a Holocene sea-level curve was constructed by Compton (2001) using facies distribution and ^{14}C dating of sediment deposits in the Langebaan Lagoon. Compton and Wiltshire (2009) correlated quartz and glauconite sand content from cores located near the Cape Canyon to the marine oxygen isotope record. It

was found that sand export onto the shelf is closely related to glacial and interglacial sea-level fluctuations. During the slow transition to glacial periods, there is a general increase in sand content, while the sand content decreases abruptly during rapid rise of sea level from glacial to interglacial periods. Although the magnitude differed the general trend followed the Waelbroeck curve shown in Figure 15.

2.4 Regional Sediment Dynamics

The sediment system of False Bay and the Cape Peninsula is complicated and not only affected by wind and waves, but in recent history it has also been altered and affected by human activities (Tinley, 1985). On a regional scale sediment moves in an anti-clockwise direction around False Bay, exits the bay at Cape Point and is transported up the Atlantic coast past Table Bay and beyond (Figure 11). Du Plessis and Glass (1991) showed varied transport directions in the surf zone of False Bay which is strongly influenced by the swell direction affecting the bay. Significant sediment inputs are found in the form of rivers discharging into False Bay, Hout Bay and Table Bay. Sediment headland bypass systems can be recognized at several bays along the False Bay and Hout Bay coasts.

2.5 Climate

The Western Cape of South Africa is situated in a sub-tropical, Mediterranean-type climate with predominantly winter rain fall. Winters are mild and wet while summers are warm, dry and windy. The highest rain fall occurs during June and July, while lowest rainfall and hottest months are during January and February. The climate is generally dominated by a bi-modal wind regime (Figure 16), in summer the south-easterly wind is the predominant wind, while in winter the north-westerly is the predominant wind (Schulze, 1965).

The dominant meteorological features which influence the summer versus winter wind regimes are two semi-permanent high pressure systems located in the South Atlantic and South Indian oceans respectively. These high pressure 'Hadley cells' form as a result of hot air circulating southwards from the tropics (Figure 17). The air in the Hadley cells move in an anti-clockwise rotation around the centre of the high pressure system.

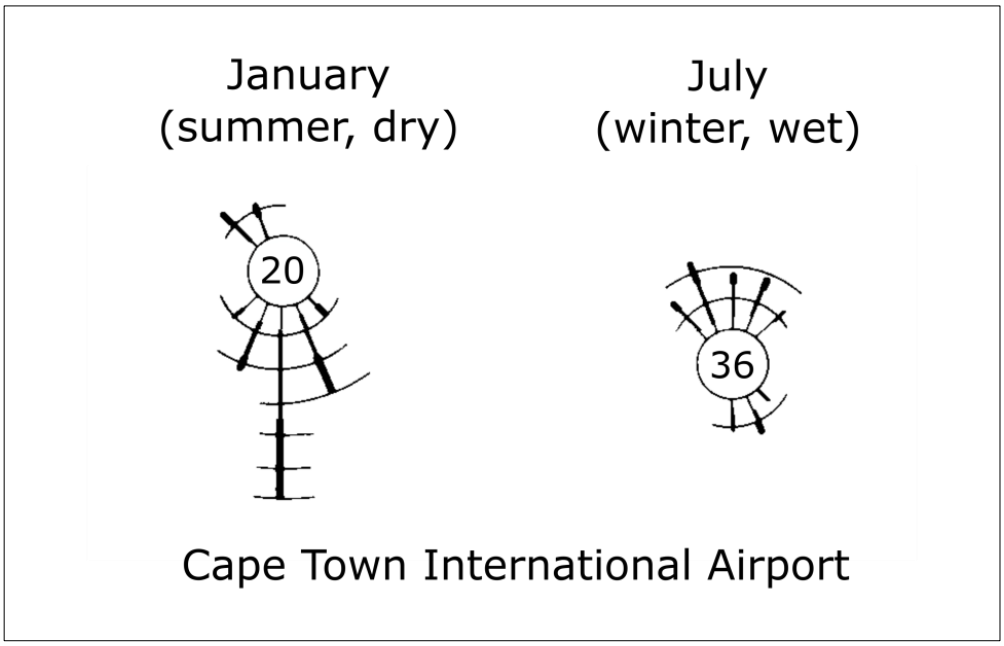

Figure 16: Wind data for Cape Town (Cape Town Int. Airport) between 1956 and 1970, indicating the dominance of strong southerlies during the dry summer months and strong north easterlies during the wet winter months. The number in the centre represents number of calm days (Stapor Jr. et al., 1983).

Low pressure systems are created in the South Atlantic by disturbed air in the Ferrel westerlies (or mid-latitude cell) which spiral eastwards around the globe. These low pressure systems and associated cold fronts are the source of the winter rain and wind regimes. During summer the high pressure systems push the low pressure systems further south into the South Atlantic and they pass south of the coast (Rossouw, 1989). The southerly and south-easterly wind directions caused by the anticyclonic movement of air of the Hadley cells during summer results in offshore wind directions during summer (Figure 16). Further up the west coast the climate is dominated by southerly winds which also cause surface water to move offshore by a process called Ekman transport. Inshore surface waters are thus moved offshore and replaced with cold Antarctic bottom water. This is called coastal upwelling and results in colder water temperatures along the Atlantic coast during summer (Tinley, 1985).

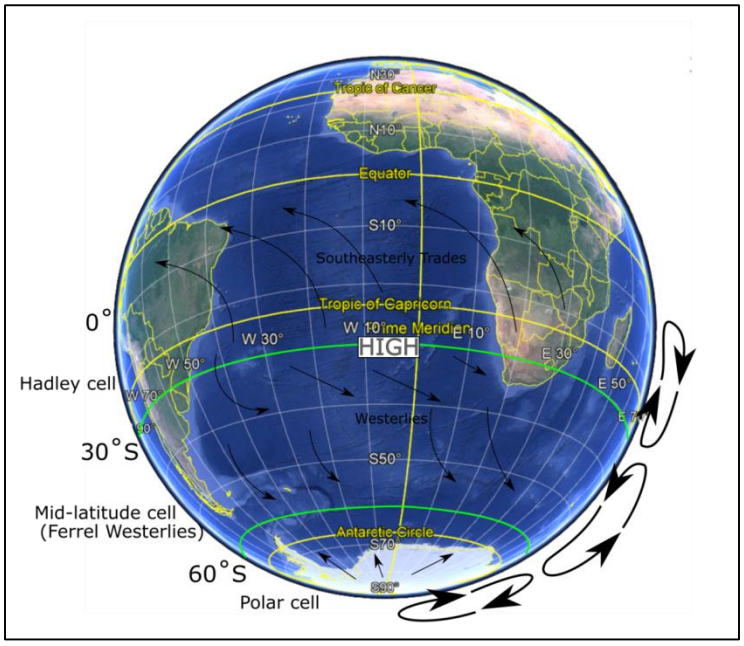

Figure 17: Atmospheric circulation responsible for the seasonal weather patterns along the South African west coast (Globe image from Google Earth).

2.6 Wave Regime

The passage of the low pressure systems and their associated cold fronts, coming from the Southern Ocean, are the main source for large ocean waves affecting the South African coastline (Tyson et al., 2000). The wave regime along the South African coast has been studied in detail by (Rossouw, 1989) using wave data collected by the CSIR at Slangkop between 1976 and 1988 (Figure 18). The Slangkop wave rider was situated 14 km offshore of the Slangkop lighthouse in a water depth of 170 m. The Slangkop wave rider has subsequently been relocated to a position closer inshore in water depth of 70 m (Zietsman, 2014). From the Slangkop data a significant wave height (H_s) which is defined as the average of the highest one-third of all wave heights measured, were calculated (Rossouw, 1989). From analysis of H_s estimates can be made of the median (H_m) and the expected return periods of extreme events (Table 1).

Significant wave height Hs	
Median value	2.54m
Yearly extreme event	7.61m
1 in 10 year extreme event	9.37m
1 in 100 year extreme event	11.11m

Table 1: Significant wave height statistics of Slangkop wave rider in a water depth of 170 m (from work by Rossouw 1989).

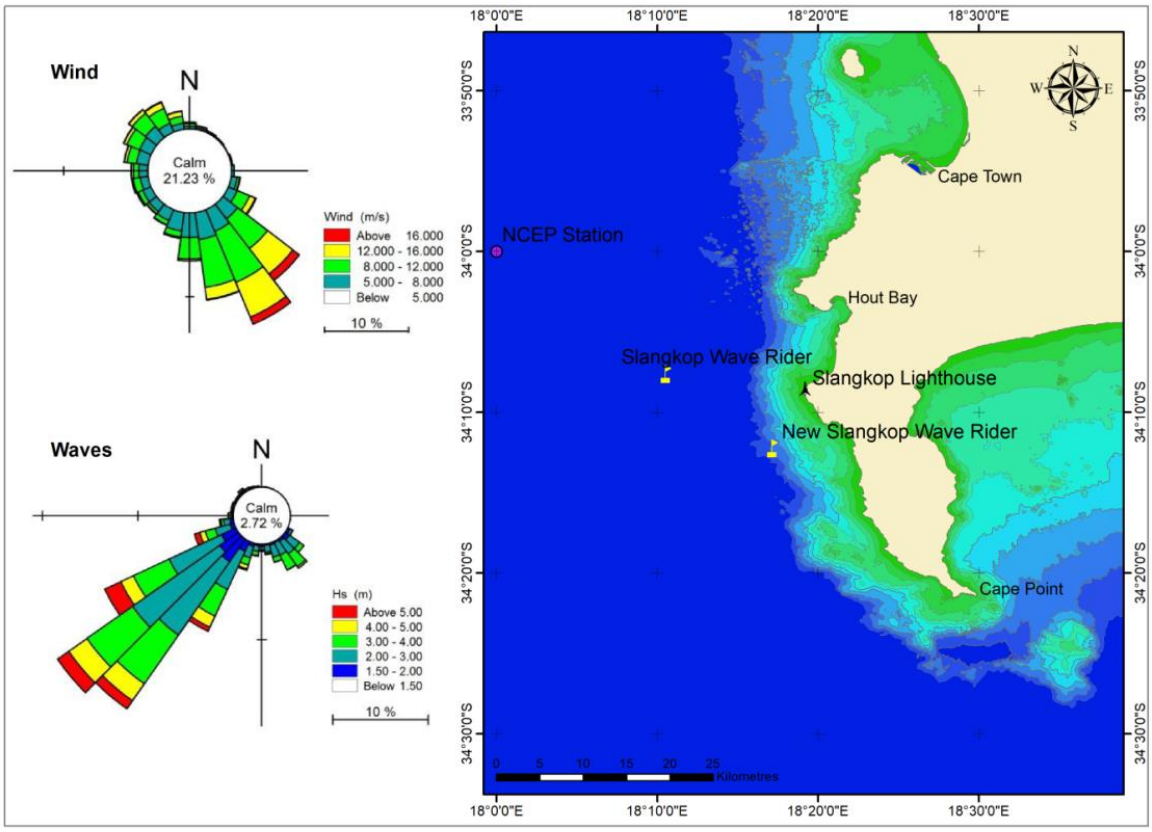

Figure 18: Annual wind and wave roses derived from National Centres of Environmental Prediction (NCEP) data for the Cape Peninsula (modified from CSIR, 2014).

Wave directions along the coast are influenced by the weather patterns. In the South Atlantic the Ferrel westerlies cause waves in a westerly direction which passes to the south of South Africa at latitudes about 40˚S. Due to the position of passing cold fronts along the south western coast the dominant direction of waves is between northwest and southwest. Further north along the west coast the north-westerly component disappears and the coast is mainly influenced by south-westerly waves. Along the Cape south coast the passing cold fronts cause mostly waves with a south-westerly and southerly component (Rossouw, 1989). More recent data from 2000 and 2003 have shown that big wave events have a more restricted measured direction of between 200˚ and 260˚ (Zietsman, 2014). The result of the seasonal wind and wave regime is a high-energy coast subject to major storm events mostly during the winter season. A computer generated model in Figure 19 shows dominant waves from the south west (247.4˚) Changing slightly to a more westerly orientation as it refracts around Duiker Point and reaching the shallow water of the Atlantic Seaboard.

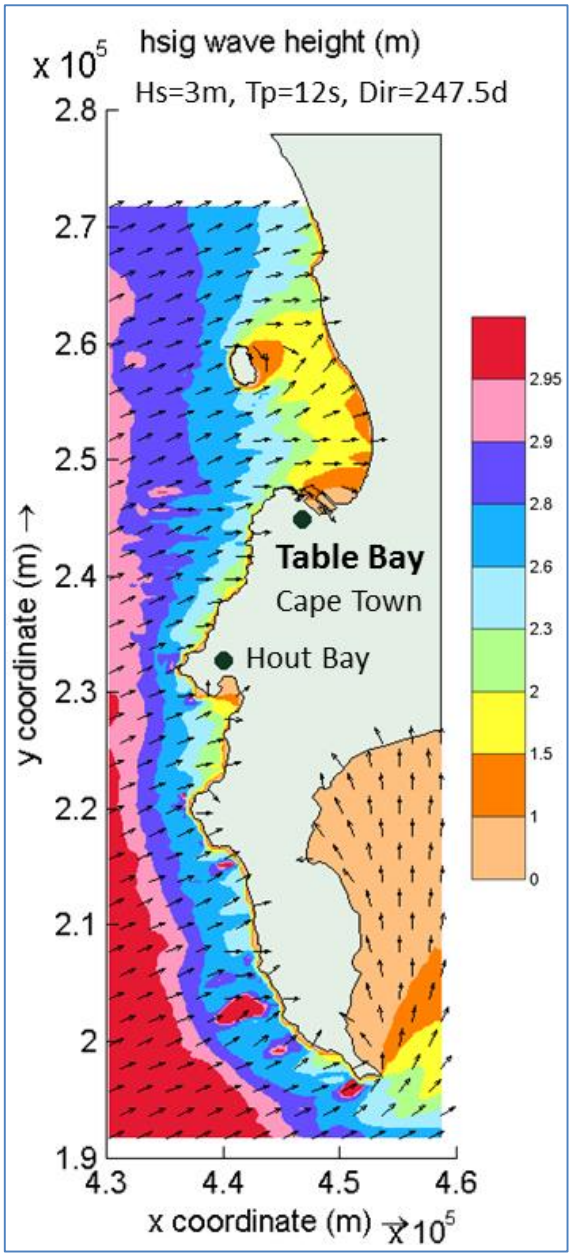

Figure 19: Wave vector plot indicating the significant wave height for the Cape Peninsula (CSIR, 2014).

2.7 Tides

The tidal range around the Cape Peninsula is relatively low and varies between 1.8 m and 1.9 m depending on the location (SA Tides, 2017). The South African coast therefore experiences a microtidal range (Woodroffe, 2002).

2.8 Inshore Currents

Inshore currents along the Atlantic coast have been studied extensively by Sea Fisheries (1960's – 1970's) and later by the University of Cape Town (Harris, 1978). Statistics of ships' drift have shown a marked difference in current directions between winter and summer. Between Cape Point and Slangkop a predominantly northward trend was observed during summer with 61% going north, 7% going south and 32% slack conditions. During winter the north and southward tends were similar with 37% north going, 25% south going and 37% slack conditions. Between Slangkop and Cape Town the predominant current was northward during both summer and winter with 50 – 60% north going, 3 – 8% south going and 40% slack conditions. The discrepancy between the two stretches of coastline can be explained by the coastline's orientation. From Cape Point to Slangkop the coast has a NW-SE orientation, which is roughly parallel to both wind regimes, while the Atlantic Seaboard has a NE-SW orientation which is almost perpendicular to the dominant wind directions. Comparisons between currents and surface temperatures suggest a strong correlation between wind direction, upwelling and currents. Atkins (1965) conducted studies at Camps Bay by tracking floats. He found little correlation between wind and current inshore, probably due to the protected nature of Camps Bay.

3 Methods

This study used a combination of hydrographic, geophysical and sedimentological methods to create detailed bathymetry, seafloor geology and sediment maps of the Atlantic Seaboard. Remote sensing data were ground-truthed with samples collected offshore. The coverage extends from the high water mark to about 70 m BMSL.

3.1 High-Resolution Bathymetry

High-resolution bathymetry data were collected using a multibeam echosounder (MBES). Although the multibeam echosounder can collect data up to 30cm grid size, these data were binned and gridded to achieve a 1m grid.

3.1.1 Operating principles of multibeam echosounders

The general operating principles of an MBES system are shown in Figure 20. A sonar transducer transmits acoustic pulses, propagated within a wide across-track and narrow along-track orientation. The receiver array, which is orientated perpendicular to the transmitting array uses a large number of receive beams that are narrow across-track. The receive beams are directionally steered by a beamforming process (Penrose et al., 2005). MBES operate at high frequencies with short pulse lengths and narrow beams, enabling them to resolve small features at a high resolution.

MBES systems are a valuable tool for data collection when full bottom coverage is required. MBES data do not only produce a high-resolution digital terrain model (DTM), but can also provide information on seabed classification and geological structure of the seabed. Prior to the development of MBES systems, full bottom coverage was only possible with 2-dimensional side scan sonars, which did not provide any bathymetry or DTM information (Denbigh, 1982)

Due to the high resolution nature of these data and the effect that the sea surface has on a floating survey platform, means that extremely accurate measurements for positioning, heave, roll, pitch and heading are required (International Hydrographic Organization, 2005). Positioning must be differentially corrected with vertical datum “tie-ins” being applied

realtime to the data (RTK) or post-processing using suitable tidal corrections. Calibration of the MBES for pitch, roll and yaw offsets must be carried out after installation of the system and before a survey can commence. Additionally, precise offset measurements are required to interface all components of the system.

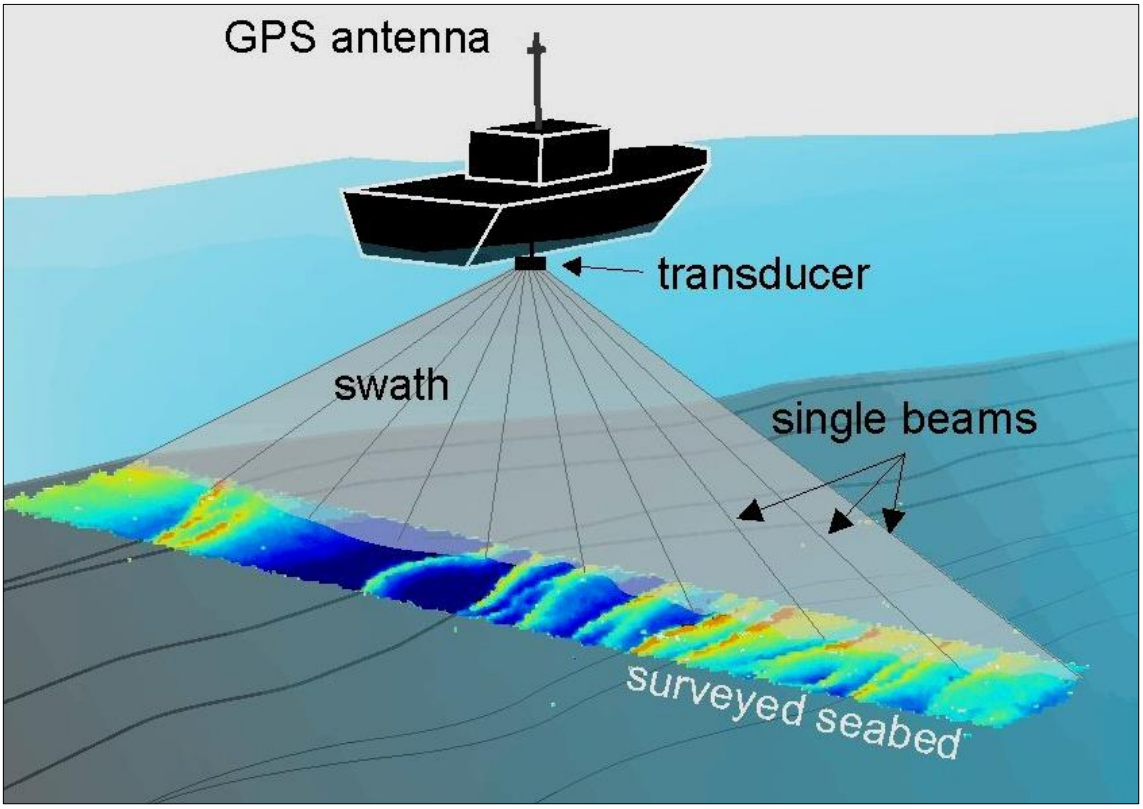

Figure 20: Operating principles of a swath multibeam echosounder (Penrose et al., 2005).

3.1.2 Reson 7125 SeaBat

The Reson 7125 SeaBat MBES, which was used in this survey, is an ultra-high resolution system with an operating frequency of 400 kHz. It is a wide-sector, wide-band, MBES utilising 512 dynamically-focused receive beams at 0.5° across-track beam-width separation. The system measures a 128° swath across the seafloor, detecting the bottom and delivering the measured ranges at a depth resolution of 5 mm up to 50 Hz. The MBES system is shown in Figure 21.

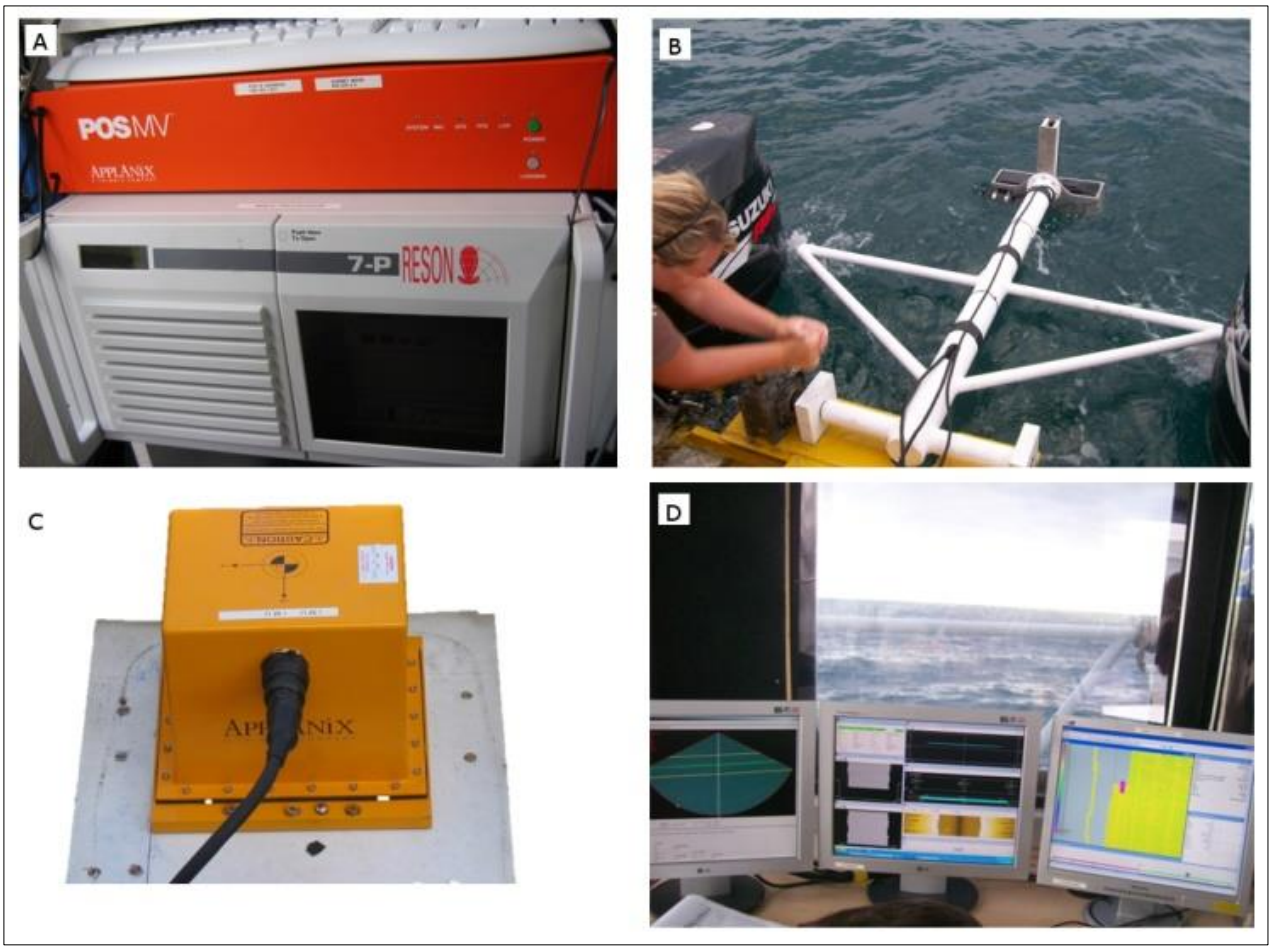

Figure 21: A. Reson 7-P and POS MV processor units, B. Multibeam sonar head being deployed, C. POS MV motion reference unit, D Multibeam RAW display on the left with acquisition and navigation displays centre and right.

3.1.3 POS MV

For accurate measurements of position, heading and motion the MBES system was interfaced with an Applanix POS MV 320 motion reference unit (MRU) with L1/L2 RTK capability (Figure 21). As an integrated GPS/inertial reference system, the POS MV outputs all motion variables at high rates of up to 200 Hz even in the presence of GPS dropouts or degraded differential GPS corrections. These data output variables include RTK positioning and elevation, velocity, 3D attitude (roll, pitch and true heading), heave (and true heave), acceleration vectors and angular rate vectors. This high-specification system is the highest precision motion reference unit for use with MBES systems.

3.1.4 Multibeam data collection

High-resolution multibeam bathymetry data were collected during three separate campaigns for the project. Data were collected during February 2012 and then again during July and September of 2014 (Table 2). Data were collected using the MGU and Marine Data Consultants' (MDC) Reson 7125, mounted on the survey vessel *Geo Manzi*, using Qinsy data acquisition software. Motion and position was supplied by interfacing a POS MV to the 7125 and using a C-NAV 3050 as auxiliary GPS. Tidal data were supplied by the SA NAVY Hydrographic Office from their tide gauge located in Cape Town harbour.

Campaign	Date	Number of days
1st	February 2012	3
2nd	July 2014	5
3rd	September 2014	5

Table 2: Multibeam survey operations.

At the start of each survey campaign a 'patch test' was conducted to calibrate the vessel and multibeam transducer offsets. The patch test corrects for pitch, heading and yaw. This had to be redone each time the equipment configuration was changed or if the equipment was removed from the vessel between surveys. At the start of each day a sound velocity cast was done using the Digibar SVP. These data were downloaded and imported into Qinsy data acquisition software, where it was used to steer the beams. The survey was conducted in order to achieve full bottom coverage. The completed coverage is shown in Figure 22.

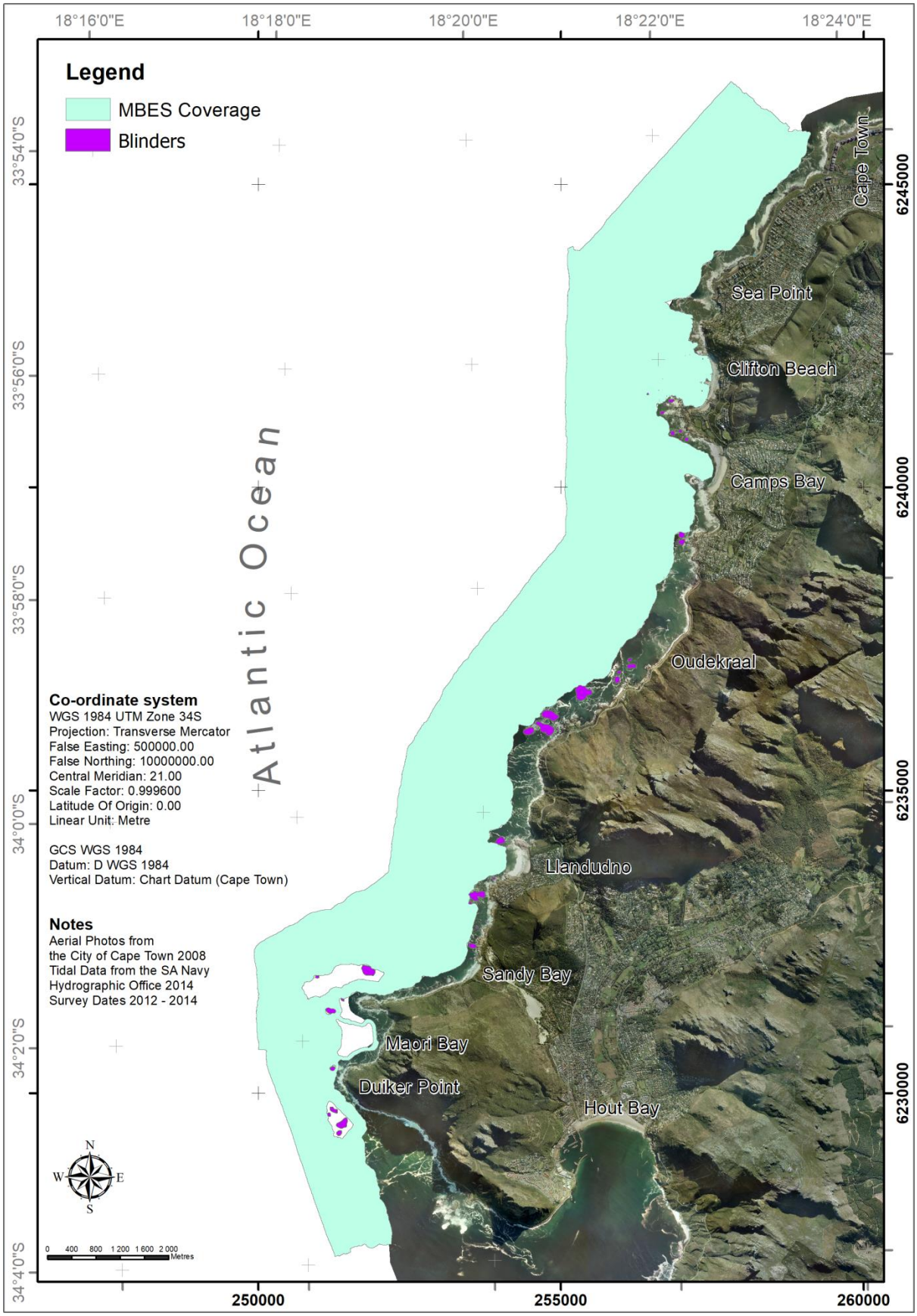

Figure 22: Multibeam coverage for the Atlantic Seaboard, data collected between 2012 and 2014.

3.1.5 Tidal corrections

To collect multibeam bathymetry data without the use of RTK positioning, the use of supplementary tide data were required to reduce elevations to an acceptable datum (International Hydrographic Organization, 2005). Tidal information for February 2012 were obtained from predicted tides, generated by the South African Navy Hydrographic Office (SANHO) (Figure 23). Tidal data for 2014 were recorded data, obtained the SANHO tide Gauge located in Granger Bay (-33.9 S; 19.417 E) Data for July 2014 is shown in Figure 24.

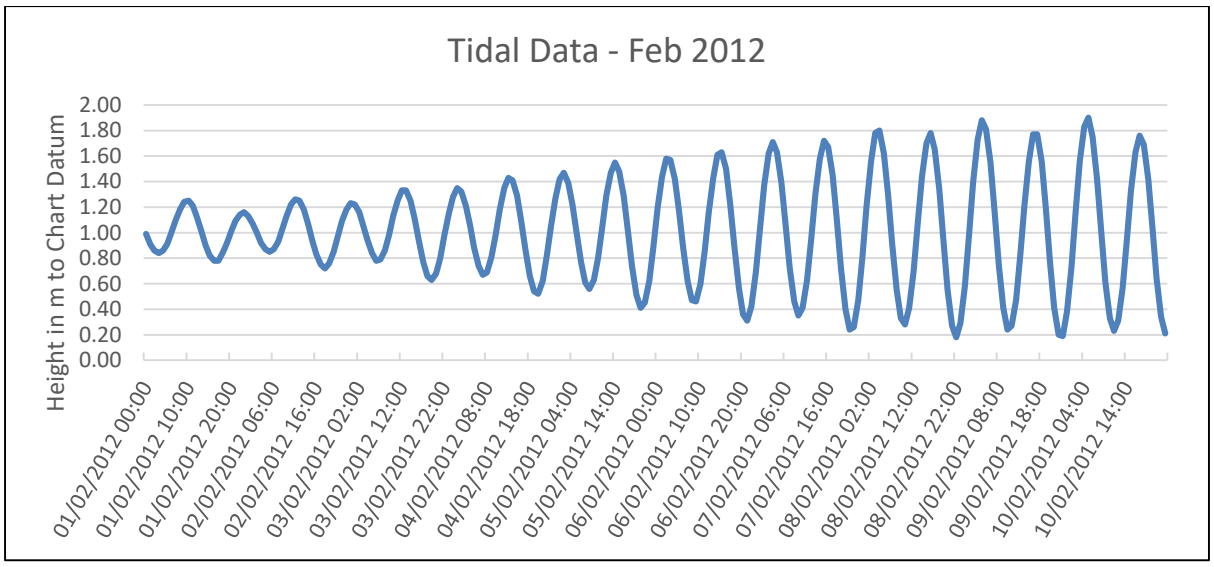

Figure 23: Predicted tidal data for 1st to 10th February 2012 for Granger Bay, supplied by SANHO.

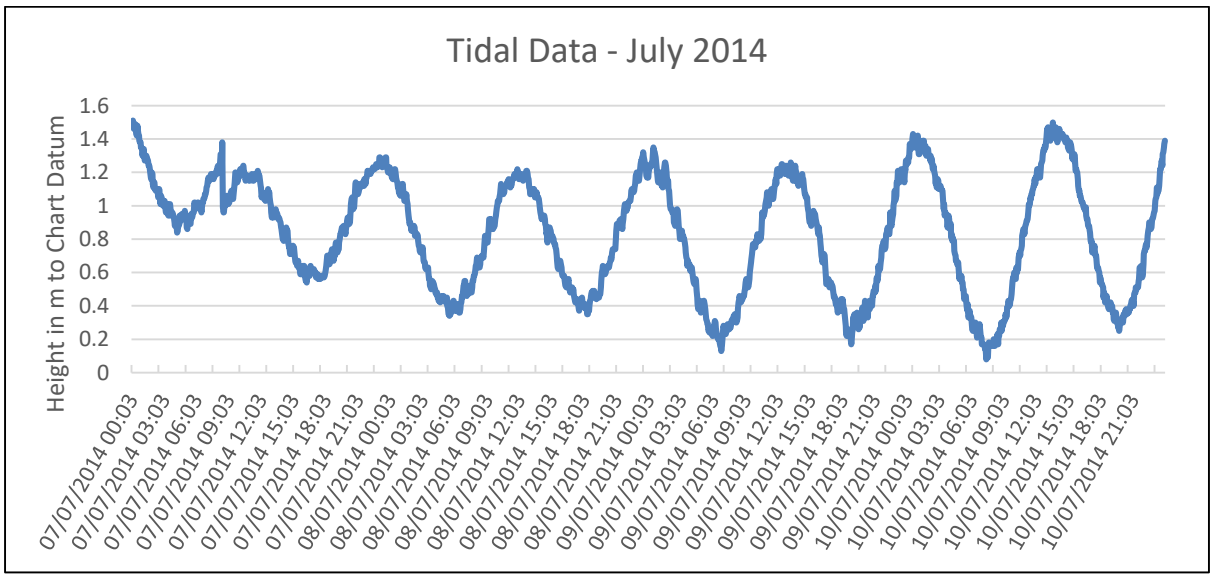

Figure 24: Recorded tidal data for 7th to 10th July 2014 from the Granger Bay tide gauge, supplied by SANHO.

3.2 Seafloor Facies

3.2.1 Operating principles of side scan sonars

Side scan sonar has traditionally been used to map the extent of sediment distribution (Klein, 1982). More recently the use of multibeam bathymetry data, including backscatter mosaics derived from the multibeam data have also become more widespread (Parkinson, 2001). Until the development of MBES systems, side scan sonar was the only acoustic system that could provide full bottom coverage and was the preferred method for surficial seabed mapping (Blondel and Murton, 1997). Side scan sonar transducers are typically mounted on either side of a towed vehicle or fish (Figure 25). In some instances, the transducers can also be mounted on a survey vessel, Remotely Operated Vehicle (ROV) or Autonomously Operated Vehicle (AUV). From the transducers the side scan sonar emits a thin, fan shaped pulse perpendicular to the direction of travel. The receiver "listens" for the returning backscatter that is reflected back from the seafloor and records it for an extended period of time to create a detailed image of the seafloor. The reflectivity of the seafloor depends on the texture or hardness of the seafloor material. Softer fine grained material has a low reflectivity, while coarser harder material has a high reflectivity (Penrose et al., 2005).

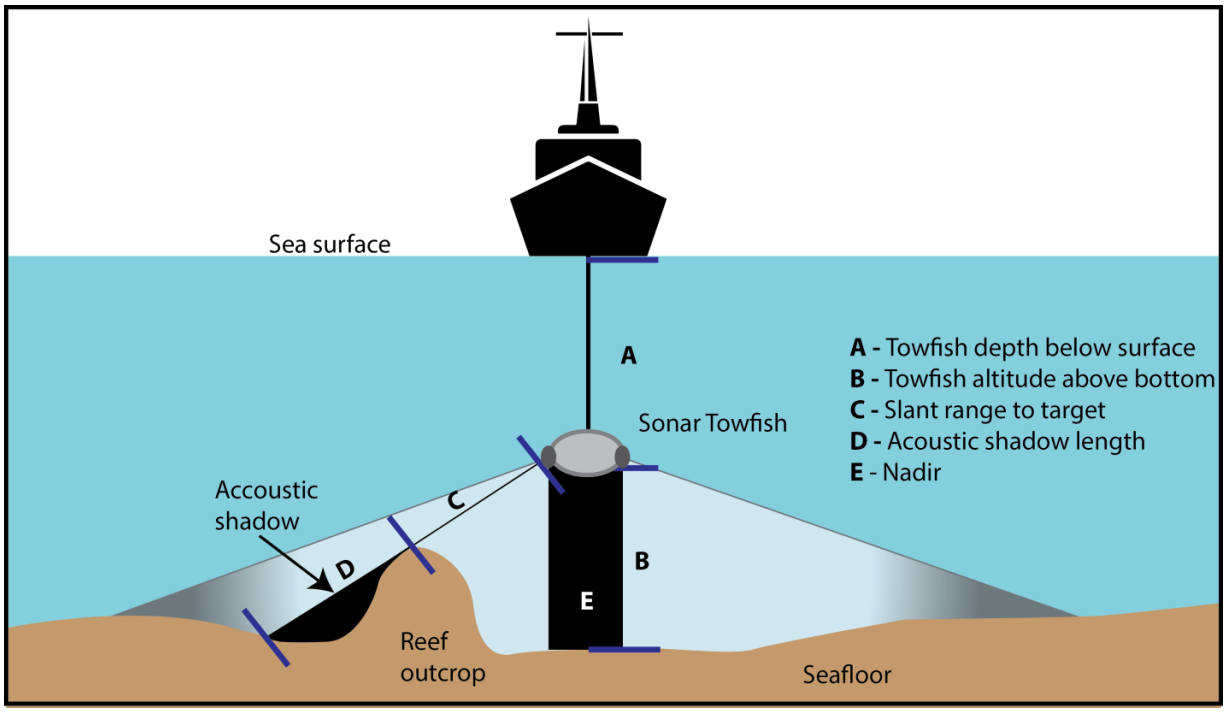

Figure 25: Side scan sonar operating principles (modified from Blondel and Blondel, 2009).

To correctly understand side scan sonar imagery one needs to understand side scan sonar geometry. Typically the towfish is towed at an elevation above the seafloor that is equal to ~10% of the scan range (Parkinson, 2001). The tow fish uses dual channels to be able to scan on both sides of the fish. The tow fish geometry can also be explained as follows: the transmitted pulse produces a black line at the start of the display for each channel. Next there will be a period of time when the sonar pulse is moving through the water column and not returning any echoes (Mazel, 1985) This is displayed as a black area below the fish. The first return should be that of the seafloor and then targets spanning the scan range of the sonar (as the pulse moves outwards). The distances seen on the record are in fact slant ranges and not true distances, although the true distance can be easily calculated (Figure 25).

3.2.2 Klein 3000 side scan sonar

A Klein System 3000 digital side scan sonar (Figure 26) was used to collect the acoustic seafloor data during the project. This is a dual frequency (100/500 kHz) digital side scan sonar system. The system comprises a Transceiver Processor Unit (TPU), a laptop operating Klein SonarPro software for data acquisition, and a towfish. In addition to the two side facing dual frequency transducers, the towfish contains depth, heading, roll and pitch sensors.

Figure 26: Klein System 3000 digital towfish (top), Klein 3000 TPU (bottom) and acquisition PC with SonarPro (right).

3.2.3 Side scan sonar data acquisition

Side scan sonar data were collected for a reef habitat mapping project for the South African Environmental Observation Network (SAEON) during two survey campaigns (Table 3) in 2010 (Van Zyl, 2010). These were collected from the survey vessel *Geo Manzi*, with the side scan sonar tow fish towed behind the vessel using a kevlar soft tow cable. Positioning was obtained from a C-NAV 3050. The position of the tow fish was calculated with the acquisition software by means of a layback calculation, using cable length and tow fish depth. A scan range of 75 m was used with a line spacing of 130 m, resulting in data overlap of 13%. Navigation was setup in Hypack while side scan sonar data were collected in .sdf format in SonarPro. Side scan sonar data were processed using MGU in-house NavLog software. Automatic time varied gain (TVG) was applied to all lines and bottom tracking was corrected. These data were divided into survey blocks and exported into tiles. This allowed for a high resolution (0.1 m/pixel) at a manageable size. Tiles were mosaicked and geo-referenced using ER Mapper (Van Zyl, 2010).

Campaign	Date	Number of days
1st	March 2010	1
2nd	April 2010	5

Table 3: side scan sonar operations.

3.2.4 Seafloor facies interpretation

Six different seafloor acoustic facies were identified from side scan sonar for the SAEON project. For this project the facies were modified and the “Sediment facies” were split into “Fine to medium grained sand facies” and “Bioclastic gravel facies” with “Boulder beach facies” and “Low relief facies” added, resulting in nine facies (Table 4). Example facies as seen in the raw side scan sonar data are shown in Figure 27 and Figure 28.

Seafloor Facies	Description
Prominent Reef	High relief reef with variable topography, including visible joint and fracture patterns.
Striated Reef	Low relief reef with clear bedding planes. Structural features such as folding and
Scattered Reef	High to moderate relief reef areas, interspersed with sediment, mostly a thin
Low Relief Reef	Low relief reef with no distinct bedding planes or bedform orientation.
Bioclastic Gravel	Rippled gravel, consisting mostly of shell fragments.
Fine to Medium Grained Sand	Unconsolidated sediment, consisting of quarzitic sand and up to 30% shell.
Boulder Beach	Well-rounded cobbles and boulders.
Scree	Unconsolidated, angular cobbles and boulders; generally accumulated at the
Anthropogenic Features	Man-made objects and features, such as buildings, sea walls, pipelines, shipwrecks.

Table 4: Seafloor facies used to describe the seafloor.

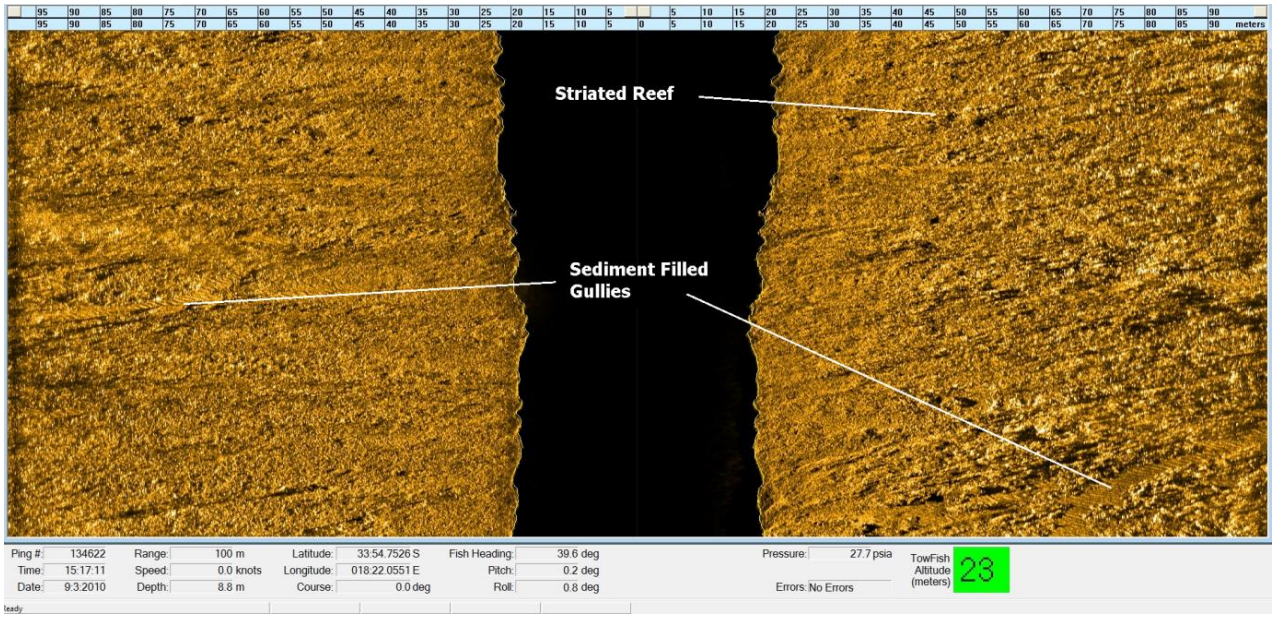

Figure 27: Example of side scan sonar data showing striated reef facies.

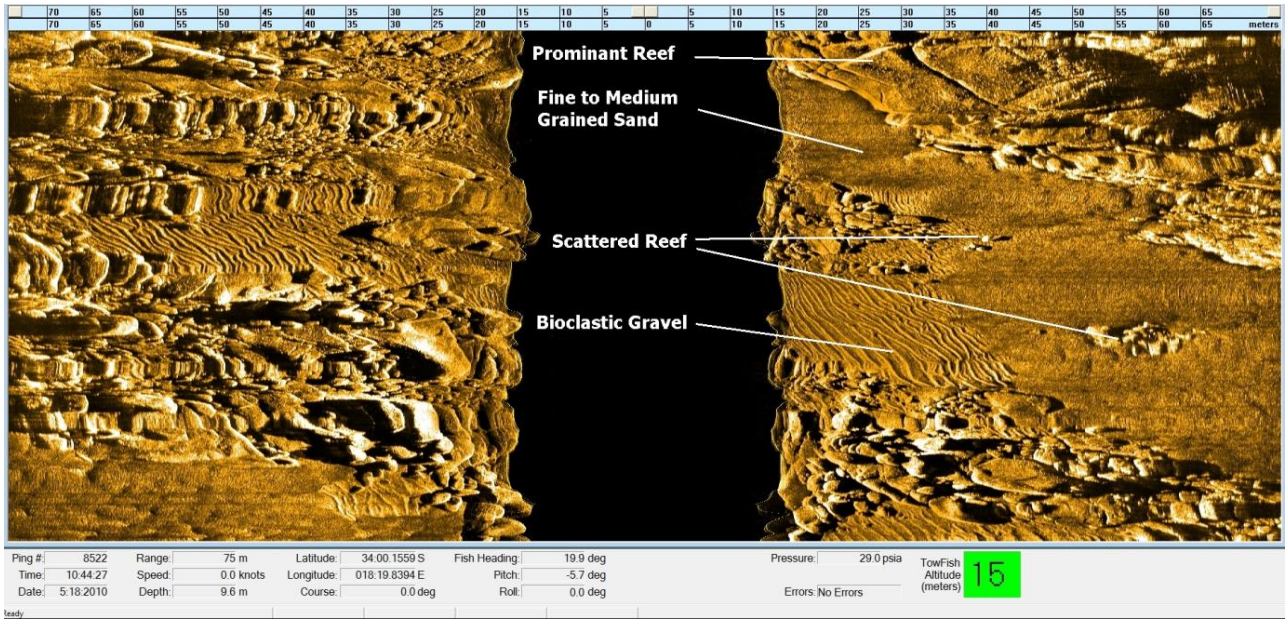

Figure 28: Example of side scan sonar data showing prominent reef, scattered reef, fine to medium grained sand and bioclastic gravel.

3.2.5 Expanding the seafloor facies interpretation

In areas with no available side scan sonar data, high resolution bathymetry data and Google Earth were used to expand the seafloor facies interpretation. The bathymetric data were especially valuable in the offshore area where the water depth was too great for the application of side scan with the available tow cable length. Most facies could be easily interpreted using these high-resolution bathymetric data (Figure 29).

Distinguishing between bioclastic gravel and fine to medium grained sand was problematic. The boundaries could easily be identified, but the facies classification was not always clearly identifiable. To overcome this, boundaries were extrapolated from the side scan sonar coverage, and the facies were interpreted according to known adjacent facies and by extending the known side scan sonar interpretation into the bathymetry only areas.

On the inshore where no side scan sonar or multibeam data were available historical Google Earth images were used to digitize areas of sediment (Figure 30). Images with clear visibility can be found by looking through the historical images. The presence of high relief reef could be identified in most areas where it was present. Distinguishing between bioclastic gravel and fine to medium grained sand facies were subject to the same difficulty than using the

multibeam data, and required interpreting sediment sampling data and making educated guesses in other areas.

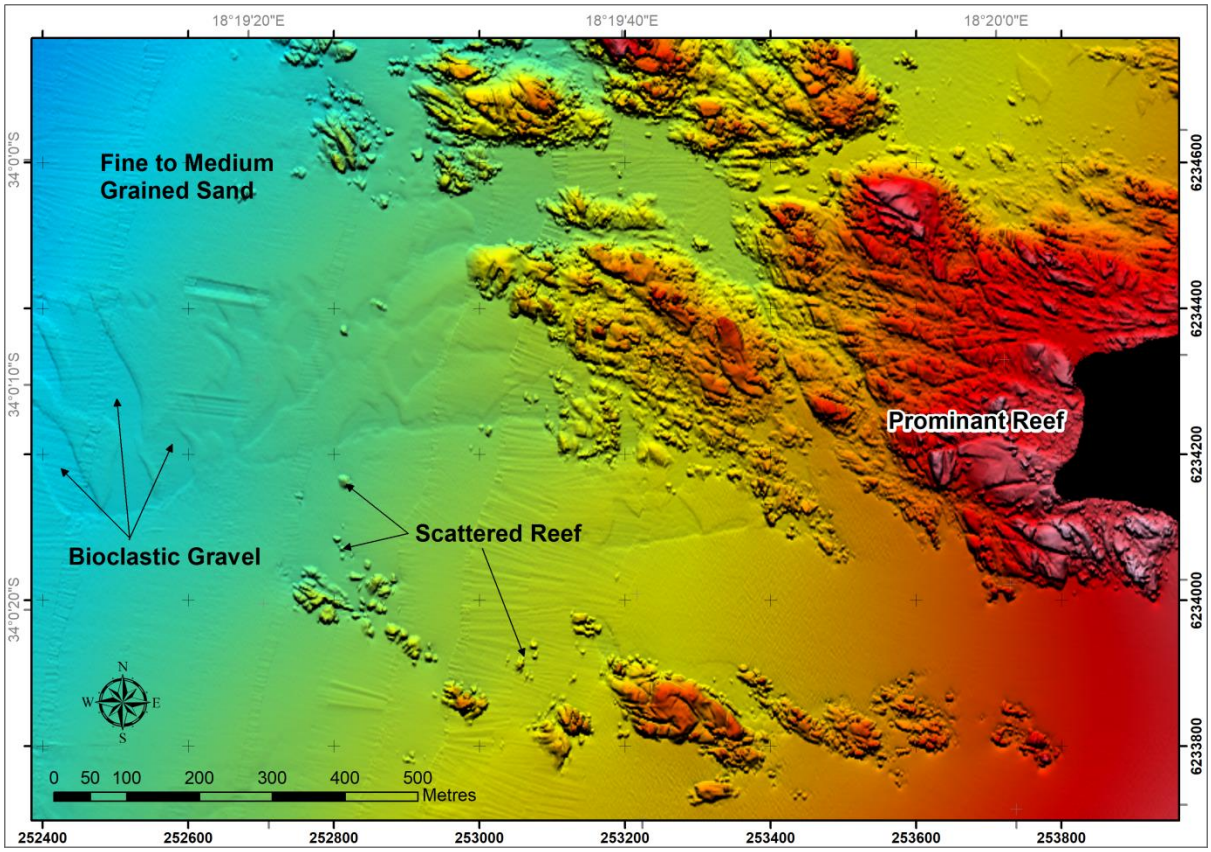

Figure 29: Multibeam bathymetry data with examples of prominent reef, scattered reef (Granite), bioclastic gravel and fine to medium grain sand facies.

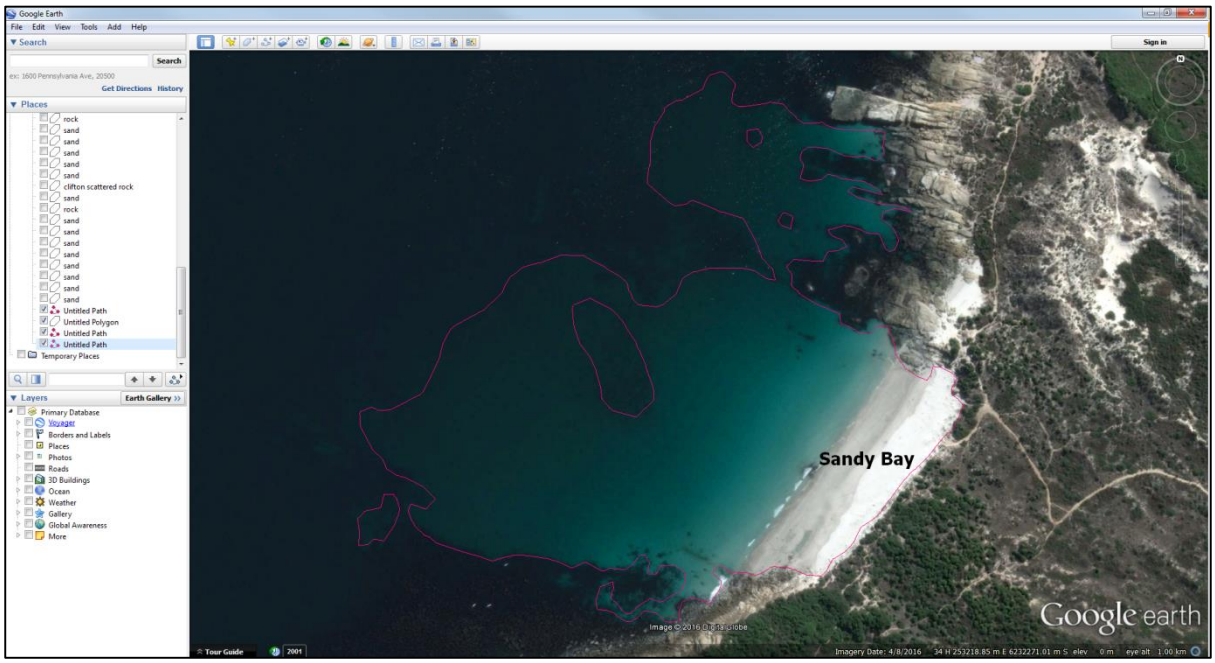

Figure 30: Digitising sediment areas and beaches in Google Earth.

3.2.6 Coastal mapping

The coast was mapped utilising a combination of field observations, Google Earth and existing geological mapping (Von Veh, 1983). The mapped area included exposed rock and beach sediments which extended from the vegetation- or building line across the shore face into shallow water where exposed reef and sediment could be identified off aerial photographs and historical Google Earth images. Exposed offshore 'blinders' or reef, which breaks the water surface and could not be mapped with side scan sonar and MBES data, were included. The coastal mapping extended the offshore facies and geological map onto the shore and it was possible to map between 100 and 200 m of coast into the nearshore area. Some areas where there was no clearly visible reef, sediment had to be inferred to close the gap between the offshore survey data and the shoreline. With the assistance of some shoreline observations, the seafloor facies could be identified from the Google Earth and aerial images. Prominent reef and scree could easily be identified while scattered reef was more problematic. As with the MBES data, sediment could not easily be separated into fine to medium grained sand or bioclastic gravel. In these areas interpretation from the side scan sonar were extrapolated into the coastal mapping areas.

3.3 Marine Magnetics

3.3.1 Operating principles of marine magnetometers

A magnetometer is used to measure magnetic flux density and can therefore detect changes in Earth's magnetic field (Hrvoic, 2007). Dynamic anomalies are due to activity in Earth's molten core, solar flares and storms from space. Static anomalies are caused by magnetic material in Earth's crust or man-made objects.

3.3.2 Seaspy magnetometer

The magnetometer used for the survey is a Marine Magnetics SeaSpy magnetometer (Figure 31). The SeaSpy is a high-sensitivity, total field magnetometer which contains an Overhauser sensor. The sensitivity of the SeaSpy is 0.01 nT (nano Tesla) with a resolution of 0.001 nT. It has no "dead zone" and is unaffected by heading offsets and ambient temperature.

Figure 31: Marine Magnetics SeaSpy magnetometer.

3.3.3 Marine magnetic data collection

Marine magnetic data were collected to supplement the seabed mapping. Due to the large extent of the survey area, data were collected over 4 separate days when weather permitted (Figure 32). Using the survey vessel *Tethys*, data were collected from Granger Bay on 5 November and 16 November and from Hout Bay on 13 February and 5 March (Table 5). Coast-parallel lines were planned with 250 m line spacing. The coast parallel lines increased the survey efficiency of the project and also ensured that dykes with their expected N-E orientation would be perpendicular to the survey lines. The magnetometer was towed 30 m behind the survey vessel, which is more than the minimum of 3 times the length of the vessel to prevent magnetic interference. Data were collected at a sampling frequency of 1 Hz. Data were recorded using Marine Magnetics propriety software SeaLink, with navigation supplied by Hypack and a CSI wireless dGPS.

Campaign	Date	Number of days
1st	5 November 2012	1
2nd	16 November 2012	1
3rd	13 February 2013	1
4th	5 March 2013	1

Table 5: Magnetometer survey operations.

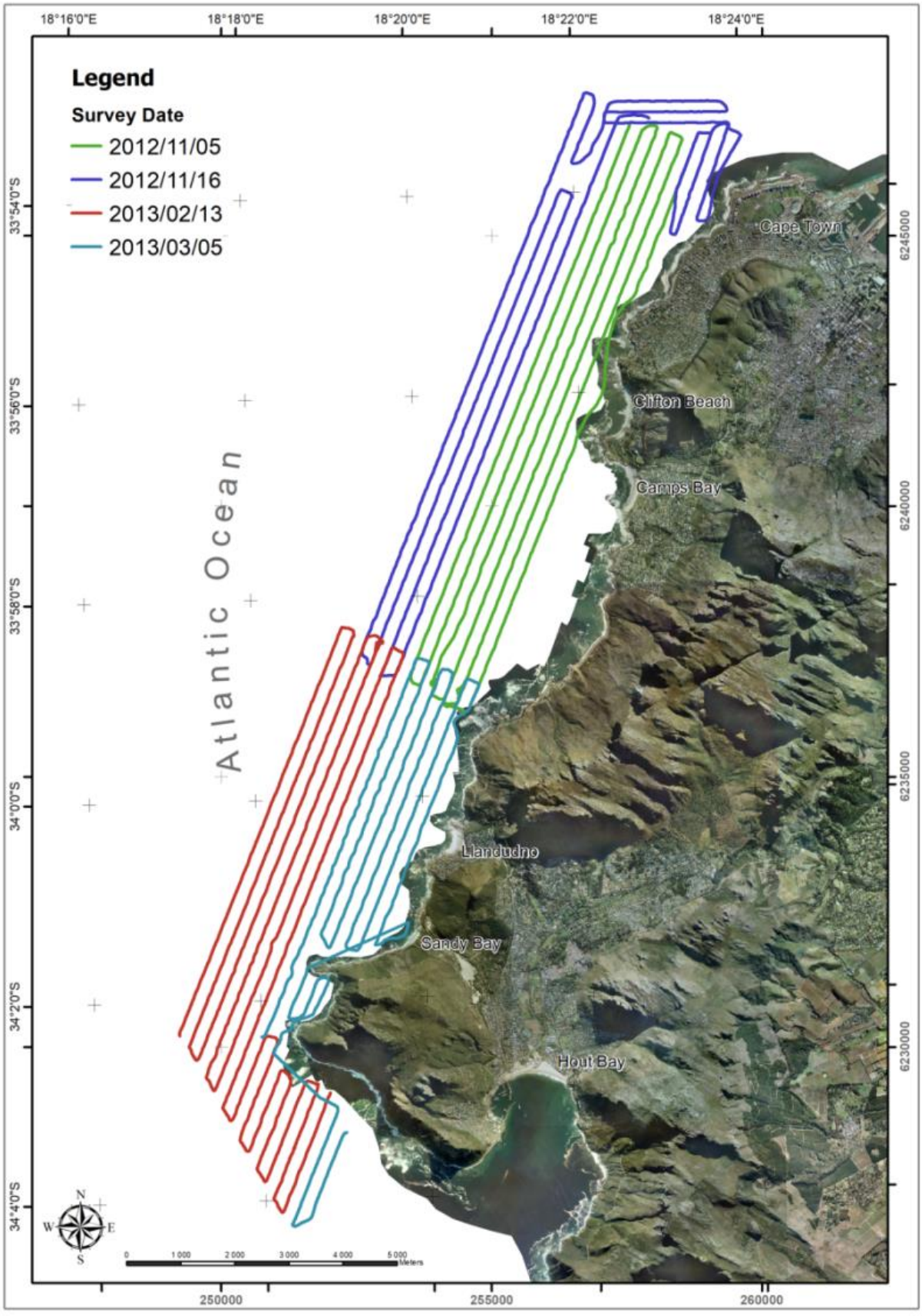

Figure 32: Track chart of magnetic data collected between 2012 and 2013.

3.3.4 Marine magnetic processing

Magnetic data are recorded as Total Field Intensity measured in nT. Processing of magnetometer data involved several corrections to be applied. The first step is to remove any diurnal variations from these data. This will remove changes due to sunspot activity and normalise surveys conducted over several days. The diurnal variations are removed by applying corrections recorded from a base station setup in a magnetically quiet area. For this survey data were supplied by the South African National Space Agency (SANSA) from the Hermanus Magnetic Observatory (Gouws et al., 2011). Diurnal data obtained for the survey is shown in Figure 33. This allows for the combination of data sets collected during different surveys and differing ambient magnetic levels.

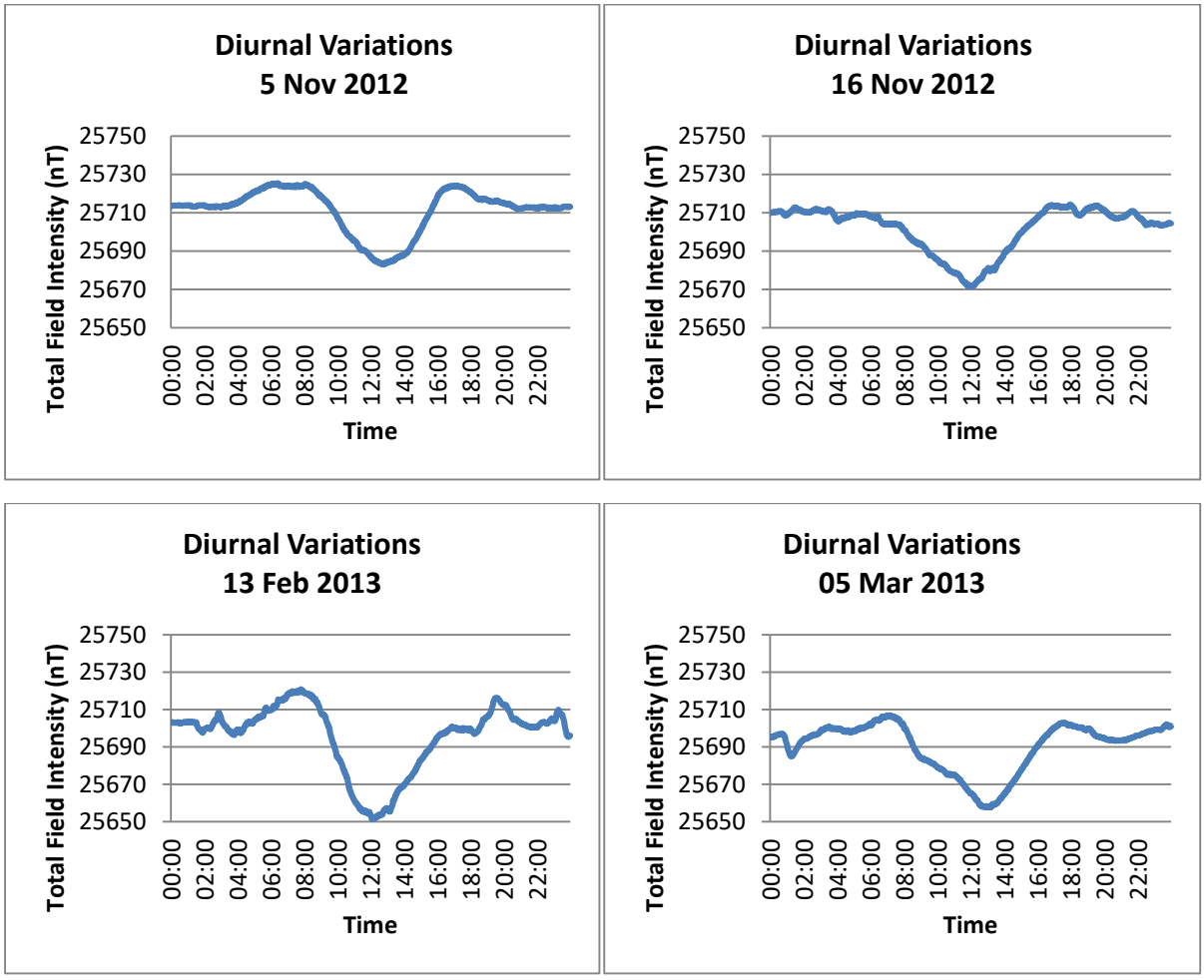

Figure 33: Diurnal variation data received from SANSA at the Hermanus Magnetic Observatory for each survey date.

The magnetic field of the earth is constantly changing (Hrvoic, 2007). To correct for this change in the earth's magnetic field the International Geomagnetic Reference Field (IGRF) is applied to these data (Figure 34). The IGRF is a mathematical description of the earth's main magnetic field and is updated and maintained by the International Association of Geomagnetism and Aeronomy (IAGA).

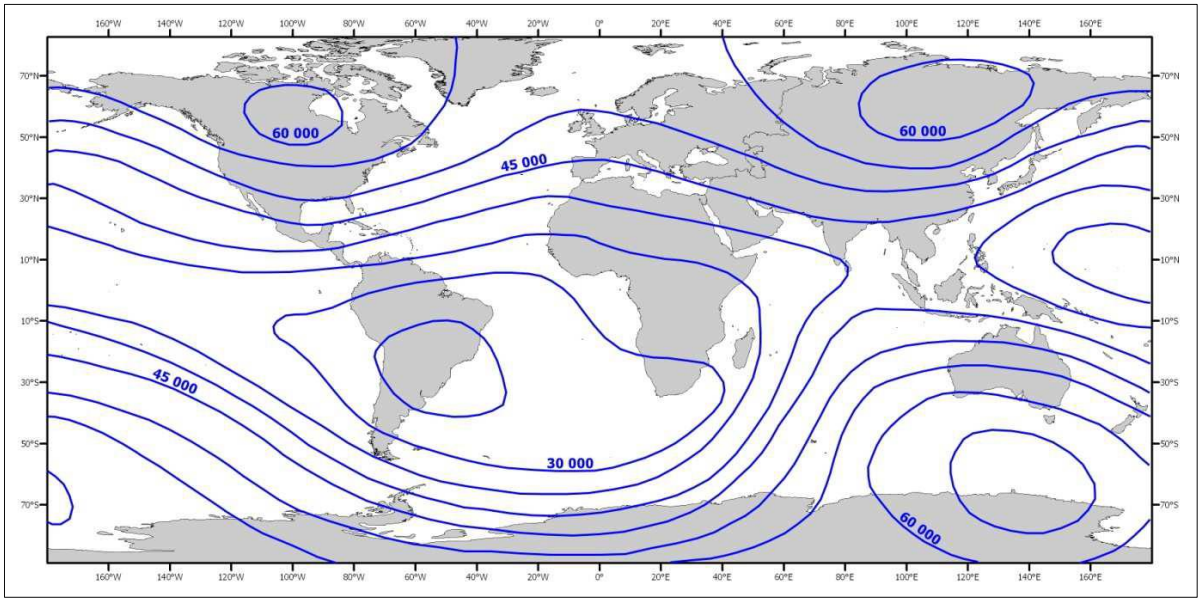

Figure 34: Contour map of the total magnetic field intensity over the surface of the Earth, as of 1995 (contour interval is 5 000 nT), (modified from Hrvoic, 2007).

Once the magnetic data have been processed, magnetic anomalies or lineations were identified. To assist with the identifying the source of the magnetic anomalies their location was compared to mapped onshore geological features (Theron, 1984) and marine magnetic data by previous authors (Day, 1986; Reid et al., 1991; Backeberg et al., 2011; MacHutchon, 2013). The magnetic lineations identified as geological features were digitised and later adjusted to correlate with the bathymetry and side scan sonar data.

3.4 Sub-bottom Profiling

3.4.1 Operating principles of seismic systems

In seismic surveys, sound waves are generated using a sound source which is towed or mounted on a vessel. These sound waves are sent through the water column and into the seafloor, where some of the energy is reflected by layers of different competence

(International Assosiation of Oil and Gas Producers, 2011). The returning sound is recorded by means of hydrophones as an electrical signal which can be processed and displayed digitally as two-way travel time measured in milliseconds. The strength of the returning signal which travels as a pressure wave through the water column depends on the several factors such as the energy of the source, the water depth, the velocity of sound in the water and the seafloor and the competence of the different lithological layers from which the signal is being reflected (Parkinson, 2001). Seismic data can be used to draw cross sections of the sub-bottom strata to give a better understanding of the geology. When acquiring seismic lines in a tightly spaced grid the volumes of the different lithologies can be calculated. This will be useful in determining the amount of unconsolidated sediment in the study area. Although there are numerous types of sub-bottom profilers available, this study used a boomer seismic instrument, which was selected according to its depths of penetration and ability to resolve relatively shallow deposits on the continental shelf.

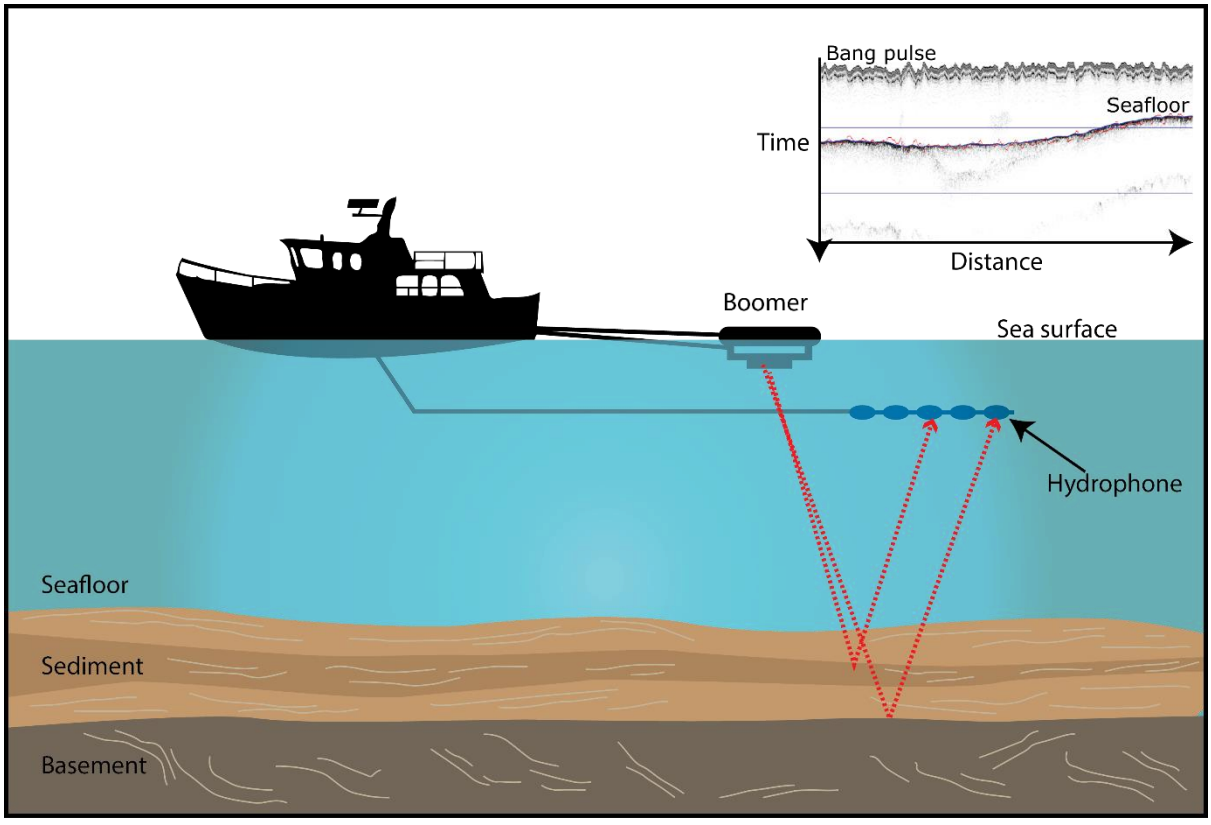

Figure 35: Towed boomer seismic array (modified from Stoker et. al, 1997).

3.4.2 CSP1000

The first Boomer survey was conducted using an Applied Acoustic Engineering CSP1000 power supply that produces a maximum energy output of 1 000 J/s and a Design Projects high frequency 500 J boomer plate as a sound source. The boomer plate is mounted on a catamaran float which is towed behind the survey vessel.

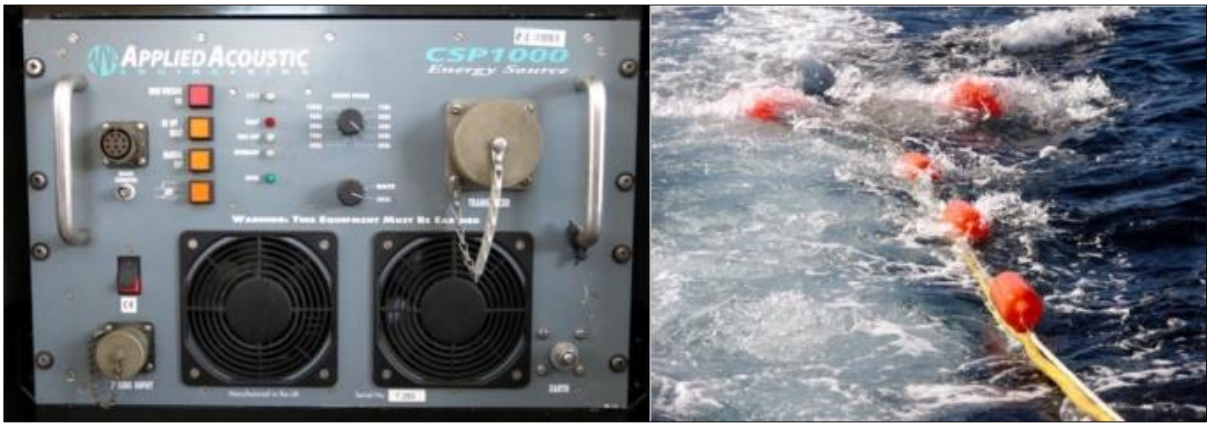

Figure 36: Applied Acoustics CSP1000 power supply with 500J plate in tow behind the survey vessel on the right.

3.4.3 CSP –P

The second seismic survey was conducted using a system which consists of an Applied Acoustics CSP-P power supply, with a max output of 350 Joules and a 200 J boomer plate, also by Applied Acoustics. The CSP-P has a lower power output, but benefits from a clearer crisper sound source, resulting in a more detailed cleaner image.

Figure 37: Applied Acoustics CSP-P Boomer power supply with 200J plate on the right.

3.4.4 Hydrophone

A hydrophone is device used to record soundwaves underwater. They are passive devices and only listen for sounds and do not transmit any sound. The analogue sound signal is converted into a voltage range which then needs to be sent to an analogue to digital converter (Parkinson, 2001). This project used an eight element Design Projects hydrophone array. The hydrophone is connected to a Geo Acoustics pre-amp to boost the signal strength before connecting it to the Octopus 760D via a BNC cable for data recording.

3.4.5 Coda Octopus 760D

Seismic data were recorded on an Octopus 760D analogue to digital processor. It is used for real-time processing, digital recording and as a post-processing workstation. On-board processing facilities include swell filtering, stacking, water column blanking, time varied band pass filtering, time varied gain, and automatic bottom tracking. These data are digitally stored in seg-y format. The Octopus is responsible for the triggering of the seismic system.

Figure 38: Coda Octopus 760D seismic acquisition system.

3.4.6 Seismic data collection

Two seismic surveys were conducted during 2014 (Table 6). The first seismic survey was a regional boomer line, conducted on the 30th July 2014 and consisted of two long traverse lines to 15 nm offshore.

Campaign	Date	Number of days
Regional Transect	30 July 2014	1
Inshore Grid	24 April 2015	1

Table 6: Seismic survey operations.

The MGU CSP 1000 boomer was use for this survey conducted from the survey vessel Geo Manzi. The plate was fired at 500 J with a trigger interval of 600 ms and a sweep length of 600 ms. The vertical resolution of this system is close to 1 m. Line 1 started close inshore near Sandy Bay and headed directly offshore for 15 nm, which is the operational limit of the survey vessel. The return line 2 was cut short due to worsening weather conditions (Figure 39).

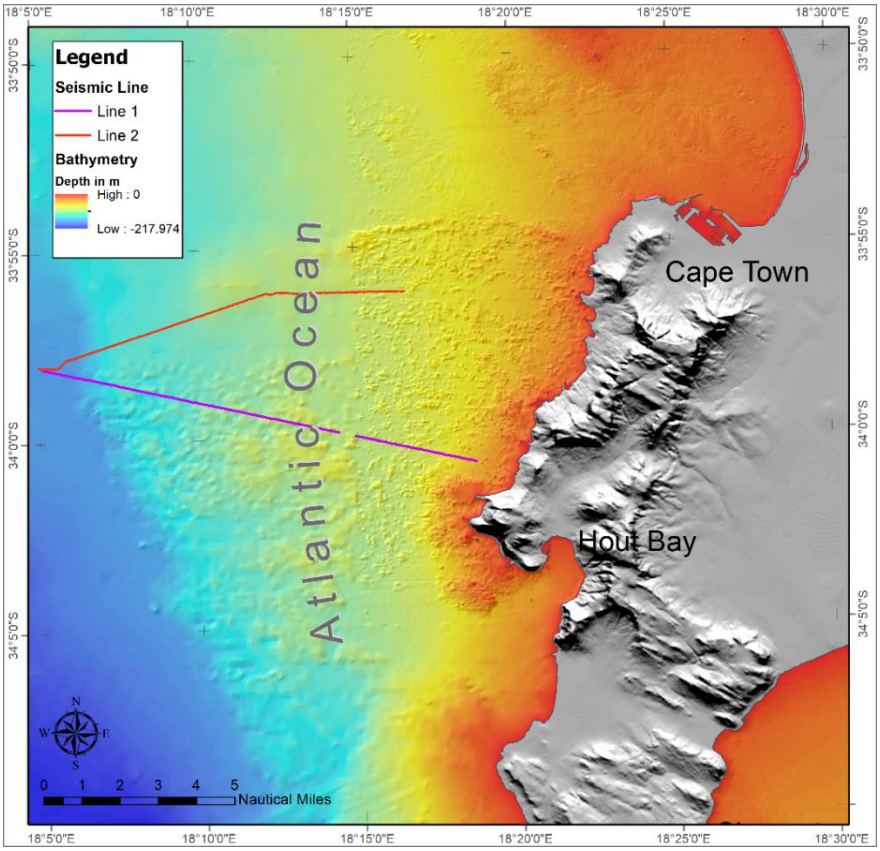

Figure 39: Regional boomer transect, extending to 15 nautical miles offshore of Sandy Bay, with a return line towards Cape Town.

The second seismic survey was an inshore survey, conducted using the MGU CSP-P boomer. The plate was fired at 200 J with a trigger interval of 500 ms and a sweep length of 400 ms. This system has a vertical resolution slightly better than 1 m. The survey was conducted from the survey vessel *Geo Manzi* in the Sandy Bay area. Lines were spaced approximately 200 m apart and planned offshore of Sandy Bay and Llandudno in areas of sediment mapped from side scan sonar and MBES data (Figure 40).

In both surveys navigation was supplied through Hypack using a C-NAV 3050 GNSS receiver. Data were collected using the Octopus 760D at a sampling frequency of 24 kHz. The boomer plate and hydrophone were towed 20 m behind the vessel on either side of the outboard motors. The swash zone created by the motors creates a blanking effect directly between the boomer plate and the hydrophone, reducing size of the initial bang pulse.

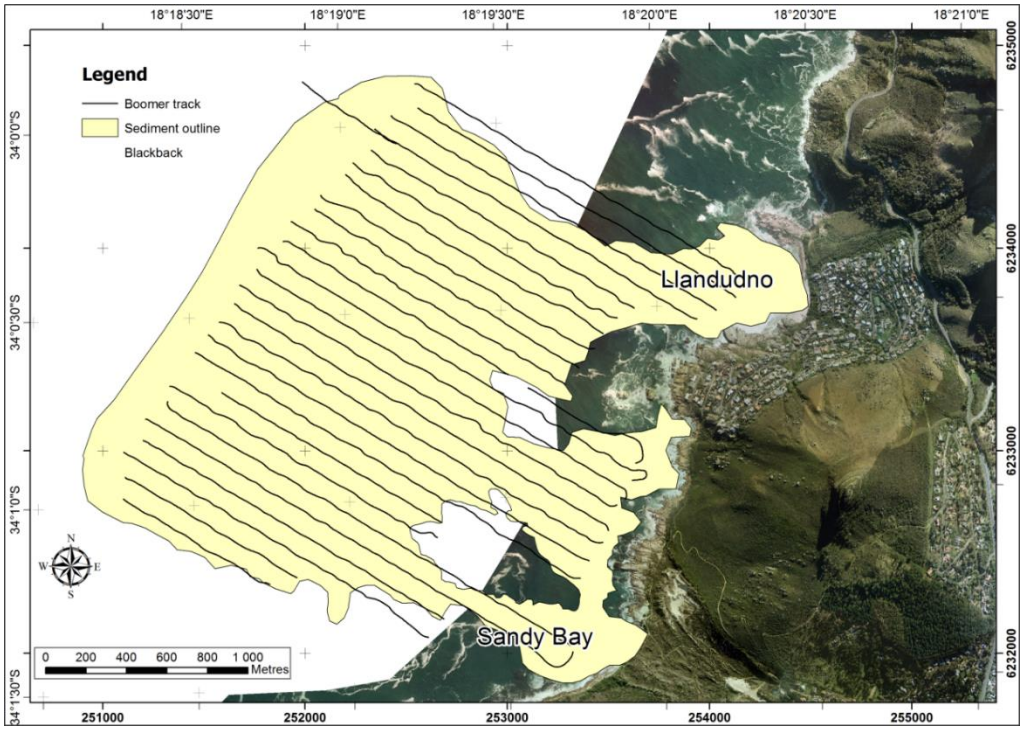

Figure 40: Sandy Bay boomer survey track chart of the inshore grid, data collected during 2015.

The seismic data were processed in the seismic component of NavLog processing software. The software was used to correct the layback, do bottom tracking and pick the different sediment horizons. A band pass filter was applied with a low cut off of 500 Hz and a high cut off of 2000 Hz. This removed most of the low frequency noise in the record.

3.5 Beach Profiling

3.5.1 Carlson Surveyor+

The Carlson Surveyor+ is a rugged dual frequency GNSS RTK receiver and field controller. The receiver is GPS and GLONASS enabled. RTK precision can be achieved by connecting to the NTRIP network over the internet or by connecting to an RTK base station via radio modem. RTK precision for the Carlson+ is 1 cm ± 2 ppm in the horizontal and 2 cm ± 2 ppm in the vertical. The device can be used for precise position and height measurements. The field controller is preloaded with SurvCE data collection software for navigation and data collection.

Figure 41: Carlson Surveyor+ controller with external antenna and di-pole GSM antenna for better mobile reception (Top), Carlson surveyor+ setup in a backpack ready for beach profiling (right).

3.5.2 Beach profile data collection

Beach profiling was conducted on Camps Bay beach, Sandy Bay beach and the Karbonkelberg sediment bypass between Hout Bay and Sandy Bay. The surveys were conducted at the end of winter (August) at the start of summer (October/November) and towards the end of summer (January/February) (Table 7). The profiling was carried out using a Carlson surveyor+ RTK GPS. Data were collected with the GPS antenna mounted on a back pack. The height of the antenna above ground is measured and entered into the handheld controller. At Sandy Bay and Camps Bay there was sufficient mobile reception to receive RTK corrections from the NTRIP network over the mobile internet connection built into the

Carlson controller. On the sand bypass dune there were some areas with no mobile reception. For this survey the C-NAV 3050 was setup near the dune as an RTK base station. The RTK corrections were received from the base station via radio modems. The Carlson Surveyor+ was set to record data points containing position and elevation continuously every metre while walking transects across the beach at 20 m intervals. These transects extended from the top of the beach where the vegetation started to waist deep into the surf zone. Several coast parallel lines were walked on the beach surveys to act as tie lines. Survey dates were selected close to spring low tide to maximize the exposed beach which could be surveyed. Several coast parallel lines were walked to increase data density and serve as tie lines. The survey data were exported from the Carlson as a text file and gridded with Surfer using the Kriging algorithm.

Campaign	Date	Season	Beaches
1st	August 2013	End of winter	Camps Bay Sandy Bay Hout Bay Dune
2nd	November 2013	End of spring	Camps Bay Sandy Bay Hout Bay Dune
3rd	January 2013	End of Summer	Camps Bay Sandy Bay

Table 7: Beach profiling dates.

The first topographic survey conducted on the Karbonkelberg sediment bypass or dune was conducted on 23rd August 2013, a few days after the City of Cape Town started transporting sand to the dune. To avoid the artificial transport of sand influencing the results, the first survey only included 2 transects on the slip face of the dune, this area did not show any disturbance by sand dumping at the time. Unfortunately, bulldozers where already flattening sand dumped by trucks towards the Hout Bay side and thus, this side could not be surveyed. On the 3rd of December 2013 just more than a month after the artificial sand transport was completed, another survey was conducted. This survey included a grid of the slip face, the ridge and the rise on the Hout Bay side.

3.6 Sediment Sampling

A total of 236 sediment samples were collected during several campaigns between 2010 and 2014 offshore of Camps Bay and Clifton beach, Sandy Bay beach and some offshore dive sites in the survey area. Beach samples were collected on the beach at Sandy Bay, Camps Bay, Bakhoven beach, the Karbonkelberg sediment bypass and the road and beach in Hout Bay. The offshore samples were collected using a small Van Veen grab deployed from the surey vessel *Tethys*. Sample sites were planned in areas draped by sediment. Onshore samples were collected on the back beach, beach berm and swash zone in several profiles along each beach. Samples on the sediment bypass were taken in two profiles down the face of the dune. Navigation and sample target sites were loaded into Hypack with positioning provided by a CSI Wireless DGPS. Samples were collected by hand in 250 ml jars and plastic sample bags, each sample marked with sample number and collection time. The sample time was later reconciled with the Hypack target file to get the position of each sample. Positions of beach samples were recorded using the Carlson controller or handheld GPS, depending on what was available. Ten samples were collected by scuba divers. Position of these samples was recorded using a GPS in a float, towed by the diver. The position and depth were calculated by reconciling the diver's dive computer time with the GPS time and position. The Van Veen Grab sampler was subject to some fine sediment loss (Figure 42). The loss might influence the grain size distribution to some degree.

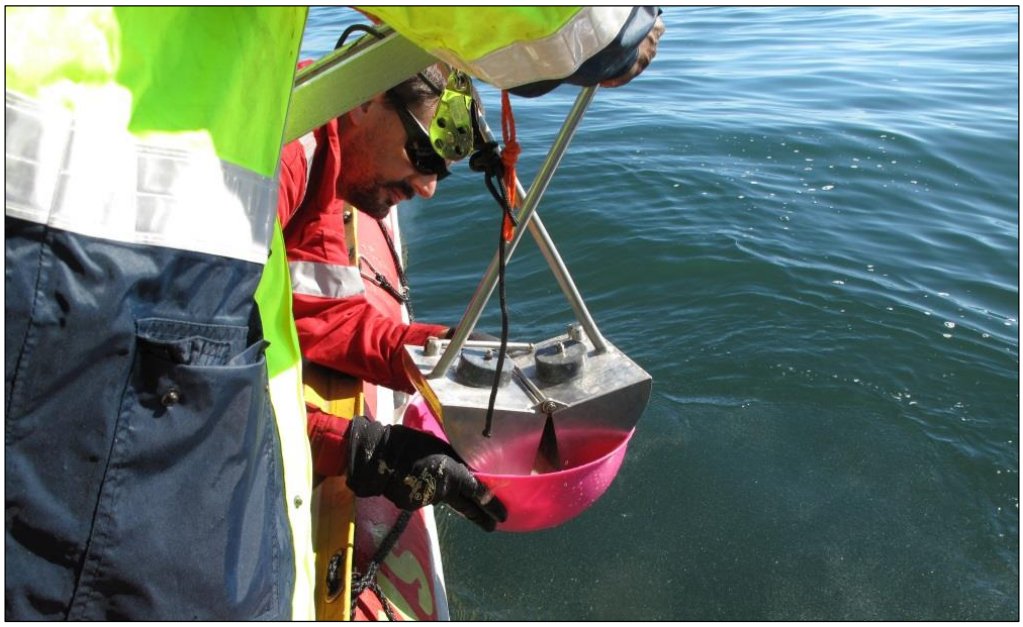

Figure 42: Sediment sample in the process of being collected by grab sampler from Tethys.

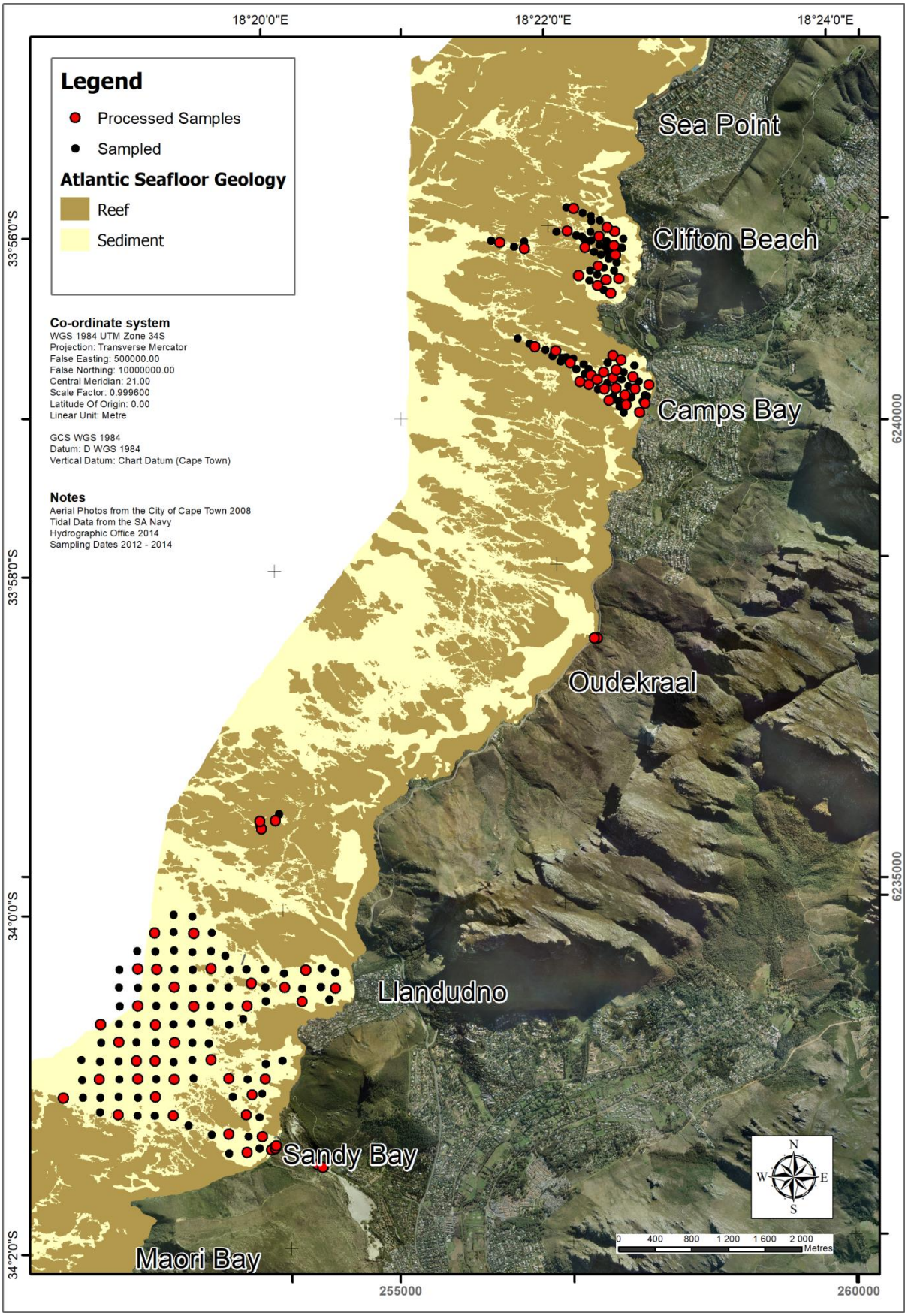

Figure 43: Sediment samples collected and processed from the Atlantic Seaboard, processing results are presented in Appendix A.

3.7 Sediment Analysis

Sediment analysis was performed on a subset of the samples collected for the project. The subset of sample points was selected using an ArcGIS extension called Hawth's Tools (Hawth's tools 2009). The extension contains a tool for randomly selecting a subset within an existing dataset by specifying the number of samples required in the subset. A selection of 71 samples was processed in the CGS sediment lab in the Western Cape office. Sediment grain size classification is done according to (Wentworth, 1922) and the major size fractions used are gravel (> 2000 µm), sand (63 – 2000 µm) and mud (< 63 µm) (Figure 44).

Millimeters (mm)		Micrometers (µm)	Phi (φ)	Wentworth size class		Rock type
	4096		-12	Boulder	Gravel	Conglomerate/Breccia
	256		-8	Cobble		
	64		-6	Pebble		
	4		-2	Granule		
	2	2000	-1	Very coarse sand	Sand	Sandstone
	1		0	Coarse sand		
1/2	0.50	500	1	Medium sand		
1/4	0.25	250	2	Fine sand		
1/8	0.125	125	3	Very fine sand		
1/16	0.0625	63	4	Coarse silt	Mud	Siltstone
1/32	0.031	31	5	Medium silt		
1/64	0.0156	15.6	6	Fine silt		
1/128	0.0078	7.8	7	Very fine silt		
1/256	0.0039	3.9	8	Clay		Claystone
	0.00006	0.06	14			

Figure 44: Grain size classification (Wentworth, 1922).

Processing followed procedures were modified from De Decker (1987) and Folk (1980). A flow diagram of the process is presented in Figure 45. The process, which was further developed in this project, started with drying of the bulk sample collected during the sampling phase.

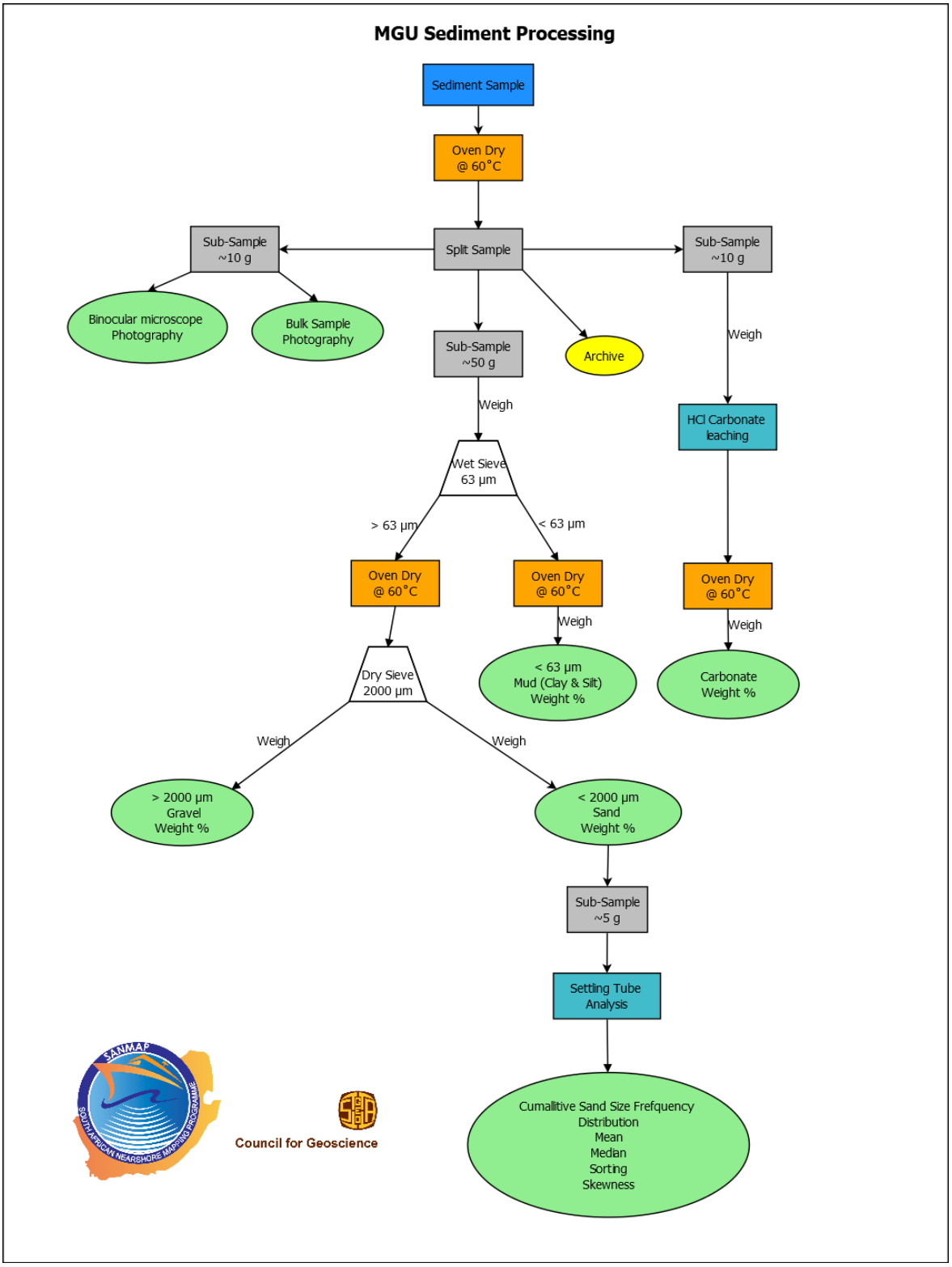

Figure 45: Sediment analysis flow diagram.

The samples were first partially dried in the sun before being placed in a drying oven in the lab. Three sub-samples were taken from the dried bulk sample for the various processes to follow. The sub-samples were split from the bulk sample using a statistical sediment splitter to get even splits from the bulk sample. The first sub-sample of 10 g was used to study under a stereo microscope. The second sub-sample where used to test for carbonate content. The third sub-sample was used for size frequency analysis.

3.7.1 Carbonate content

To calculate the carbonate shell content of a sample, the carbonate was dissolved from a sample of known weight with hydrochloric acid. The process can be explained be the following equation:

$$2HCl_{(aq)} + CaCO_{3(s)} \longrightarrow CaCl_{2(aq)} + CO_{2(g)} + H_2O_{(l)}$$

Equation 1: Calcium carbonate and hydrochloric acid reaction.

Adding hydrochloric acid (HCl) to carbonate material ($CaCO_3$) will produce a dissolved calcium chloride salt ($CaCl_2$), a gas (CO_2) which dissipates in the air and water (Equation 1). Quartz sand and other minerals in the sample do not react with the HCl and will remain behind. Once the carbonate has been removed the sample is washed, dried and weighed again and the carbonate dissolved is calculated by subtracting the remaining sediment weight from the original sample weight (Folk, 1980).

The sample was prepared by weighing about 10 g of sample into a glass beaker. Small amounts of HCl were added to the beaker. The reactions would cause the sample to foam as the CO_2 is given off. HCl was added in small amounts while stirring the sample to prevent the foam from spilling out of the beaker. To assist the process samples with a large amount of shell was crushed with a mortar and rubber pestle. Once the reaction is complete the acid and dissolved $CaCl_2$ salt is rinsed through a 63µm sieve. This process will cause some loss of fines, but it was found to be negligible compared to the $CaCl_2$ which precipitates during the drying process.

The remaining material is weighed and the percentage carbonate is calculated by subtracting the remaining weight from the original sample before the acid was added. Because same samples contained fine grained material which stuck to the beaker once dried, it was easier to weigh the empty beaker before adding the sample. The carbonate would then be calculated by subtracting the beaker weight from the remaining sample including the beaker, before subtracting this from the original sample weight.

3.7.2 Dry sieving

Samples were first split into gravel, sand and mud fractions using SABS-approved sieves. The sieves used were 2000 µm, 600 µm and 63 µm aperture sieves (Figure 46). The sieves with material were run on a shaker for 3 min. Material caught in the 2000 µm sieve was classed as gravel, material from the 600 µm and 63 µm sieves were combined to give the sand fraction. The remaining material from the bottom pan was classified as mud. The 600 µm sieve was used to split the sand fraction to reduce the chance of material from the mud fraction to be trapped in the sand fraction. Each fraction was weighed to obtain the weight percentage of gravel, sand and mud.

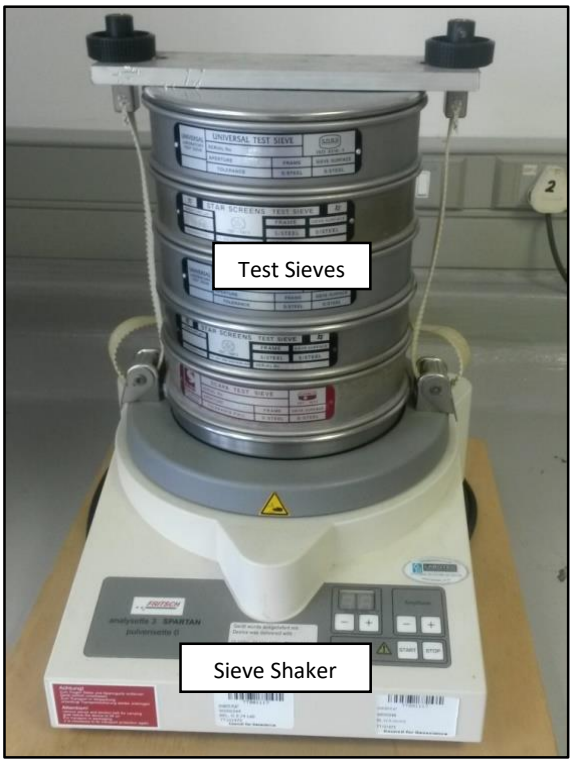

Figure 46: Image of the sieves used to separate the sediment samples into the different clast size ranges and the sieve shaker.

3.7.3 Settling tube analysis

The MGU sediment settling tube is shown below in Figure 47. It consists of an Adam Equipment PGL 203 balance which is accurate to three decimal places and has been calibrated for laboratory use. The balance is mounted onto a wooden shelf so that it is orientated directly above a 2 m long, clear PVC tube that has been filled with water. A collection pan has been suspended from underneath the balance at the base of the water column. The balance measures the relative weight accumulation of sand grains and feeds these values to a computer so that the grain size statistics and calculations can be computed for the selected sample. The software is triggered to start logging by an optical trigger that has accurately been aligned to the top of the water column.

3.7.4 Theory of the settling tube design

The theory behind a settling tube is that when sediment falls through a water column the grains the different grains will reach their maximum settling velocity depending on their respective grain size. This results in larger, coarser grains settling faster and smaller, finer grains settling slower, there by sorting the original sample.

The equation that governs how fast a particle will settle in water is Stoke's Law:

$V = \frac{(\rho_s - \rho_f) g r^2}{18\mu}$	Where: • V = the settling velocity of the particle • ρs = the density of the particle • ρf = the density of the water • g = the acceleration due to gravity • r = the radius of the particle • μ = the dynamic viscosity of the water

Equation 2: Stoke's Law.

This formula, however, tends to overestimate the observed settling velocity of a sphere as the size of the sphere increases. Gibbs et al. (1971) developed a formula which more accurately approximates the observed settling velocity of glass spheres of various sizes. This formula is as follows:

$V = \frac{-3\mu + \sqrt{9\mu^2 + gr^2\rho_f(\rho_s - \rho_f)(0.015476 + 0.19841r}}{\rho_f(0.011607 + 0.14881r}$	Where: • V = the settling velocity of the particle • ρ_s = the density of the particle • ρ_f = the density of the water • g = the acceleration due to gravity • r = the radius of the particle • μ = the dynamic viscosity of the water

Equation 3: Gibbs *et al.*, (1971) settling velocity equation.

This equation can be rearranged so that the equivalent spherical diameter for a specific settling velocity can be calculated by measuring the time it travels over a known distance. This equation is as follows:

$$\frac{0.015476V^2\rho_f + \sqrt{0.003114V^2{\rho_f}^2 + \left[g\left(\rho_s - \rho_f\right)\right][4.5\mu V + 0.008705V^2\rho_s]}}{g(\rho_s - \rho_f)}$$

Equation 4: Gibbs *et al.*, (1971) equivalent spherical diameter equation.

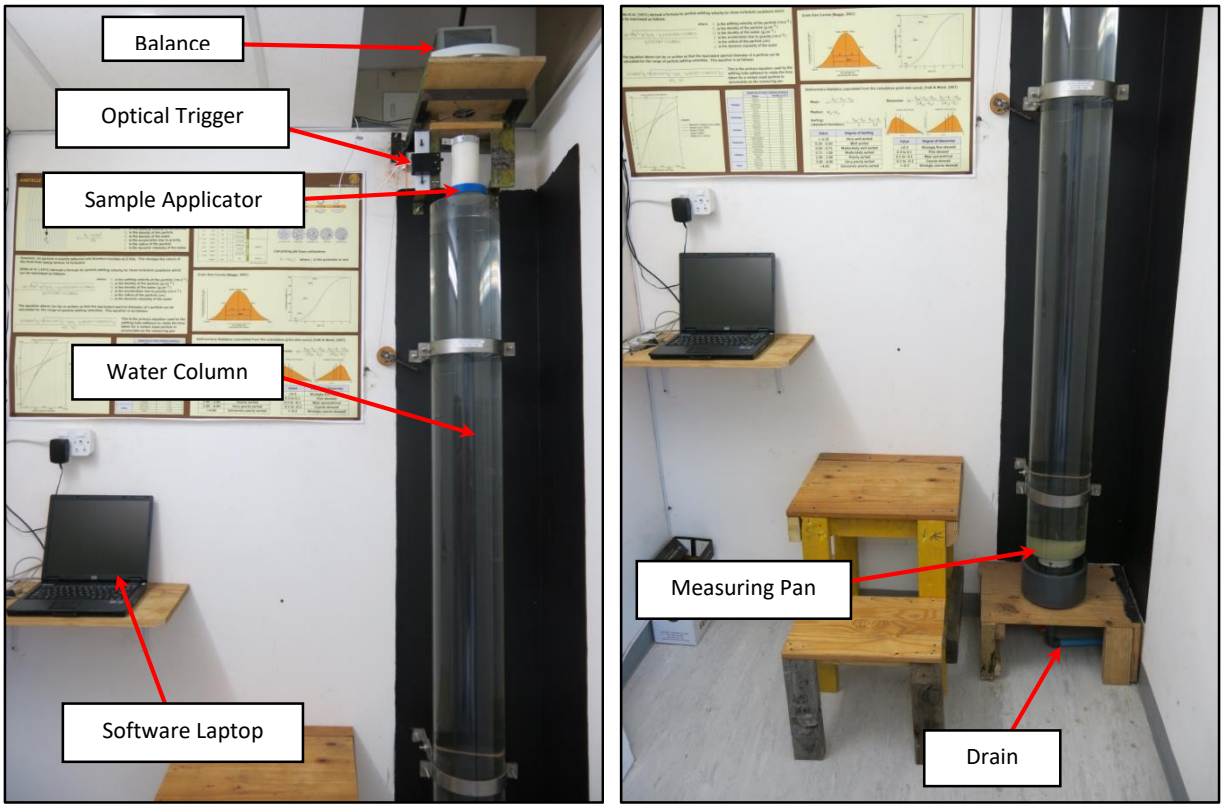

Figure 47: Pictures of the MGU settling tube.

3.7.5 Sediment grain size analysis

Before a sample can be started, the relevant project information and environmental variables must be entered into the software. These include the project name, location, operator, temperature of the water column, distance to the pan and weight and density of the sample. Once the settling tube software and trigger is ready, a measure of between 4 and 5 g of a representative sample is placed on the sample applicator at the top of the settling tube. The grains adhere to the applicator due to surface tension. The applicator is gently lowered into the water column, at which time the surface tension is broken and the grains start to settle through the water column towards the collection pan. At the same time the optical trigger starts the logging of the time and weight from the balance on the connected computer programme. The programme records the weight increase on the pan over time, to produce a cumulative weight percentage plot. This is one of the methods used for graphically displaying sediment size distributions (Boggs, 2011). The way the settling tube software displays the recorded data is shown in Figure 48. From this curve, grain sizes for corresponding weight percentiles are extracted to calculate common sedimentary statistics. These percentiles are shown graphically below.

3.7.6 Sediment statistics

The different sediment statistics reported are mean grain size, median grain size, sorting and skewness (Folk, 1980) (Figure 49). The mean (average) grain size (μ) uses different percentile ranges for the cumulative weight percentage of the grain size in the sample, expressed as Φ (phi) units. The reported statistic provides an indication of the energy required to transport the sediment (Pethick, 1984). The median value (M_d) is that value which separates the lower half of the grain size population from that of the higher half. This value is sometimes the same as the mean (Pethick, 1984). The median can be defined as the 50^{th} percentile of Φ. The sorting (σ) of the sample is equivalent to the standard deviation of the grain size population (Folk, 1980). The sorting of a sediment sample is an indication of how effective the depositional medium is at separating the grains into their respective size classes (Pethick, 1984). Small values of sorting indicate low standard deviation and selective transport and deposition with the converse holding firm for high values of sorting (Pethick, 1984). Factors influencing sorting include sediment source, transport mode and depositional

environment and sorting generally increases from proximal to distal environments (Pethick, 1984).

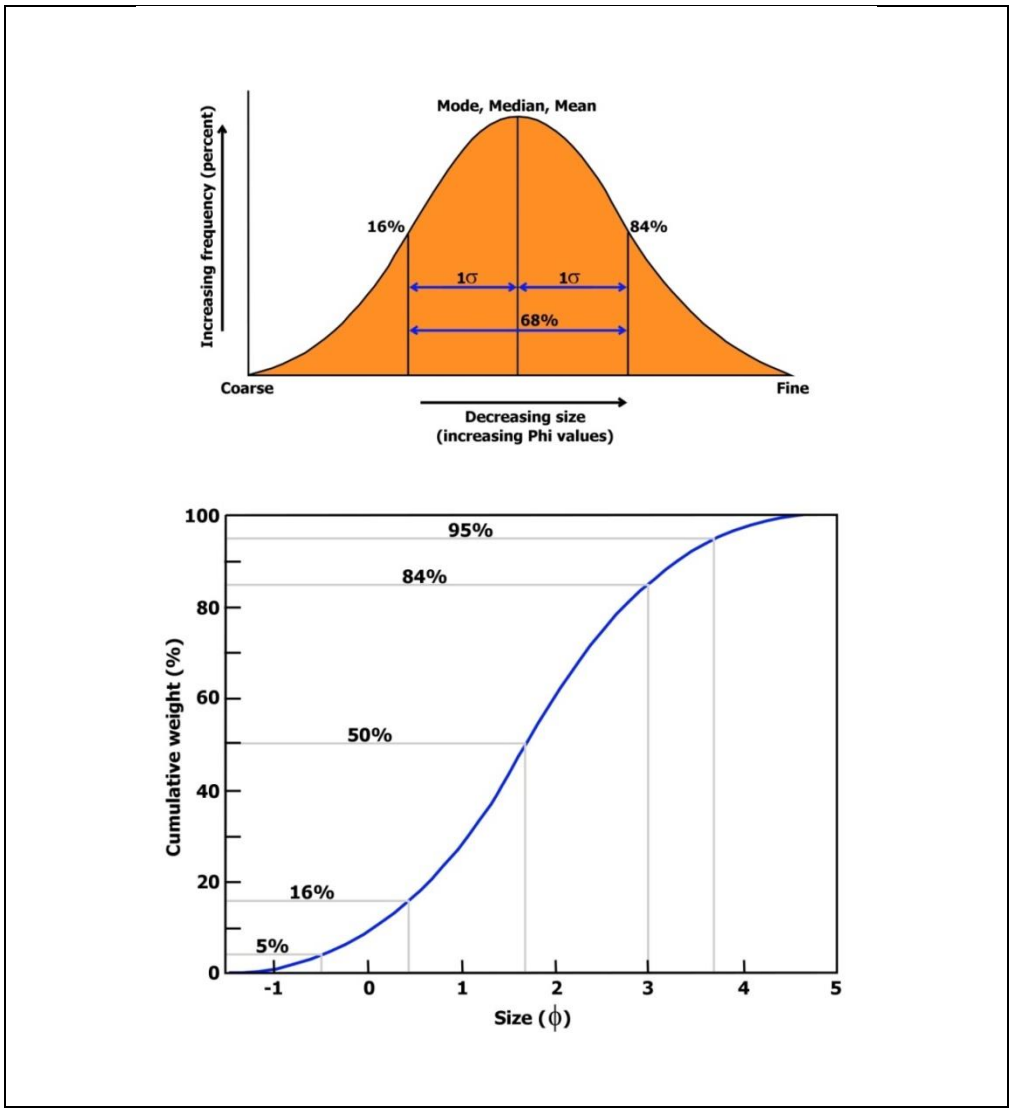

Figure 48: Graphical representations of grain size distribution in terms of frequency (top) and cumulative weight percent (bottom), (modified from Boggs (2011) and MacHutchon et al. (2014)).

Skewness (sk) is a measure of the symmetry of the grain size distribution within the sample and is related to erosional and depositional processes (Pethick, 1984). A negative skew (coarse tail) indicates a mode of finer grained sediment with a large coarse tail with the converse holding firm for a positive skew (Pethick, 1984; Boggs, 2011). The different sedimentary statistics calculated by the software are as follows:

Sedimentary Statistics (calculated from the cumulative grain size curve) (Folk & Ward, 1957)

Mean: $\mu = \frac{\phi_{16} + \phi_{50} + \phi_{84}}{3}$

Median: $M_d = \phi_{50}$

Sorting: **(standard deviation)** $\sigma = \frac{\phi_{84} - \phi_{16}}{4} + \frac{\phi_{95} - \phi_5}{6.6}$

Skewness: $sk = \frac{\phi_{84} + \phi_{16} - 2\phi_{50}}{2(\phi_{84} - \phi_{16})} + \frac{\phi_{95} + \phi_5 - 2\phi_{50}}{2(\phi_{95} - \phi_5)}$

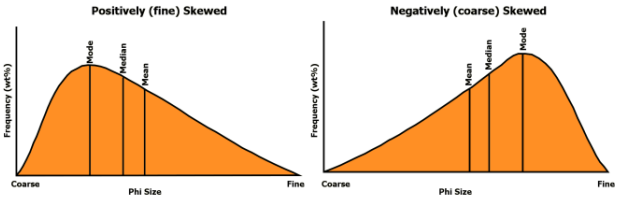

Value	Degree of Sorting
< 0.35	Very well sorted
0.35 - 0.50	Well sorted
0.50 - 0.71	Moderately well sorted
0.71 - 1.00	Moderately sorted
1.00 - 2.00	Poorly sorted
2.00 - 4.00	Very poorly sorted
>4.00	Extremely poorly sorted

Value	Degree of Skewness
>0.3	Strongly fine skewed
0.3 to 0.1	Fine skewed
0.1 to -0.1	Near symmetrical
-0.1 to -0.3	Coarse skewed
<-0.3	Strongly coarse skewed

Figure 49: Equations for calculating sedimentary statistics, (modified from Folk, 1980; MacHutchon et al., 2014)

Once the grain size parameters have been determined from the lab results the various characteristics must be gridded. Mean grain size and calcium carbonate percentage are gridded with Golden Software Surfer using the Kriging statistical analysis method. Using the sediment characteristics of mean grain size, skewness and sorting, transport vectors are calculated using the following statements:

1. Finer grained sediment can be placed into suspension more readily than coarse grained sediment and is therefore preferentially transported.
2. Theoretically sediment in transport becomes finer, better sorted and more negatively skewed in the downstream direction.
3. Alternatively a lag deposit becomes coarser, better sorted and more positively skewed in the downstream direction (McLaren and Bowles, 985).

The limitation of using these grain size characteristics is that it only indicates the direction of transport and not the transport rate (Pedreros et al., 1996). The composition of the sediment is useful in indicating the source of the sediment. The type of minerals present can give an indication of the host rock or the carbonate content can indicate the direction of transport from biogenic input on offshore reefs.

3.8 Additional Equipment

3.8.1 Geo Manzi

The MGU survey vessel *Geo Manzi* (Figure 50) was utilized to collect the majority of the geophysical data for the project. *Geo Manzi* is an 8.5 m aluminium catamaran power by two Suzuki 175 HP outboard motors. The vessel has a large enclosed cabin to set up equipment, and is well suited for geophysical and hydrographic survey work. A stable, repeatable mounting pole is situated between the motors which can be used to mount survey equipment such as bathymetric echosounders or seismic transducers. A large, open deck is available to deploy towed survey equipment such as a side scan sonar towfish or boomer seismic systems.

Figure 50: MGU research vessels, *Geo Manzi* on the left and Tethys on the right.

3.8.2 Tethys

The Survey vessel *Tethys* (Figure 50) is a 6 m semi-rigid inflatable boat. The vessel is easily launched from most slipways and has a range of 80 km per day at survey speed of 5 – 6 knots. The vessel was utilized for smaller surveys and sediment grab sampling during the project. The deck is versatile for various applications at sea, depending on the task being conducted. For survey work a frame with a box containing the survey equipment was mounted. The box was removed and replaced with an over-the-side A-Frame for sediment grab sampling or a cylinder rack for SCUBA diving surveys.

3.8.3 Positioning and navigation

To obtain accurate positioning for geophysical and hydrographic surveys, Global Navigation Satellite Systems (GNSS) were utilised. These include the American GPS and the Russian GLONASS systems. Most modern GNSS receivers can receive GPS and GLONASS signals. Due to inaccuracies in the receiver's electronics, non-mitigated ionospheric and tropospheric

delays and ephemeris errors, a GNSS receiver in standalone has an accuracy of 100 m (Parkinson, 2001). This level of accuracy is generally not sufficient for geophysical and hydrographic surveys, especially in the case of multibeam bathymetric surveys. Some GNSS receivers can receive a correction from a base station to increase the level of accuracy. The most accurate level of positioning is RTK or Real Time Kinematic satellite navigation which can have a horizontal accuracy of a 1 cm and vertical accuracy of 2 cm (Parkinson, 2001). One level down in accuracy from RTK is the proprietary NAVCom RTG (Real Time GIPSY) correction. An RTG enabled receiver receives corrections not from a locally setup base station but from a global network of base stations. The signal is received via a satellite connection. This type of system can achieve decimetre accuracy, typically 10 cm horizontally and 15 cm vertically (Morton, 2015). An additional way to receive deferential GPS corrections is via radio broadcast from permanent base stations situated along the coastline at various locations. These base stations broadcast a Minimum Shift Keying (MSK) radio signal which the receiver utilizes to correct the satellite signal. The accuracy of this system is close to 1 m (Parkinson, 2001). All data for this project were collected, processed and displayed in UTM 34 S with a WGS 84 datum as described in Table 8.

Co-ordinate System	WGS 1984 UTM Zone 34S
Projection	Transverse Mercator
False Easting	500 000
False Northing	100 000 000
Central Meridian	21
Scale Factor	0.9996
Latitude of Origin	0
Linear Unit	Metre
Geographical Co-ordinate System	WGS 1984
Datum	WGS 1984
Vertical Datum	Chart Datum (Cape Town 0.825m BMSL)

Table 8: Co-ordinate system used during the project.

C-Nav DGPS

The C-Nav 3050 GNSS receiver (Figure 51) is a combined GPS/GLONASS receiver which provides decimetre positioning. GNSS Precise Point Positioning corrections are received via satellite as a subscription service. The corrections increase the GPS accuracy to sub-10 cm. The multi-constellation receiver tracks both GPS and GLONAS satellites. In conjunction with external radio modems or an internet connection, the 3050 receiver can be enabled to be used as a RTK base station or rover.

Figure 51: C-Nav 3050 GNSS positioning system.

CSI Wireless DGPS

The CSI Wireless DGPS Max (Figure 52) with MSK corrections is a combined 12-channel GPS with an integrated MSK beacon receiver that provides positional corrections enabling sub-metre horizontal accuracy. The system has an update rate of up to 5Hz or 5 times per second. MSK corrections are received via radio beacons located at the Cape Columbine and Cape Agulhas lighthouses.

Figure 52: CSI Wireless DGPS Max system.

Software

Hypack software was used for navigation and positioning of the survey vessel for the side scan sonar and magnetometer surveys and sediment sample collection.

Qinsy QPS software was used for navigation, to collect and process MBES data for this project. During the survey operations, Qinsy recorded real-time bathymetric coverage in a sounding grid file which was projected on the navigation display. The sounding grid was used to check bottom coverage and to identify shallow objects below the sea surface. The software records and combines the different sensors and offsets required to conduct a MBES survey. Once these data are collected, the software is used to process these data for sensor offsets, tidal corrections, sound velocity corrections and removing noise in the water column.

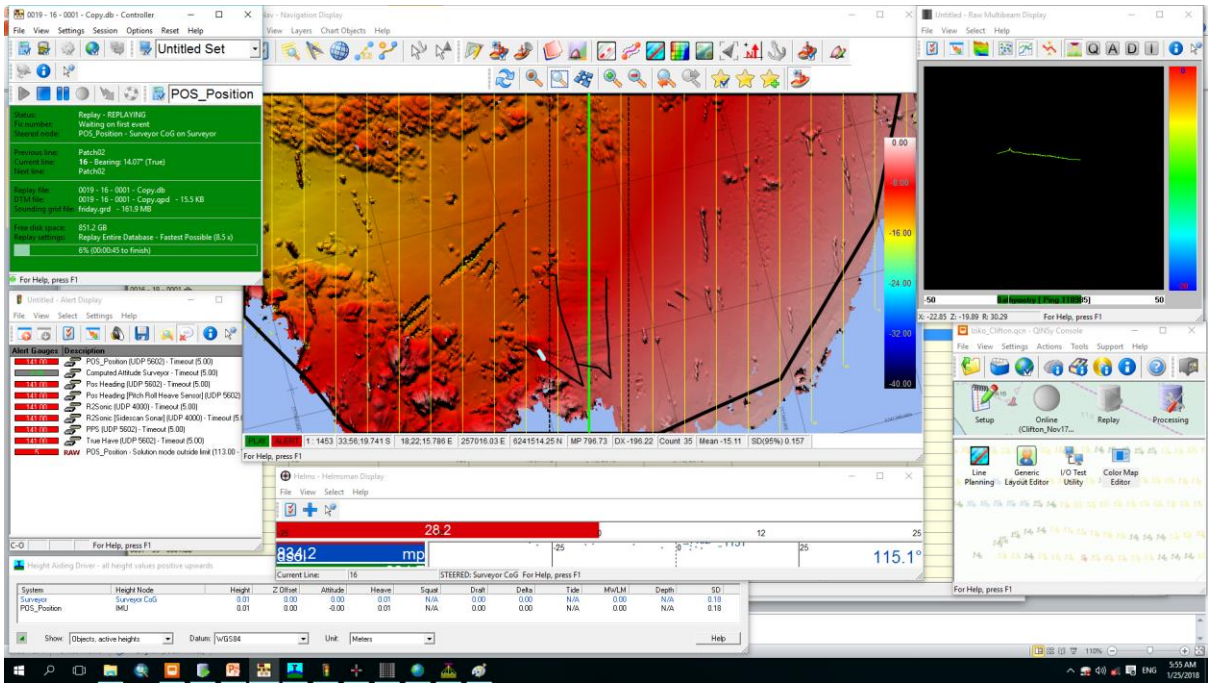

Figure 53: QPS Qinsy multibeam acquisition software with screens for navigation, online data recording, equipment error warnings and position status.

3.8.4 Sound velocity probe

The velocity of sound or acoustic waves through water is influenced by several factors and properties of the water, including temperature, salinity, pressure and density. Temperature variations within the survey area and water column are the most important variable and as an example a 1°C change in water temperature can cause a 4.5m/s change in sound velocity (International Hydrographic Organization, 2005). Depending on the requirement of the survey instrument, the sound velocity probe (SVP) can either record a complete sound velocity profile of the water column or calculate an average reading.

Figure 54: Odom Digibar S sound velocity probe, used to correct for speed of sound in water.

The Odom Digibar S was used for all sonar equipment requiring accurate sound velocity information. The Digibar S is a rugged, stainless steel, un-tethered SVP with a maximum depth rating of 500 m. The probe measures speed of sound, pressure and temperature. It uses a 2 MHz transducer to measure the speed of sound across a known distance directly. The Digibar S can store up to 255 casts.

3.9 Geological Map Production

Combining the datasets obtained from the previous sections a seafloor facies chart was created, which extends from beach or backshore above water, to between 40 and 70 m BMSL, from Vulcan Rock in the South to Mouille Point in the north. The seafloor has been interpreted as various types of facies according to Table 10. The location of dolerite dykes as interpreted from the marine magnetics was plotted as an overlay on the facies chart. Once the general location of a dyke is identified through the magnetic data, the dyke is pinpointed by tracing gullies or linear features in the bathymetry data. Additionally, the sediment sampling data were used to ground truth the interpreted facies, especially where multibeam data were used and some uncertainty existed. The facies results were then correlated to geological units and combined with CGS onshore data from the 1:50 000 map series to create a continuous, uninterrupted onshore-offshore map of the geology of the Atlantic Seaboard (Appendix E).

4 Results

4.1 Bathymetry

During the bathymetry data collection a total area of 36 km^2 of seafloor were covered along 22 km of coastline (Figure 55 and Appendix C). These data are presented in more detail as charts 1- 4 in Figure 56 to Figure 59. The survey extended from as close to the coast as possible, keeping vessel and equipment safety in mind, to between 1.5 and 2.5 km offshore. Due to a faulty sound velocity probe used during the survey, a height discrepancy exists in some areas between adjacent lines. The incorrect sound velocity reading causes these data on the outer beams of the swath to curve upwards resulting in a concave-shaped swath. This is most noticeable in flat sediment area such as Sandy Bay (Figure 58). Adjusting the sound velocity manually removed most of the visible discrepancies.

Maori Bay is the only large area without full bottom coverage. Maori Bay could not be covered due to logistical and budgetary issues (Figure 59). Smaller areas in the survey area are also missing data. These areas are mostly due to safety concerns for the vessel and equipment. The two areas on either side of Maori Bay were not surveyed due to blinders or exposed/shoaling reef or very shallow submerged reef (Figure 59). Small areas of exposed reef are located offshore from Camps Bay. These areas are locally known as the Lion's North and South Paws, which are exposed at low tide (Figure 56).

The survey area can be split into two distinct bathymetric zones based on the geomorphology (Figure 55). Zone A starts at Sea Point and continues to the northern extent of the survey area at Mouille Point. This zone consists of low-relief, parallel ridges with a general northwest to southeast orientation. Sediment is generally restricted to gullies with the same orientation as the overall dominant fabric observed in the reef. An anticlinal fold axis can be observed in the offshore area (Figure 56). The fold limbs are spaced approximately 200 m apart and the fold axis can be traced for up to 800 m in a south east to northwest direction. Several negative relief structural lineaments with different orientations can be observed.

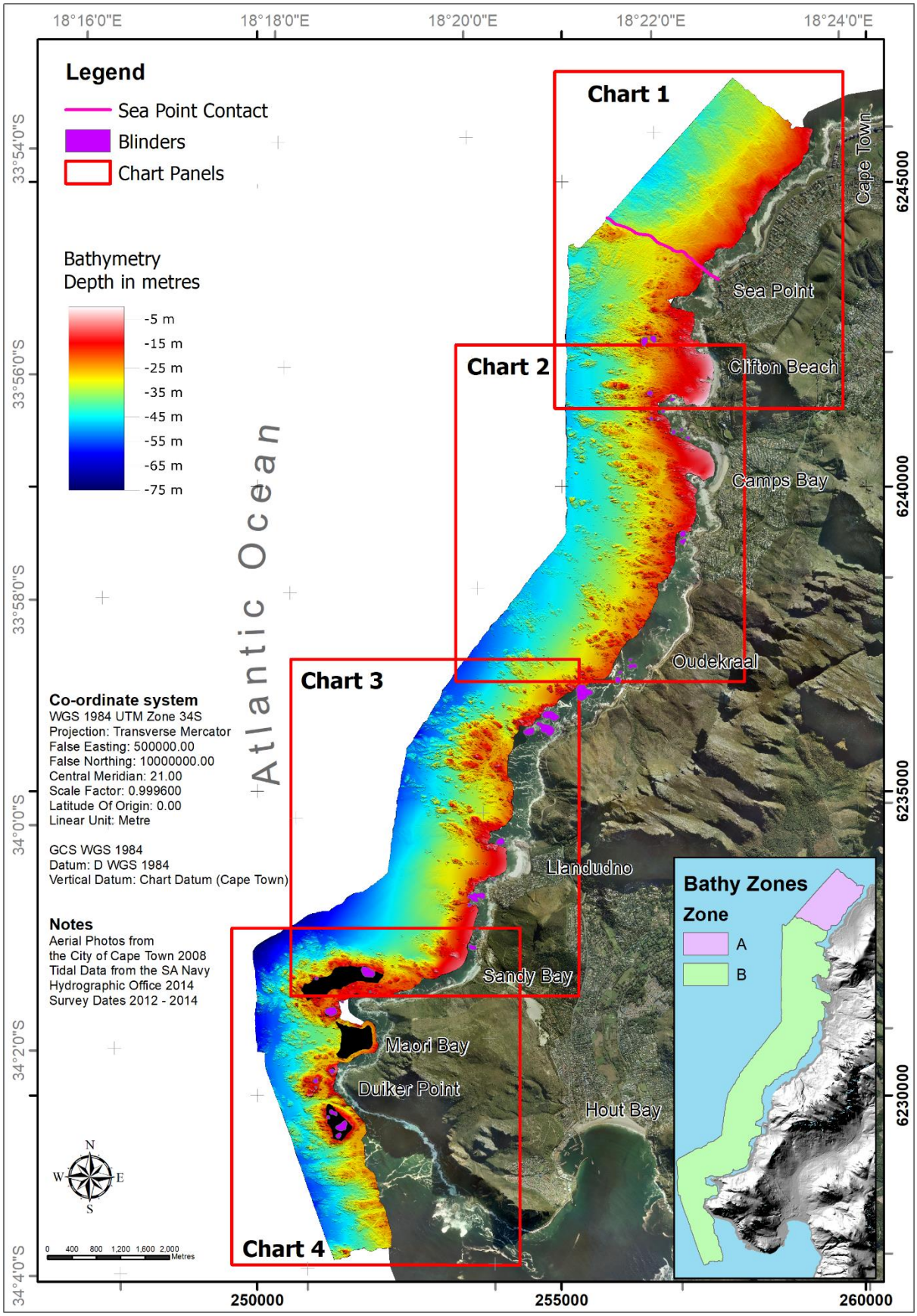

Figure 55: Multibeam bathymetry of the Atlantic Seaboard, bathymetric zones indicated on the insert (See Appendix C for enlarged multibeam bathymetry chart).

The first is a north east to south west lineation which can be traced for more than 3 km. The second lineation has a curved orientation starting on the offshore with an east-west orientation and changing to north east on the inshore. The third lineation has a north west to south east orientation and continues for 1.4 km.

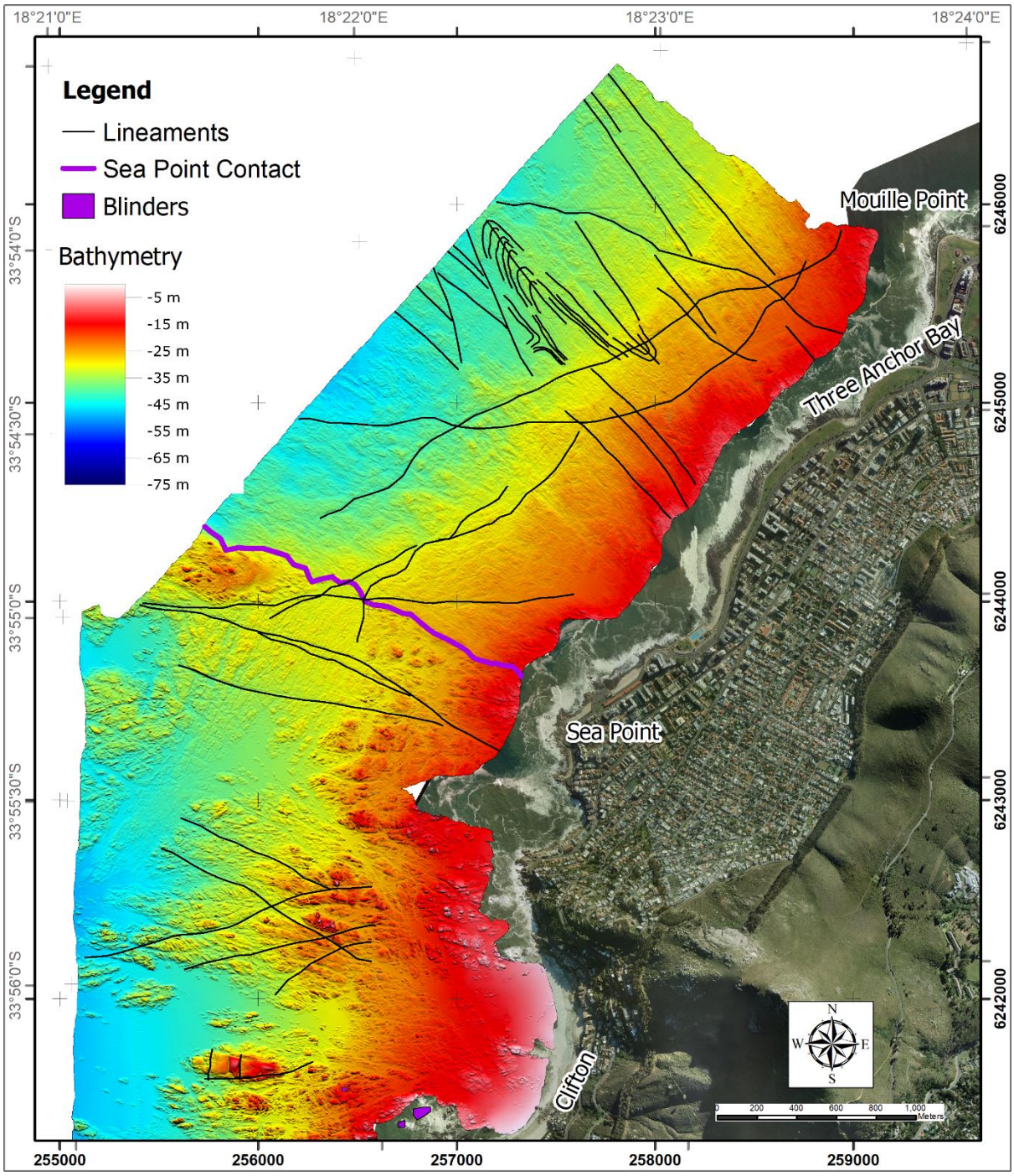

Figure 56: Chart 1 multibeam bathymetry, Mouille Point to Clifton, indicating the Sea Point contact, Zone A will north of the contact and Zone B will be south of the contact.

Zone B extends from Sea Point to the southern extent of the study area. The bathymetry in this zone is highly variable, with high-relief reef shoaling from more than 30 m depth to exposed rock outcrop or blinders at the surface over short distances. Several large reef complexes can be found, generally associated with headlands onshore. Examples of this are Duiker Point in the south (Figure 59), the headland north of Llandudno Figure 58)

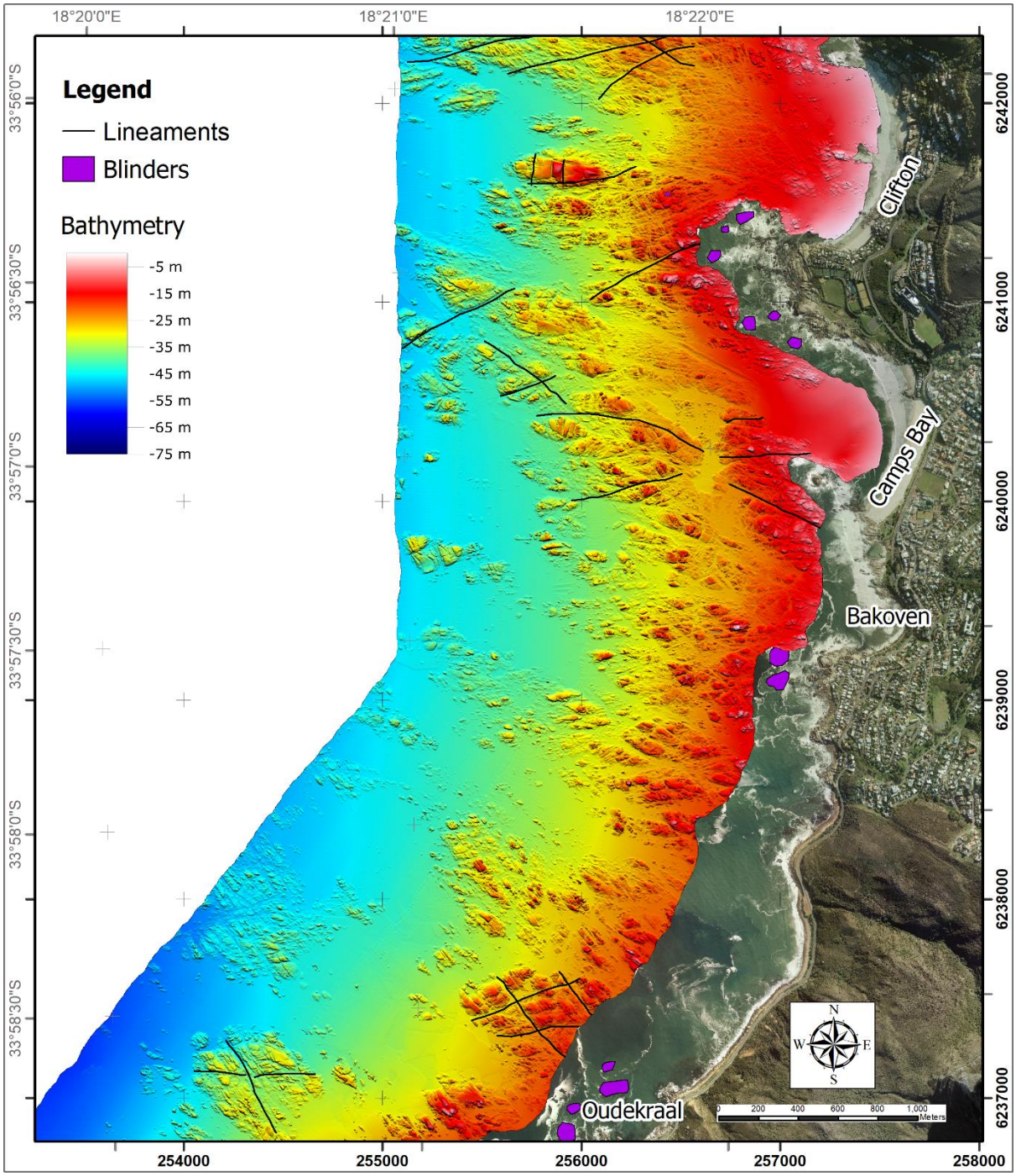

Figure 57: Chart 2 multibeam bathymetry, Clifton to Oudekraal.

and the headlands bounding either side of Clifton beach, locally known as the Lion's North and South paws (Figure 57). Small, low-relief reefs are found scattered throughout the survey area. The reef areas are surrounded by sediment-filled depressions, sloping gently towards the offshore. Conjugate joint sets in the reef are common throughout the zone with angles of 130˚ and 50˚ between sets. The orientations of the joints are mostly NNW and NNE.

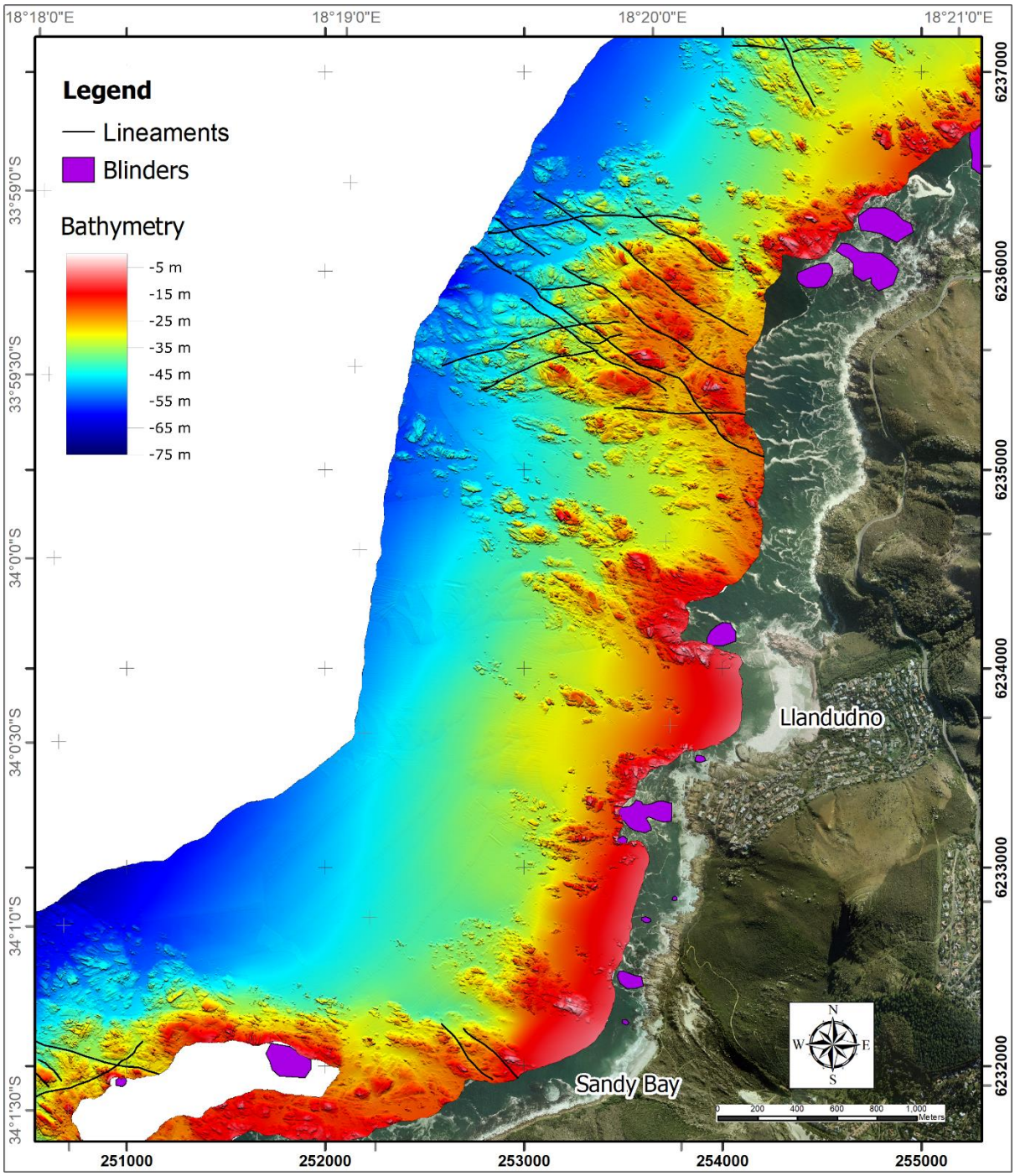

Figure 58: Chart 3 multibeam bathymetry, Oudekraal to Sandy Bay.

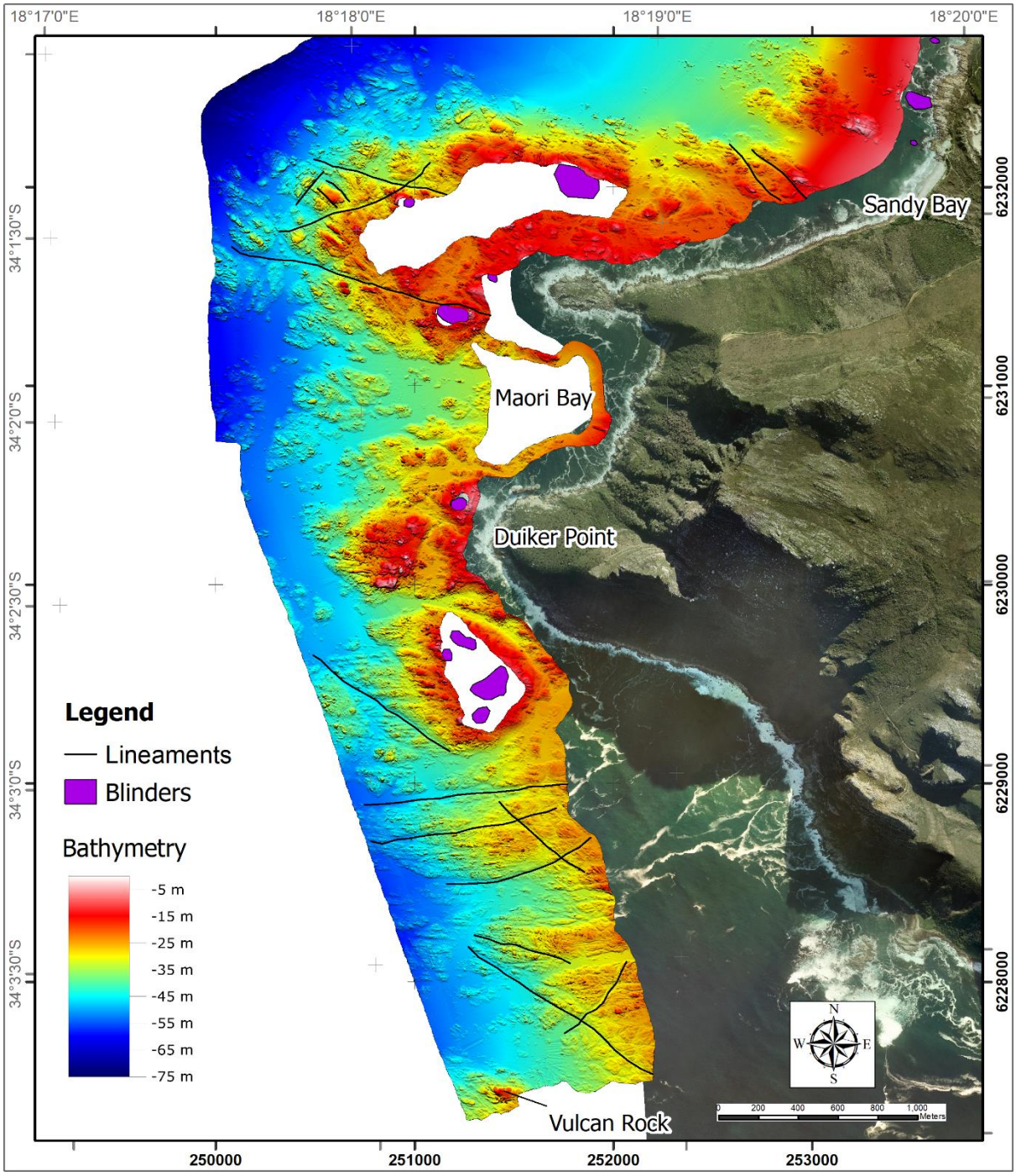

Figure 59: Chart 4 multibeam bathymetry, Sandy Bay to Vulcan Rock.

4.2 Side Scan Sonar Mosaic

A mosaic was created from the side scan sonar data. The mosaic is presented in Figure 60. More detailed mosaics are shown in Figure 61 to Figure 64.

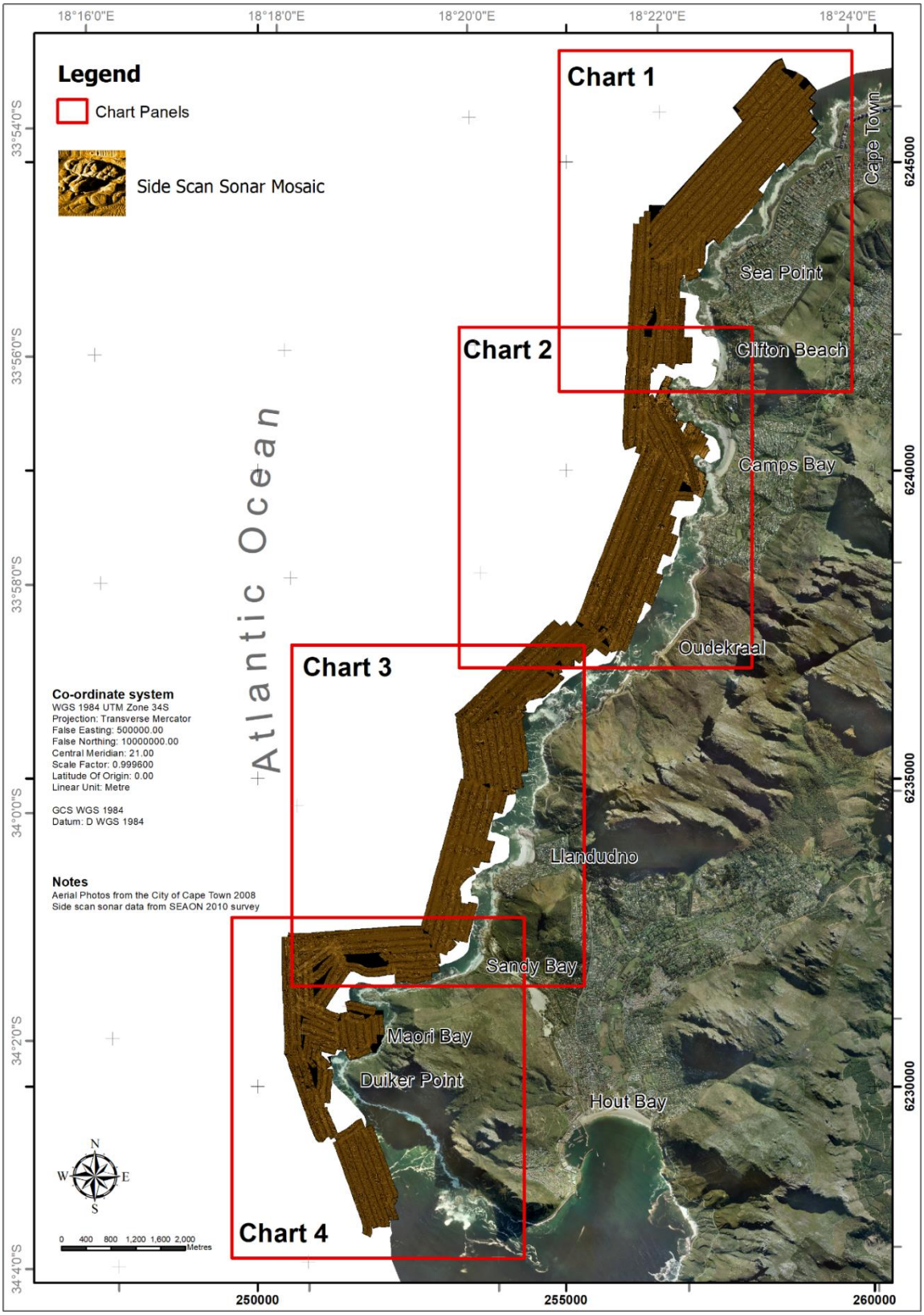

Figure 60: Side scan sonar mosaic of the Atlantic Seaboard.

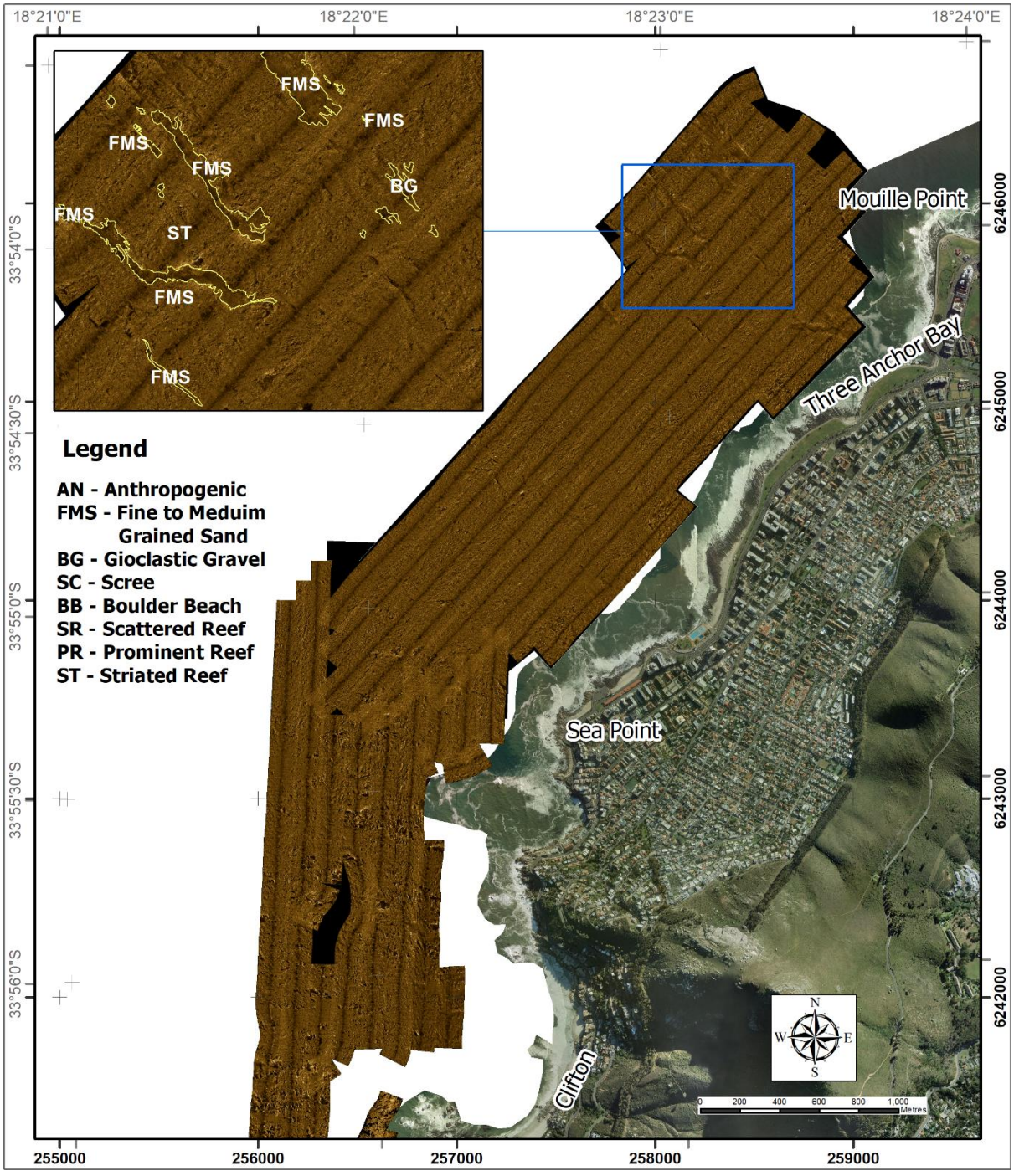

Figure 61: Side scan sonar mosaic between Clifton Beach and Mouille Point

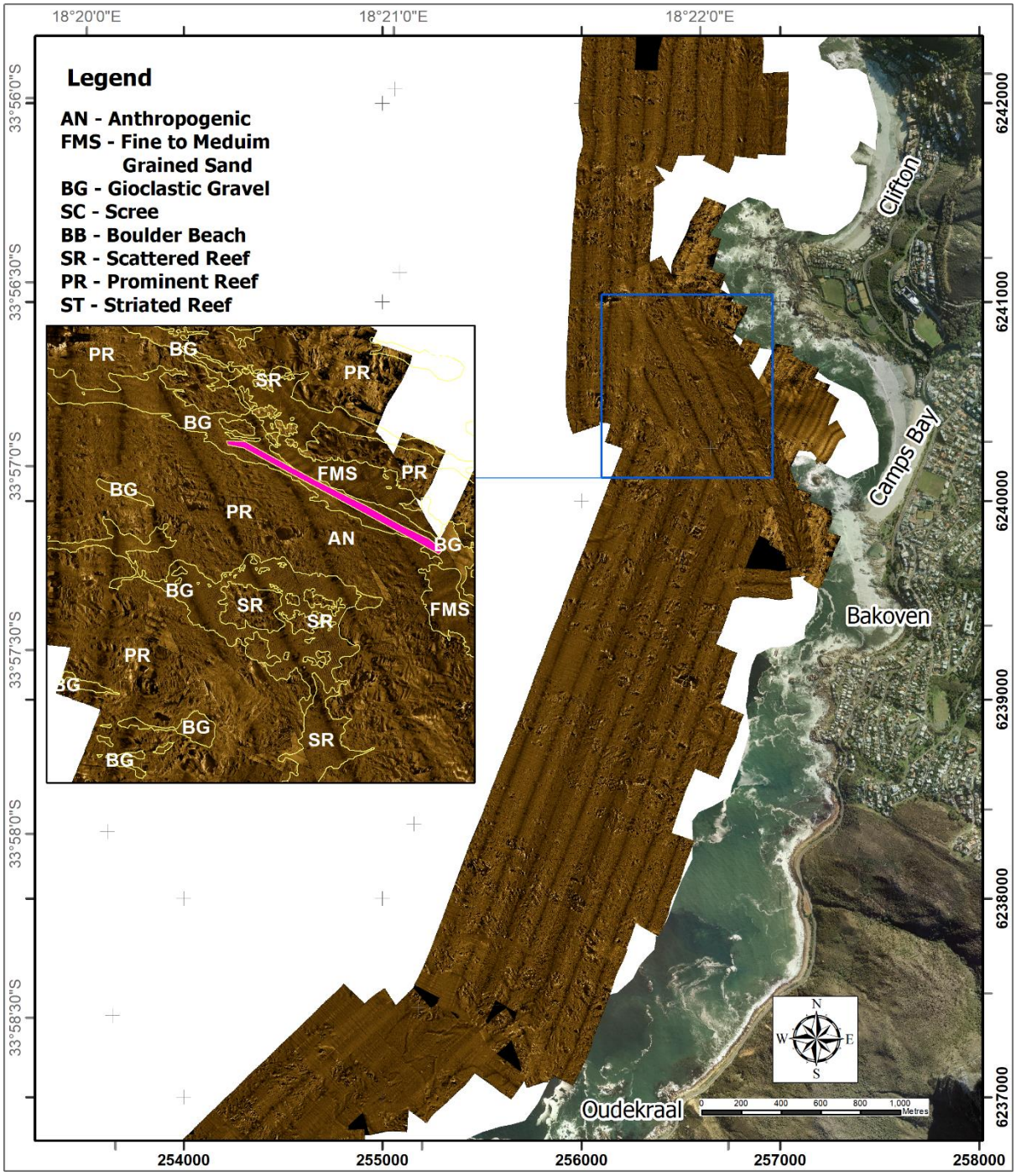

Figure 62: Side scan sonar mosaic between Clifton Beach and Oudekraal, Camps Bay out-fall pipe line indicated in pink.

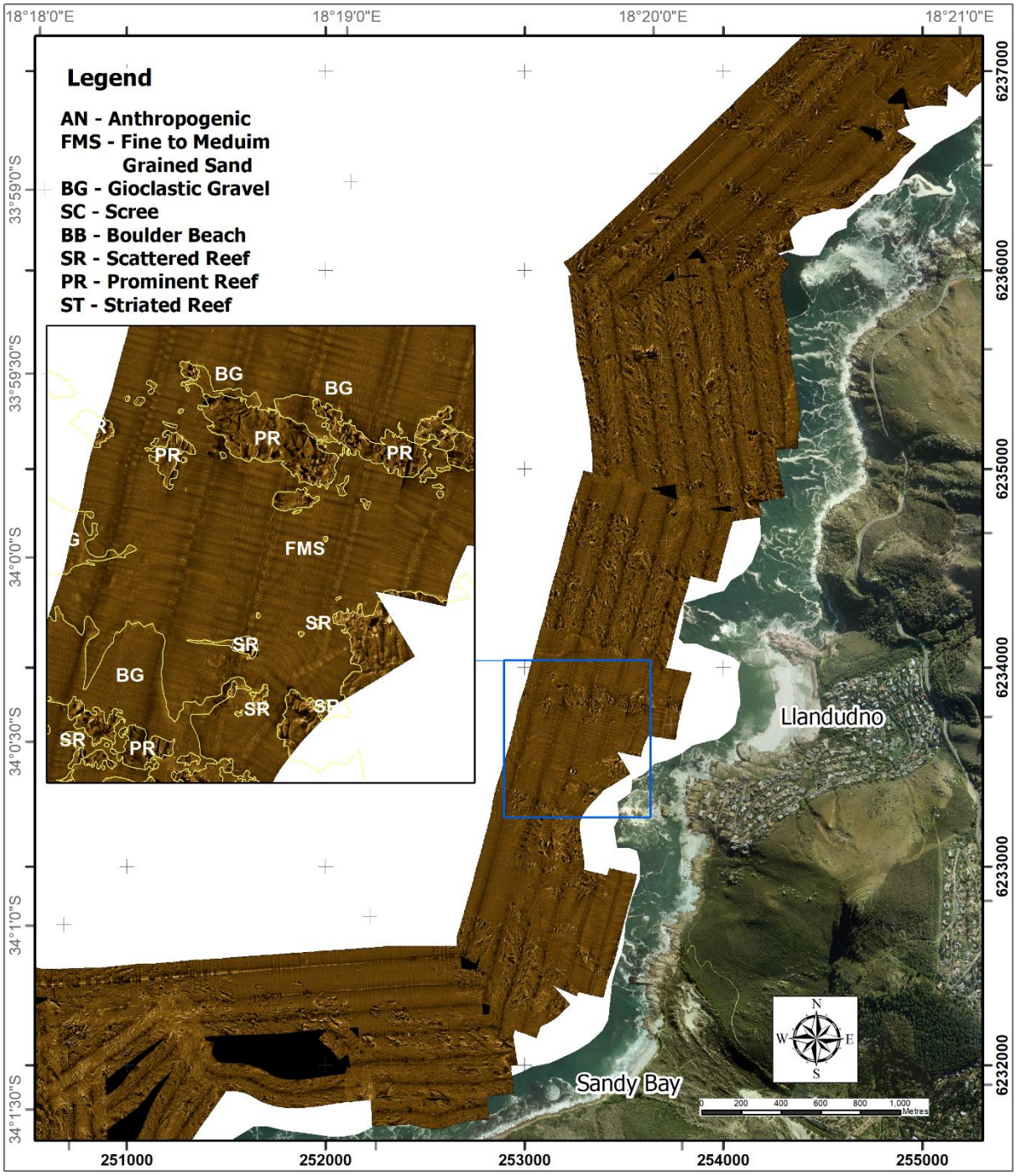

Figure 63: Side scan sonar mosaic between Oudekraal and Sandy Bay

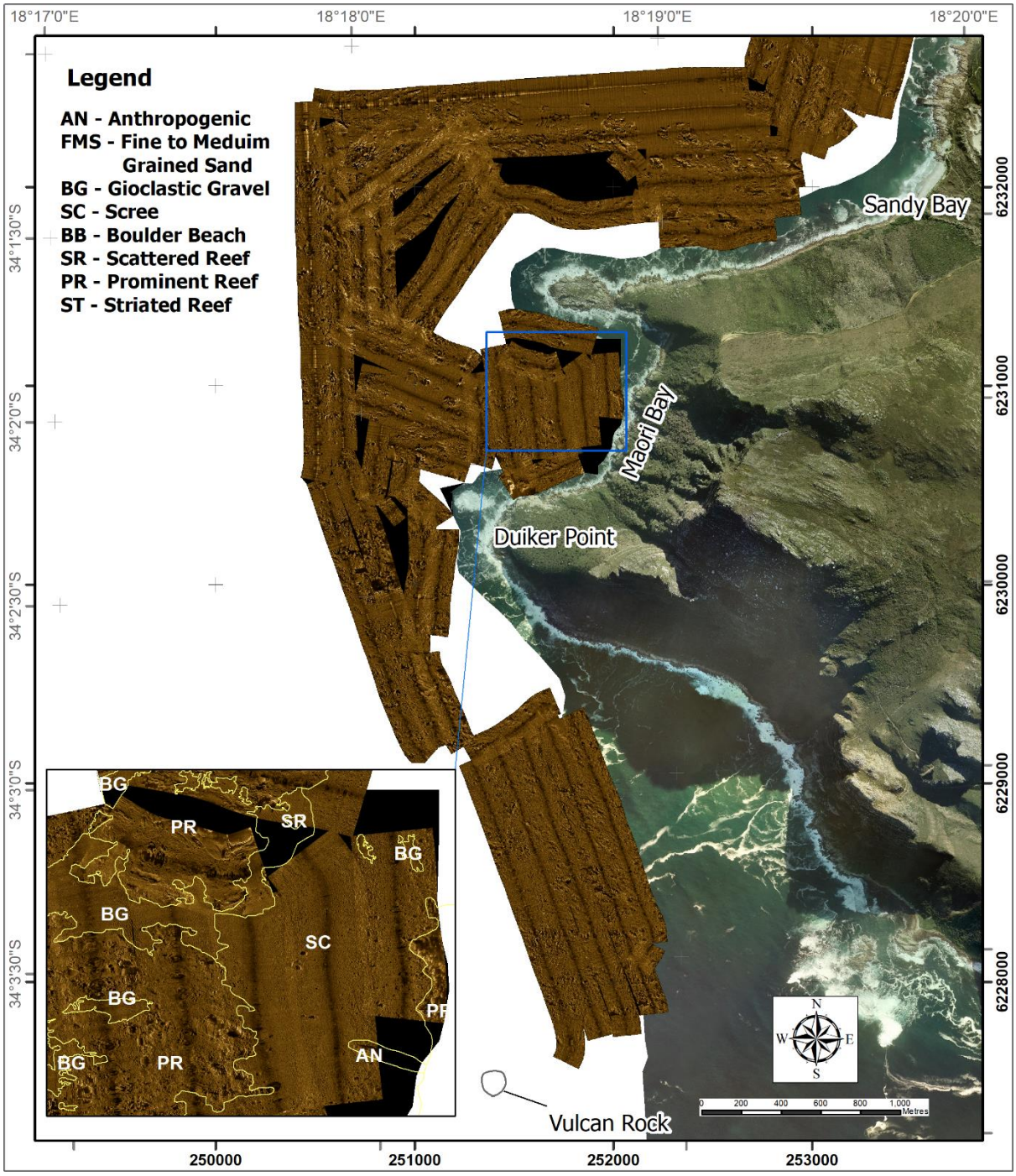

Figure 64: Side Scan sonar mosaic between Sandy Bay and Vulcan Rock

4.3 Magnetic Anomalies

From the regional magnetometer survey, several linear anomaly features have been identified. The features generally follow a NW-SE trend. The features have strong magnetic signatures, some positive and some negative. A total of 14 magnetic anomalies have been identified, numbered A through N (**Figure 65**). Two strongly positive magnetic anomalies are

located to the north (A and B). They are located at Green Point and Three Anchor Bay, respectively. Anomaly C is a weaker magnetic anomaly located just north of Sea Point. Anomalies D and E are two strong positive anomalies located off Clifton 3rd and 4th Beach. Just south of Bakoven are two weak negative anomalies F and G. Between Llandudno and Oudekraal, there are four positive anomalies H, I, J and K, with K being the strongest. L, M and N are located offshore of Sandy Bay and Maori Bay, with M being negative. The anomalies seem to be grouped into clusters A – B; C; D – E; F – G; H – I – J – K and L – M – N. The four anomalies further south of Maori Bay are extensions of magnetic anomalies described by MacHutchon (2013), and will not be discussed here. The dolerite dykes identified in the study area are presented in Table 9 with the corresponding dykes from Reid et al. (1991).

Magnetometer Number	Reid et al., (1991) Number	Location
A		Green Point
B		Three Anchor Bay
C	1	Sea Point
D	2	Clifton 2
E	3	Clifton 1
F	4	Bakhoven
G	5	Kasteelpoort
H	6	Oudekraal 1
I	7	Oudekraal 2
J	8	Llandudno Ravine
K	9	Logies Bay
L	10	Sandy Bay
M		Maori Bay 1
N	(11)	Maori Bay 2 (Chapmans Pk 1)

Table 9: List of identified dolerite dykes from the False Bay Dolerite Swarm located in the Atlantic Seaboard in this study numbered A to N, with corresponding numbers from Reid et al. (1991).

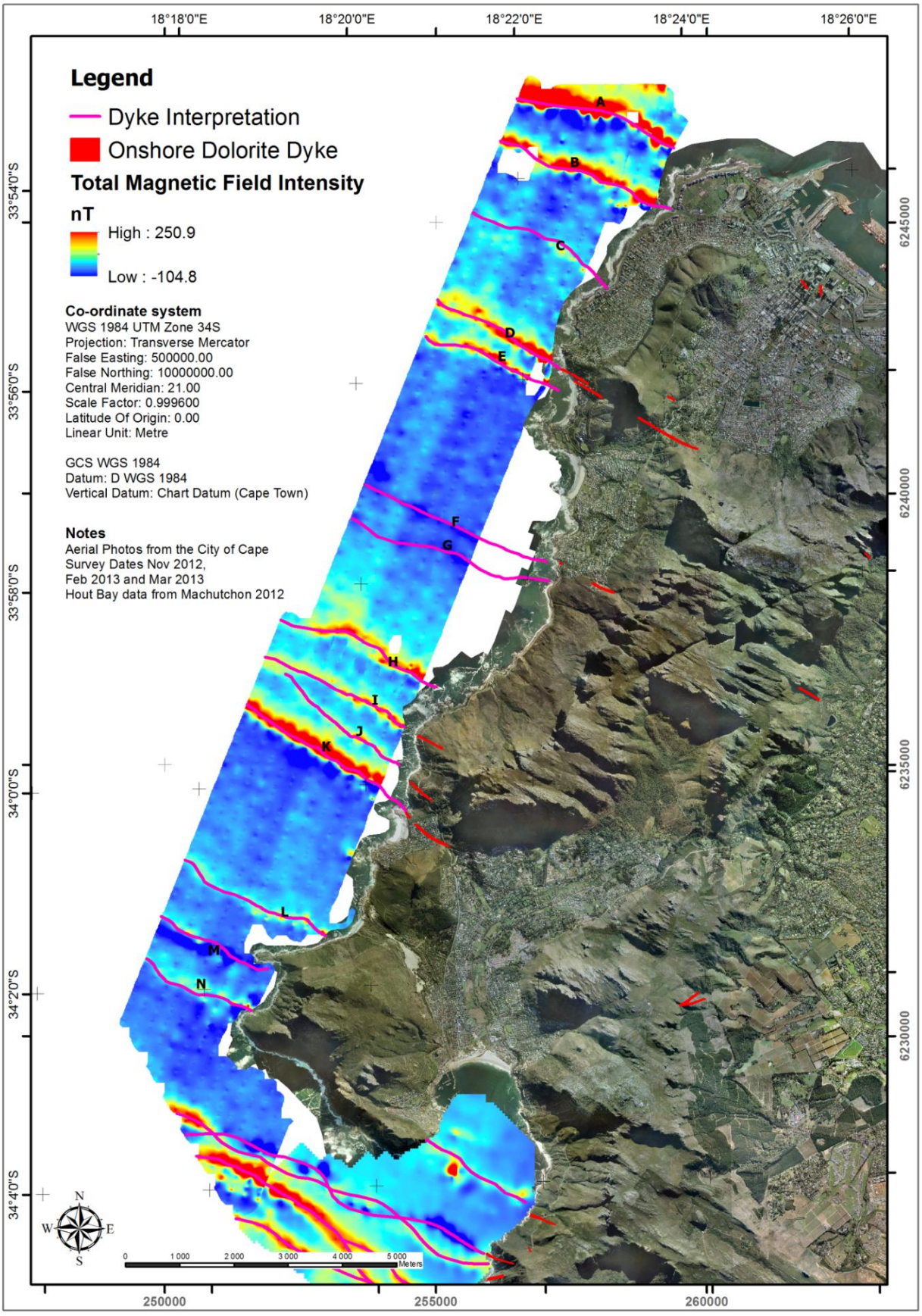

Figure 65: Total Magnetic field results from marine magnetometer survey conducted during 2012 and 2013, Hout Bay data from MacHutchon (2013) onshore dykes from CGS 1:50 000 map series.

4.4 Beach Profiling

4.4.1 Camps Bay

Camps Bay is a north-south trending sandy beach enclosed with rocky outcrops on both sides (Figure 66). The beach is contained on the backshore by an artificial grass embankment and road infrastructure. The backshore is relatively flat along most of the beach. A variable beach berm develops at certain times of the year, from where the beach slopes down steeply to the foreshore and towards the nearshore. A large granite outcrop dissects the beach about 130 m from the northern end of the beach. The granite outcrop measures about 60 m x 60 m and extends from the grass embankment into the surf zone. At spring low tide, the foreshore is exposed seaward of the outcrop. Beach profiling was not conducted to the north of the granite outcrop.

In August 2013, beach elevation varied between 4 m and -1 m MSL. The beach width was between 80 and 95 m with a length of 650 m up to the northern granite outcrop. Beach elevation was generally low, with some erosion evident by exposed boulders and pipeline. The beach berm was poorly developed and set back far towards the backshore. To the northern side of the survey area large cobbles and boulders were observed in the surf zone. The northern section of the beach had a steep sloping foreshore. On the southern end of the beach the foreshore slope was much less. Two beach bars were noted in the immediate nearshore area.

There was a pronounced increase in beach elevation measured during November, especially on the foreshore. The beach berm was more pronounced and had migrated towards the foreshore. On the northern side of the survey area the boulders were completely covered by sand. The elevation of the backshore remained stable. The nearshore sand bars observed during August were no longer present.

During the January survey the beach berm migrated further towards the foreshore. Backshore elevations seem to have decreased slightly. During January it was possible to walk around the granite outcrop on the northern side of the survey area, suggesting an increase in sediment volumes in the foreshore and nearshore.

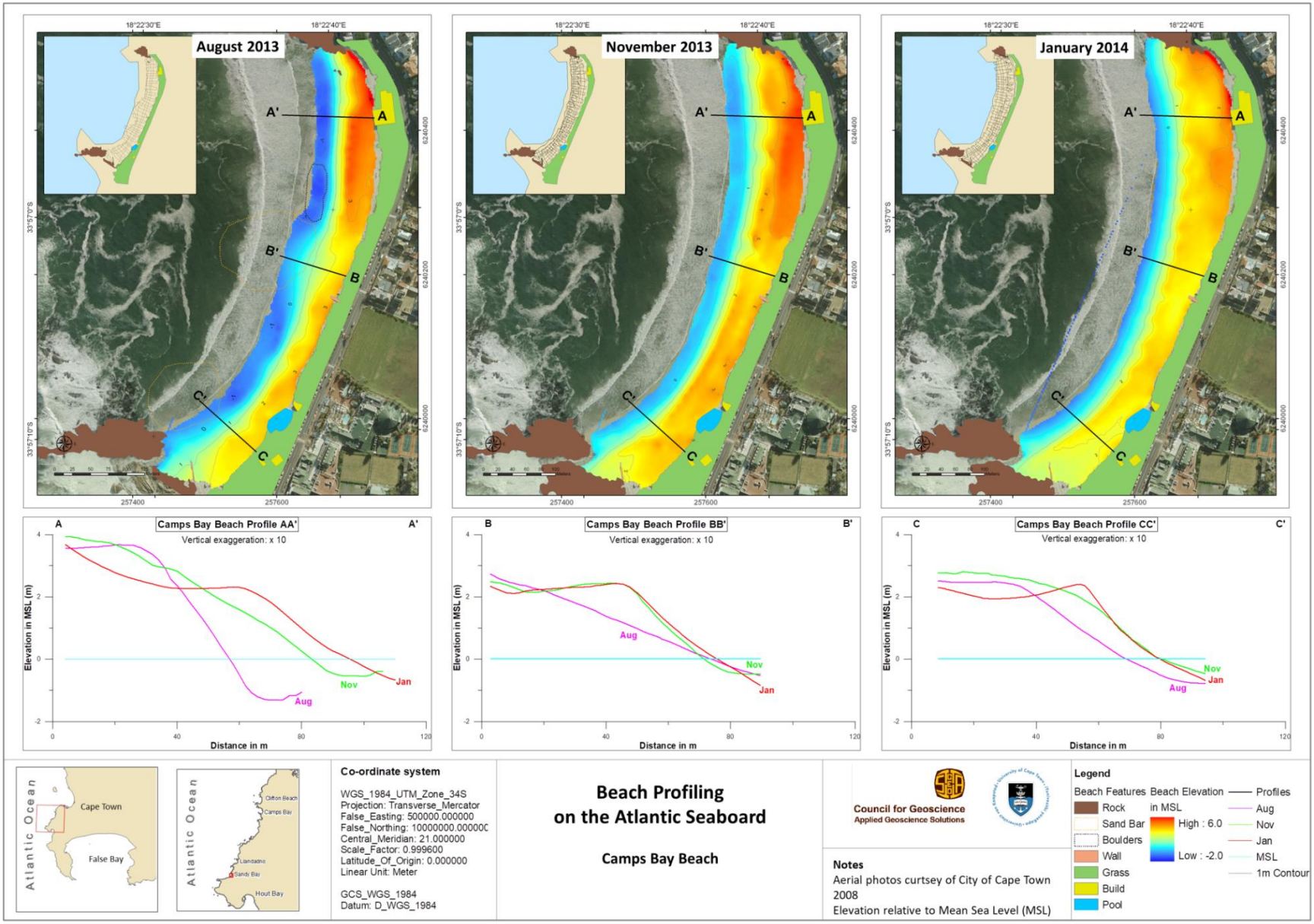

Figure 66: Camps Bay beach profiling surveys with time series sections at 3 locations along the beach showing the change in elevation at each survey.

4.4.2 Sandy Bay

Sandy Bay beach is a NW facing beach about 370 m long and between 50 and 70 m wide (Figure 67). To the north it is enclosed by granite outcrop that extends to the beach at Llandudno. To the south the shoreface consist of large boulders that spilled down the steep mountain slope directly into the sea. The boulders consist of Table Mountain Group sandstone from the top of Karbonkelberg. Occasional granite outcrops are present along the coast. The landward margin of the beach is bordered by fynbos growing on what remains of the relic dune bypass from Hout Bay. Towards the southern part of the beach there is an increase in the occurrence of large boulders. The sand eventually disappears until only the boulder field remains. A small sandy beach is located just north of the main beach. This small beach is surrounded by granite outcrop and not connected to the surf zone.

In August the beach elevation varied between -1 and 3 m MSL. Most of the beach had a gentle, evenly graded slope, with only a small berm present on the northern side of the beach. A sand bar was noticed in the surf zone in the central part of the beach, and a channel located on the northern side next to the rock outcrop. By October there was a more pronounced beach berm all along the beach. There was a definite increase in sediment with the back beach elevation now at 4 m. The amount of boulders exposed on the southern side of the beach was much reduced and the rock outcrop on the northern side was set back further to the north. In January the sand volumes increase further, mostly with an increase in berm height. The boulder line on the southern side of the beach was set back by more than 100 m in places, increasing the overall length of the beach. Some of the rocky outcrops outlined in previous surveys completely disappeared.

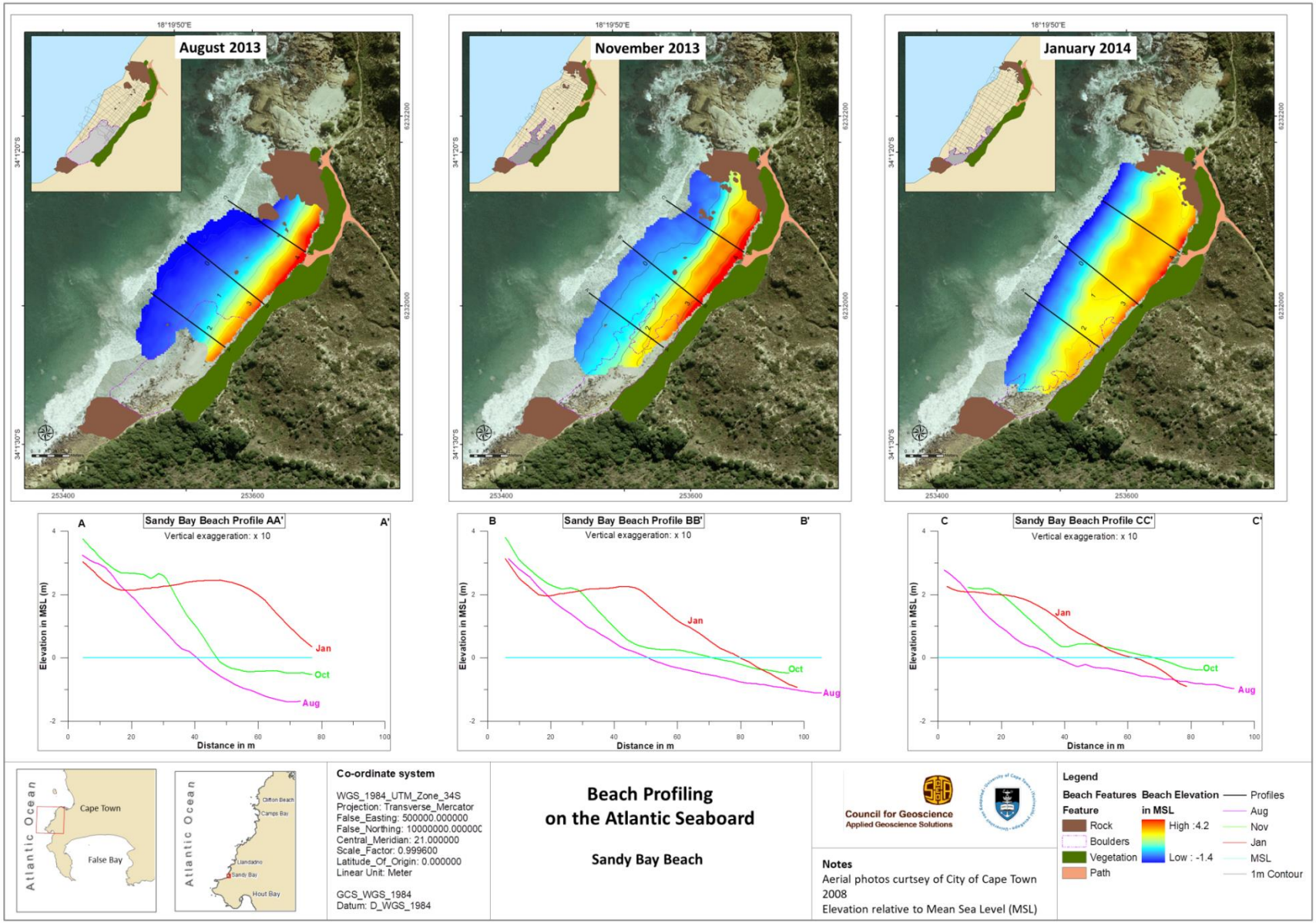

Figure 67: Sandy Bay beach profiling surveys with time series sections at 3 locations along the beach showing the change in elevation at each survey.

4.4.3 Karbonkelberg Sediment Bypass

On the Hout Bay side of the dune crest the dune slope is narrow with a gentle slope dipping towards Hout Bay (Figure 69). Closer to the crest the dune is between 30 and 40 m in width. About 160 m down the slope the dune starts to widen gradually until it reaches its maximum width of 290 m about 580 m from the crest. The dune extends further towards Hout Bay to a maximum distance of 1.2 km from the crest. The slip face on the Sandy Bay side of the crest is steep and consists of two steps to the base, which is only 138 m away from the crest. The width of the slip face is about 58 m at the maximum. The current aerial extent of the dune as measured from Google Earth images of 2015 is 13.123 ha, which is similar to the aerial extent measured in 2010 by MacHutchon (2013).

During 2014 the City of Cape Town started removing sand which was building up in the parking lot on the beach front in Hout Bay by truck and dumped it at the top of the Karbonkelberg sediment bypass dune crest. An estimated 30 000 cubic meters of sand were transported to the dune between 12 August 2013 and 25 October 2013 (pers. comm., Amy Davidson, 2016). The sand was flattened with a bulldozer, mostly towards the Hout Bay side, with the remainder towards Sandy Bay (Figure 68).

Figure 68: City of Cape Town disturbing the sediment on the crest of the Karbonkelberg dune.

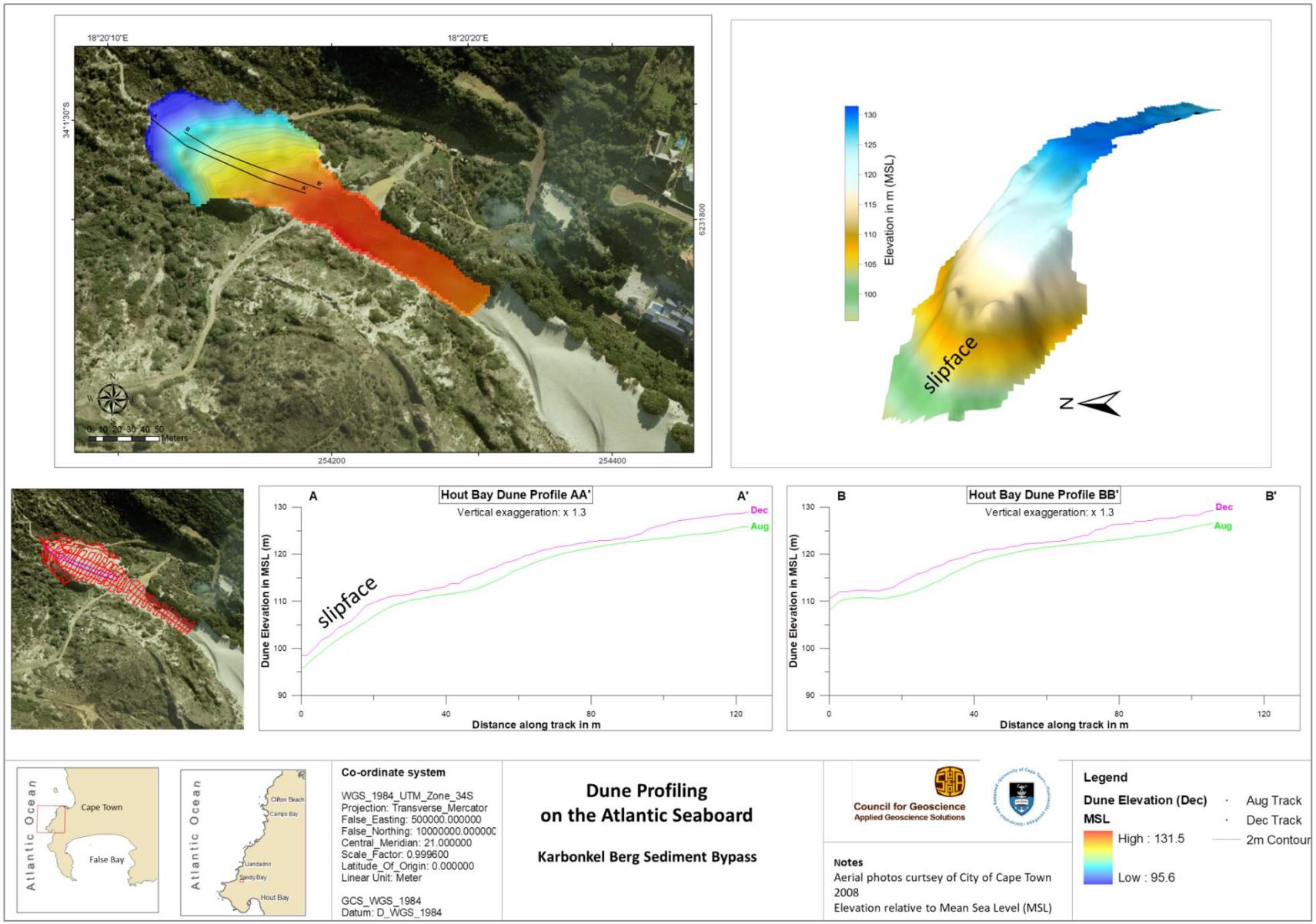

Figure 69: Dune profiling of the Karbonkelberg sediment bypass with 3D digital terrain model and profiles for each survey.

4.5 Sub-bottom Seismics

4.5.1 Regional seismic line

Inshore the regional seismic line shows a granite basement with a cover of sediment (Figure 71). The granite crops out occasionally to form high relief reef or in some cases scattered reef. The granite basement forms notable topographic highs at 60 m and 90 m BMSL. Pockets of Holocene sediment are found to the inshore of these topographic highs at 55 m and 100 – 105 m BMSL respectively. Possible marine terraces are seen at 120 m, 130 and 150 m BMSL. The offshore is covered by two thin Palaeogene or possibly Cretaceous deposits which on-laps onto the granite basement. These deposits are most likely of the Cape St Blaize Formation (Dingle and Siesser, 1975). These units have not been sampled during this project, there location has been interpreted from Dingle and Siesser (1975) and unpublished MGU data for the Cape Town sheet (Figure 11). Similar features were seen in a seismic line located to the north of the study area in Table Bay (Figure 70). This line crossed the Malmesbury Group (MacHutchon et al., 2018).

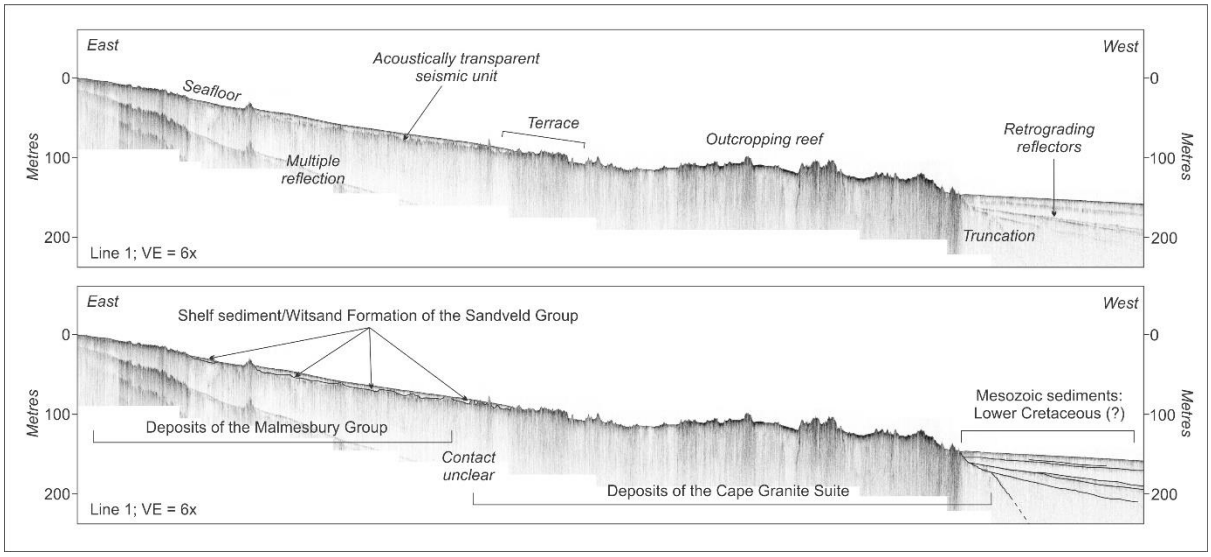

Figure 70: Seismic interpretation of a boomer line in Table Bay, (MacHutchon et al., 2018).

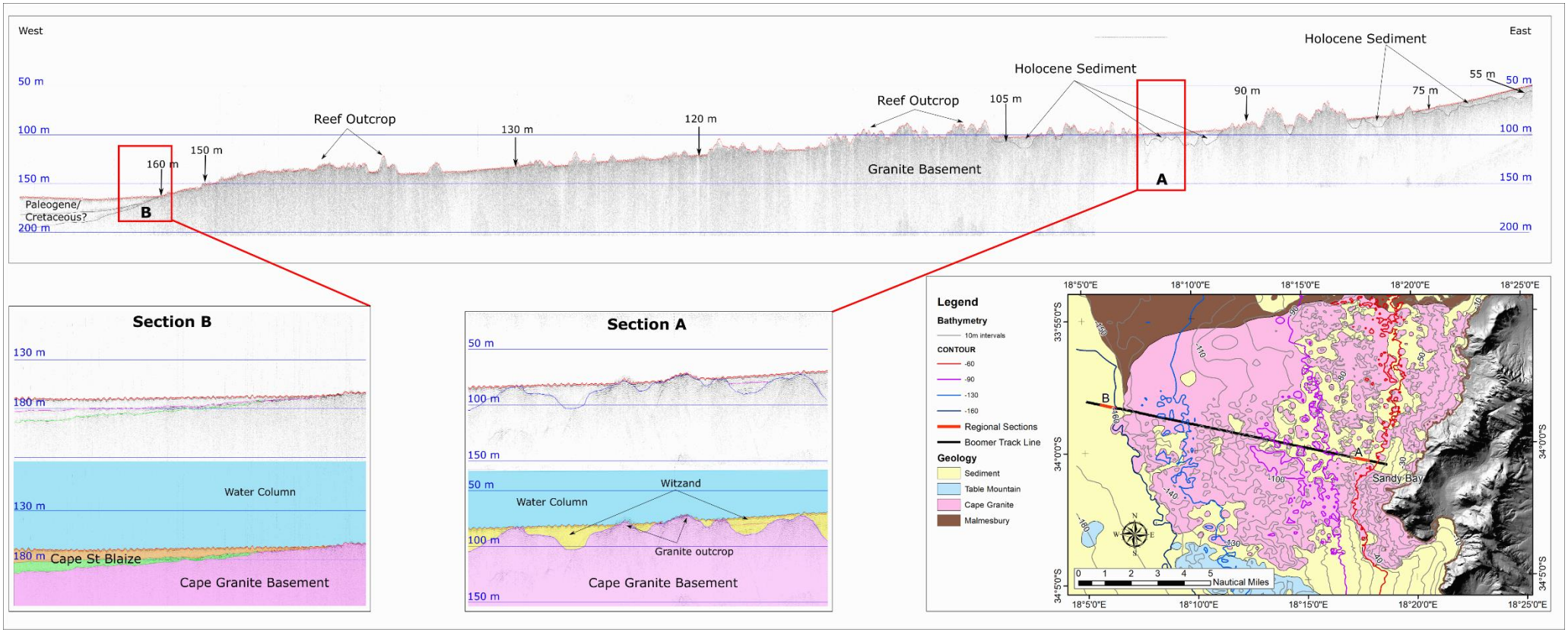

Figure 71: Regional seismic section, with raw (above) and interpreted (below) detail shown in section A and B, horizontal distance of the main profile is 22 km.

4.5.2 Inshore seismic survey

The inshore seismic survey resulted in 26 seismic profiles with a shore perpendicular orientation. The lines varied between 800 m and 2500 m in length. Two example lines are shown in Figure 72 and Figure 74 below. In most lines there is a change in slope about 650 m from the shore at a water depth between -33 and -36 m.

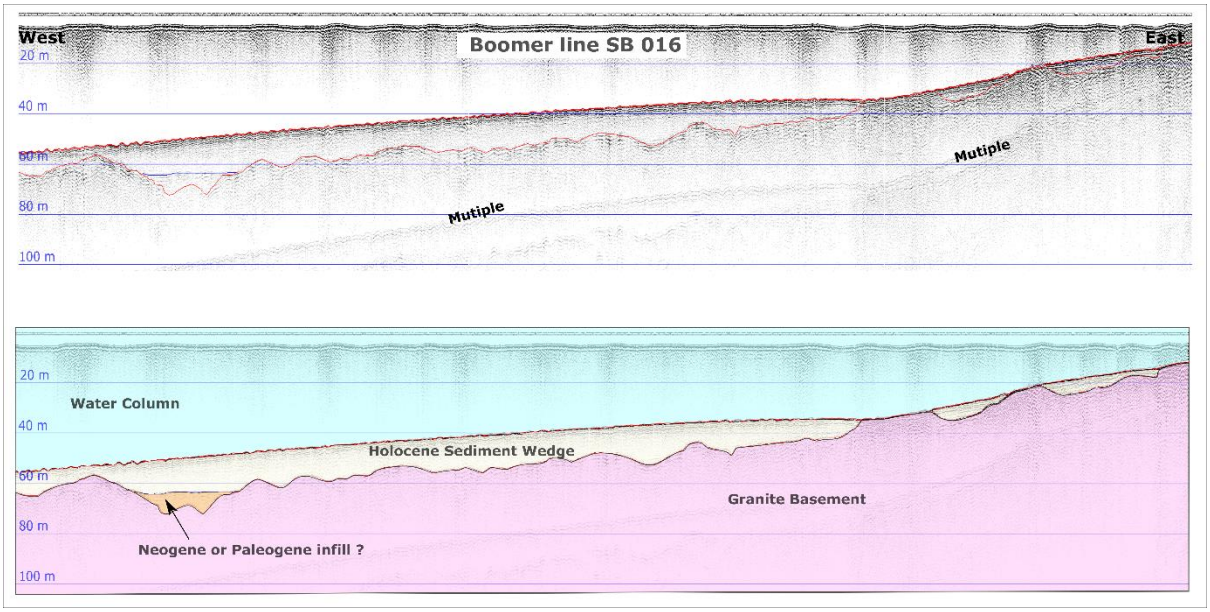

Figure 72: Seismic section SB 016 located in Sandy Bay, see Figure 74 for location, horizontal distance 2.2km.

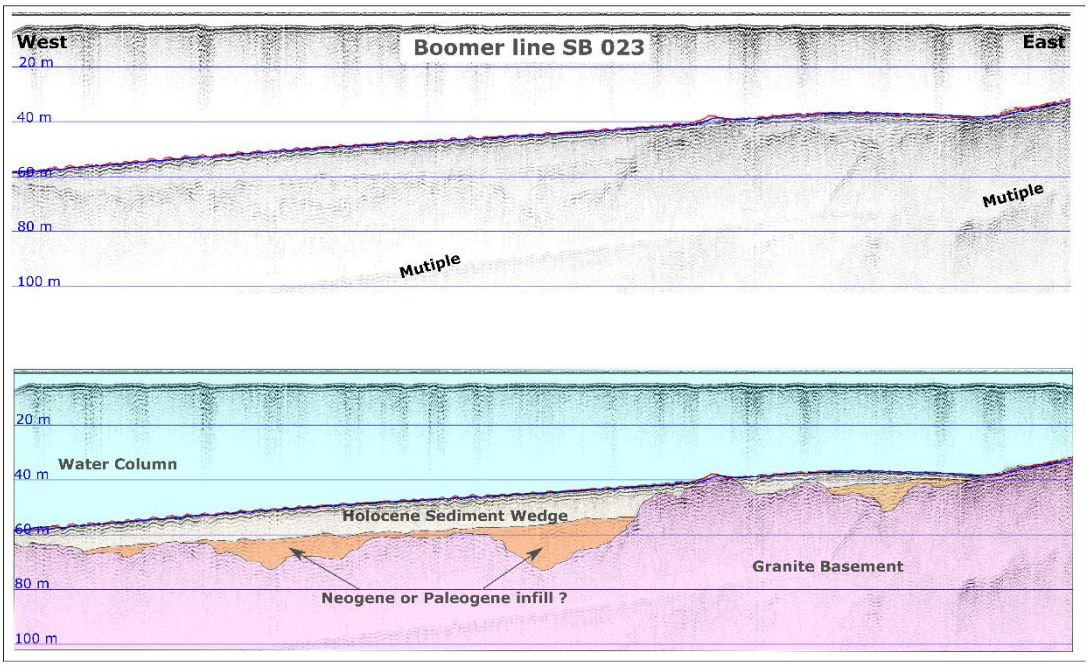

Figure 73: Seismic section SB 021 located in Sandy Bay, see Figure 74 for location, horizontal distance 1.7km.

Sediment filled pockets are confined by basement depressions, but a general increase is present towards the offshore. The basement has been interpreted as Cape Granite with two sedimentary packages within the basement depressions. An unidentified sediment deposit is present in some of the deeper basement depressions. This unit might be Neogene or Pleistocene in age, but without sampling and dating it is not conclusive. The Seafloor is mostly covered with Holocene sediments consisting of fine to medium grained sand and bioclastic gravel. The seismic record did not resolve the extent of the fine to medium grained sand vs the bioclastic gravel.

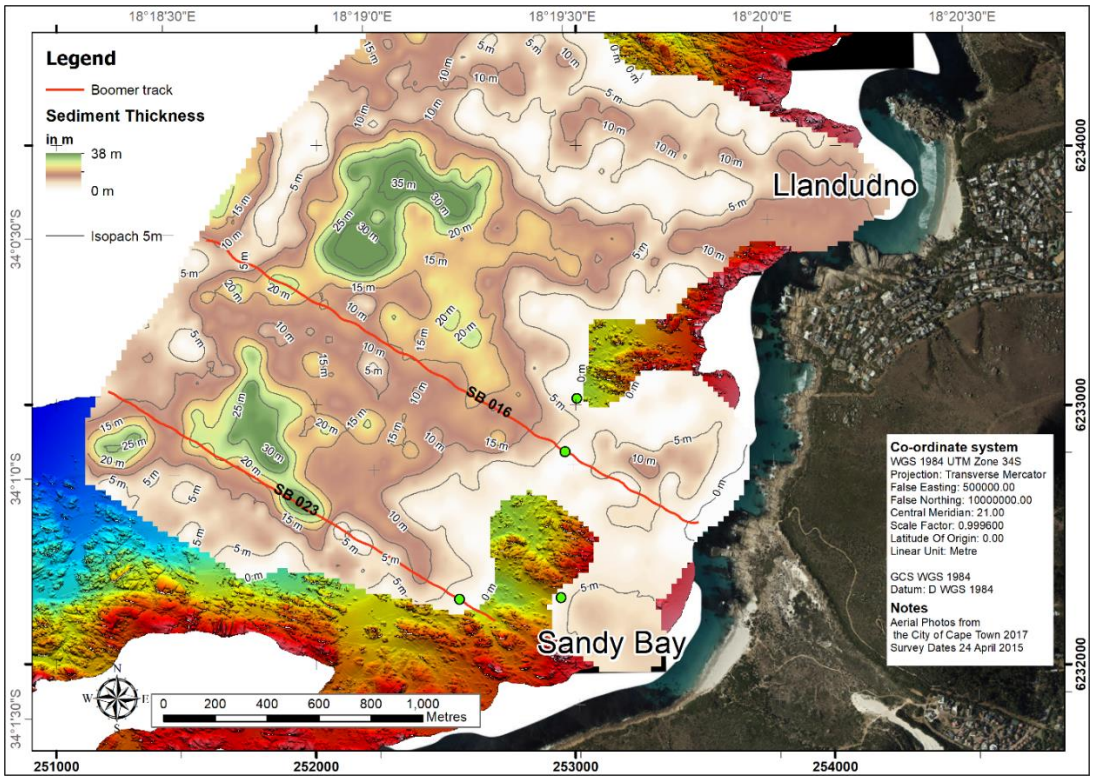

Figure 74: Sediment isopach chart derived from boomer data in the Sandy Bay area, with location of boomer lines SB016 and SB 023 indicated.

The sediment thickness or sediment isopach chart was derived from gridding the inshore seismic boomer data (Figure 74). The thickness shows unconsolidated sediment thickness to basement and no differentiation was made between different internal reflectors. The contours are drawn at 5 m intervals and show two deep depressions in the centre of the bay, reaching a thickness of up to 38 m in some places. The sediment thickness decreases towards the beaches where it reaches a maximum thickness of 5 m. The sediment thickness generally tapers off on the sides of the basin against rocky outcrops.

4.6 Sedimentology

The sedimentology results and settling tube plots for the study are shown in Appendix A. The carbonate content and mean grain size have been gridded and are displayed in Figure 75 and Figure 76, respectively. Figure 75 shows the distribution of percentage carbonate in the Sandy Bay area. The highest concentration of cabonate is located to the south west of the bay where the percentage is generally above 70%. Except for two high points in the centre of the bay the percentages decrease in a notherly direction reaching less then 40% in the northern extent of the sampled area. Close to Sandy Bay and Llandudno beaches the carbonate percentage is much lower. On and close to the beaches, the percentage starts at about 24%, gradually increasing away from the beach to about 40%.

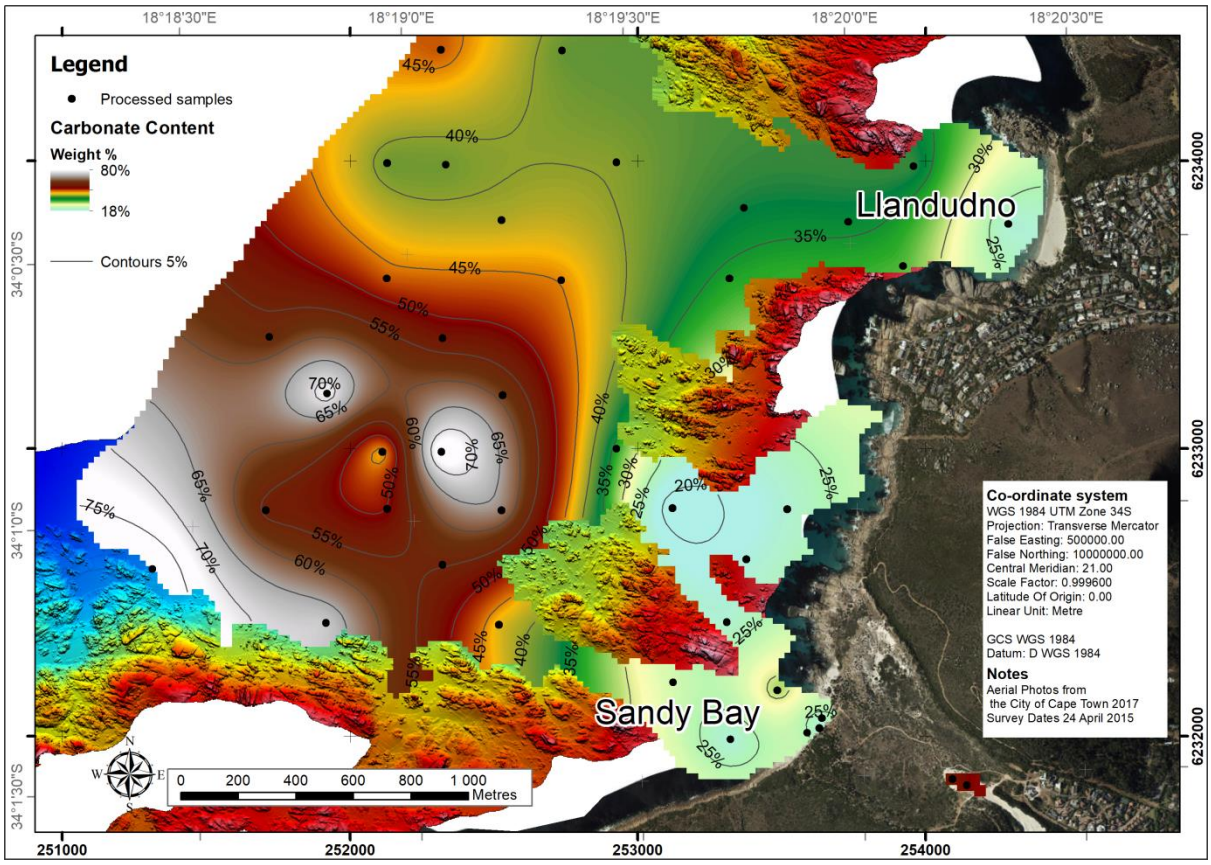

Figure 75: Percentage carbonate content for Sandy Bay.

The mean grain size grid shown in Figure 76 shows a very similar trend to the carbonate content grid. The largest particles are found to the southwest of the bay from where it decreases from 0.8 mm to 0.3 mm in the north of the bay. The mean grain size close to Sandy Bay and Llandudno beaches first decreases in size slightly before it increases again. In the case of Sandy Bay beach, the grain size starts with 0.36 mm on the beach, decreasing to 0.28 mm and increasing to 0.40 mm before transitioning into the large grain size area to the southwest. The mean grain size of Llandudno starts off slightly higher at 0.40 mm, decreasing to 0.30 mm further offshore.

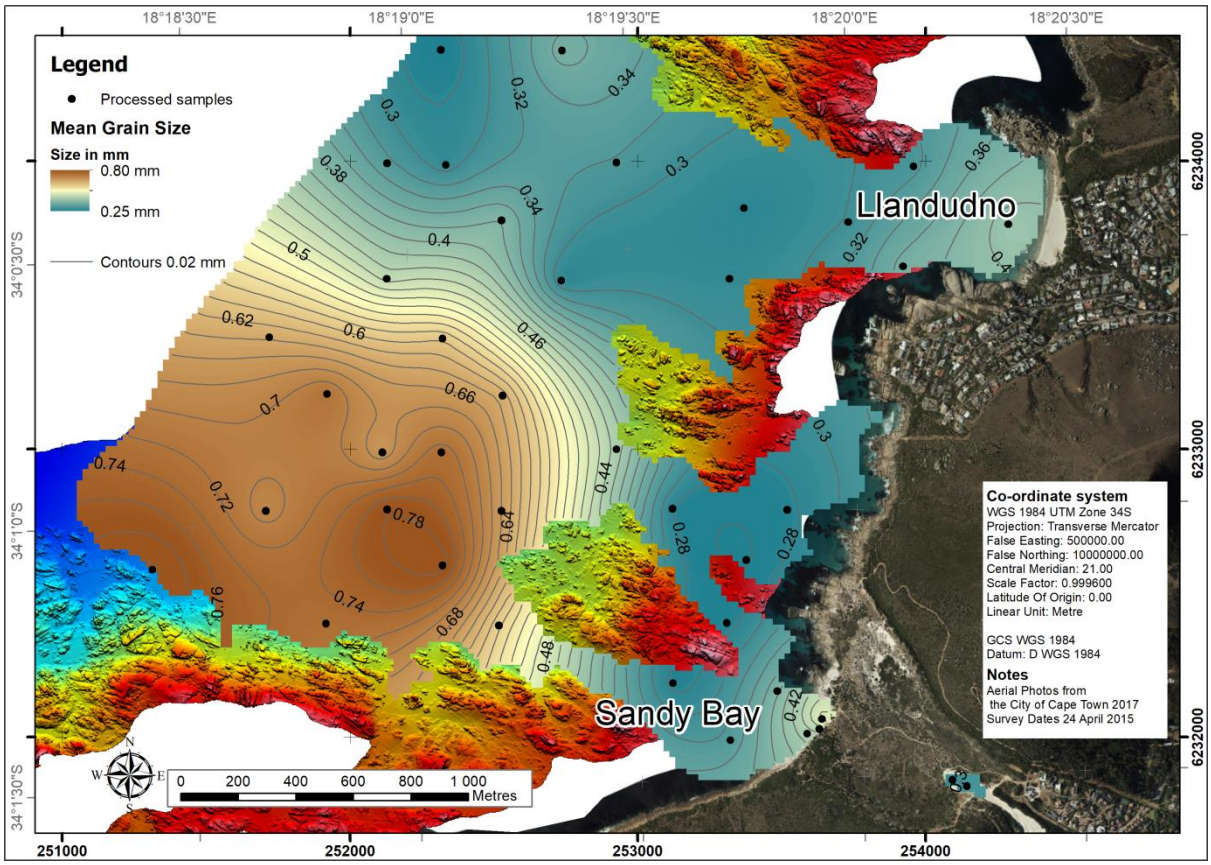

Figure 76: Mean grainsize (in mm) distribution for Sandy Bay.

4.7 Seafloor Geology

The geophysical, hydrographic and sedimentological results have been consolidated to create an acoustic seafloor facies chart (Figure 77). The seafloor facies chart is shown in more detail as charts 1 to 4 in Figure 78 to Figure 81. The coastline in the study area consists mostly of a steep rocky shoreline with isolated sandy beaches. The sandy beaches constitute only 2.7 km of the 33.3 km of coastline. The four main beaches are found between Duiker Point and Mouille Point, namely Sandy Bay, Llandudno, Camps Bay and Clifton Beach (Figure 77). Some smaller sandy beaches are found, mostly in the northern part of the survey, but these tend to be located behind a rocky surf zone on the back beach. Boulder beaches can be found between Bakhoven and Oudekraal (Figure 79). Some areas of scree were identified near Oudekraal, the southern end of Sandy Bay and Maori Bay (Figure 81). Scree is classified as angular cobbles and boulders at the base or on the slope of mountain sides. These occurrences of scree consist of angular sandstone cobbles and large boulders with a limited transport history from the adjacent Table Mountain Group sandstone higher up the mountain.

Several large prominent rocky reef complexes are found along the Atlantic Seaboard study area. These reef complexes are associated with adjacent onshore mountains or headlands which extend into the ocean. In the southern extent of the survey area, a large prominent reef complex can be observed in association with Karbonkelberg and Duiker Point (Figure 81). Karbonkelberg is a resistant Table Mountain Group sandstone peak with a height of 653m AMSL (Theron et al., 1992). It drops down steeply to the coastline at its base from where the reef system extends to -70 m. Between Llandudno and Camps Bay is a series of mountain ridges known as the Twelve Apostles. This coastal range varies between 700 and 900 m AMSL and descends steeply to the coastline on the seaward margin. The second largest offshore reef complex extends out to sea from the southern end of the Twelve Apostles range (Figure 80). A shallow pinnacle within the reef complex is locally known among divers as the Thirteenth Apostle. Another substantial reef complex can be found at the northern extent of the Twelve Apostles, offshore of Camps Bay (Figure 79). This reef extends from the shoreline south of Camps bay beach in a north westerly direction to about 3 km offshore. The fourth large reef complex in the study area lies offshore of Clifton Beach

(Figure 78). Above Clifton Beach is the iconic Cape Town mountain peak known as Lion's Head.

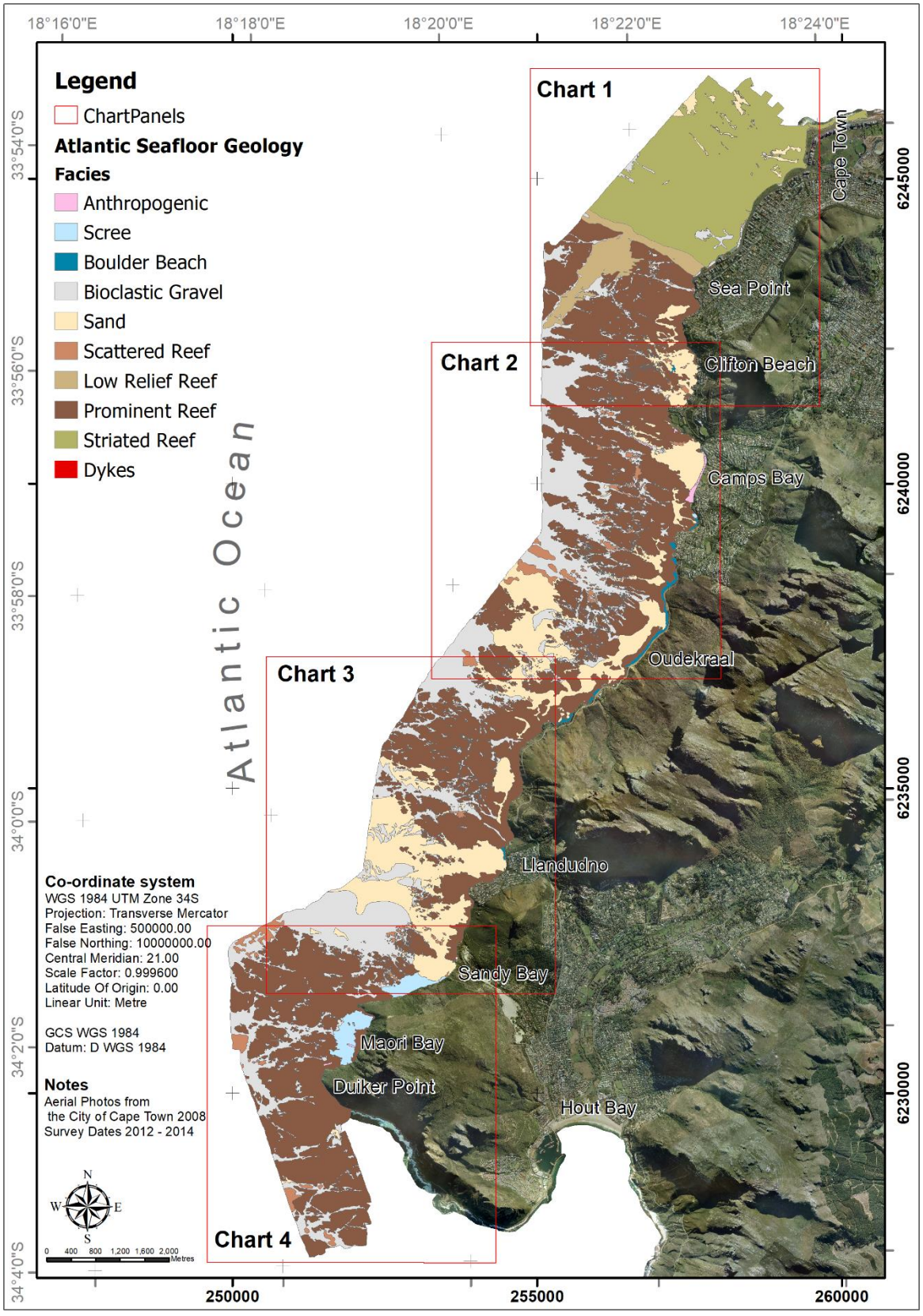

Figure 77: Interpreted facies of the Atlantic Seaboard, combining side scan sonar, multibeam bathymetry and coastal mapping results (See Appendix D and Figure 78 - Figure 81 for enlarged seafloor facies chart).

Clifton Beach is enclosed by two ridges which extend down from Lion's Head extending offshore to form what is locally known as Lion's North and South paws. The fifth prominent reef complex crops out of Bantry Bay and Sea Point. This reef consists of the Prominent Reef facies which outcrops close inshore and a smaller outcrop is situated in the offshore extent of these data. This smaller outcrop is the northern most occurrence of the Prominent Reef facies.

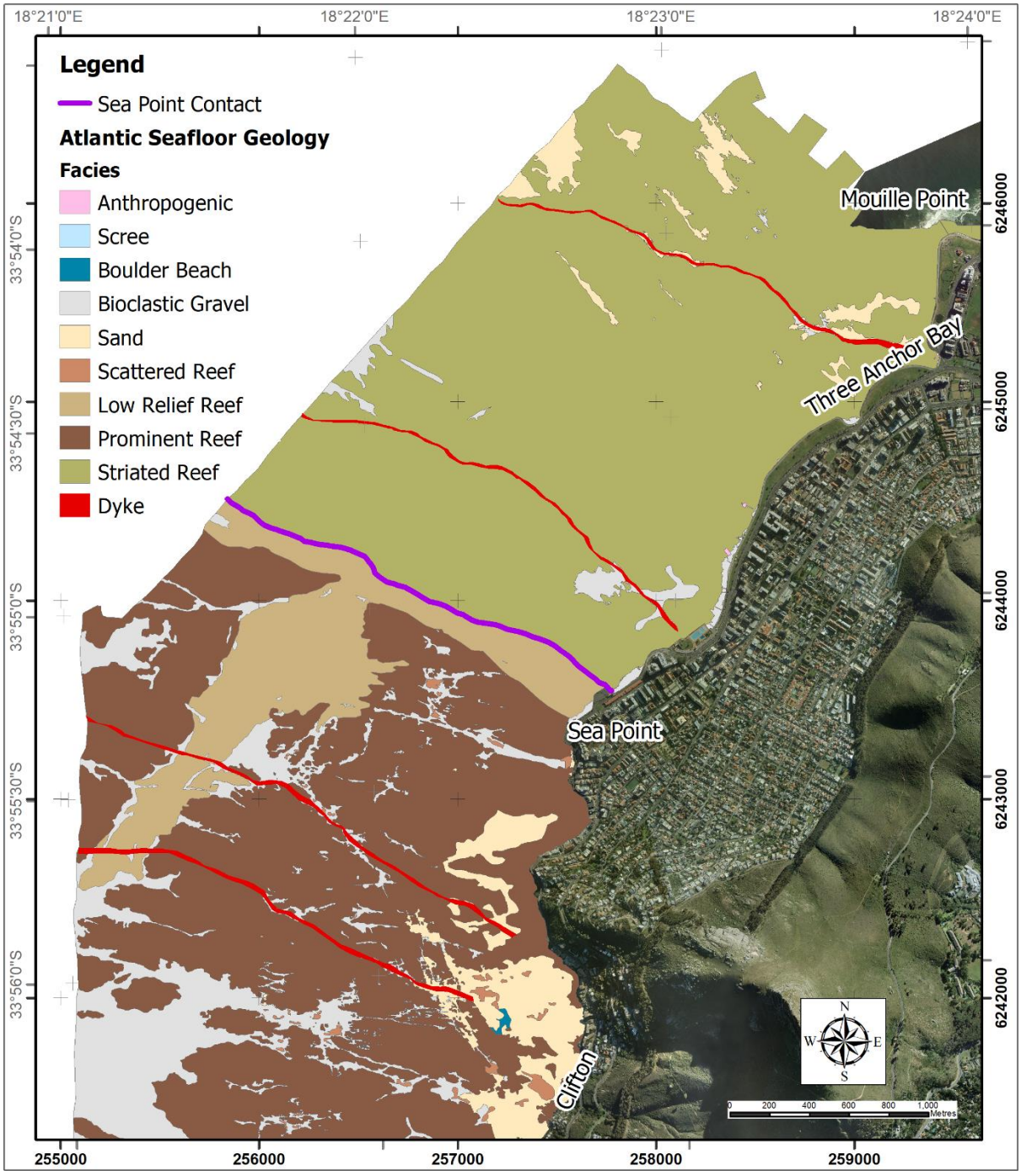

Figure 78: Interpreted facies chart 1, striated reef dominates the north of the Sea Point contact, and prominent reef to the south. Fine to medium grained sand is found inshore on the Clifton pocket beach and in inshore channels, while bioclastic gravel are found further offshore.

Smaller areas of prominent reef interspersed with scattered reef and unconsolidated sediment occur in the Sandy Bay/Llandudno area and the Oudekraal/Bakoven area. In these two areas, small reef complexes are found scattered within larger unconsolidated sediment areas. In both locations the unconsolidated sediment coverage increases further offshore.

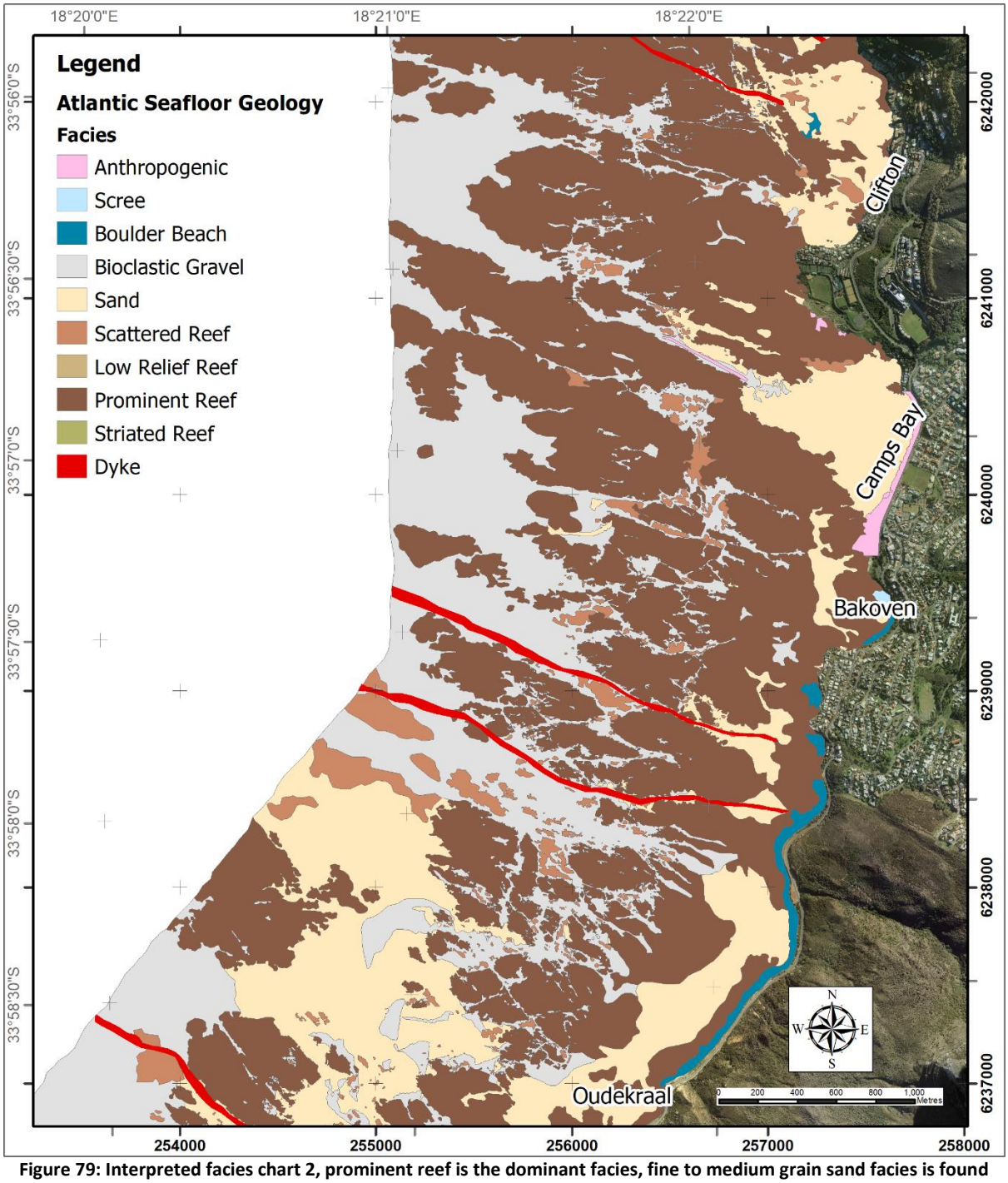

Figure 79: Interpreted facies chart 2, prominent reef is the dominant facies, fine to medium grain sand facies is found inshore on pocket beaches and sediment filled channels north of Oudekraal and in deposits offshore of Oudekraal. Sediment further offshore is mostly bioclastic gravel. Boulder beaches are located on the shore line between Oudekraal and Bakoven.

The largest continuous area of unconsolidated sediment is located offshore of Sandy Bay and Llandudno. The sediment area, which stretches from Karbonkelberg reef complex in the south to the Twelve Apostles reef complex in the north, is 2.8 km at its widest and extending 1.2 km offshore to the extent of the survey and beyond.

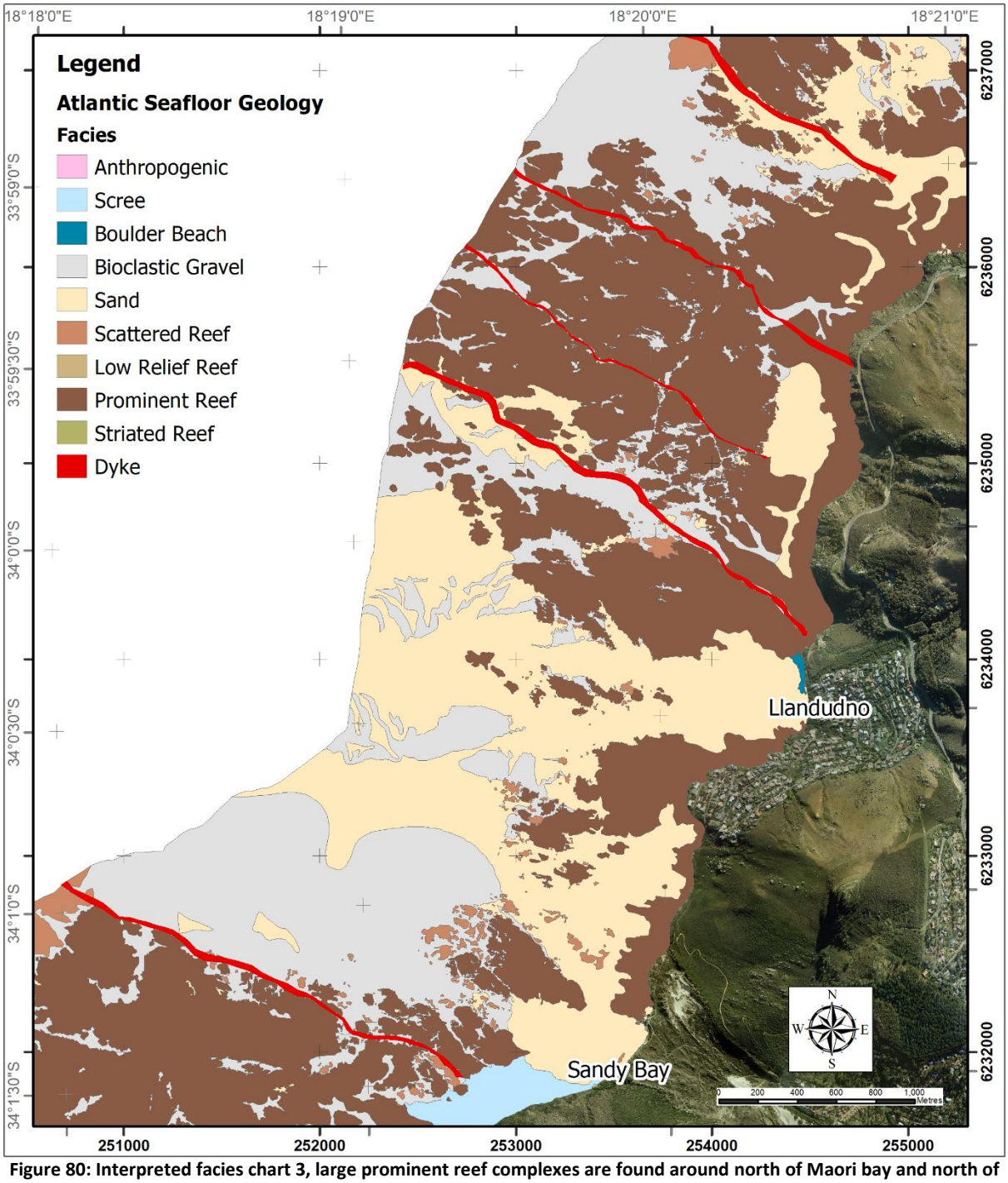

Figure 80: Interpreted facies chart 3, large prominent reef complexes are found around north of Maori bay and north of Llandudno, a large area of fine to medium grained sand facies are located between Sandy Bay and Llandudno with some inshore channels continuing north of Llandudno. Bioclastic gravel is located to the north of each of the reef complexes.

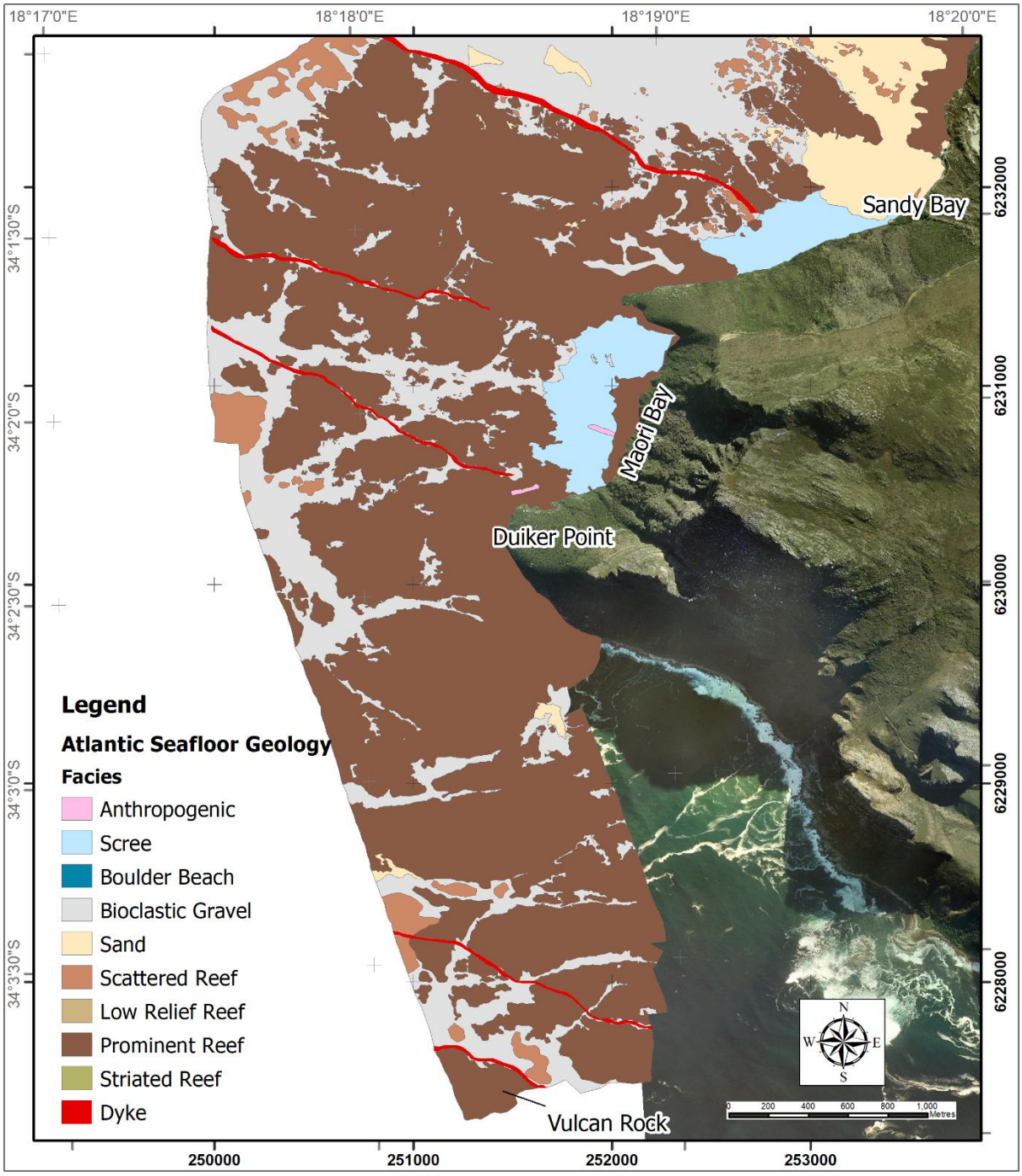

Figure 81: Interpreted facies chart 4, dominated by prominent reef associated with the Duiker Point headland, small areas of scree located close to shore and on the south of Sandy Bay beach. The sediment filled channels between the prominent reef consist mainly of bioclastic gravel.

Narrow, coast-parallel, channels with sediment fill can be observed close inshore between 100 and 300 m from the shoreline. The channels vary in width between just a few metres up to 300 m. The channels form an almost continuous connection from Sandy Bay in the south to Bantry Bay in the north. The channels are interrupted in several locations by prominent

reef outcrops, for example the headland at Little Lion's Head between Sandy Bay and Llandudno, the southern extent of Camps Bay and the southern extent of Clifton Beach or Lion's South Paw. Sediment filled channels with a northwest south east orientation running from inshore to offshore can be observed in most areas along the coastline.

North of Sea Point the seafloor changes to low-relief striated reef. The reef areas display clearly defined bedding planes. The area contains few, relatively small sediment patches, mostly contained within linear gullies. The coastal plain tends to be wider with a gentler slope descending from the mountain ridge between Lion's Head and Signal Hill, which forms the "rump" of the lion. The coastline in this area has been altered extensively by built structures in the form of concrete sea walls, tidal pools, outfall pipes and breakwater constructions.

5 Discussion

Many of the coastal features in this study can be related to the underlying bedrock geology. The coastal geomorphology is determined by the way the bedrock weathers, which in turn determines the location of pocket beaches vs rocky headlands. The principal rocks are discussed here from oldest to youngest in terms of how they influence coastal morphology, bathymetry and other aspects of the coast. Table 10 presents the seafloor facies and how the facies relates to the geological units present in the study area.

Seafloor Facies	Geology	Description
Prominent Reef	Cape Granite Suite	High relief reef with variable topography, including visible joint and fracture patterns.
Striated Reef	Malmesbury Group	Low relief reef with clear bedding planes. Structural features such as folding and faulting can be observed.
Scattered Reef	Minor outcrops of Cape Granite Suite within sediment	High to moderate relief reef areas, interspersed with sediment, mostly a thin veneer covering prominent reef areas.
Low Relief Reef	Micro Granite and Sea Point contact zone	Low relief reef with no distinct bedding planes or bedform orientation.
Bioclastic Gravel	Witzand Formation	Rippled gravel, consisting mostly of shell fragments.
Fine to Medium Grained Sand	Witzand Formation	Unconsolidated sediment, consisting of quarzitic sand and up to 30% shell.
Boulder Beach	Quaternary Cover	Well-rounded cobbles and boulders.
Scree	Quaternary Cover	Unconsolidated, angular cobbles and boulders; generally accumulated at the bottom of steep slopes.
Anthropogenic Features		Man-made objects and features, such as buildings, sea walls, pipelines, shipwrecks. and other built structures

Table 10: A description of the seafloor facies used and the equivalent geological unit.

5.1 Malmesbury Group

The rocks on the seafloor between Sea Point and Mouille Point have been mapped as the Tygerberg Formation which forms part of the Malmesbury Group (Zone A in Figure 55). Although the Malmesbury Group deposits are poorly exposed onshore with only narrow strips exposed at the coast (Theron et al., 1992; Von Veh, 1983), it is extensively exposed offshore between Sea Point and Robben Island, as shown in unpublished Joint Geological Survey and University of Cape Town Marine Geoscience Unit data from the 1970's and 1980's. These datasets include Thomas B Davie cruise SF88, and Technical Report 14 (Woodborne, 1983).

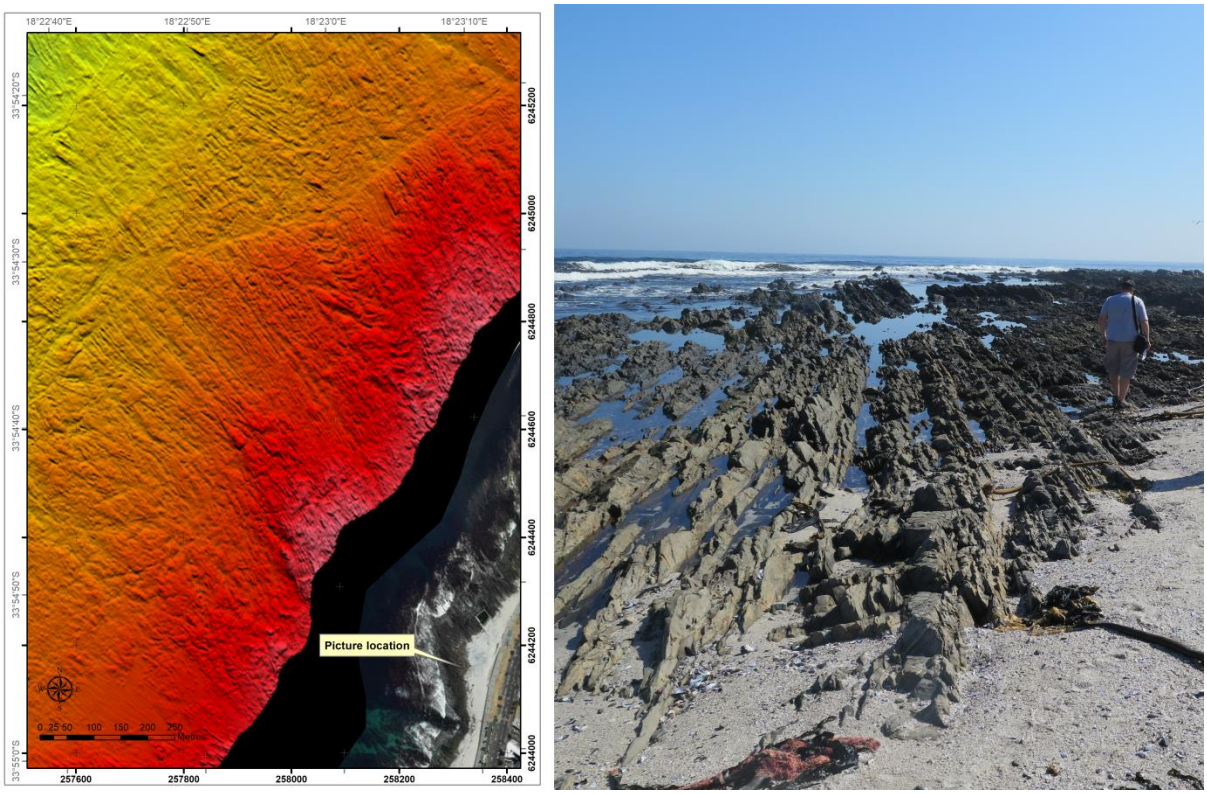

Figure 82: Malmesbury Group rocks exposed near Sea Point during low tide. The NNW orientated bedding results in the striated nature of the facies in the side scan sonar and multibeam bathymetry data.

The Malmesbury Group rocks can be identified on the multibeam and side scan sonar data collected during this project by their striated nature (striated reef facies) which are a result of upturned bedding planes, alternating beds of variably resistance, and the low relief seafloor (Figure 82). The orientation of the bedding planes is mostly NNW, except in the case of a tight anticlinal fold structure on the seafloor between Sea Point and Three Anchor Bay. This fold structure consists of a tight anticline-syncline pair and can probably be connected to the syncline fold axis described at Rocklands Bay by Von Veh (1983). The fold

axis seems to be offset, but this could be explained by a number of faults running coast parallel inferred by Von Veh (1983) and observed on the multibeam data. The general NNE orientation of the bedding on the offshore data matches well with observations and measurements done onshore by Von Veh (1983).

5.2 Sea Point Contact

The Sea Point contact is a mixing zone between 200 and 300 m in width located between the Malmesbury Group rocks to the north and the Cape Granite Suite rocks to the south (Von Veh, 1983). Onshore the contact can be seen at Sea Point with the dark Malmesbury Group rocks the north and the lighter coloured Cape Granite to the south (Figure 83). On the CGS 1:50 000 Cape Town sheet it has been mapped as microgranite and hybridic microgranite with hornfels xenoliths (Theron et al., 1992).

Figure 83: The Sea Point Contact, with the dark Malmesbury Group rocks on the left and the lighter coloured Cape Granite on the right and Lions Head in the background.

The unpublished historical offshore data boundary seems to be on the northern side of the contact and thus includes the transition zone with the Cape Granite Suite. The transition zone cannot be distinguished as a clear separate lithological facies on the most recent geophysical and hydrographic data collected for this project. The zone has therefore been digitized by extrapolating the onshore contact zone boundaries in some places (Figure 78). An anomalous low relief extension can be seen extending from the contact boundary in a

SW direction, eventually tapering out at about 2 km from the contact boundary (Figure 56 and Figure 78). Identification of the feature proved to be problematic, the low relief seems to compare with the Malmesbury Group relief, but the fabric orientation does not seem to fit with the normal NNW direction. This feature has therefore been interpreted as part of the contact zone and classified as microgranite and probably came as the result of weathering of the granite by a lower sea level between 27 and 32 m BMSL. Possible erosional features which appears as drainage channels on the MBES data supports this theory (Figure 56).

5.3 Cape Granite Suite

From Sea Point south, almost the entire exposed prominent reef and scattered reef acoustic facies can be classified as part of the Cape Peninsula Pluton of the Cape Granite Suite. Granite has been mapped onshore all along the coast from Sea Point to Hout Bay (Figure 77). Exposed rocks close to the shoreline can be confidently interpreted as granite (Figure 84).Granite has been identified offshore on numerous dives during the project (Figure 85). A typical characteristic of granite in the area is the presence of conjugate joint sets (Figure 86). The joint sets are widely spaced, which results in the granite weathering into large boulders. Granite tends to weather by a process of exfoliation, which results in the characteristic rounded boulders or core-stones seen along the coastline.

Figure 84: Exposed granite core-stones near Oudekraal, with Lion's head in the background.

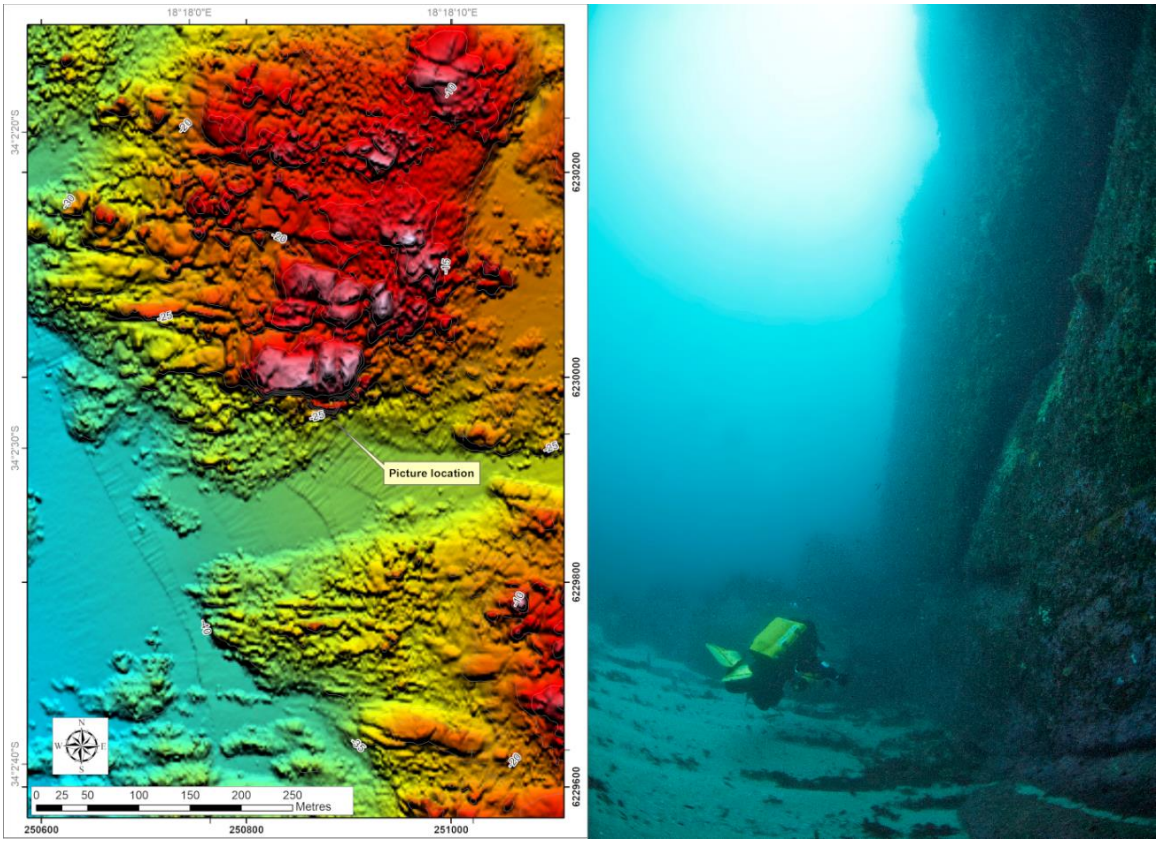

Figure 85: Example of prominent reef facies, identified as granite on the left. A diver at 30 m water depth next to the same vertical wall of granite, extending to just below the surface at 5 m water depth. (photo credit Jean Tresfon).

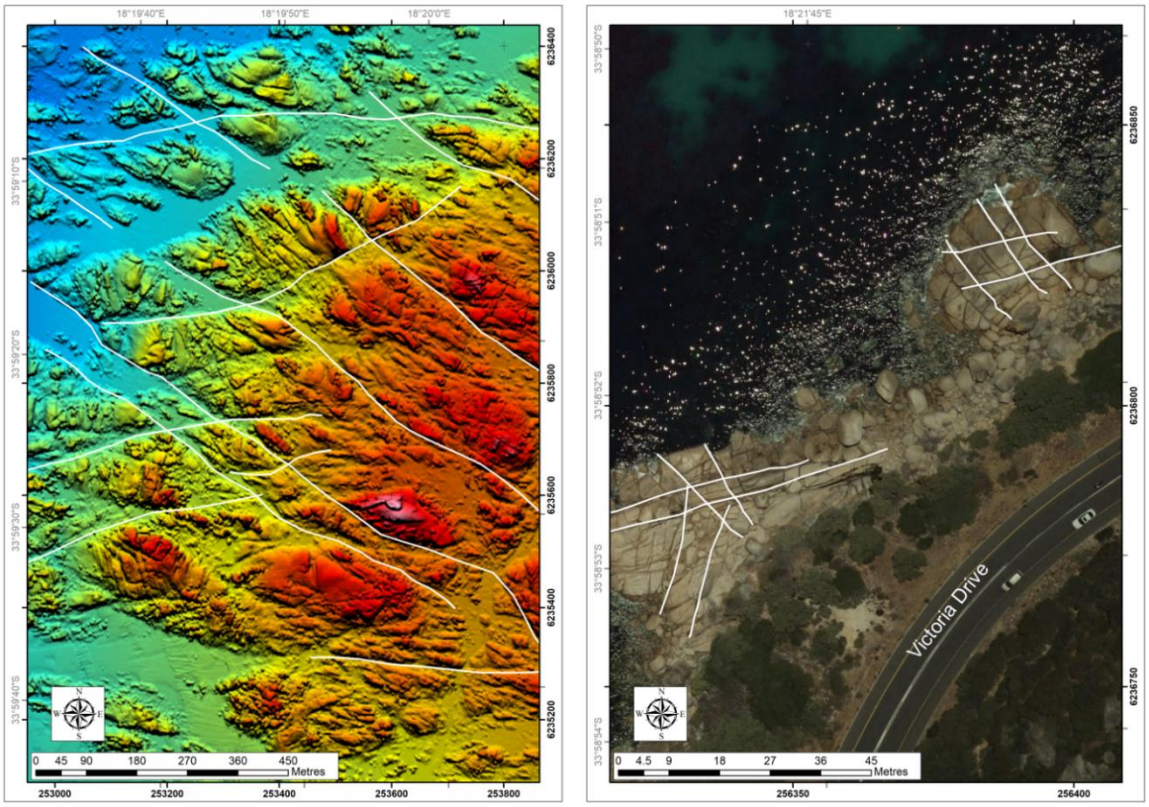

Figure 86: Conjugate joint sets shown in the multibeam data on the left and onshore from Aerial photography on the right, both charts located in the Oudekraal area along Victoria Drive.

5.4 Table Mountain Group

Although the TMG sandstones are not represented on the seafloor anywhere in the study area, these deposits are represented by the mountain range immediately onshore of the area and play an important part in the coastal geomorphology of the study area, by forming a resistant outlier of the Cape Super Group (Compton, 2004). The resistant Peninsula Formation forms the iconic Table Mountain which also has an influence on the local weather patterns of the peninsula, by influencing wind and rainfall patterns.

5.5 Dolerite Dykes

Dolerite dykes show up as distinct linear anomalies, which can be either positive or negative. The magnetic signature of the dolerite is due to the presence of magnetite in the dolerite dyke, while the different magnetic orientation is due to the dykes being emplaced at different times with different orientations in Earth's magnetic field (Ogg et al., 2016).

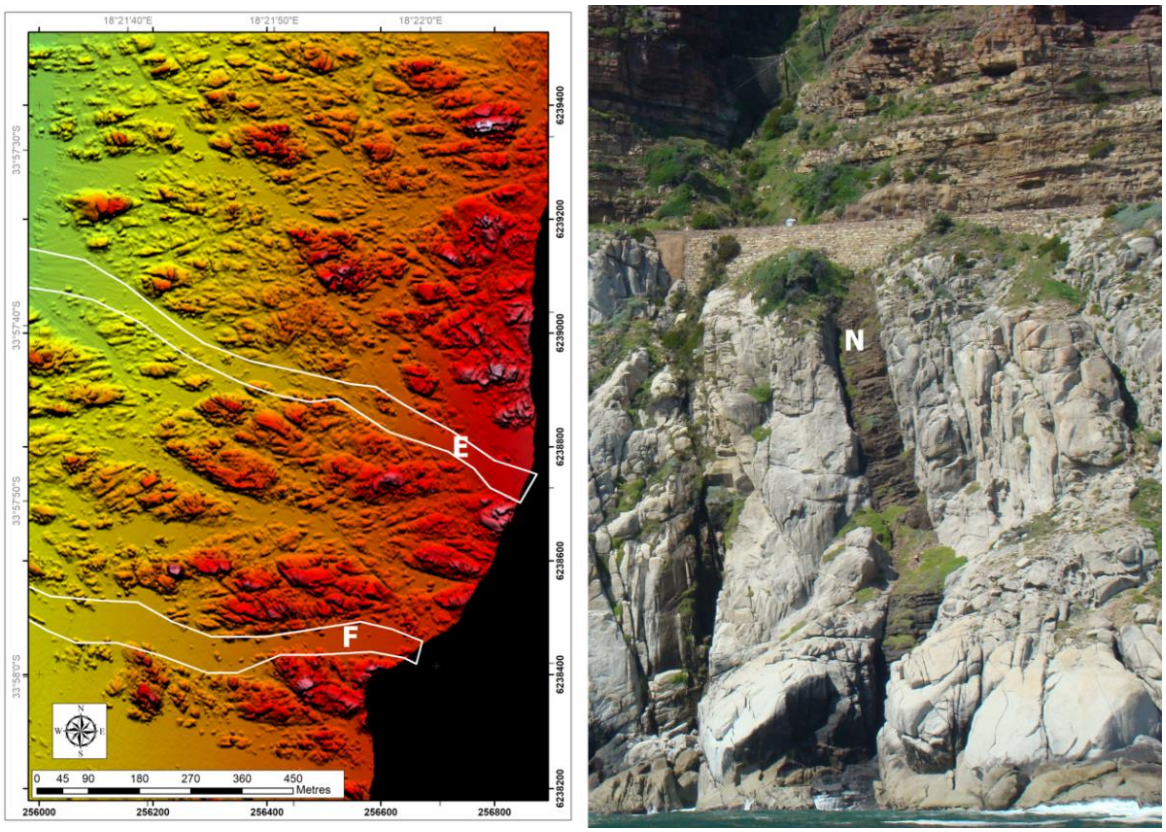

Figure 87: Dykes E and F near Oudekraal, appearing as sediment filled gullies in the granite basement on the left, on-shore equivalent of dyke N cutting into the granite basement below Chapman's Peak Drive on the right (see Table 9) (photo credit Hayley Cawthra)

The dykes weather as negative gully features in most cases (Figure 87), suggesting that the dyke material is more susceptible to weathering than the host rock (granite or Malmesbury). The gullies representing the dykes are mostly sediment filled and the actual dolerite rocks are seldom exposed (and perhaps why their onshore outcrop is often not mapped). Previous studies, both onshore and offshore have identified numerous dykes in the area (Day, 1986; Reid et al., 1991). Reid et al. (1991) identified 10 dolerite dykes belonging to the False Bay Dyke Swarm in the area. An 11th dyke mapped in Maori Bay probably corresponds to one of the dykes exposed on Chapman's Peak (Table 9). To the south, MacHutchon (2013) identified several dykes with a similar orientation in the Hout Bay area, which could be traced to Chapman's Peak.

5.6 Cenozoic Deposits

5.6.1 Witzand Formation

The Holocene Witzand Formation is well represented in the study area by dune fields, pocket beaches and offshore sediment deposits. The beaches within the study area consist mostly of fine to medium grained quartzose sand with a carbonate content of about 30% (Holmes and Luger, 1996; MacHutchon, 2013). Offshore, the sediment composition is more varied and can grade from a fine to medium grained quartz sand with 30% carbonate content to bioclastic, shelly gravel with carbonate content in excess of 90%. The shelly gravel is mostly found close to reef outcrops and present as a rippled texture on the side scan sonar data. The carbonate content and grain size gradually decrease away from the outcrop.

The possible reason for this phenomenon is the reefs are the source of the bioclastic gravel or shell, as this is where many of the sessile shell organisms live (mostly limpets and the black mussel *Choromytilius meridionalis*); the shell content then disperses away from the reef. The grain size decreases away from the reef either due to preferential transportation of smaller grain size particles, or the transport process tends break the shell into smaller particles as it is transported over time and distance.

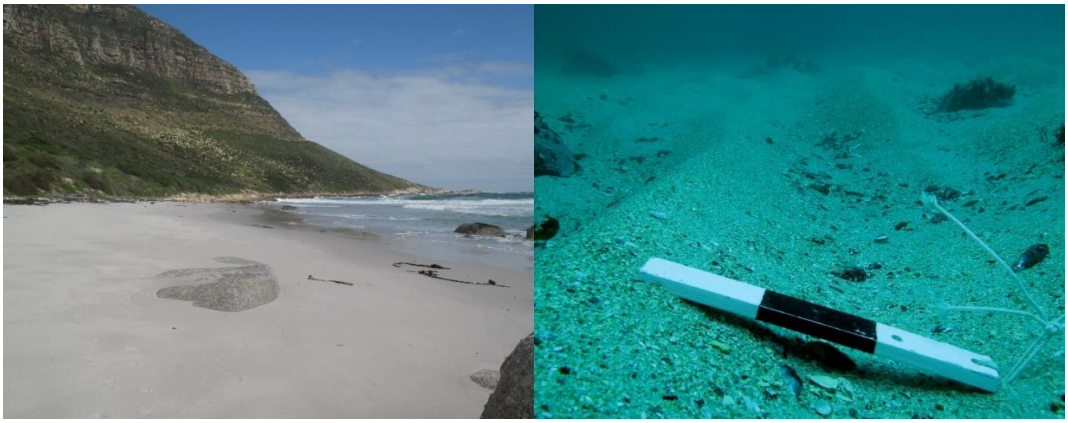

Figure 88: Fine to medium grained sand on Sandy Bay and rippled bioclastic gravel offshore of Oudekraal. Scale bar equals 30 cm in length.

5.6.2 Scree

Scree can be found in the southern part of the study area, most notably on the seafloor in Maori Bay and the southern end of Sandy Bay beach. The scree consists of large boulders and cobbles of TMG sandstone scattered on the slopes of the Karbonkelberg and extending to the surf zone. Scree is generally found in areas where there are steep slopes. Angular cobbles and boulders of granitic origin are found in some places, notably close to current sea level where large granite outcrops have started to break up due to weathering and wave action (Figure 89). Due to the angular nature of these cobbles and boulders it can be inferred that they have not been transported any significant distance and most probably remained where the original granite intruded.

Figure 89: A mix of well-rounded sandstone boulders and angular granite boulders seen at Oudekraal at current sea level.

5.6.3 Boulder beaches

Boulder beaches are present in the study area, with the most prominent one just to the south of Bakoven along the shoreline (Figure 90). The boulder beach consists of large cobbles to boulder size, well-rounded mostly sandstone and minor occurrences of granite rock. On the southern end of Sandy Bay beach, the boulders are periodically covered with sand from the beach during the seasonal changes in sand volume. Remnants of a paleo boulder beach were found on a dive in the Oudekraal region. The boulders follow a coast parallel trend between 9 and 10 m water depth. It is therefore very likely that other boulder beach deposits are found offshore where they are mostly covered by shifting sediment deposits.

Figure 90: Boulder beach located south of Bakoven next to Victoria Drive.

In some areas the differentiation between scree and boulder beach can become difficult to resolve as there can be a considerable amount of mixing. At Oudekraal, just above mean sea level, the well-rounded sandstone boulders are well-mixed with more recently weathered, angular granite boulders. In this case the well-rounded sandstone boulders are interpreted to be remnants of an older boulder beach with granite material deposited more recently close to the current shoreline.

5.7 Anthropogenic Features

5.7.1 Engineering structures

Anthropogenic modification of the coastline can be observed, particularly in the northern part of the study area. To protect the coastal infrastructure, a sea wall has been constructed extending from Sea Point to Mouille Point. The sea wall varies in height from 4 to 6 m and leaves only a narrow exposure of rock and beach, exposed during low tide (Figure 91). There are four small pocket beaches between the sea wall and the exposed Malmesbury Group rock outcrops consisting of coarse bioclastic gravel and medium-grained sand clasts. These sea walls are under constant threat of being damaged by large winter storms. During a recent storm of 2017, the sea breached the sea walls and caused extensive damage by flooding in Sea Point and Three Anchor Bay. With rising sea levels and climate change this type of event can be expected to occur on a more regular basis (Woodroffe, 2002; Chen et al., 2017).

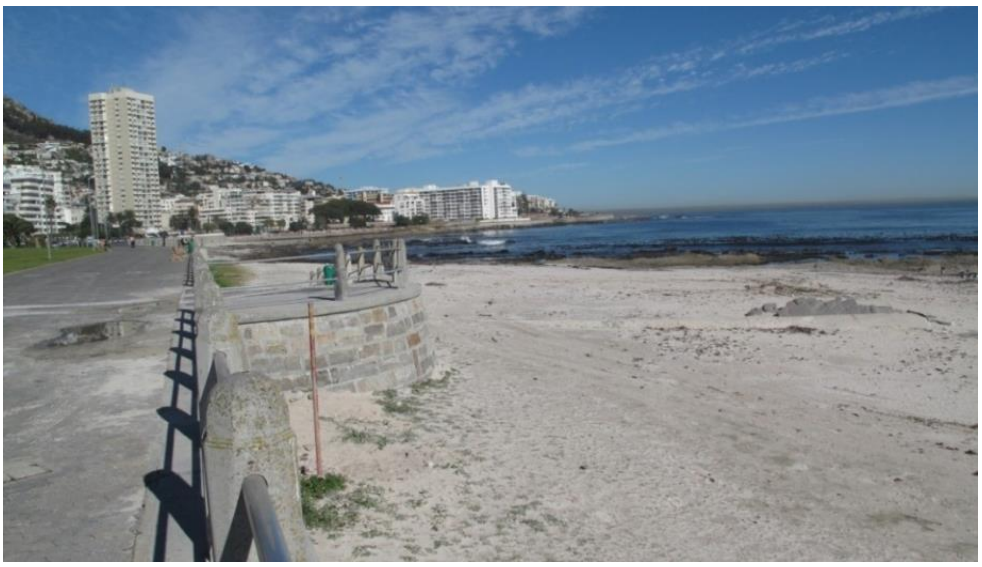

Figure 91: Sea Point promenade protected by a sea wall with outcrop of Malmesbury Group rocks and pocket beaches. These beaches are mostly above the high water mark and only affected by waves during storm events.

Between Sea Point and Camps Bay large, apartment buildings have been constructed close to the high water mark. These buildings are at risk due to storm surges and sea-level rise. Several artificial cement-walled tidal pools are located along the coast between Three Anchor Bay and Camps Bay. Various storm water and sewerage out-fall pipes are located in the sturdy area. Storm water pipes generally terminate in the surf zone and several can be seen between Sea Point and Mouille Point. The two sewerage outfall pipes are known to be

in the area are located in Camps Bay and Green Point. The pipe extending into Camps Bay can be identified on both the multibeam (Figure 57) and side scan sonar data (Figure 62).

5.7.2 Ship wrecks

The Cape peninsula has a long history of ship wrecks dating back as long ago as the 1400's. Due to the high-energy coastal environment along the Atlantic Seaboard most of the older wrecks have been broken up to such an extent that they are no longer recognisable by geophysical survey equipment. Most wrecks also tend to beach very close to shore and are therefore located inside the inaccessible shallow water zone where no geophysical data were available. Some of the more well-known wrecks in the area are listed in Table 11.

Ship Wreck	Location	Year
SS Maori	Maori Bay	1909
SS Oakburn/Boss 400	Maori Bay	1906/1994
SAS Gelderland	Maori Bay	1988
MV Romelia	Llandudno	1977
MV Antipolis	Oudekraal	1977
Het Huis de Kraaisteen	Oudekraal	1698

Table 11: List of ship wrecks located within the study area; see Chart in Appendix C.

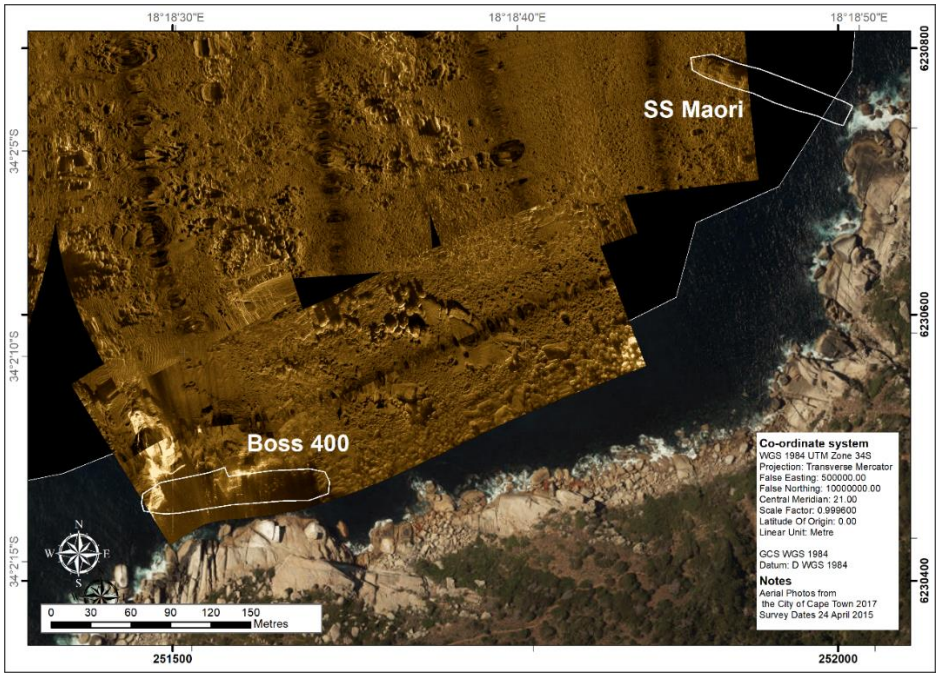

Figure 92: Ship wreck detected on side scan sonar in Maori Bay.

5.8 Coastal morphology

The orientation and physiography of the coast along the Cape Peninsula is closely related to the bedrock geology and the distribution of the Malmesbury Group, Cape Granite Suite and TMG. The low grade metamorphic rocks of the Malmesbury Group are more easily weathered than the intrusive igneous Cape Granite and quartz arenite sandstones of the TMG. This can be observed by the flatly eroded nature of the Malmesbury bedrock along the coast and in the offshore. The exception to this is the Malmesbury Group outcrops which form Signal Hill and the Tygerberg Hills (Figure 93). In these areas the Malmesbury Group rocks were heated to a higher degree, resulting in the more resistant rocks forming these hills (Compton, 2004).

Cape Granite is more resistant to weathering than the Malmesbury Group and forms headlands extending out to sea, plunging coastal cliffs and extensive offshore reefs with high bathymetric variability and relief (Figure 94). A similar trend can be observed further afield along the Western Cape, such as at Cape Columbine. North of the study area the coast, which consist of Malmesbury Group basement is much wider, forming a low-lying coastal plain. On the southern Peninsula and eastern False Bay with its granite basement and the quartz arenite of the TMG, there are steep plunging cliffs along the coast line. On a regional scale the differential weathering of the different geological units results in a coastline with a general NE orientation where there is Cape Granite and or TMG quartz arenite sandstone outcrops, and a NW orientated coastline with a flat, wide coastal plain with log spiral bays (such as Table Bay) where there is Malmesbury Group bedrock. During times of lowered sea level, the coastline would have looked much different from today. Extensive offshore sediment deposits can be seen which would have formed beaches at lower sea levels. Long sandy coastlines would have been present at -9 m, -60 m and -90 m (Figure 71). On these beaches longshore drift is interpreted to have been the main process transporting sediment in a northerly direction. It might have looked very similar to the coastline north of Robben Island and 16 Mile Beach, which is located between Yzerfontein and the Langebaan Lagoon on the West Coast.

A rapid rise in sea level will affect the different areas of coastline in different ways. Due to the low relief of the coastal zone in the northern side of the Atlantic Seaboard, even a small rise in sea level will cause an increase in flooding events due to storms surges. With the increase in energy and shifting of the surf zone, these will most likely result in the disappearance of the pocket beaches in the area. Eventually with a 4 – 5m rise in sea level the coastal plain in the Sea Point area will be permanently inundated. In the southern part of the Atlantic Seaboard, sea-level rise will mostly impact the pocket beaches such as Clifton, Camps Bay, Llandudno and Sandy Bay and a few low-lying areas such as Bakoven. The rest of this section of coastline consists of steep plunging cliffs and sea level will have to rise substantially in order to have an effect on the coastline.

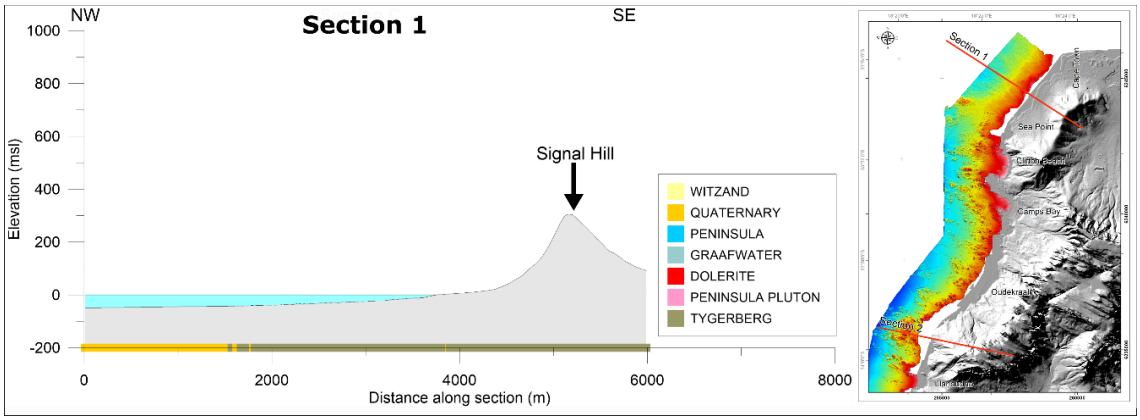

Figure 93: Elevation cross section C, showing coastal elevation derived from MBES bathymetry data and 25m DEM topographic data. In areas of Malmesbury Group rocks there is a wider coastal plain with a gently dipping slope towards the offshore.

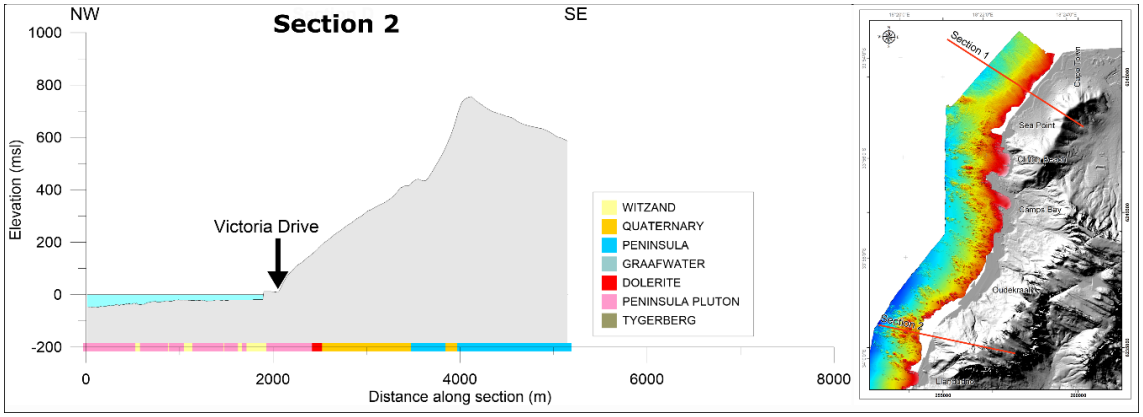

Figure 94: Elevation cross section D, showing coastal elevation derived from MBES bathymetry data and 25m DEM topographic data. In areas of Granite and TMG there is steeply plunging coastal cliffs and uneven bottom topography in the offshore.

5.9 Sediment Distribution

The geophysical data collected during this project considerably increased the known extent and detail of sediment deposits in the nearshore environment compared to the available historic maps and charts. Three major sediment deposits have been identified within the study area with a fourth deposit recognised just to the south of the study area at Noordhoek Beach and a fifth further offshore. The three deposits in the study area are the Sandy Bay deposit, the Oudekraal deposit and the Camps Bay deposit. The Noordhoek deposit which is just to the south plays an important function in the sediment dynamics of the Atlantic Seaboard as a major source of offshore sediment (Figure 95).

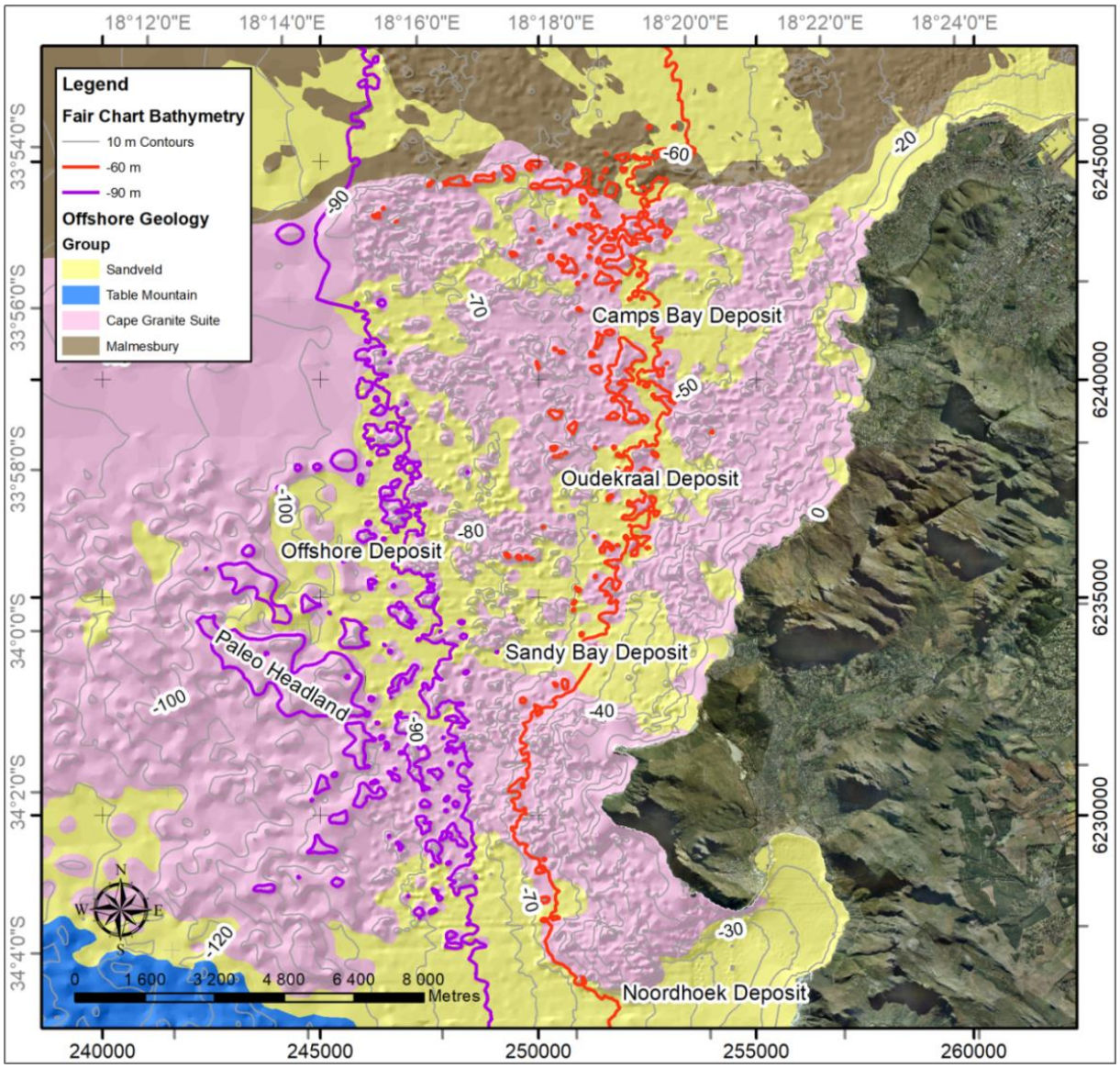

Figure 95: Regional offshore geology in relation to the bathymetry, -60 m and -90 m contours highlighted in red showing two paleo shorelines. The -90 m shoreline is protected by a headland or possible peninsula to the south.

The Sandy Bay deposit is located offshore of Sandy Bay and Llandudno (Figure 80 and Figure 81). It is bounded by Duiker Point and Maori Bay to the south and a large offshore reef which extends from Judas Peak in the north. The mapped area of this deposit is just over 5 km^2. This is only part of a much larger sediment deposit extending offshore from Sandy Bay. When using the low resolution historical data to extend the mapped sediment distribution, the sediment extent could be as much as 32 km^2. The results of the seismic survey conducted in Sandy Bay indicate a deep, sediment-filled depression in the bay (see Figure 72 and Figure 73 for seismic section). The sediment thickness was measured to in excess of 30 m in places (Figure 74). The surficial facies are evenly distributed between bioclastic gravel facies and fine to medium-grained sand facies (Figure 80). The Oudekraal deposit is located north of Llandudno and Judas Peak and extends past Oudekraal to Bakoven (Figure 79 and Figure 80). The deposit consists of a large proportion of fine to medium grain sand, which extends close to the shore line. The Camps Bay deposit is mostly found further offshore except for the two pocket beaches of Camps Bay and Clifton Beach, which are connected to the offshore deposit by narrow gullies (Figure 79). The offshore deposit consists mostly of bioclastic gravel, which is derived from biogenic production on local reefs, while the inshore pocket beaches have a higher medium grained sand component. Although sand can be transported offshore through these gullies, they tend to be very narrow (between 20 and 40 m) and the sand transport from the inshore to the offshore appears to be limited. The supply of bioclastic gravel could be of such high volumes from the offshore reefs that any fine to medium grained sand is covered by the bioclastic gravel. An almost continuous sediment corridor is present closer inshore running from south to north. This corridor can be traced most of the way from Llandudno to Sea Point, with only an occasional break in connectivity caused by reef outcrop.

Once the Sediment facies was split into “Fine to medium grained sand” and “Bioclastic (shelly) gravel”, patterns in the distribution and transport of sediment became clear. The distribution of bioclastic gravel vs. fine to medium grained sand is closely related to the occurrence of the prominent reef facies, or granite outcrop and rocky headlands. In areas immediately surrounding prominent reef facies, the sediment consists mostly of bioclastic gravel. Further away from the prominent reef and headlands, the mean grain size decreases and the carbonate content decreases in a northerly direction until the sediment becomes

better sorted and is comprised of fine to medium grained sand. Sediment deposits and pocket beaches found close inshore were mostly fine to medium grained sand as can be seen from sediment sampling results in Sandy Bay and Camps Bay (Figure 76).

The largest continuous inshore sediment deposit along the Cape Peninsula is located just to the south of the study area at Noordhoek Beach (Figure 11). The Noordhoek deposit extends from Noordhoek Beach in the south to Hout Bay Beach in the north (Figure 95). It extends almost 20 km to the west where it eventually connects to the sediment deposits further offshore though narrow channels.

The sediment characteristics for Sandy Bay and Llandudno beaches appear to be anomalous. The carbonate content (Figure 75) on the beaches is much lower than the Karbonkelberg dune (which is the proposed source) or the immediate offshore deposits. The mean grain size appears to be coarser on the beach than on the dune and the immediate offshore area. The explanation for this is in the wave energy of the beach and the proximity of the different sources. The higher energy available in the surf zone and beach will tend to remove the finer fraction of sand and move it offshore. The carbonate content is lower on the beach and surf zone for the same reason; the wave energy will tend to break the shell (which consists of calcium carbonate) into smaller pieces, assisting in the dissolution of calcium and carbonate.

The offshore deposit appears to be related to a bathymetric high to the south (Figure 95). The bathymetric high can also be identified on the regional seismic section in Figure 71. This bathymetric feature would have formed a headland or peninsula allowing sediment to accumulate on the lee side of the feature, where wave energy would be lower, when sea level was between -100 MSL and -90 MSL about 15 kyr ago (Figure 15).

5.10 Sediment Sources

5.10.1 Karbonkelberg sediment bypass and Hout Bay

The Karbonkelberg sediment bypass, sometimes referred to as the Hout Bay dune or a headland bypass dune, has been a major bypass system for fine to medium grained sand in the past and a major contributor of sediment to the Atlantic Seaboard (Holmes and Meadows, 2012). This can clearly be observed when examining the seafloor geology interpretation (Figure 77), historical offshore geology charts (Figure 95) and historical aerial photos (Figure 96) of the area.

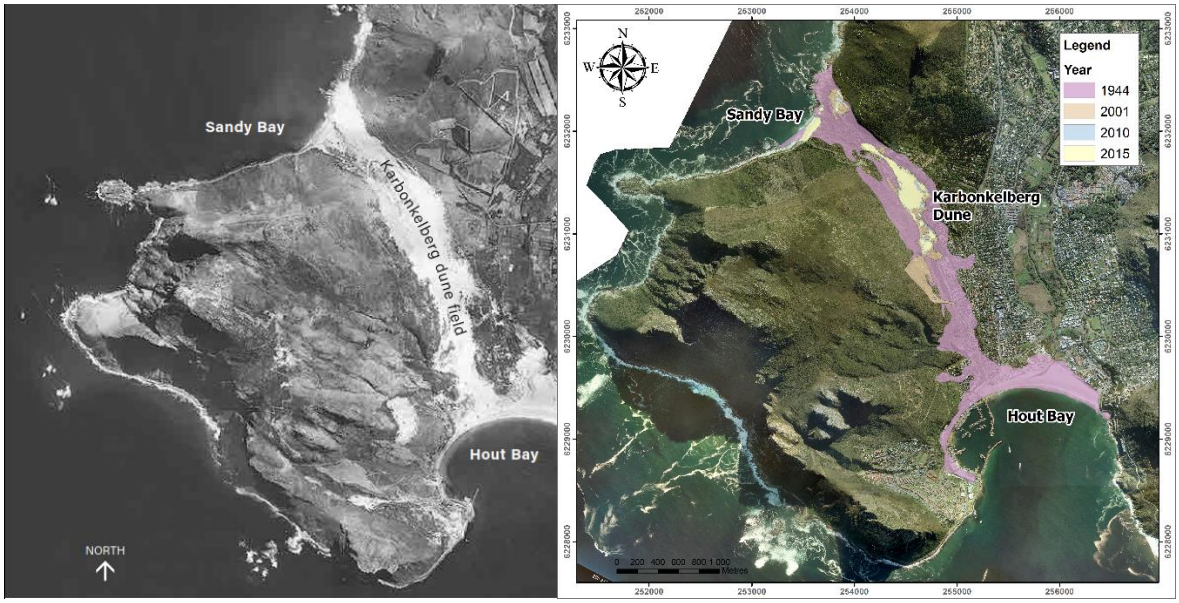

Figure 96: Aerial photo showing the extent of the Karbonkelberg sediment bypass during the 1940's obtained from NGI, Department of Rural Development and Land Reform, compared to current extent from Google Earth 2017.

In historic times the dune field would have formed a continuous stretch of sand from Dias Beach at Hout Bay over the neck to Sandy Bay for a total of 3.2 km. At present the dune field is visible only on the slopes for about 1 km, cascading over the neck for another 200 m towards Sandy Bay. The width of the dune field varies from a few tens of metres to about 300 m at its widest.

Urban development from the last few decades and encroachment of alien invasive species like *Acacia cyclops,* have been interfering with the movement of sediment and the proper functioning of the bypass system. Various attempts have been made in the past to stabilize the dunes on Hout Bay Beach, by planting grass, erecting hedges and irrigating the dunes.

Most dune rehabilitation attempts did not last very long before sand started moving into roads and infrastructure (CSIR, 1989; Louw and Van Eeden, 2013)(Figure 97).

Figure 97: Sand migration across the road Harbour and covering infrastructure in Hout Bay.

Some studies have suggested that the functioning of the system has been effectively destroyed by human influence (Holmes and Meadows, 2012) and no sediment is currently transported to Sandy Bay

In the undisturbed sediment bypass system, sand is deposited on the beach in Hout Bay by wave action (MacHutchon, 2013). The fine sand is then transported onto a beach dune system by wind, which is mostly the southeaster that blows during summer months. The sediment then continues to migrate up into the sediment bypass system until it forms a spill-over dune at the top of the ridge between Hout Bay and Sandy Bay (Holmes and Luger, 1996). The transport mostly occurs during the summer months, during dry and windy conditions. From the crest of the dune, windblown sand continues down the slope to Sandy Bay Beach. Some sediment will be transported back towards Hout Bay during the winter months when the north westerly winds are dominant, but due to wetter conditions and less wind than in summer, the net movement is towards Sandy Bay (Holmes and Luger, 1996).

Figure 98: Sandy Bay Beach with the much reduced Karbonkelberg sediment bypass dune visible in the back ground. In the past the dune would have covered most of the area shown in the picture in yellow.

Even if the bypass system is no longer functioning, it did supply sediment to Sandy Bay in the past before development took over. Grain size characteristics and composition (from carbonate content) do correlate well between sediment samples from the top of the dune and from Sandy Bay beach. The samples taken (presented in Appendix A) on top of the dune consist of well sorted medium sand (Φ 1.6 – 1.8) with about 50% carbonate while the beach consists of well sorted medium sand (Φ 1.0 – 1.21) with about 30% carbonate. Further offshore the carbonate content becomes much higher. This could either mean that the fine grained material and carbonate have been removed from the beach before sampling, or that the bypass is indeed no longer functioning and that the fine grained sand is no longer replenished in the beach. With the beach located in a wind shadow, a fraction of fine to very fine sediment could be transported further offshore by wind and bypassing the beach all together.

5.10.2 Biogenic carbonate production

From the sediment analysis results, local calcium carbonate production seems to act as a much more important source of sediment than was expected at the start of the project. Carbonate content of samples collected around reef outcrops to the south of Sandy Bay is as high as 80% (Figure 75). This concentration rapidly decreases away from the reef to about 40% towards the north. Closer towards the beaches of Sandy Bay and Llandudno, the carbonate content is much lower and not much more than 30%, indicating a different source for the beach sediment. This also applies to the samples taken on Sandy Bay Beach which had a carbonate content of between 21% and 25%. MacHutchon (2013) found similar trends in the Hout Bay area, with calcium carbonate reaching concentrations of up to 95% near reef outcrop to the south of the bay and averaging between 30 and 40% inside the bay. These trends together with grain size distribution, has been attributed to direction of longshore drift with in Hout Bay.

Samples collected on the crest of the Karbonkelberg dune produced similar results to what MacHutchon (2013) obtained on the beach at Hout Bay of about 50% carbonate. This is much higher than the results for Sandy Bay Beach and on the shoreface near the beach where results were between 20 and 30%. The samples were taken before the City of Cape Town started artificial transport of sediment from Hout Bay to the dune crest.

5.10.3 Weathering of local bedrock formations

Three major bedrock types are present in or near the study area; Cape Granite, Malmesbury Group rocks and TMG sandstone. The weathering of TMG probably produced a large portion of the quartzose sand found on the continental shelf. This is suggested because of the dominant grain size of fine to medium-grained sand and the dominant grain composition of quartz. Some large boulders of TMG have been noticed on Sandy Bay and Bakoven. The input of sediment from TMG, first as large boulders becoming scree, which is eventually weathered further due to mechanical weathering to form quartzose sand, is likely. Local deep weathering of granite has been observed in several locations along the coastline. Pockets of gravel with a granitic origin containing quartz and feldspar can be seen at several locations such as Oudekraal, Bakoven (Figure 99) and in some offshore sediment samples.

Granite weathering can be seen in road cuttings along Victoria Drive between Bakoven and Llandudno. Granite is therefore an important local source of sediment. Lastly, the Malmesbury Group rocks are found only to the north of the study area, in the direction of proposed sediment transport. Due to the low relief of the seabed and lack of large sediment traps, any material derived from this source will probably exit the system relatively quickly on its northward bound transportation.

Figure 99: Gravel from weathered granite and sandstone bounders found on the shoreline at Oudekraal.

5.10.4Sediment input from rivers

Sediment discharge by rivers into the study area appears to be limited. There are no major perennial rivers located along the Atlantic Seaboard itself. Some small intermittent streams are present, but they generally have small catchment areas and low annual sediment yields. Three ravines can be seen passing through Camps Bay and Bakoven and another in Llandudno. These ravines might have been important sediment sources during wetter climates, transporting aforementioned weathered TMG sand to the coast. The Disa River discharging into Hout Bay is probably the most significant river contributing sediment to the system today. MacHutchon (2013) estimated the annual fluvial discharge of the Disa River to be $0.024 \times 10^6 m^3$. Further afield rivers which would contribute sediment to the regional system includes the Lourens River, Eerste River, Zeekoe and Zandvlei, all located in False

Bay, therefore not having short term influence on the sediment supply along the Atlantic Seaboard.

5.10.5 Relic offshore sediment

As can be seen from Figure 95 and Figure 71, during times of lower sea levels there were extensive sandy beaches along the Atlantic Seaboard. Notable deposits can be seen between the -100 and -105 m and the -75 and - 60 m isobaths. From the seismic section in Figure 71 the deposits appear to be confined to basement depressions and protected by bathymetric highs of the -90 m and -50 m contours. With the rapid rise in sea level after the last glacial maximum these deposits have been left behind on the inner shelf as relic sediment deposits. Although these sediments are below wave base during normal wave conditions, some movement and re-deposition might occur during large storm events or with the presence of strong wind or upwelling generated bottom currents.

5.11 Sediment Transport

Sediment transport in the Atlantic Seaboard is closely linked to seasonal variations in weather patterns. Sediment is mostly transported by aeolian processes, wave action or currents. Nearshore currents are created by either wave action or wind, and waves are created by wind as well (Flemming, 1981). In the Western Cape the seasonal weather patterns result in south easterly winds dominating in summer and north westerlies dominating in winter and high-energy wave conditions occur mostly during the winter from the south west originating from winter storms in South Atlantic. The direction of the dominant wave regime and the orientation of the Atlantic Seaboard coastline should produce conditions that results in a net northward direction of transport of sediment. Waves predominantly hit the coastline obliquely from the south west, which would result in longshore drift to the north. The rocky nature of the coastline however will affect sediment transport, forming sediment traps and sediment barriers in places along the coast.

5.11.1 Beaches

Beach profiling data provided insight into the processes and movement of sediment on beaches and the surf zone. Erosion and accretion on beaches relates largely to seasonal variations in the amount of wave energy (Figure 100). During winter months, high- energy

wave events (storms) erode beaches and during the summer months, relatively low- energy wave conditions allow sediment accretion (Figure 66 and Figure 67). High- energy wave events are generally associated with winter storms and it can therefore be said that sediment movement on beaches are a seasonal occurrence, during summer small waves deposit sediment onto the beach to form a beach berm and during winter large storm waves move sediment offshore to form a bar (Figure 101). Aubrey (Aubrey, 1979) determined two pivotal points at -6 m and -3 m on a beach profile in his study area about which the sediment movement changes. To determine the pivotal points for this study area, additional repeat onshore and offshore surveys will have to be conducted over several seasons.

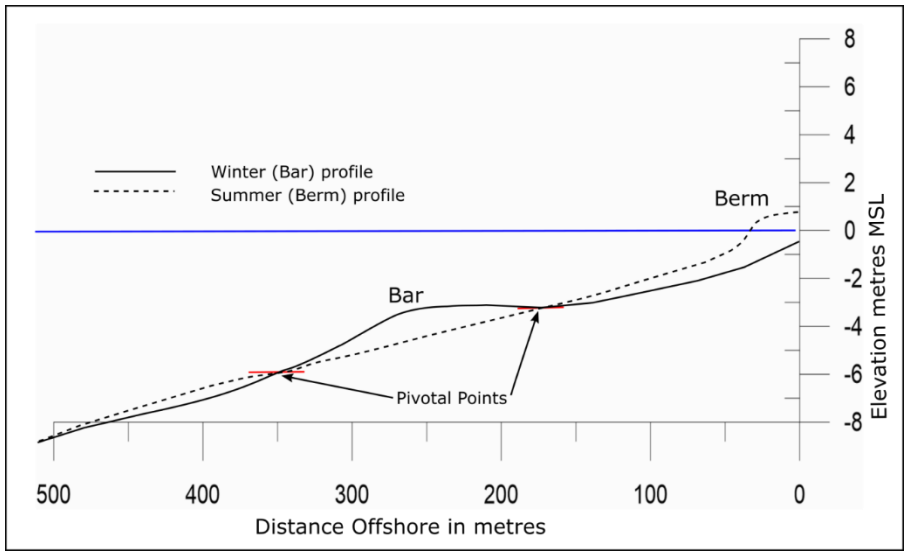

Figure 100: Example of a winter – summer profile, during summer sediment moves onshore and forms a beach berm and during winter sediment moves offshore to form a bar, modified from (Aubrey, 1979).

According to public perception, sand on Sandy Bay beach is slowly disappearing. Whether this is accurate is open to some debate. Similar trends do occur however with sediment building up on the beach during summer and getting eroded during winter. During beach profiling data collection sand bars where observed offshore of the beach in the surf zone which were not present during the summer surveys. It is therefore assumed that most of the seasonal sediment movement that occurs only happens between the surf zone and the foreshore. A similar trend was observed at Camps Bay Beach, where sand is deposited on the beach during summer, creating a gently sloping beach. During winter high-energy storm

waves erode the beach, forming a steep beach berm. Similar to Sandy Bay, the sand appears to move only a short distance offshore to from sand banks or bars just beyond the surf zone.

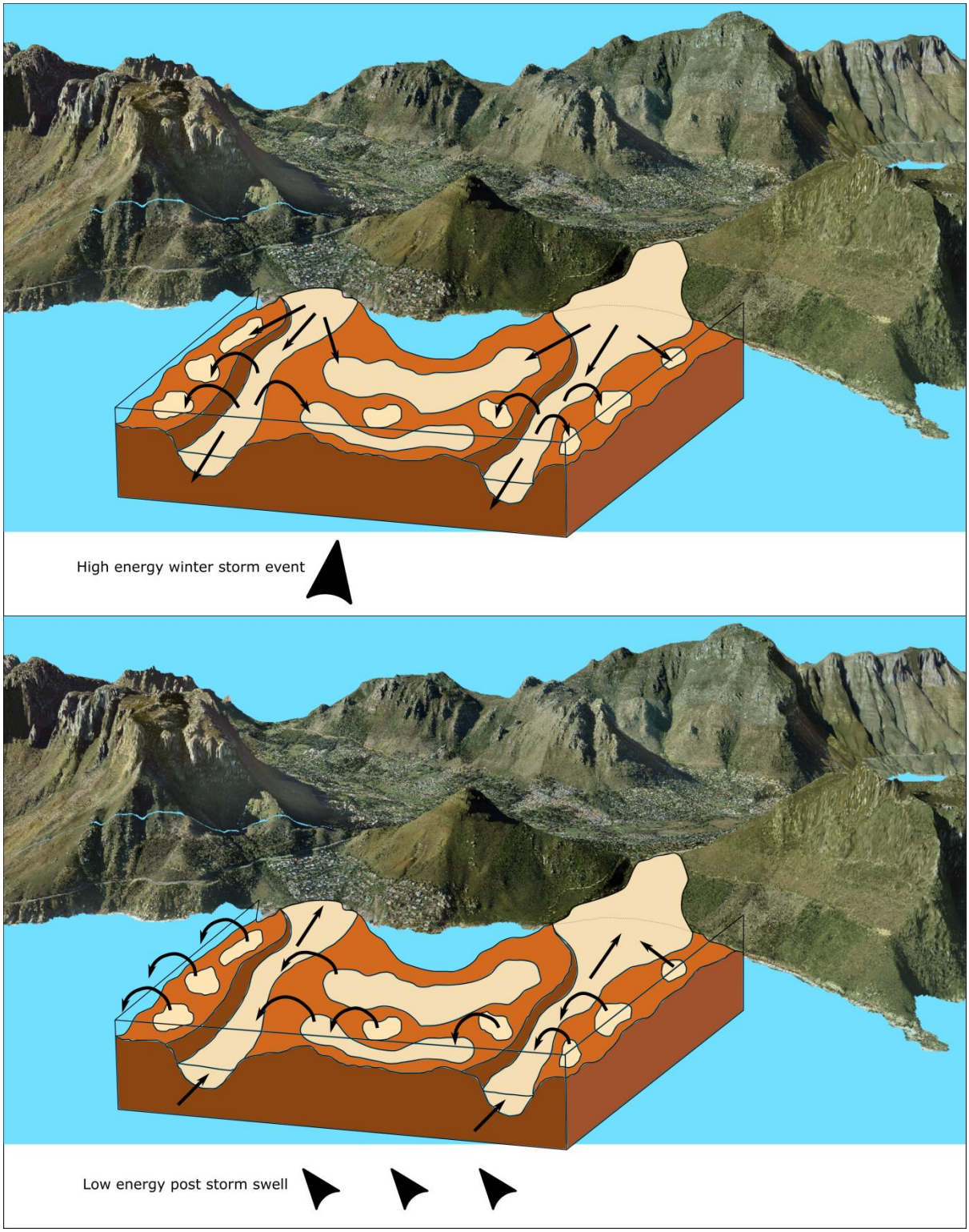

Figure 101: High-energy storm events (Top), which occur mostly during winter, remove sediment from beaches and sediment channels, while low-energy post storm conditions (Bottom), which occur mostly between winter storms and during summer move sediment back onto beaches and northwards though longshore drift.

5.11.2 Nearshore sediment transport

Along rocky coastlines such as the Atlantic Seaboard, the rocky headlands that separate the sandy pocket beaches act as barriers for sediment movement by wave induced longshore drift (Tait, 1995). Headlands and reef outcrops create protected areas where the effects of storm waves are less and finer sediment can accumulate in lower energy conditions. To overcome the barriers imposed by the rocky headlands, sediment needs to be transported outside of the surf zone (Tait, 1995). Storm events are generally required to move sediment offshore and past headlands for sediment to be transported alongshore (Storlazzi and Field, 2000). Historical offshore marine data (unpublished Marine Geoscience data and maps) show that there is very little sediment in the nearshore and therefore little sediment available for transport by longshore drift. But this does not seem to be the case when looking at interpreted seafloor geology in Figure 77**.** From the sediment distribution interpreted during this project there appears to be substantially more sediment available in the nearshore areas from Llandudno, past Oudekraal towards Camps Bay and Clifton beaches than previously shown. From Sandy Bay sediment filled channels and embayments can be traced close inshore almost continuously to Camps Bay (Figure 102). The first major bathymetric barrier for the northward moving sediment can be found north of Camps Bay in the form of the headland formed by the Lion's 'South Paw'. Here sediment needs to move offshore before it can continue its transport up the coast. North of Clifton's beaches the sediment-filled channels resume until they reach the Malmesbury Group at Sea Point. Because of the low relief of the Malmesbury Group rock, the sediment is often not confined to sediment-filled channels, but it is rather spread out as a thin sediment veneer. The Malmesbury Group rocks therefore do not create such a large barrier to sediment movement as the high-relief reef out crop off the Cape Granite.

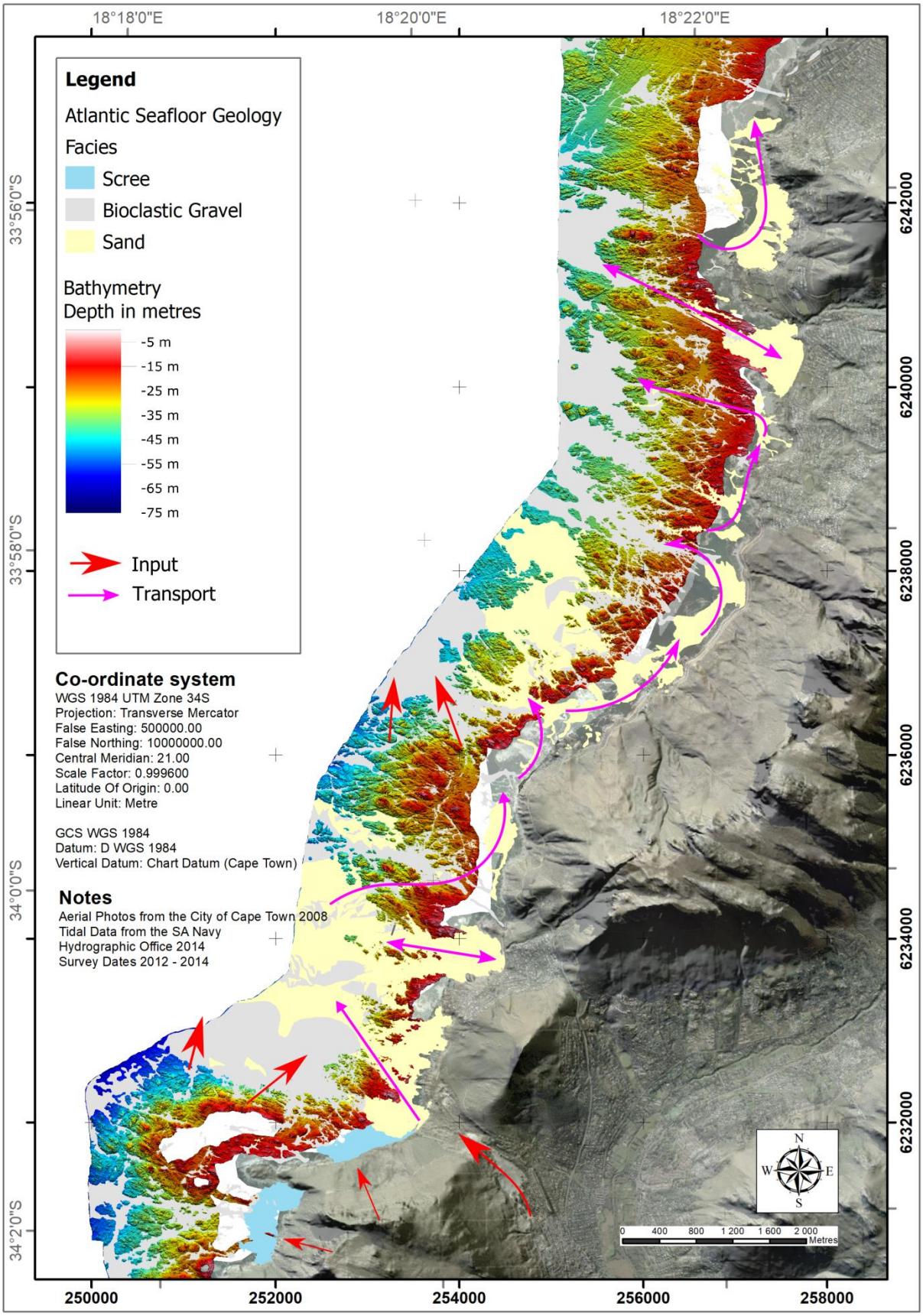

Figure 102: Sediment input (red arrows) and potential transport pathways (magenta arrows) between Sandy Bay and Clifton Beach.

5.12 Human Impact

Human activities along the coastline severely influenced the potential for sediment to be transported though aeolian processes across shore, such as at the Karbonkelberg sediment bypass, thereby reducing the input of fine grained sand to the system. This will eventually have an influence on the quality of sand on beaches such as Sandy Bay, Llandudno, Camps Bay and Clifton Beach. With the added effect of sea-level rise, resulting in increased wave energy at beaches, the volume of fine to medium grained quartzitic sand will be reduced at an even higher rate. With climate change and sea-level rise, storm surges will become a more severe and frequent occurrence (Cai et al., 2014; Trenberth et al., 2015), which will affect sea walls and infrastructure.

In future, beach nourishment strategies might be the only solution to stop the deterioration of beaches and coastal infrastructure. Beach nourishment has been used successfully to protect beaches in many parts of the world (Corbella and Stretch, 2012). One way to conduct beach nourishment is to dredge suitable sand from an offshore location with a dredger and then to pump the sand onshore or near shore at a beach. Several potential sediment sources are located within the study area (Figure 95), but these deposits will have to be investigated further with sampling and vibrocoring to determine the suitability of grain size and composition at depth. An additional option would be to dredge sand from within Hout Bay for use in beach nourishment. This option should solve two problems; a reduction in sand migrating onto Hout Bay Beach, thus reducing the necessity for stabilizing the dunes on the beach and the mechanical transport of sand from the beach to the Karbonkelberg sand dune, and a relatively near source of sand available for beach nourishment along the Atlantic Seaboard or even in Table Bay.

6 Conclusion

The basement geology of the Atlantic Seaboard consists of two zones with the boundary at Sea Point, known as the Sea Point Contact. North of the Sea Point contact the basement consists of the Neoproterozoic rocks of the Tygerberg Formation which is part of the Malmesbury Group. South of the Sea Point contact the basement consist of the intrusive rocks of the Cape Granite Suite. The geomorphology of the coastal zone is closely linked to the type of basement rock of the area, with Malmesbury Group rocks resulting in a NE orientated coastline, low-relief offshore reefs and wide coastal plains during times of lowered sea level, while the Cape Granite Suite rocks results in a NW orientated coastline, high-relief offshore reefs and steep, plunging coastal cliffs with intermittent pocket beaches.

Sediment distribution, composition and transport are similarly affected by the underlying basement rock. In the north, the low-relief seafloor offers almost no barriers to sediment transport, resulting in few beaches and offshore sediment deposits. In contrast, the high-relief reef, plunging cliffs and protruding headlands of the Cape Granite Suite supply ample transport barriers to trap and retain sediment deposits and sandy pocket beaches.

Three primary sources of sediment were identified along the Atlantic Seaboard, the input of the Karbonkelberg dune sand as part of the sediment bypass at Sandy Bay, biogenic input of carbonate from shelly organisms living on offshore reefs and in sandy beaches, weathering of local rock (granite) and weathering of the adjacent sandstone mountains (TMG). Secondary sources of sediment include longshore drift from the south and sediment from offshore deposits, but these probably only play a role during storm events.

The high percentage of carbonate present in the sediment samples indicates that biogenic carbonate production plays an important role in the sediment supply of the Atlantic Seaboard, while the reduction in size of the Karbonkelberg sediment bypass in recent decades is becoming less important as a source and might even completely disappear. Although this will take many years or even decades to take effect with the currently available offshore deposits, it will eventually change the composition of sediment on beaches of the Atlantic Seaboard, which will become increasingly carbonate shell rich.

Sediment transport and deposition is not only affected by the basement geology, but also by seasonal weather patterns. During summer mostly calm sea conditions facilitate the deposition of sediment onto beaches, while during winter storm events move sediment offshore and facilitate moving sediment past headlands and bathymetric barriers.

A geological legend (Figure 103) and an on-offshore geological map (Figure 104) is presented here, with an enlarged print presented in Appendix E.

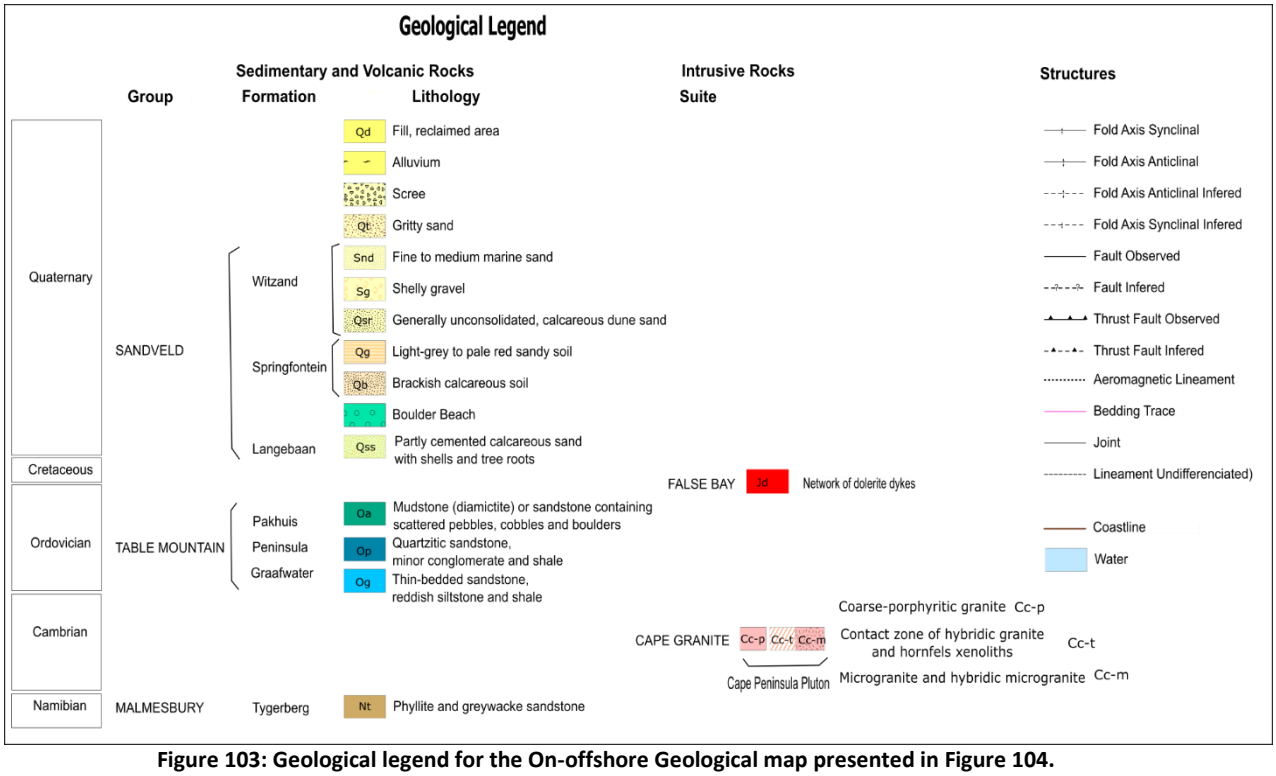

Figure 103: Geological legend for the On-offshore Geological map presented in Figure 104.

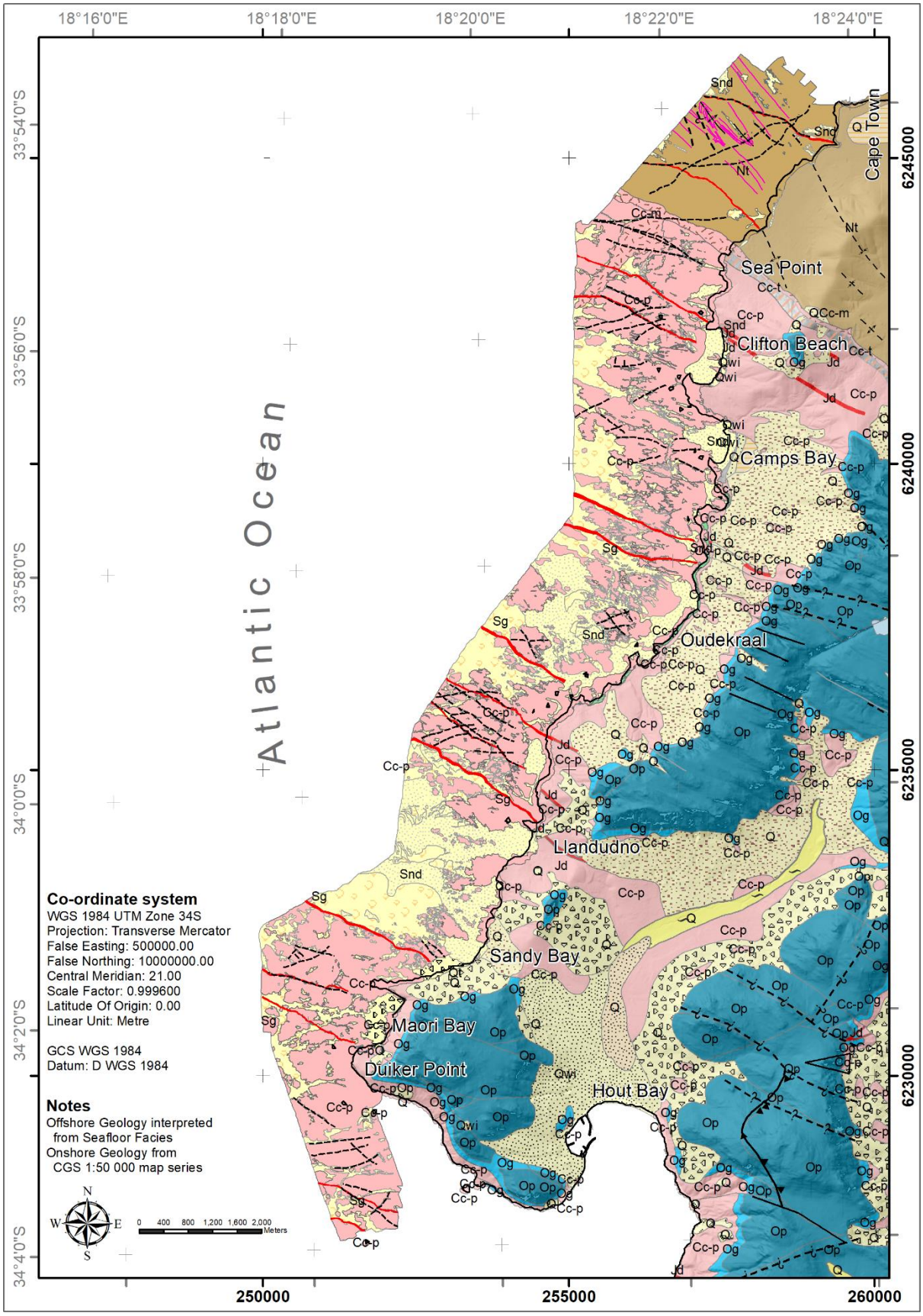

Figure 104: Onshore-offshore geology map of the Atlantic Seaboard, offshore data interpreted from the Seafloor Facies chart in Figure 77, onshore data from the CGS 1:50 000 Geology map series (See Appendix E for enlarged On-offshore Geology map).

7 References

Atkins, G.R., 1965. Camps Bay Outfall Investigation (Contract Report). Institute of Oceanography, University of Cape Town, Cape Town.

Aubrey, D.G., 1979. Seasonal patterns of onshore/offshore sediment movement. Journal of Geophysical Research 84, 6347–6354. https://doi.org/10.1029/JC084iC10p06347

Backeberg, N.R., 2012. Petrogenesis of the False Bay Dyke Swarm, Cape Peninsula, South Africa (MSc). University of Cape Town, Cape Town.

Backeberg, N.R., Reid, D.L., Trumbull, R.B., Romer, R.L., 2011. Petrogenesis of the False Bay Dyke Swarm, Cape Peninsula, South Africa: Evidence for Basement Assimilation. South African Journal of Geology 114, 335–352. https://doi.org/10.2113/gssajg.114.3-4.335

Bagnold, R.A., 1973. The Nature of Saltation and of "Bed-Load" Transport in Water. Proceedings of the Royal Society of London. A. Mathematical and Physical Sciences 332, 473–504. https://doi.org/10.1098/rspa.1973.0038

Bayram, A., Larson, M., Hanson, H., 2007. A new formula for the total longshore sediment transport rate. Coastal Engineering 54, 700–710. https://doi.org/10.1016/j.coastaleng.2007.04.001

Belcher, R.W., Kisters, A.F.M., 2003. Lithostratigraphic correlations in the western branch of the Pan-African Saldania belt, South Africa: the Malmesbury Group revisited. South African Journal of Geology 106, 327–342. https://doi.org/10.2113/106.4.327

Blondel, P., 2009. The Handbook of Sidescan Sonar. Springer, Berlin; New York; Chichester, UK; Praxis Pub.

Blondel, P., Murton, B.J., 1997. Handbook of Seafloor Sonar Imagery, Wiley-Praxis series in remote sensing. Wiley published in association with Praxis Pub, Chichester, UK; New York.

Boeyinga, J., Dusseljee, D.W., Pool, A.D., Schoutens, P., Verduin, F., van Zwicht, B.N.M., Klein, A.H.F., 2010. The effects of a bypass dunefield on the stability of a headland bay beach: A case study. Coastal Engineering 57, 152–159. https://doi.org/10.1016/j.coastaleng.2009.10.002

Boggs, S., 2011. Principles of Sedimentology and Stratigraphy, 5th ed. Pearson, Boston.

Brown, A.C., 1971. The Ecology of the Sandy Beaches of the Cape Peninsula, South Africa. Part 1: Introduction. Transactions of the Royal Society of South Africa 39, 247–279. https://doi.org/10.1080/00359197109519119

Cai, W., Borlace, S., Lengaigne, M., van Rensch, P., Collins, M., Vecchi, G., Timmermann, A., Santoso, A., McPhaden, M.J., Wu, L., England, M.H., Wang, G., Guilyardi, E., Jin, F.-F., 2014. Increasing frequency of extreme El Niño events due to greenhouse warming. Nature Climate Change 4, 111–116. https://doi.org/10.1038/nclimate2100

Chen, X., Zhang, X., Church, J.A., Watson, C.S., King, M.A., Monselesan, D., Legresy, B., Harig, C., 2017. The increasing rate of global mean sea-level rise during 1993–2014. Nature Climate Change 7, 492–495. https://doi.org/10.1038/nclimate3325

Church, J.A., White, N.J., 2006. A 20th century acceleration in global sea-level rise: An Acceleration in Global Sea-Level Rise. Geophysical Research Letters 33. https://doi.org/10.1029/2005GL024826

City of Cape Town, 2015. Research on the economic value of tourism in the City of Cape Town. Grant Thornton, Cape Town.

Collie, J.S., Adamowicz, W.L. (Vic., Beck, M.W., Craig, B., Essington, T.E., Fluharty, D., Rice, J., Sanchirico, J.N., 2013. Marine spatial planning in practice. Estuarine, Coastal and Shelf Science 117, 1–11. https://doi.org/10.1016/j.ecss.2012.11.010

Compton, J.S., 2004. The Rocks and Mountains of Cape Town. Double Storey Books, Cape Town, South Africa.

Compton, J.S., 2001. Holocene sea-level fluctuations inferred from the evolution of depositional environments of the southern Langebaan Lagoon salt marsh, South Africa. The Holocene 11, 395–405.

Compton, J.S., Wiltshire, J.G., 2009. Terrigenous sediment export from the western margin of South Africa on glacial to interglacial cycles. Marine Geology 266, 212–222.

Corbella, S., Stretch, D.D., 2012. Coastal defences on the KwaZulu-Natal coast of South Africa: a review with particular reference to geotextiles. Journal of the South African Institution of Civil Engineering 54, 55–64.

CSIR, 2014. Metocean Conditions & Vulnerability - Medium resolution wave climate & run-up (No. ECCS112 (/AT1)), South African Coastal Vulnerability Assessment: Phase 2. DEA - CSIR, Stellenbosch.

CSIR, 1989. Dune Management Plan and the Hout Bay Estuary. CSIR, Stellenbosch.

Day, R.W., 1986. Magnetic Mapping of the False Bay Dolerites, Cape Town (Technical Report No. 16). Joint Geological Survey/University of Cape Town Marine Geoscience Unit, Cape Town.

De Decker, R.H., 1987. The Geological Setting of Diamondiferous Deposits on the Inner Shelf between the Orange River and Wreck Point, Namaqualand. Bulletin of the Geological Survey 86.

Denbigh, P.N., 1982. A Review of Rapid Depth Measuring Techniques and the Development of a Bathymetric Side Scan Sonar, in: W.G.A Russell-Cargill (Ed.), Recent Developments in Side Scan Sonar Techniques. Central Acoustics Laboratory, Cape Town, p. 141.

Dingle, R.V., Siesser, W.G., 1975. Geology of the Continental Margin Between Walvis Bay and Ponta Do Ouro. Marine Geoscience Series 2.

Dingle, R.V., Siesser, W.G., Newton, A.R., 1983. Mesozoic and Tertiary Geology of Southern Africa. A.A. Balkema; Distributed in the U.S.A. & Canada by M.B.S, Rotterdam: Salem, N.H., U.S.A.

Du Plessis, A., Glass, J.G., 1991. The Geology of False Bay. Transactions of the Royal Society of South Africa 47, 495–517.

FitzGerald, D.M., Fenster, M.S., Argow, B.A., Buynevich, I.V., 2008. Coastal Impacts Due to Sea-Level Rise. Annual Review of Earth and Planetary Sciences 36, 601–647. https://doi.org/10.1146/annurev.earth.35.031306.140139

Flemming, B.W., 1981. Factors controlling shelf sediment dispersal along the southeast African continental margin. Marine Geology 42, 259–277. https://doi.org/10.1016/0025-3227(81)90166-3

Folk, R.L., 1980. Petrology of sedimentary rocks. Hemphill Pub. Co, Austin, Tex.

Fuller, A.O., 1985. A contribution to the conceptual modelling of pre-Devonian fluvial systems. South African Journal of Geology 88, 189.

Galvin, C., J., 1972. Wave Breaking in Shallow Water, in: Meyer, R.E. (Ed.), Waves on Beaches and Resulting Sediment Transport. Academic Press, pp. 413–456. https://doi.org/10.1016/B978-0-12-493250-0.50015-1

Garrison, T., 2005. Oceanography: an invitation to marine science, 5th ed. ed. Thomson Brooks/Cole, Belmont, CA.

Gibbs, J.R., Mathews, M.D., Link, D.A., 1971. The relationship between sphere size and settling velocity. Journal of Sedimentary Petrology 41, 7–18.

Gouws, D.J., Saunderson, E.F., McKinnell, L.A., 2011. The Hermanus Magnetic Observatory as a space physics facility. EDP Sciences 9.

Harris, T.F.W., 1978. Review of Coastal Currents in Southern African Waters (No. 30), South African National Scientific Programmes Report. South African National Committee for Oceanographic Research.

Hartnady, C.J.H., Newton, A.R., Theron, J.N., 1974. The stratigraphy and structure of the Malmesbury Group in the southwestern Cape. Bulletin of Precambrian Research 15, 193–213.

Holmes, P.J., Luger, A., 1996. Geomorphic implications of the stabilisation of a headland bypass dune system in the Cape Peninsula, South Africa. Zeitschrift Fur Geomorphology 107, 63–77.

Holmes, P.J., Meadows, M.E., 2012. Southern African geomorphology: recent trends and new directions. Sun Media, Bloemfontein, Bloemfontein.

Hopley, D. (Ed.), 2011. Encyclopedia of modern coral reefs: structure, form and process, The encyclopedia of earth sciences series. Springer, Dordrecht.

Horn, J., 2009. Seapoint contact revisited (MSc). University of Stellenbosch, Stellenbosch.

Hrvoic, D., 2007. SeaSPY Overhauser Magnetometer Technical Application Guide rev 1.4. Marine Magnetics Corporation.

Illenberger, W.K., 1993. Variations of sediment dynamics in Algoa Bay during the Holocene. South African Journal of Science, Xth SASQUA Conference 89, 187–196.

International Assosiation of Oil and Gas Producers, 2011. An Overview of Marine Seismic Operations (No. 448). International Assosiation of Oil and Gas Producers, London.

International Hydrographic Organization, 2005. Manual on Hydrography, 1st ed. International Hydrographic Bureau, Monaco.

Kisters, A.F.M., Agenbach, C., Frei, D., 2015. Age and Tectonic Significance of the Volcanic Bloubergstrand Member in the Pan-African Saldania Belt, South Africa. South African Journal of Geology 118, 213–224. https://doi.org/10.2113/gssajg.118.3.213

Klein, M., 1982. A modular sonar system for seabed mapping., in: Russell-Cargill, W.G.A. (Ed.), Recent Developments in Side Scan Sonar Techniques. Cape Town, p. 141.

Komar, P.D., 1998. Beach processes and sedimentation, 2nd ed. ed. Prentice Hall, Upper Saddle River, N.J.

Komar, P.D., Inman, D.L., 1970. Longshore sand transport on beaches. Journal of Geophysical Research 75, 5914–5927. https://doi.org/10.1029/JC075i030p05914

Louw, A.B., Van Eeden, J.D., 2013. Management and Rehabilitation Plan for the Hout Bay Dunes Volume 1 (No. PO 4501955067). Vula Environmental Services, Vredenburg.

MacHutchon, M.R., 2013. The Geological Evolution and Sedimentary Dynamics of Hout Bay, South Africa. Bulletin of the Council for Geoscience 148.

MacHutchon, M.R., Cawthra, H.C., Van Zyl, F.W., Salzmann, L., 2018. Geophysical Investigation of Table Bay, Cape Town (Annual Technical Report No. 2018– 0030). Bellville.

MacHutchon, M.R., Van Zyl, F.W., Daniels, W., 2014. Sediment Budget and Dynamics of the Western Cape (Annual Technical Programme Review No. 2014– 0169). Council for Geoscience, Bellville.

Mangor, K., Drønen, N.K., Kærgaard, K.H., Kristensen, S.E., 2017. Shoreline Managment Guidlines. Danish Coastal Authority, Copenhagen.

Martin, A.K., Flemming, B.W., 1986. The Holocene Shelf Sediment Wedge Off the South and East Coast of South Africa. Canadian Society of Petroleum Geologists, Shelf Sands and Sandstones Memoir 11, 27–44.

Master, S., 2012. Darwin as a geologist in Africa – dispelling the myths and unravelling a confused knot. South African Journal of Science 108. https://doi.org/10.4102/sajs.v108i9/10.994

Mazel, C., 1985. Side Scan Sonar Training Manual. Klein associates, Inc, Salem, New Hampshire.

McLachlan, A., Illenberger, W.K., Burkinshaw, J.R., Burns, M.E.R., 1994. Management Implications of Tampering with Littoral Sand Sources. Journal of Coastal Research, Coastal Hazards: Perception, Susceptibility and Mitigation 51–59.

McLaren, P., Bowles, D., 985. The effects of sediment transport on grain-size distributions. Journal of Sedimentary Petrology 55, 457–470.

McMillan, I.K., 1990. Foraminifera from the late Pleistocene (latest Eemian to earliest Weichselian) shelly sands of Cape Town City Centre, South Africa. Annals of the South African Museum 99, 121–186.

Miller, K.G., 2005. The Phanerozoic Record of Global Sea-Level Change. Science 310, 1293–1298. https://doi.org/10.1126/science.1116412

Morton, R., 2015. C-nav gnss services: providing confidence through redundancy, integrity, independence, and choice.

Neumann, B., Vafeidis, A.T., Zimmermann, J., Nicholls, R.J., 2015. Future Coastal Population Growth and Exposure to Sea-Level Rise and Coastal Flooding - A Global Assessment. Plos One 10, e0118571. https://doi.org/10.1371/journal.pone.0118571

Nichols, G., 2009. Sedimentology and stratigraphy, 2nd ed. ed. Wiley-Blackwell, Chichester, UK; Hoboken, NJ.

Ogg, J.G., Ogg, G., Gradstein, F.M., 2016. A concise geologic time scale 2016. Elsevier, Amsterdam, Netherlands.

Parkinson, R., 2001. High resolution site surveys. Spon Press, London; New York.

Partridge, T.C., Maud, R.R., 1987. Geomorphic evolution of Southern Africa since the Mesozoic. South African Journal of Geology 90, 179.

Pedreros, R., Howa, H.L., Michel, D., 1996. Application of grain size trend analysis for the determination of sediment transport pathways in intertidal areas. Marine Geology 135, 35–49. https://doi.org/10.1016/S0025-3227(96)00042-4

Penrose, J.D., Siwabessy, P.J.W., Gavrilov, A., Parnum, I., Brooke, B., Ryan, D.A., Kennedy, P., 2005. Acoustic Techniques for Seabed Classification (Technical Report No. 32). Cooperative Research Centre for Coastal Zone Estuary and Waterway Managment.

Pethick, J., 1984. An introduction to coastal geomorphology. E. Arnold, London ; Baltimore, Md., U.S.A.

Playfair, J., Hall, B., 1813. Account of the structure of Table Mountain and other parts of the peninsula of the Cape; drawn up by Prof. Playfair, from the observations made by Capt. Basil Hall. Transactions of the Royal Society of Edinburgh 7, 269–278.

Ramsay, P.J., 1996. 9000 Years of sea-level change along the southern African coastline. Quaternary International 31, 71–75. https://doi.org/10.1016/1040-6182(95)00040-P

Ramsay, P.J., Cooper, J.A.G., 2002. Late Quaternary Sea-Level Change in South Africa. Quaternary Research 57, 82–90. https://doi.org/10.1006/qres.2001.2290

Reading, H.G. (Ed.), 1991. Sedimentary environments and facies, 2. ed., reprinted. ed. Blackwell, Oxford.

Reid, D.L., Erlank, A.J., Rex, D.C., 1991. Age and correlation of the False Bay dolerite dyke swarm, South-western Cape, Cape Province. South African Journal of Geology 94, 155–158.

Roberts, D.L., 2006. Sandveld Group, in: Johnson, M.R. (Ed.), Catalogue of South African Lithostratigraphic Units. pp. 25–26.

Roberts, D.L., Botha, G.A., Maud, R.R., Pether, J., 2006. Coastal Cenozoic Deposits, in: Johnson, M.R., Anhauesser, C.R., Thomas, R.J. (Eds.), The Geology of South Africa. Geological Society of South Africa & The Council for Geoscience, Cape Town, pp. 605–628.

Rossouw, J., 1989. Design Waves for the South African Coastline (Doctor of Philosophy). University of Stellenbosch, Stellenbosch.

Rowe, C.D., Backeberg, N.R., Van Rensburg, T., Maclennan, S.A., Faber, C., Curtis, C., Viglietti, P.A., 2010. Structural Geology of Robben Island: Implications for the Tectonic Environment of Saldanian Deformation. South African Journal of Geology 113, 57–72. https://doi.org/10.2113/gssajg.113.1-57

Rozendaal, A., Gresse, P.G., Scheepers, R., Le Roux, J.P., 1999. Neoproterozoic to Early Cambrian Crustal Evolution of the Pan-African Saldania Belt, South Africa. Precambrian Research 97, 303–323. http://dx.doi.org/10.1016/S0301-9268(99)00036-4

Rust, I., 1973. The Evolution of the Paleozoic Cape Basin, Southern Margin of Africa, in: Nairn, A.M., Stehli, F. (Eds.), The South Atlantic, The Ocean Basins and Margins. Springer US, pp. 247–276.

Rust, I.C., 1991. Environmental geology of the coastal zone: a South African perspective. South African Journal of Marine Science 10, 397–405. https://doi.org/10.2989/02577619109504647

Scheepers, R., 1995. Geology, geochemistry and petrogenesis of Late Precambrian S-, I- and A-type granitoids in the Saldania belt, Western Cape Province, South Africa. Journal of African Earth Sciences 21, 35–58. https://doi.org/10.1016/0899-5362(95)00087-A

Scheepers, R., Schoch, A.E., 2006. The Cape Granite Suite, in: Johnson, M.R., Anhauesser, C.R., Thomas, R.J. (Eds.), The Geology of South Africa. Geological Society of South Africa & The Council for Geoscience, Cape Town, pp. 421–432.

Schulze, B.R., 1965. General Survey. Climate of South Africa (No. Part 8 WB 28). South African Weather Bureau, Department of Environment Affairs, Pretoria.

Shone, R.W., 2006. Onshore Post-Karoo Mesozoic Deposits, in: Johnson, M.R., Anhauesser, C.R., Thomas, R.J. (Eds.), The Geology of South Africa. Geological Society of South Africa & The Council for Geoscience, Cape Town, pp. 541–552.

Short, A.D., Hesp, P.A., 1982. Wave, beach and dune interactions in Southeastern Australia. Marine Geology 48, 259–284. https://doi.org/10.1016/0025-3227(82)90100-1

Smith, G.G., Mocke, G.P., 2002. Interaction between breaking/broken waves and infragravity-scale phenomena to control sediment suspension transport in the surf zone. Marine Geology 187, 329–345.

Stapor Jr., F.W., May, J.P., Barwis, J., 1983. Eolian Shape-Sorting and Aerodynamic Traction Equivalence in the Coastal Dunes of Hout Bay, Republic of South Africa. Developments in Sedimentology Volume 38, 149–164. http://dx.doi.org/10.1016/S0070-4571(08)70794-5

Stoker, M.S., Pheasant, J.B., Josenhans, H., 1997. Seismic Methods and Interpretation, in: Davies, T.A., Bell, T., Cooper, A.K., Josenhans, H., Polyak, L., Solheim, A., Stoker, M.S., Stravers, J.A. (Eds.), Glaciated Continental Margins: An Atlas of Acoustic Images. Springer Netherlands, Dordrecht, pp. 9–26. https://doi.org/10.1007/978-94-011-5820-6_2

Storlazzi, C.D., Field, M.E., 2000. Sediment distribution and transport along a rocky, embayed coast: Monterey Peninsula and Carmel Bay, California. Marine Geology 170, 289–316.

Tait, J.F., 1995. Rocky coasts and inverse methods: sediment transport and sedimentation patterns of Monterey Bay National Marine Sanctuary. University of California, Santa Cruz.

Tankard, A.J., Jackson, M.P.A., Eriksson, K.A., Hobday, D.K., Hunter, D.R., Minter, W.E.L., 1982. Fragmentation and Mesozoic Paleogeography, in: Crustal Evolution of Southern Africa. Springer New York, New York, NY, pp. 407–423. https://doi.org/10.1007/978-1-4613-8147-1_12

Thamm, A.G., Johnson, M.R., 2006. The Cape Super Group, in: Johnson, M.R., Anhauesser, C.R., Thomas, R.J. (Eds.), The Geology of South Africa. Geological Society of South Africa & The Council for Geoscience, Cape Town, pp. 443–460.

Theron, J.N., 1984. The Geology of Cape Town and Environs. Explanation: Sheet Maps 3318 CD and DC, 3418 AB, AD and BA.

Theron, J.N., P.G. Gresse, H.P. Siegfried, J. Rogers, 1992. The Geology of the Cape Town area. Republic of South Africa, Dept. of Mineral and Energy Affairs, Geological Survey, Pretoria.

Tinley, K.L., 1985. Coastal Dunes of South Africa (No. SANSP Report 109), South African national scientific programmes General science, engineering & technology. CSIR.

Trenberth, K.E., Fasullo, J.T., Shepherd, T.G., 2015. Attribution of climate extreme events. Nature Climate Change 5, 725–730. https://doi.org/10.1038/nclimate2657

Turner, B.R., 1990. Continental sediments in South Africa. Journal of African Earth Sciences (and the Middle East) 10, 139–149. https://doi.org/10.1016/0899-5362(90)90051-F

Tyson, P.D., Preston-Whyte, R.A., Preston-Whyte, R.A., 2000. The weather and climate of southern Africa, 2nd ed. ed. Oxford University Press, Cape Town ; New York.

USACE - CERC, 1984. Shore Protection Manual. Department of the Army, U.S. Corps of Engineers, Coastal Engineering Research Centre, Washington, DC 20314.

Van Zyl, F.W., 2010. Marine Geophysical Survey Report Table Mountain Marine Protected Area, Phase 1 (Atlantic Seaboard - Mouille Point to Duiker Point) (Survey Report No. 2010– 0214). Council for Geoscience, Bellville.

Von Veh, M.W., 1983. Aspects of sedimentation, structure, and tectonic evolution in the Tygerberg terrane, southwestern Cape Province, Bulletin. University of Cape Town, Dept. of Geology, Chamber of Mines Precambrian Research Unit, Cape Town.

Waelbroeck, C., Labeyrie, L., Michel, E., Duplessy, J.C., McManus, J.F., Lambeck, K., Balbon, E., Labracherie, M., 2002. Sea-level and deep water temperature changes derived from benthic foraminifera isotopic records. Quaternary Science Reviews 21, 295–305. https://doi.org/10.1016/S0277-3791(01)00101-9

Walker, F., 1956. The dolerites of the Cape Peninsula. South African Journal of Geology, 59, 77–92.

Wentworth, C.K., 1922. A Scale of Grade and Class Terms for Clastic Sediments. The Journal of Geology 30, 377–392. https://doi.org/10.2307/30063207

Wong, P.P., Losada, I.J., Gattuso, J.-P., Hinkel, J., Khattabi, A., McInnes, K.L., Saito, Y., Sallenger, A., 2014. Coastal systems and low-lying areas, in: Field, C.B. (Ed.), Climate Change 2014: Impacts, Adaptation, and Vulnerability. Part A: Global and Sectoral Aspects. Contribution of Working Group II to the Fifth Assessment Report of the Intergovernmental Panel on Climate Change. Cambridge University Press, Cambridge, United Kingdom and New York, NY, USA, pp. 361–409.

Woodborne, M.W., 1983. Bathymetry, Solid Geology and Quaternary Sedimentology of Table Bay (No. 14), Technical Report. Joint Geological Survey/University of Cape Town Marine Geoscience Unit, Cape Town.

Woodroffe, C.D., 2002. Coasts: Form, Process and Evolution. Cambridge University Press.

Zecchin, M., Ceramicola, S., Gordini, E., Deponte, M., Critelli, S., 2011. Cliff overstep model and variability in the geometry of transgressive erosional surfaces in high-gradient shelves: The case of the Ionian Calabrian margin (southern Italy). Marine Geology 281, 43–58. https://doi.org/10.1016/j.margeo.2011.02.003

Zietsman, B., 2014. Coastal Dynamics Assessment Mouille Point Precinct One: Upgrade of Promenade Report. Element Consulting Engineers, Stellenbosch.

Websites

Hawth's Tools 2009

http://www.spatialecology.com/htools/rndselss.php

Accessed 10 December 2009

SApeople 2012

http://www.sapeople.com/2012/05/17/clifton-beach-shipwreck-photographs/

Accessed 28 June 2017

IOL 2012

https://www.iol.co.za/news/south-africa/western-cape/relief-as-eihatsu-maru-is-towed-off-1300053

Accessed 30 June 2017

SA Tides 2017

http://www.satides.co.za/

Accessed 02 August 2017

BBC 2017

http://www.bbc.co.uk/bitesize/ks3/geography/physical_processes/rivers_flooding/revision/4/

Accessed 03 August 2017

Personal communication

Andre Theron, 2014. Interview regarding sediment transport along the Atlantic Seaboard. Senior Research Engineer, Ports, Coasts and Estuaries, CSIR Built Environment, Stellenbosch.

Amy Davidson, 2016. E-mail correspondence regarding the volume of sand transported from Hout Bay to the Karbonkelberg sand dune by the City of Cape Town. State of the Environment and Sustainability coordinator, Environmental Resource Management Department, City of Cape Town.

Appendix A – Sediment Results

Sample No	X	Y	Date	Location	Sample Type	Carbonate %	Gravel %	Sand %	Mud %	Mean Φ	Median Φ	Sorting	Skewness	Mean mm	Median mm
SBG02	253322	6231988	2014/10/04	SandyBay	Grab	22.31	0.54	99.44	0.00	1.62	1.59	0.49	0.19	0.33	0.33
SBG04	253485	6232159	2014/10/04	SandyBay	Grab	31.78	0.10	99.88	0.00	1.41	1.39	0.34	0.11	0.38	0.38
SBG07	253123	6232186	2014/10/04	SandyBay	Grab	27.01	0.46	99.46	0.00	1.89	1.87	0.35	0.11	0.27	0.27
SBG10	251916	6232393	2014/11/04	SandyBay	Grab	68.47	45.88	54.09	0.03	0.46	0.43	0.32	0.50	0.73	0.74
SBG13	252517	6232388	2014/11/04	SandyBay	Grab	42.37	30.52	69.46	0.01	0.78	0.73	0.32	0.20	0.58	0.60
SBG16	251313	6232581	2014/11/04	SandyBay	Grab	79.49	91.99	7.93	0.03	0.31	0.13	0.60	0.97	0.81	0.91
SBG21	252321	6232596	2014/11/04	SandyBay	Grab	55.19	17.81	82.14	0.02	0.34	0.34	0.38	0.26	0.79	0.79
SBG24	253376	6232615	2014/10/04	SandyBay	Grab	22.36	0.00	99.98	0.00	1.96	1.94	0.29	0.11	0.26	0.26
SBG26	251706	6232784	2014/11/04	SandyBay	Grab	53.64	18.84	81.10	0.02	0.54	0.45	0.51	0.47	0.69	0.73
SBG28	252128	6232790	2014/11/04	SandyBay	Grab	49.65	38.99	60.90	0.02	0.36	0.30	0.42	0.68	0.78	0.82
SBG30	252526	6232786	2014/11/04	SandyBay	Grab	63.64	38.38	61.56	0.02	0.60	0.58	0.38	0.27	0.66	0.67
SBG32	253120	6232793	2014/10/04	SandyBay	Grab	17.52	0.00	99.82	0.14	1.85	1.85	0.23	0.02	0.28	0.28
SBG34	253519	6232789	2014/10/04	SandyBay	Grab	23.08	0.00	99.89	0.02	1.87	1.85	0.29	0.10	0.27	0.28
SBG39	252112	6232988	2014/11/04	SandyBay	Grab	41.94	6.10	93.80	0.02	0.60	0.52	0.42	0.59	0.66	0.70
SBG40	252317	6232988	2014/11/04	SandyBay	Grab	76.62	23.68	76.24	0.02	0.45	0.45	0.35	0.29	0.73	0.73
SBG43	252926	6232999	2014/10/04	SandyBay	Grab	33.88	0.26	99.68	0.04	1.21	1.19	0.28	0.11	0.43	0.44
SBG46	251920	6233190	2014/11/04	SandyBay	Grab	73.23	34.93	65.00	0.06	0.47	0.47	0.39	0.43	0.72	0.72
SBG49	252530	6233185	2014/11/04	SandyBay	Grab	58.88	1.74	98.16	0.02	0.66	0.66	0.27	0.08	0.63	0.63
SBG52	251720	6233387	2014/10/04	SandyBay	Grab	56.39	4.26	95.66	0.02	0.65	0.64	0.33	0.38	0.64	0.64
SBG55	252321	6233383	2014/11/04	SandyBay	Grab	52.30	1.02	98.86	0.00	0.74	0.72	0.31	0.16	0.60	0.61
SBG62	252127	6233591	2014/11/04	SandyBay	Grab	46.26	0.17	99.78	0.02	1.15	1.05	0.44	0.64	0.45	0.48
SBG65	252734	6233584	2014/10/04	SandyBay	Grab	44.96	0.16	99.82	0.00	1.83	2.23	0.43	-1.28	0.28	0.21
SBG68	253319	6233590	2014/10/04	SandyBay	Grab	34.20	0.02	99.96	0.00	1.79	1.77	0.31	0.09	0.29	0.29
SBG69	253921	6233634	2014/10/04	SandyBay	Grab	33.00	0.00	99.96	0.00	1.44	1.41	0.30	0.15	0.37	0.38

SBG75	252526	6233793	2014/10/04	SandyBay	Grab	41.08	0.44	99.54	0.01	1.39	1.33	0.42	0.24	0.38	0.40
SBG79	253369	6233835	2014/10/04	SandyBay	Grab	36.31	0.06	99.82	0.04	1.84	1.83	0.29	0.03	0.28	0.28
SBG81	253732	6233787	2014/10/04	SandyBay	Grab	35.62	0.00	99.94	0.04	1.73	1.72	0.35	0.06	0.30	0.30
SBG84	254287	6233780	2014/10/04	SandyBay	Grab	22.50	0.13	99.71	0.02	1.28	1.27	0.31	0.15	0.41	0.41
SBG86	253958	6233980	2014/10/04	SandyBay	Grab	37.24	0.05	99.89	0.00	1.68	1.67	0.35	0.03	0.31	0.32
SBG88	252128	6233992	2014/10/04	SandyBay	Grab	38.73	0.00	99.84	0.09	1.62	1.56	0.47	0.33	0.33	0.34
SBG89	252332	6233985	2014/10/04	SandyBay	Grab	38.92	0.03	99.86	0.02	1.79	1.79	0.44	0.08	0.29	0.29
SBG92	252927	6233995	2014/10/04	SandyBay	Grab	39.73	0.05	99.88	0.01	1.65	1.62	0.34	0.25	0.32	0.33
SBG104	252315	6234385	2014/10/04	SandyBay	Grab	46.63	0.03	99.76	0.07	1.93	1.90	0.49	0.17	0.26	0.27
SBG106	252736	6234382	2014/10/04	SandyBay	Grab	38.53	0.18	99.75	0.03	1.43	1.37	0.40	0.36	0.37	0.39
DIV05	253627	6235612	2010/10/03	12thApostle	Diver	97.21	61.71	38.29	0.00	0.10	0.11	0.21	-0.04	0.93	0.93
DIV07	253477	6235524	2010/10/03	12thApostle	Diver	80.05	80.78	19.12	0.00	-0.10	-0.09	0.23	0.00	1.07	1.06
DIV09	253458	6235603	2010/10/03	12thApostle	Diver	95.89	74.89	24.99	0.02	-0.09	-0.07	0.22	-0.03	1.06	1.05
HBD25	254093	6231852	2013/06/09	HB_dune	Beach	53.39	0.00	100.00	0.00	1.80	1.78	0.23	0.06	0.29	0.29
HBD23	254144	6231830	2013/06/09	HB_dune	Beach	50.48	0.00	99.98	0.04	1.69	1.68	0.33	0.05	0.31	0.31
SBB20	253590	6232012	2013/06/09	SandyBay	Beach	25.49	0.00	100.00	0.00	1.21	1.19	0.23	0.05	0.43	0.44
SBB16	253631	6232028	2013/06/09	SandyBay	Beach	21.58	0.00	100.00	0.00	1.19	1.18	0.24	0.08	0.44	0.44
SBB14	253640	6232063	2013/06/09	SandyBay	Beach	23.78	0.00	100.00	0.00	1.00	1.01	0.29	0.01	0.50	0.50
CBB11	257605	6240073	2013/06/09	CampsBay	Beach	10.93	0.00	100.00	0.00	0.99	1.00	0.29	-0.11	0.50	0.50
CBB09	257666	6240174	2013/06/09	CampsBay	Beach	9.25	0.04	99.96	0.00	1.03	1.03	0.23	0.01	0.49	0.49
CBB02	257706	6240372	2013/06/09	CampsBay	Beach	8.33	0.66	99.30	0.00	0.40	0.40	0.37	-0.04	0.76	0.76
BKB01	257140	6237608	2015/04/27	Bakhoven	Beach	10.94	0.00	99.98	0.00	1.47	1.43	0.21	0.09	0.36	0.37
BKB10	257111	6237608	2015/04/27	Bakhoven	Beach	9.64	0.00	99.96	0.00	1.23	1.21	0.19	0.04	0.43	0.43
CCG15	257341	6241797	2012/07/24	Clifton	Grab	15.91	0.27	99.74	0.00	1.14	1.13	0.30	0.07	0.45	0.46
CCG13	257163	6241994	2012/07/24	Clifton	Grab	13.32	1.37	98.53	0.00	0.94	0.97	0.37	-0.14	0.52	0.51
CCG59	256464	6240794	2012/08/24	CampsBay	Grab	18.58	45.29	54.68	0.03	-0.08	-0.07	0.25	0.01	1.06	1.05
CCG88	256688	6240744	2012/08/24	CampsBay	Grab	32.34	0.12	99.86	0.00	1.26	1.27	0.33	-0.02	0.42	0.42
CCG55	256850	6240615	2012/08/24	CampsBay	Grab	29.83	0.99	98.93	0.00	1.33	1.42	0.52	-0.56	0.40	0.37
CCG68	256952	6240412	2012/08/24	CampsBay	Grab	18.84	0.00	99.98	0.00	1.28	1.28	0.28	0.01	0.41	0.41

CCG83	257272	6240202	2012/08/24	CampsBay	Grab	12.96	0.23	99.70	0.00	0.49	0.53	0.31	-0.13	0.71	0.69
CCG62	257458	6240156	2012/08/24	CampsBay	Grab	17.83	0.00	99.98	0.00	1.13	1.14	0.30	-0.06	0.46	0.45
CCG75	257528	6240462	2012/08/24	CampsBay	Grab	21.14	0.23	99.72	0.00	0.91	0.95	0.44	-0.28	0.53	0.52
CCG48	257446	6240261	2012/08/24	CampsBay	Grab	16.50	1.00	98.98	0.00	0.77	0.86	0.52	-0.49	0.59	0.55
CCG52	257071	6240477	2012/08/24	CampsBay	Grab	30.93	0.06	99.91	0.00	1.50	1.49	0.31	0.01	0.35	0.36
CCG73	257212	6240512	2012/08/24	CampsBay	Grab	27.49	0.03	99.93	0.00	1.50	1.51	0.25	-0.04	0.35	0.35
CCG80	257313	6240695	2012/08/24	CampsBay	Grab	27.01	0.32	99.63	0.02	1.02	1.04	0.39	-0.04	0.49	0.49
CCG72	257315	6240448	2012/08/24	CampsBay	Grab	13.38	0.00	99.98	0.00	1.14	1.13	0.23	-0.01	0.45	0.46
CCG41	256938	6241567	2012/08/24	Clifton	Grab	80.92	77.90	22.00	0.04	-0.13	-0.18	0.24	0.13	1.09	1.13
CCG39	257142	6241455	2012/08/24	Clifton	Grab	17.43	3.85	96.08	0.03	1.25	1.23	0.26	0.00	0.42	0.43
CCG29	257377	6241532	2012/08/24	Clifton	Grab	12.16	0.00	99.98	0.00	1.12	1.10	0.25	0.09	0.46	0.47
CCG03	257329	6242047	2012/08/24	Clifton	Grab	18.68	0.18	99.77	0.00	1.27	1.26	0.30	-0.02	0.41	0.42
CCG43	256349	6241865	2012/08/24	Clifton	Grab	76.49	66.58	33.37	0.00	0.06	0.06	0.24	0.02	0.96	0.96
CCG45	256079	6241929	2012/08/24	Clifton	Grab	90.47	43.53	56.32	0.11	0.34	0.34	0.23	0.01	0.79	0.79
CCG67	257050	6240377	2012/08/24	CampsBay	Grab	17.79	0.00	100.00	0.00	1.12	1.11	0.32	0.09	0.46	0.46
CCG65	257222	6240330	2012/08/24	CampsBay	Grab	25.80	0.66	99.24	0.00	0.59	0.60	0.33	-0.01	0.66	0.66
CCG69	257556	6240329	2012/08/24	CampsBay	Grab	18.76	0.34	99.66	0.00	1.07	1.13	0.43	-0.29	0.48	0.46
CCG49	257342	6240337	2012/08/24	CampsBay	Grab	19.43	0.00	99.94	0.00	0.92	0.92	0.25	-0.02	0.53	0.53
CCG51	257142	6240432	2012/08/24	CampsBay	Grab	23.93	0.00	99.98	0.00	1.17	1.17	0.39	-0.14	0.44	0.44
CCG77	257348	6240536	2012/08/24	CampsBay	Grab	19.30	0.09	99.88	0.00	1.12	1.13	0.37	-0.14	0.46	0.46
CCG37	257290	6241371	2012/08/24	Clifton	Grab	9.94	0.07	99.84	0.00	1.08	1.07	0.27	0.01	0.47	0.48
CCG32	257151	6241666	2012/07/24	Clifton	Grab	11.65	1.34	98.58	0.00	0.92	0.94	0.23	-0.07	0.53	0.52
CCG34	257238	6241521	2012/08/24	Clifton	Grab	15.15	0.00	99.86	0.00	1.32	1.29	0.27	0.09	0.40	0.41
CCG21	256815	6242053	2012/07/24	Clifton	Grab	32.23	0.07	99.72	0.04	2.18	2.18	0.44	-0.08	0.22	0.22
CCG08	256882	6242299	2012/07/24	Clifton	Grab	31.64	0.88	99.03	0.02	1.83	1.86	0.33	-0.17	0.28	0.28
CCG28	257010	6241876	2012/07/24	Clifton	Grab	20.11	0.06	99.91	0.01	1.27	1.26	0.30	0.05	0.41	0.42
CCG11	257321	6241893	2012/07/24	Clifton	Grab	25.88	0.00	99.93	0.00	1.53	1.52	0.43	0.09	0.35	0.35
CCG79	257403	6240647	2012/08/24	CampsBay	Grab	15.66	0.19	99.81	0.00	1.05	1.11	0.45	-0.43	0.48	0.46
CCG04	257252	6242095	2012/08/24	Clifton	Grab	23.46	0.04	99.96	0.00	1.48	1.46	0.28	0.01	0.36	0.36

Appendix B – Settling Tube Results

COUNCIL FOR GEOSCIENCE
SETTLING TUBE ANALYSIS

Council for Geoscience

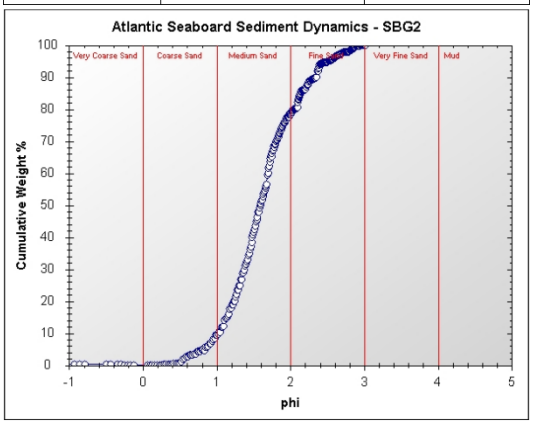

Project and Sample Details:			
Sample Number:	SBG2	Client:	University of Cape Town
Analysis By:	Wilhelm van Zyl	Project Name:	Atlantic Seaboard Sediment Dynamics
Date Analysed:	2015/10/23	Project Location:	Cape Town

Sediment Statistics:			
Mean (mm):	0.34	Median (mm):	0.33
Mean (phi):	1.62	Median (phi):	1.59
Sorting:	0.49	Skewness:	0.19

Grain Size Classification after Wentworth (1922)
All formulas used to calculate settling velocities and grain size radii after Gibbs (1971)

COUNCIL FOR GEOSCIENCE
SETTLING TUBE ANALYSIS

Council for Geoscience

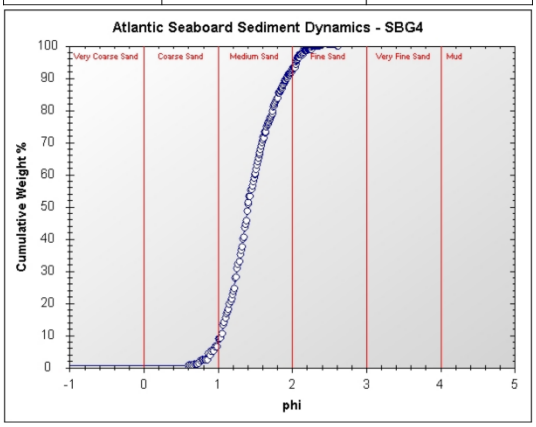

Project and Sample Details:			
Sample Number:	SBG4	Client:	University of Cape Town
Analysis By:	Wilhelm van Zyl	Project Name:	Atlantic Seaboard Sediment Dynamics
Date Analysed:	2015/10/23	Project Location:	Cape Town

Sediment Statistics:			
Mean (mm):	0.38	Median (mm):	0.38
Mean (phi):	1.43	Median (phi):	1.40
Sorting:	0.35	Skewness:	0.13

Grain Size Classification after Wentworth (1922)
All formulas used to calculate settling velocities and grain size radii after Gibbs (1971)

COUNCIL FOR GEOSCIENCE
SETTLING TUBE ANALYSIS

Council for Geoscience

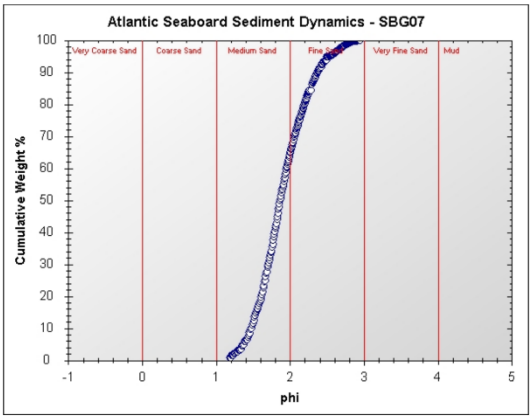

Project and Sample Details:			
Sample Number:	SBG07	Client:	University of Cape Town
Analysis By:	Wilhelm van Zyl	Project Name:	Atlantic Seaboard Sediment Dynamics
Date Analysed:	2015/08/31	Project Location:	Cape Town

Sediment Statistics:			
Mean (mm):	0.27	Median (mm):	0.27
Mean (phi):	1.89	Median (phi):	1.86
Sorting:	0.35	Skewness:	0.13

Grain Size Classification after Wentworth (1922)
All formulas used to calculate settling velocities and grain size radii after Gibbs (1971)

COUNCIL FOR GEOSCIENCE
SETTLING TUBE ANALYSIS

Council for Geoscience

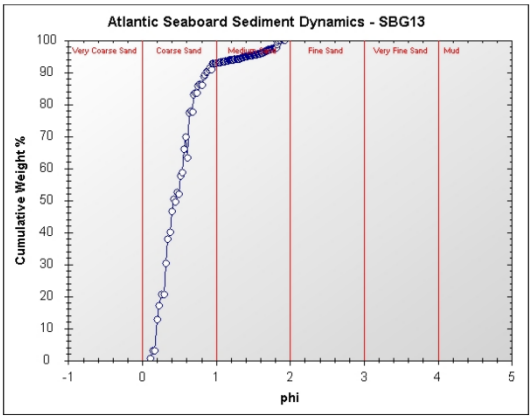

Project and Sample Details:			
Sample Number:	SBG13	Client:	University of Cape Town
Analysis By:	Wilhelm van Zyl	Project Name:	Atlantic Seaboard Sediment Dynamics
Date Analysed:	2015/08/31	Project Location:	Cape Town

Sediment Statistics:			
Mean (mm):	0.73	Median (mm):	0.74
Mean (phi):	0.46	Median (phi):	0.43
Sorting:	0.32	Skewness:	0.50

Grain Size Classification after Wentworth (1922)
All formulas used to calculate settling velocities and grain size radii after Gibbs (1971)

COUNCIL FOR GEOSCIENCE
SETTLING TUBE ANALYSIS

Council for Geoscience

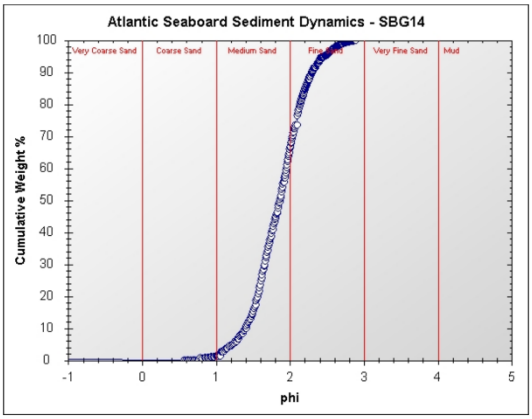

Project and Sample Details:			
Sample Number:	SBG14	Client:	University of Cape Town
Analysis By:	Wilhelm van Zyl	Project Name:	Atlantic Seaboard Sediment Dynamics
Date Analysed:	2015/09/01	Project Location:	Cape Town

Sediment Statistics:			
Mean (mm):	0.28	Median (mm):	0.28
Mean (phi):	1.85	Median (phi):	1.86
Sorting:	0.36	Skewness:	-0.03

Grain Size Classification after Wentworth (1922)
All formulas used to calculate settling velocities and grain size radii after Gibbs (1971)

COUNCIL FOR GEOSCIENCE
SETTLING TUBE ANALYSIS

Council for Geoscience

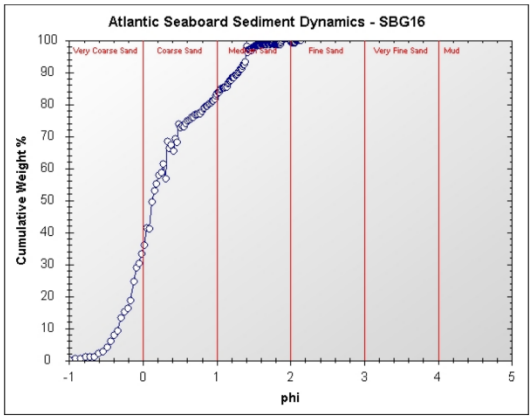

Project and Sample Details:			
Sample Number:	SBG16	Client:	University of Cape Town
Analysis By:	Wilhelm van Zyl	Project Name:	Atlantic Seaboard Sediment Dynamics
Date Analysed:	2015/09/01	Project Location:	Cape Town

Sediment Statistics:			
Mean (mm):	0.86	Median (mm):	0.91
Mean (phi):	0.31	Median (phi):	0.13
Sorting:	0.60	Skewness:	0.97

Grain Size Classification after Wentworth (1922)
All formulas used to calculate settling velocities and grain size radii after Gibbs (1971)

COUNCIL FOR GEOSCIENCE
SETTLING TUBE ANALYSIS

Council for Geoscience

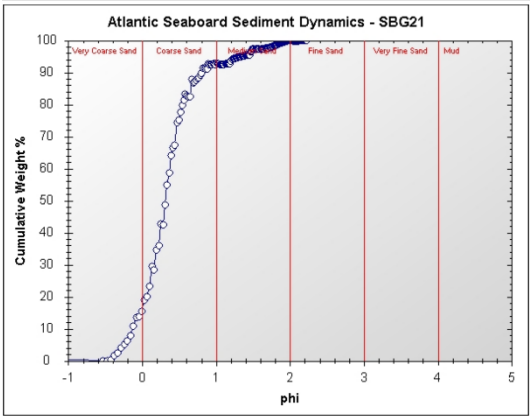

Project and Sample Details:			
Sample Number:	SBG21	Client:	University of Cape Town
Analysis By:	Wilhelm van Zyl	Project Name:	Atlantic Seaboard Sediment Dynamics
Date Analysed:	2015/09/01	Project Location:	Cape Town

Sediment Statistics:			
Mean (mm):	0.81	Median (mm):	0.80
Mean (phi):	0.32	Median (phi):	0.32
Sorting:	0.40	Skewness:	0.36

Grain Size Classification after Wentworth (1922)
All formulas used to calculate settling velocities and grain size radii after Gibbs (1971)

COUNCIL FOR GEOSCIENCE
SETTLING TUBE ANALYSIS

Council for Geoscience

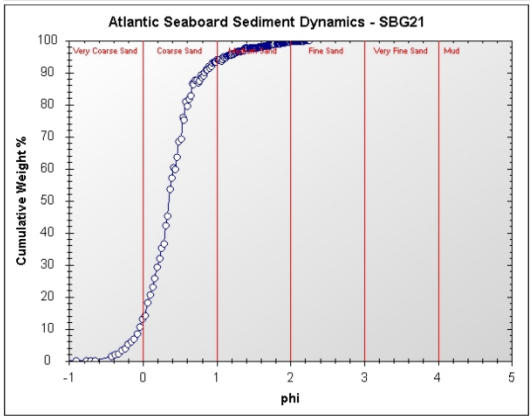

Project and Sample Details:			
Sample Number:	SBG21	Client:	University of Cape TownSBG21
Analysis By:	Wilhelm van Zyl	Project Name:	Atlantic Seaboard Sediment Dynamics
Date Analysed:	2015/09/01	Project Location:	Cape Town

Sediment Statistics:			
Mean (mm):	0.80	Median (mm):	0.78
Mean (phi):	0.35	Median (phi):	0.35
Sorting:	0.35	Skewness:	0.15

Grain Size Classification after Wentworth (1922)
All formulas used to calculate settling velocities and grain size radii after Gibbs (1971)

COUNCIL FOR GEOSCIENCE SETTLING TUBE ANALYSIS

Council for Geoscience

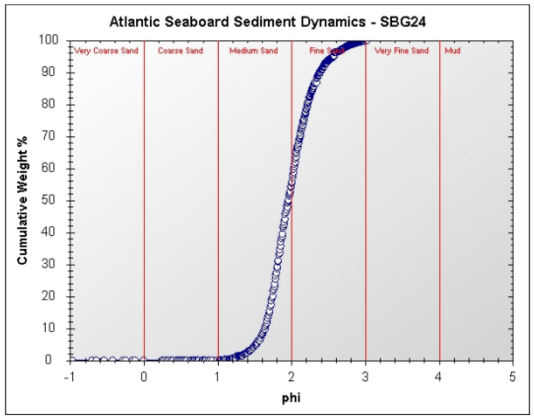

Project and Sample Details:			
Sample Number:	SBG24	Client:	University of Cape TownSBG21
Analysis By:	Wilhelm van Zyl	Project Name:	Atlantic Seaboard Sediment Dynamics
Date Analysed:	2015/09/01	Project Location:	Cape Town

Sediment Statistics:			
Mean (mm):	0.26	Median (mm):	0.26
Mean (phi):	1.98	Median (phi):	1.96
Sorting:	0.30	Skewness:	0.11

Grain Size Classification after Wentworth (1922)
All formulas used to calculate settling velocities and grain size radii after Gibbs (1971)

COUNCIL FOR GEOSCIENCE SETTLING TUBE ANALYSIS

Council for Geoscience

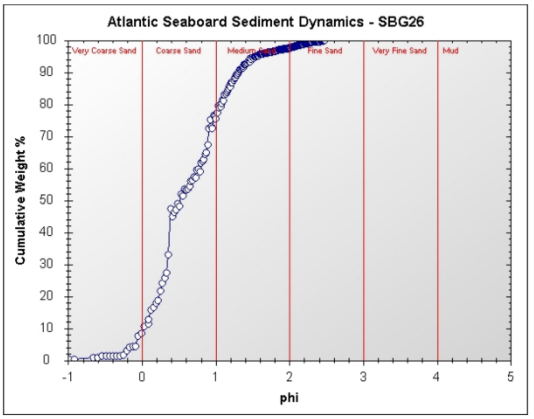

Project and Sample Details:			
Sample Number:	SBG26	Client:	University of Cape TownSBG21
Analysis By:	Wilhelm van Zyl	Project Name:	Atlantic Seaboard Sediment Dynamics
Date Analysed:	2015/09/01	Project Location:	Cape Town

Sediment Statistics:			
Mean (mm):	0.69	Median (mm):	0.70
Mean (phi):	0.60	Median (phi):	0.52
Sorting:	0.50	Skewness:	0.48

Grain Size Classification after Wentworth (1922)
All formulas used to calculate settling velocities and grain size radii after Gibbs (1971)

COUNCIL FOR GEOSCIENCE SETTLING TUBE ANALYSIS

Council for Geoscience

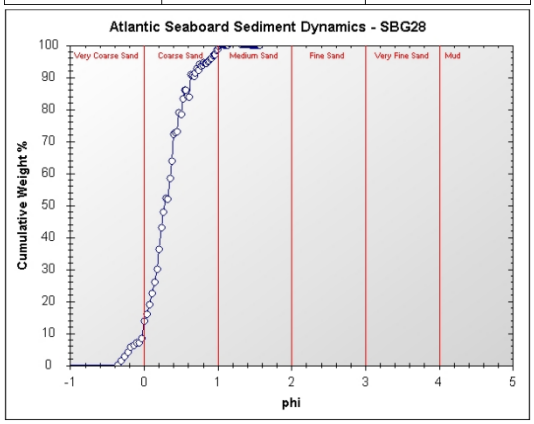

Project and Sample Details:			
Sample Number:	SBG28	Client:	University of Cape TownSBG28
Analysis By:	Wilhelm van Zyl	Project Name:	Atlantic Seaboard Sediment Dynamics
Date Analysed:	2015/09/02	Project Location:	Cape Town

Sediment Statistics:			
Mean (mm):	0.83	Median (mm):	0.82
Mean (phi):	0.29	Median (phi):	0.28
Sorting:	0.28	Skewness:	0.06

Grain Size Classification after Wentworth (1922)
All formulas used to calculate settling velocities and grain size radii after Gibbs (1971)

COUNCIL FOR GEOSCIENCE SETTLING TUBE ANALYSIS

Council for Geoscience

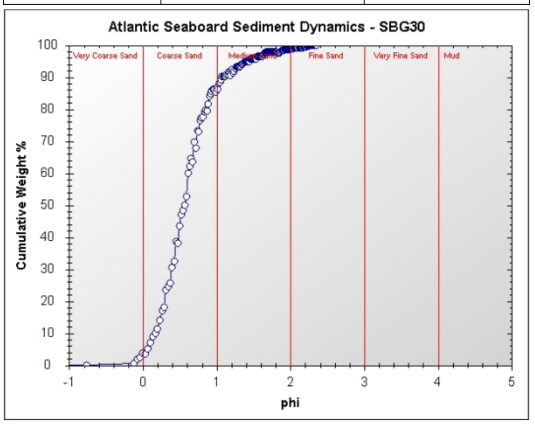

Project and Sample Details:			
Sample Number:	SBG30	Client:	University of Cape Town
Analysis By:	Wilhelm van Zyl	Project Name:	Atlantic Seaboard Sediment Dynamics
Date Analysed:	2015/09/16	Project Location:	Cape Town

Sediment Statistics:			
Mean (mm):	0.69	Median (mm):	0.68
Mean (phi):	0.57	Median (phi):	0.57
Sorting:	0.37	Skewness:	0.26

Grain Size Classification after Wentworth (1922)
All formulas used to calculate settling velocities and grain size radii after Gibbs (1971)

COUNCIL FOR GEOSCIENCE
SETTLING TUBE ANALYSIS

Council for Geoscience

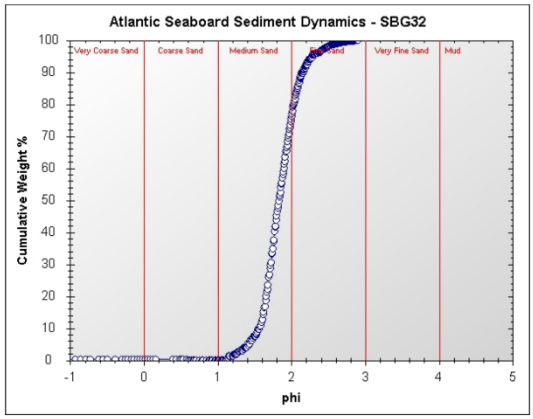

Project and Sample Details:			
Sample Number:	SBG32	Client:	University of Cape Town
Analysis By:	Wilhelm van Zyl	Project Name:	Atlantic Seaboard Sediment Dynamics
Date Analysed:	2015/09/16	Project Location:	Cape Town

Sediment Statistics:			
Mean (mm):	0.28	Median (mm):	0.28
Mean (phi):	1.84	Median (phi):	1.83
Sorting:	0.24	Skewness:	0.03

Grain Size Classification after Wentworth (1922)
All formulas used to calculate settling velocities and grain size radii after Gibbs (1971)

COUNCIL FOR GEOSCIENCE
SETTLING TUBE ANALYSIS

Council for Geoscience

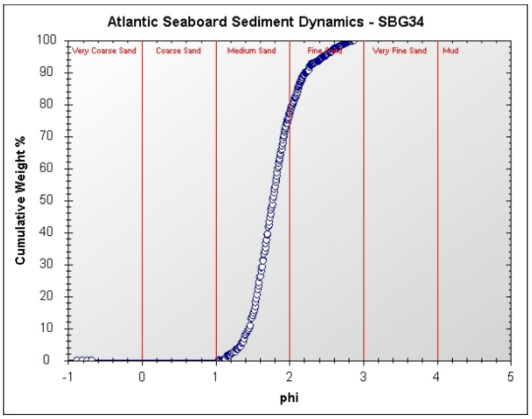

Project and Sample Details:			
Sample Number:	SBG34	Client:	University of Cape Town
Analysis By:	Wilhelm van Zyl	Project Name:	Atlantic Seaboard Sediment Dynamics
Date Analysed:	2015/09/18	Project Location:	Cape Town

Sediment Statistics:			
Mean (mm):	0.29	Median (mm):	0.29
Mean (phi):	1.82	Median (phi):	1.81
Sorting:	0.28	Skewness:	0.01

Grain Size Classification after Wentworth (1922)
All formulas used to calculate settling velocities and grain size radii after Gibbs (1971)

COUNCIL FOR GEOSCIENCE
SETTLING TUBE ANALYSIS

Council for Geoscience

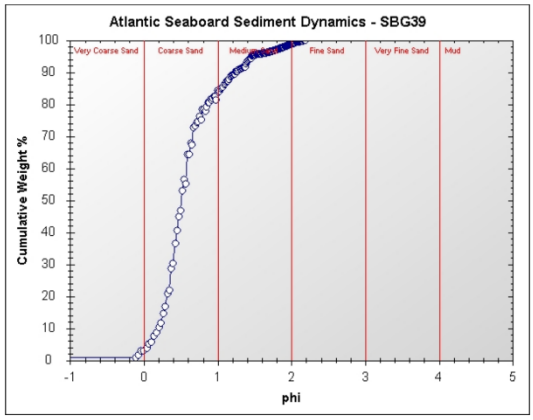

Project and Sample Details:			
Sample Number:	SBG39	Client:	University of Cape Town
Analysis By:	Wilhelm van Zyl	Project Name:	Atlantic Seaboard Sediment Dynamics
Date Analysed:	2015/09/18	Project Location:	Cape Town

Sediment Statistics:			
Mean (mm):	0.68	Median (mm):	0.70
Mean (phi):	0.59	Median (phi):	0.51
Sorting:	0.39	Skewness:	0.44

Grain Size Classification after Wentworth (1922)
All formulas used to calculate settling velocities and grain size radii after Gibbs (1971)

COUNCIL FOR GEOSCIENCE
SETTLING TUBE ANALYSIS

Council for Geoscience

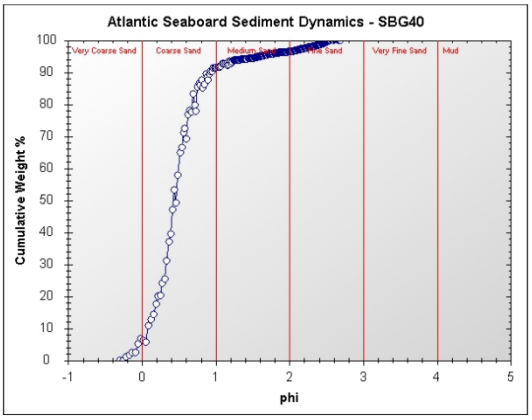

Project and Sample Details:			
Sample Number:	SBG40	Client:	University of Cape Town
Analysis By:	Wilhelm van Zyl	Project Name:	Atlantic Seaboard Sediment Dynamics
Date Analysed:	2015/10/09	Project Location:	Cape Town

Sediment Statistics:			
Mean (mm):	0.74	Median (mm):	0.74
Mean (phi):	0.45	Median (phi):	0.43
Sorting:	0.40	Skewness:	0.60

Grain Size Classification after Wentworth (1922)
All formulas used to calculate settling velocities and grain size radii after Gibbs (1971)

COUNCIL FOR GEOSCIENCE SETTLING TUBE ANALYSIS

Council for Geoscience

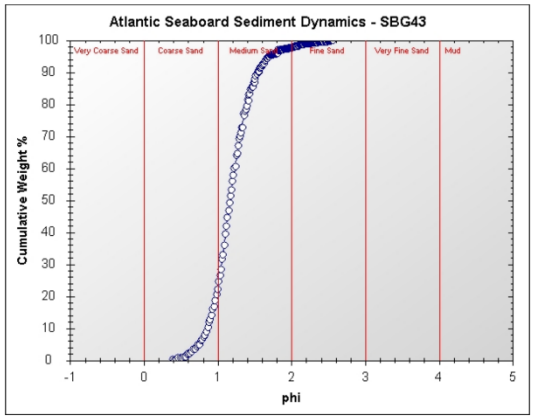

Project and Sample Details:			
Sample Number:	SBG43	Client:	University of Cape Town
Analysis By:	Wilhelm van Zyl	Project Name:	Atlantic Seaboard Sediment Dynamics
Date Analysed:	2015/10/09	Project Location:	Cape Town

Sediment Statistics:			
Mean (mm):	0.45	Median (mm):	0.45
Mean (phi):	1.18	Median (phi):	1.16
Sorting:	0.27	Skewness:	0.07

Grain Size Classification after Wentworth (1922)
All formulas used to calculate settling velocities and grain size radii after Gibbs (1971)

COUNCIL FOR GEOSCIENCE SETTLING TUBE ANALYSIS

Council for Geoscience

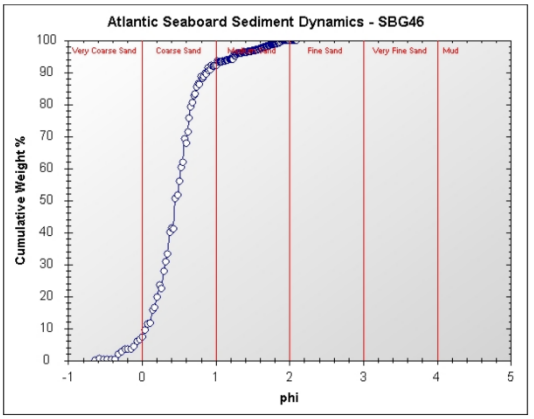

Project and Sample Details:			
Sample Number:	SBG46	Client:	University of Cape Town
Analysis By:	Wilhelm van Zyl	Project Name:	Atlantic Seaboard Sediment Dynamics
Date Analysed:	2015/10/09	Project Location:	Cape Town

Sediment Statistics:			
Mean (mm):	0.74	Median (mm):	0.73
Mean (phi):	0.45	Median (phi):	0.45
Sorting:	0.35	Skewness:	0.16

Grain Size Classification after Wentworth (1922)
All formulas used to calculate settling velocities and grain size radii after Gibbs (1971)

COUNCIL FOR GEOSCIENCE SETTLING TUBE ANALYSIS

Council for Geoscience

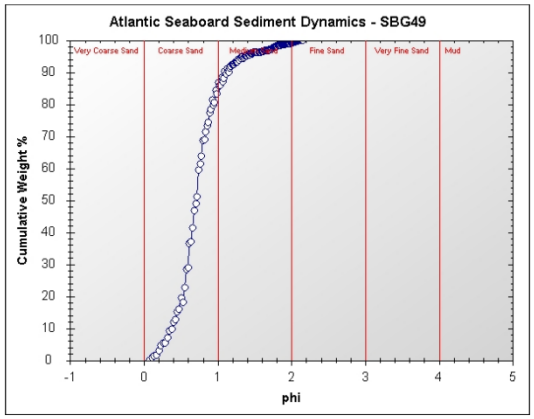

Project and Sample Details:			
Sample Number:	SBG49	Client:	University of Cape Town
Analysis By:	Wilhelm van Zyl	Project Name:	Atlantic Seaboard Sediment Dynamics
Date Analysed:	2015/10/09	Project Location:	Cape Town

Sediment Statistics:			
Mean (mm):	0.61	Median (mm):	0.61
Mean (phi):	0.72	Median (phi):	0.71
Sorting:	0.29	Skewness:	0.12

Grain Size Classification after Wentworth (1922)
All formulas used to calculate settling velocities and grain size radii after Gibbs (1971)

COUNCIL FOR GEOSCIENCE SETTLING TUBE ANALYSIS

Council for Geoscience

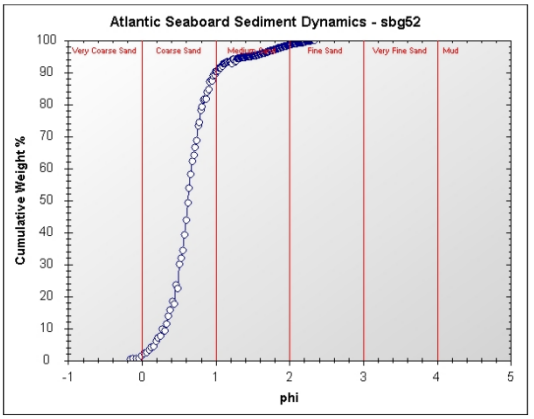

Project and Sample Details:			
Sample Number:	sbg52	Client:	University of Cape Town
Analysis By:	Wilhelm van Zyl	Project Name:	Atlantic Seaboard Sediment Dynamics
Date Analysed:	2015/10/12	Project Location:	Cape Town

Sediment Statistics:			
Mean (mm):	0.65	Median (mm):	0.65
Mean (phi):	0.63	Median (phi):	0.62
Sorting:	0.32	Skewness:	0.26

Grain Size Classification after Wentworth (1922)
All formulas used to calculate settling velocities and grain size radii after Gibbs (1971)

COUNCIL FOR GEOSCIENCE SETTLING TUBE ANALYSIS

Council for Geoscience

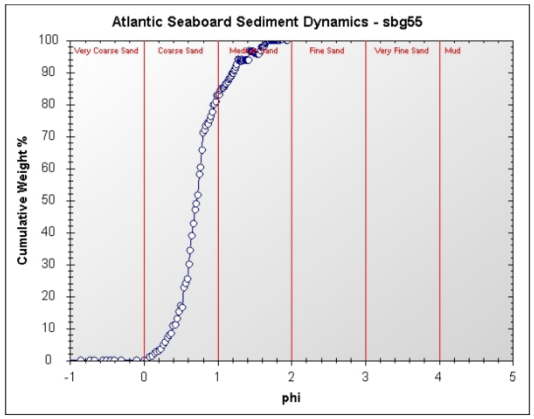

Project and Sample Details:			
Sample Number:	sbg55	Client:	University of Cape Town
Analysis By:	Wilhelm van Zyl	Project Name:	Atlantic Seaboard Sediment Dynamics
Date Analysed:	2015/10/12	Project Location:	Cape Town

Sediment Statistics:			
Mean (mm):	0.60	Median (mm):	0.61
Mean (phi):	0.74	Median (phi):	0.72
Sorting:	0.31	Skewness:	0.16

Grain Size Classification after Wentworth (1922)
All formulas used to calculate settling velocities and grain size radii after Gibbs (1971)

COUNCIL FOR GEOSCIENCE SETTLING TUBE ANALYSIS

Council for Geoscience

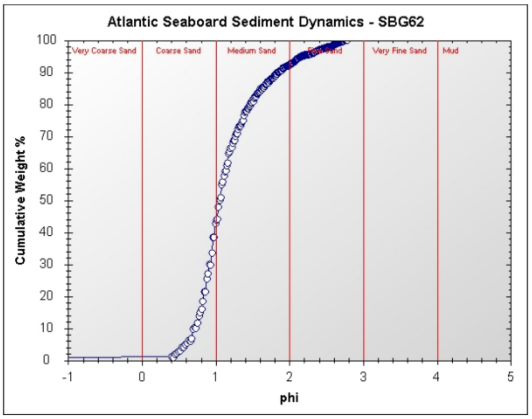

Project and Sample Details:			
Sample Number:	SBG62	Client:	University of Cape Town
Analysis By:	Wilhelm van Zyl	Project Name:	Atlantic Seaboard Sediment Dynamics
Date Analysed:	2015/10/12	Project Location:	Cape Town

Sediment Statistics:			
Mean (mm):	0.46	Median (mm):	0.48
Mean (phi):	1.15	Median (phi):	1.05
Sorting:	0.44	Skewness:	0.64

Grain Size Classification after Wentworth (1922)
All formulas used to calculate settling velocities and grain size radii after Gibbs (1971)

COUNCIL FOR GEOSCIENCE SETTLING TUBE ANALYSIS

Council for Geoscience

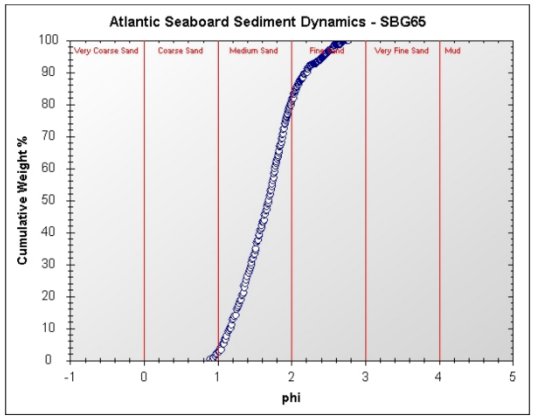

Project and Sample Details:			
Sample Number:	SBG65	Client:	University of Cape Town
Analysis By:	Wilhelm van Zyl	Project Name:	Atlantic Seaboard Sediment Dynamics
Date Analysed:	2015/10/12	Project Location:	Cape Town

Sediment Statistics:			
Mean (mm):	0.32	Median (mm):	0.31
Mean (phi):	1.66	Median (phi):	1.69
Sorting:	0.41	Skewness:	0.05

Grain Size Classification after Wentworth (1922)
All formulas used to calculate settling velocities and grain size radii after Gibbs (1971)

COUNCIL FOR GEOSCIENCE SETTLING TUBE ANALYSIS

Council for Geoscience

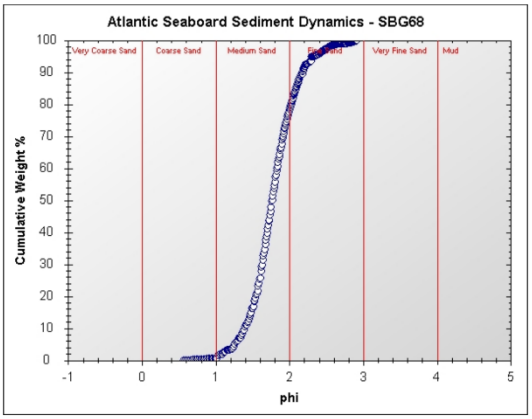

Project and Sample Details:			
Sample Number:	SBG68	Client:	University of Cape Town
Analysis By:	Wilhelm van Zyl	Project Name:	Atlantic Seaboard Sediment Dynamics
Date Analysed:	2015/10/12	Project Location:	Cape Town

Sediment Statistics:			
Mean (mm):	0.30	Median (mm):	0.29
Mean (phi):	1.78	Median (phi):	1.76
Sorting:	0.31	Skewness:	0.04

Grain Size Classification after Wentworth (1922)
All formulas used to calculate settling velocities and grain size radii after Gibbs (1971)

COUNCIL FOR GEOSCIENCE SETTLING TUBE ANALYSIS

Council for Geoscience

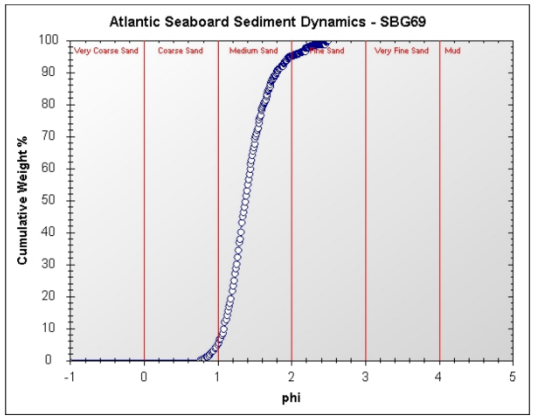

Project and Sample Details:			
Sample Number:	SBG69	Client:	University of Cape Town
Analysis By:	Wilhelm van Zyl	Project Name:	Atlantic Seaboard Sediment Dynamics
Date Analysed:	2015/10/12	Project Location:	Cape Town

Sediment Statistics:			
Mean (mm):	0.38	Median (mm):	0.39
Mean (phi):	1.40	Median (phi):	1.38
Sorting:	0.28	Skewness:	0.14

Grain Size Classification after Wentworth (1922)
All formulas used to calculate settling velocities and grain size radii after Gibbs (1971)

COUNCIL FOR GEOSCIENCE SETTLING TUBE ANALYSIS

Council for Geoscience

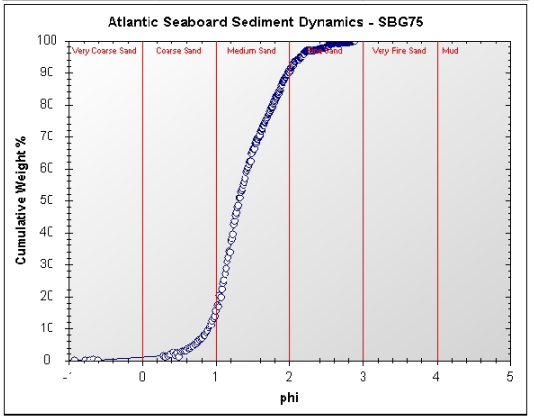

Project and Sample Details:			
Sample Number:	SBG75	Client:	University of Cape Town
Analysis By:	Wilhelm van Zyl	Project Name:	Atlantic Seaboard Sediment Dynamics
Date Analysed:	2015/10/20	Project Location:	Cape Town

Sediment Statistics:			
Mean (mm):	0.39	Median (mm):	0.40
Mean (phi):	1.39	Median (phi):	1.31
Sorting:	0.43	Skewness:	0.28

Grain Size Classification after Wentworth (1922)
All formulas used to calculate settling velocities and grain size radii after Gibbs (1971)

COUNCIL FOR GEOSCIENCE SETTLING TUBE ANALYSIS

Council for Geoscience

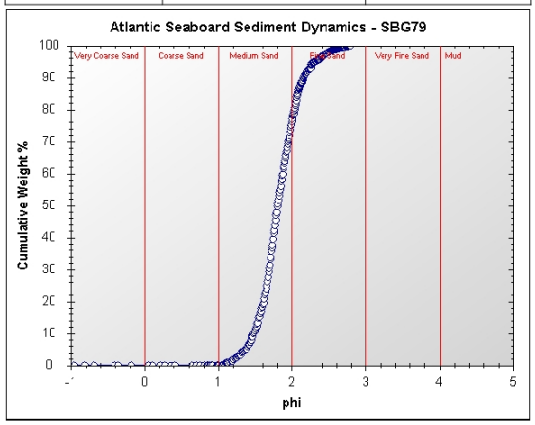

Project and Sample Details:			
Sample Number:	SBG79	Client:	University of Cape Town
Analysis By:	Wilhelm van Zyl	Project Name:	Atlantic Seaboard Sediment Dynamics
Date Analysed:	2015/10/20	Project Location:	Cape Town

Sediment Statistics:			
Mean (mm):	0.29	Median (mm):	0.29
Mean (phi):	1.81	Median (phi):	1.80
Sorting:	0.27	Skewness:	0.04

Grain Size Classification after Wentworth (1922)
All formulas used to calculate settling velocities and grain size radii after Gibbs (1971)

COUNCIL FOR GEOSCIENCE SETTLING TUBE ANALYSIS

Council for Geoscience

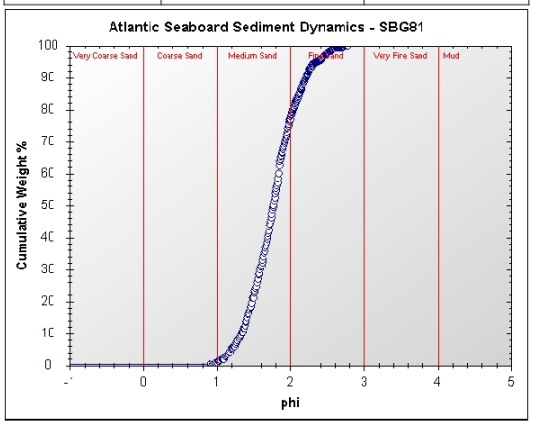

Project and Sample Details:			
Sample Number:	SBG81	Client:	University of Cape Town
Analysis By:	Wilhelm van Zyl	Project Name:	Atlantic Seaboard Sediment Dynamics
Date Analysed:	2015/10/21	Project Location:	Cape Town

Sediment Statistics:			
Mean (mm):	0.30	Median (mm):	0.29
Mean (phi):	1.77	Median (phi):	1.77
Sorting:	0.35	Skewness:	0.01

Grain Size Classification after Wentworth (1922)
All formulas used to calculate settling velocities and grain size radii after Gibbs (1971)

COUNCIL FOR GEOSCIENCE
SETTLING TUBE ANALYSIS

Council for Geoscience

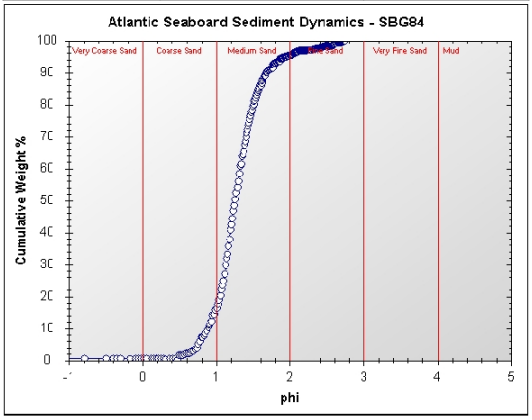

Project and Sample Details:			
Sample Number:	SBG84	Client:	University of Cape Town
Analysis By:	Wilhelm van Zyl	Project Name:	Atlantic Seaboard Sediment Dynamics
Date Analysed:	2015/10/21	Project Location:	Cape Town

Sediment Statistics:			
Mean (mm):	0.42	Median (mm):	0.42
Mean (phi):	1.27	Median (phi):	1.26
Sorting:	0.32	Skewness:	0.13

Grain Size Classification after Wentworth (1922)
All formulas used to calculate settling velocities and grain size radii after Gibbs (1971)

COUNCIL FOR GEOSCIENCE
SETTLING TUBE ANALYSIS

Council for Geoscience

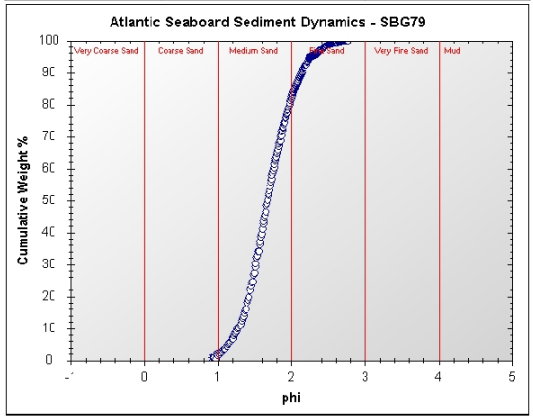

Project and Sample Details:			
Sample Number:	SBG79	Client:	University of Cape Town
Analysis By:	Wilhelm van Zyl	Project Name:	Atlantic Seaboard Sediment Dynamics
Date Analysed:	2015/10/21	Project Location:	Cape Town

Sediment Statistics:			
Mean (mm):	0.31	Median (mm):	0.31
Mean (phi):	1.69	Median (phi):	1.67
Sorting:	0.34	Skewness:	0.05

Grain Size Classification after Wentworth (1922)
All formulas used to calculate settling velocities and grain size radii after Gibbs (1971)

COUNCIL FOR GEOSCIENCE
SETTLING TUBE ANALYSIS

Council for Geoscience

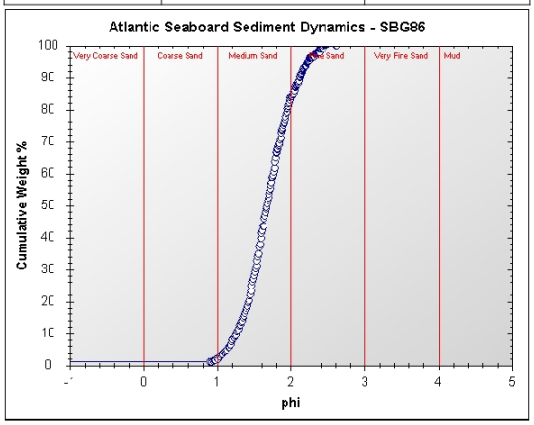

Project and Sample Details:			
Sample Number:	SBG86	Client:	University of Cape Town
Analysis By:	Wilhelm van Zyl	Project Name:	Atlantic Seaboard Sediment Dynamics
Date Analysed:	2015/10/26	Project Location:	Cape Town

Sediment Statistics:			
Mean (mm):	0.32	Median (mm):	0.31
Mean (phi):	1.68	Median (phi):	1.67
Sorting:	0.32	Skewness:	0.02

Grain Size Classification after Wentworth (1922)
All formulas used to calculate settling velocities and grain size radii after Gibbs (1971)

COUNCIL FOR GEOSCIENCE
SETTLING TUBE ANALYSIS

Council for Geoscience

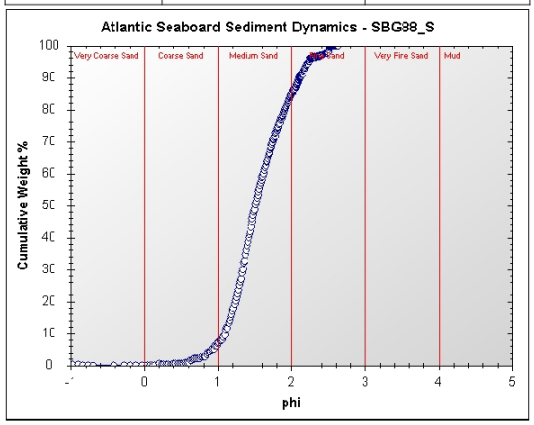

Project and Sample Details:			
Sample Number:	SBG88_S	Client:	University of Cape Town
Analysis By:	Wilhelm van Zyl	Project Name:	Atlantic Seaboard Sediment Dynamics
Date Analysed:	2015/10/26	Project Location:	Cape Town

Sediment Statistics:			
Mean (mm):	0.35	Median (mm):	0.35
Mean (phi):	1.56	Median (phi):	1.51
Sorting:	0.40	Skewness:	0.15

Grain Size Classification after Wentworth (1922)
All formulas used to calculate settling velocities and grain size radii after Gibbs (1971)

COUNCIL FOR GEOSCIENCE
SETTLING TUBE ANALYSIS

Council for Geoscience

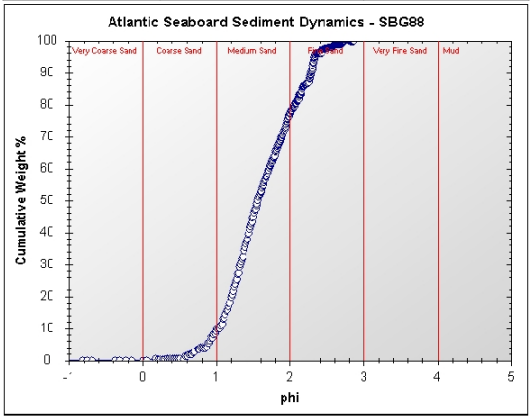

Project and Sample Details:			
Sample Number:	SBG88	Client:	University of Cape Town
Analysis By:	Wilhelm van Zyl	Project Name:	Atlantic Seaboard Sediment Dynamics
Date Analysed:	2015/10/21	Project Location:	Cape Town

Sediment Statistics:			
Mean (mm):	0.34	Median (mm):	0.34
Mean (phi):	1.62	Median (phi):	1.56
Sorting:	0.47	Skewness:	0.16

Grain Size Classification after Wentworth (1922)
All formulas used to calculate settling velocities and grain size radii after Gibbs (1971)

COUNCIL FOR GEOSCIENCE
SETTLING TUBE ANALYSIS

Council for Geoscience

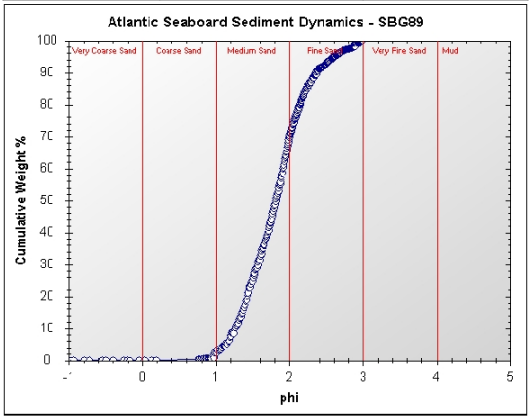

Project and Sample Details:			
Sample Number:	SBG89	Client:	University of Cape Town
Analysis By:	Wilhelm van Zyl	Project Name:	Atlantic Seaboard Sediment Dynamics
Date Analysed:	2015/10/21	Project Location:	Cape Town

Sediment Statistics:			
Mean (mm):	0.30	Median (mm):	0.28
Mean (phi):	1.80	Median (phi):	1.81
Sorting:	0.43	Skewness:	0.07

Grain Size Classification after Wentworth (1922)
All formulas used to calculate settling velocities and grain size radii after Gibbs (1971)

COUNCIL FOR GEOSCIENCE
SETTLING TUBE ANALYSIS

Council for Geoscience

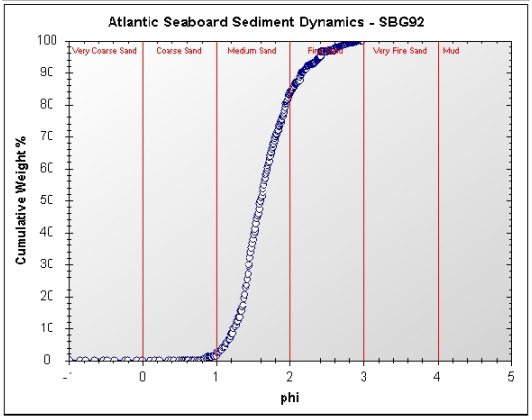

Project and Sample Details:			
Sample Number:	SBG92	Client:	University of Cape Town
Analysis By:	Wilhelm van Zyl	Project Name:	Atlantic Seaboard Sediment Dynamics
Date Analysed:	2015/10/21	Project Location:	Cape Town

Sediment Statistics:			
Mean (mm):	0.32	Median (mm):	0.33
Mean (phi):	1.65	Median (phi):	1.60
Sorting:	0.36	Skewness:	0.27

Grain Size Classification after Wentworth (1922)
All formulas used to calculate settling velocities and grain size radii after Gibbs (1971)

COUNCIL FOR GEOSCIENCE
SETTLING TUBE ANALYSIS

Council for Geoscience

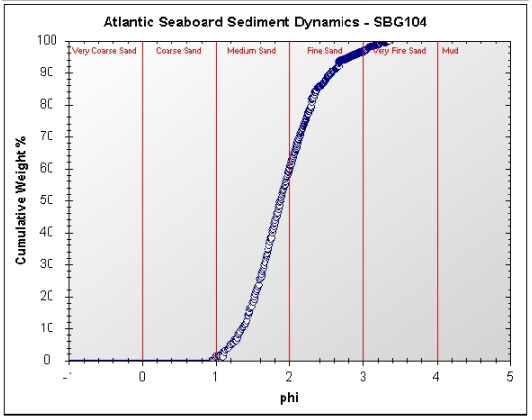

Project and Sample Details:			
Sample Number:	SBG104	Client:	University of Cape Town
Analysis By:	Wilhelm van Zyl	Project Name:	Atlantic Seaboard Sediment Dynamics
Date Analysed:	2015/10/22	Project Location:	Cape Town

Sediment Statistics:			
Mean (mm):	0.28	Median (mm):	0.27
Mean (phi):	1.90	Median (phi):	1.88
Sorting:	0.47	Skewness:	0.26

Grain Size Classification after Wentworth (1922)
All formulas used to calculate settling velocities and grain size radii after Gibbs (1971)

COUNCIL FOR GEOSCIENCE SETTLING TUBE ANALYSIS

Council for Geoscience

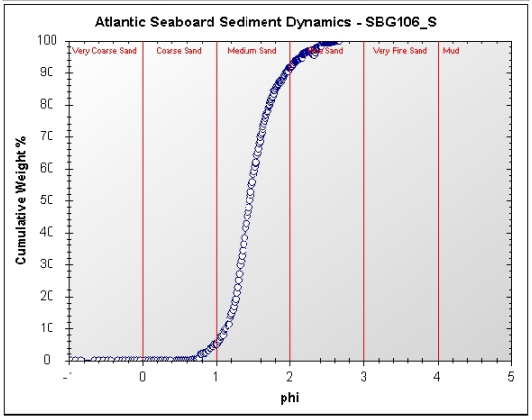

Project and Sample Details:			
Sample Number:	SBG106_S	Client:	University of Cape Town
Analysis By:	Wilhelm van Zyl	Project Name:	Atlantic Seaboard Sediment Dynamics
Date Analysed:	2015/10/26	Project Location:	Cape Town

Sediment Statistics:			
Mean (mm):	0.36	Median (mm):	0.37
Mean (phi):	1.49	Median (phi):	1.45
Sorting:	0.32	Skewness:	0.17

Grain Size Classification after Wentworth (1922)
All formulas used to calculate settling velocities and grain size radii after Gibbs (1971)

COUNCIL FOR GEOSCIENCE SETTLING TUBE ANALYSIS

Council for Geoscience

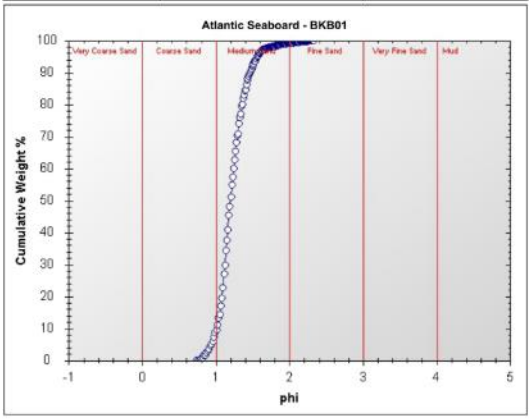

Project and Sample Details:			
Sample Number:	BKB01	Client:	University of Cape Town
Analysis By:	Wilhelm van Zyl	Project Name:	Atlantic Seaboard Sediment Dynamics
Date Analysed:	2016/09/22	Project Location:	Bakoven

Sediment Statistics:			
Mean (mm):	0.43	Median (mm):	0.44
Mean (phi):	1.22	Median (phi):	1.20
Sorting:	0.18	Skewness:	0.04

Grain Size Classification after Wentworth (1922)
All formulas used to calculate settling velocities and grain size radii after Gibbs (1971)

COUNCIL FOR GEOSCIENCE SETTLING TUBE ANALYSIS

Council for Geoscience

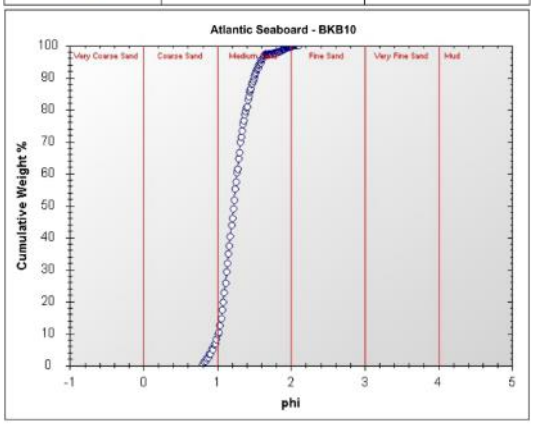

Project and Sample Details:			
Sample Number:	BKB10b	Client:	University of Cape Town
Analysis By:	Wilhelm van Zyl	Project Name:	Atlantic Seaboard Sediment Dynamics
Date Analysed:	2016/09/22	Project Location:	Bakoven

Sediment Statistics:			
Mean (mm):	0.43	Median (mm):	0.43
Mean (phi):	1.24	Median (phi):	1.22
Sorting:	0.19	Skewness:	0.03

Grain Size Classification after Wentworth (1922)
All formulas used to calculate settling velocities and grain size radii after Gibbs (1971)

COUNCIL FOR GEOSCIENCE SETTLING TUBE ANALYSIS

Council for Geoscience

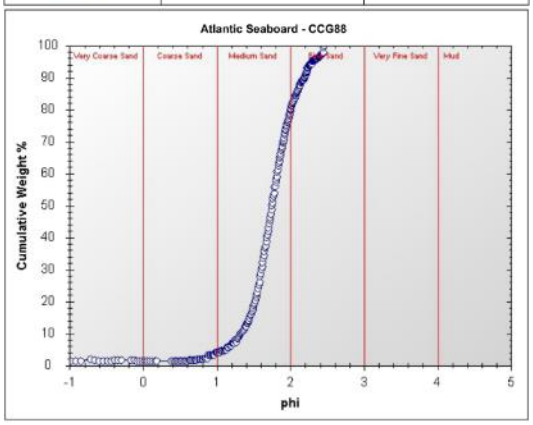

Project and Sample Details:			
Sample Number:	CCG88	Client:	University of Cape Town
Analysis By:	Wilhelm van Zyl	Project Name:	Atlantic Seaboard
Date Analysed:	2016/06/23	Project Location:	Camps Bay

Sediment Statistics:			
Mean (mm):	0.30	Median (mm):	0.30
Mean (phi):	1.76	Median (phi):	1.75
Sorting:	0.33	Skewness:	-0.03

Grain Size Classification after Wentworth (1922)
All formulas used to calculate settling velocities and grain size radii after Gibbs (1971)

COUNCIL FOR GEOSCIENCE SETTLING TUBE ANALYSIS

Council for Geoscience

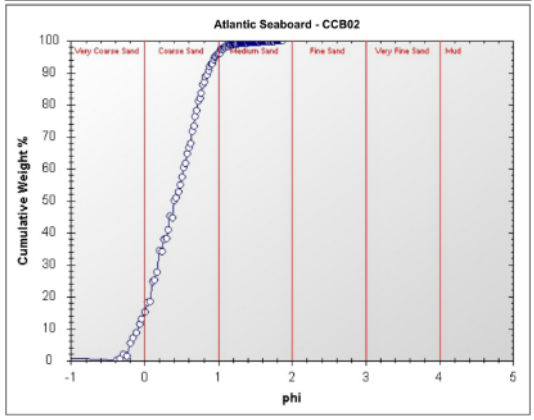

Project and Sample Details:			
Sample Number:	CCB02	Client:	University of Cape Town
Analysis By:	Leslee Salzmann	Project Name:	Atlantic Seaboard
Date Analysed:	22/02/2017	Project Location:	Camps Bay Beach

Sediment Statistics:			
Mean (mm):	0.78	Median (mm):	0.76
Mean (phi):	0.40	Median (phi):	0.40
Sorting:	0.37	Skewness:	-0.04

Grain Size Classification after Wentworth (1922)
All formulas used to calculate settling velocities and grain size radii after Gibbs (1971)

COUNCIL FOR GEOSCIENCE SETTLING TUBE ANALYSIS

Council for Geoscience

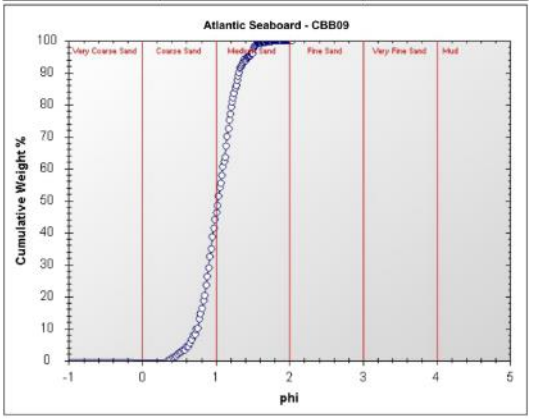

Project and Sample Details:			
Sample Number:	CBB09	Client:	University of Cape Town
Analysis By:	Leslee Salzmann	Project Name:	Atlantic Seaboard
Date Analysed:	23/02/2017	Project Location:	Camps Bay Beach

Sediment Statistics:			
Mean (mm):	0.49	Median (mm):	0.49
Mean (phi):	1.03	Median (phi):	1.03
Sorting:	0.23	Skewness:	0.01

Grain Size Classification after Wentworth (1922)
All formulas used to calculate settling velocities and grain size radii after Gibbs (1971)

COUNCIL FOR GEOSCIENCE SETTLING TUBE ANALYSIS

Council for Geoscience

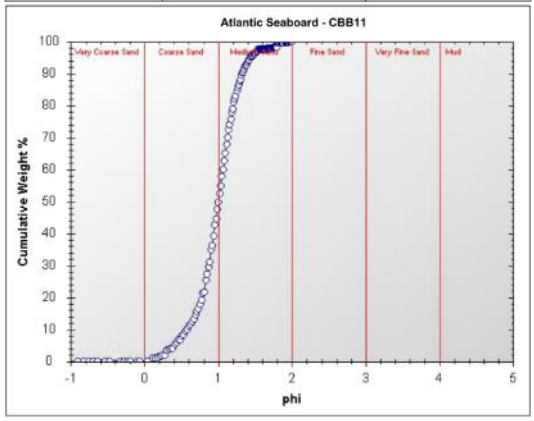

Project and Sample Details:			
Sample Number:	CBB11	Client:	University of Cape Town
Analysis By:	Leslee Salzmann	Project Name:	Atlantic Seaboard
Date Analysed:	23/02/2017	Project Location:	Camps Bay Beach

Sediment Statistics:			
Mean (mm):	0.51	Median (mm):	0.50
Mean (phi):	0.99	Median (phi):	1.00
Sorting:	0.29	Skewness:	-0.11

Grain Size Classification after Wentworth (1922)
All formulas used to calculate settling velocities and grain size radii after Gibbs (1971)

COUNCIL FOR GEOSCIENCE SETTLING TUBE ANALYSIS

Council for Geoscience

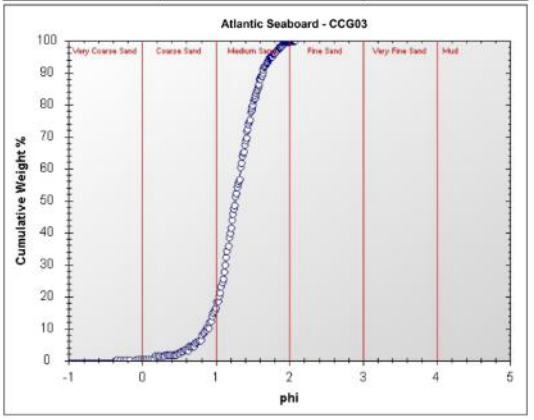

Project and Sample Details:			
Sample Number:	CCG03	Client:	University of Cape Town
Analysis By:	Wilhelm van Zyl	Project Name:	Atlantic Seaboard
Date Analysed:	2016/06/23	Project Location:	Camps Bay

Sediment Statistics:			
Mean (mm):	0.42	Median (mm):	0.42
Mean (phi):	1.27	Median (phi):	1.26
Sorting:	0.30	Skewness:	-0.02

Grain Size Classification after Wentworth (1922)
All formulas used to calculate settling velocities and grain size radii after Gibbs (1971)

COUNCIL FOR GEOSCIENCE SETTLING TUBE ANALYSIS

Council for Geoscience

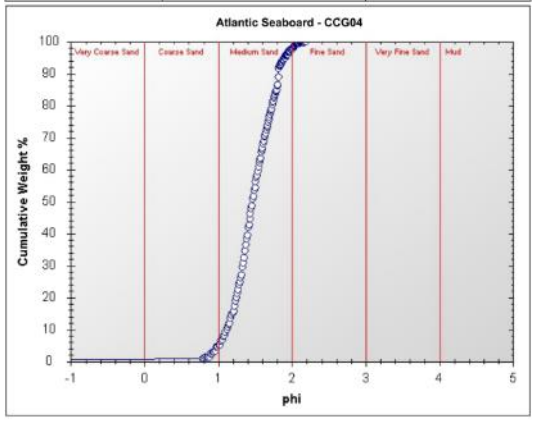

Project and Sample Details:			
Sample Number:	CCG04	Client:	University of Cape Town
Analysis By:	Leslee Salzmann	Project Name:	Atlantic Seaboard
Date Analysed:	12/06/2017	Project Location:	Camps Bay

Sediment Statistics:			
Mean (mm):	0.36	Median (mm):	0.36
Mean (phi):	1.48	Median (phi):	1.46
Sorting:	0.28	Skewness:	0.01

Grain Size Classification after Wentworth (1922)
All formulas used to calculate settling velocities and grain size radii after Gibbs (1971)

COUNCIL FOR GEOSCIENCE SETTLING TUBE ANALYSIS

Council for Geoscience

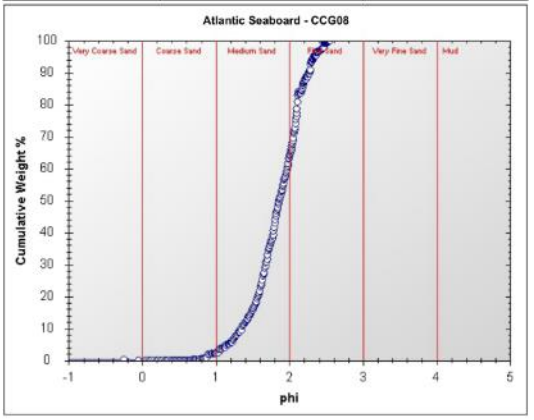

Project and Sample Details:			
Sample Number:	CCG08	Client:	University of Cape Town
Analysis By:	Wilhelm van Zyl	Project Name:	Atlantic Seaboard
Date Analysed:	2016/06/23	Project Location:	Camps Bay

Sediment Statistics:			
Mean (mm):	0.29	Median (mm):	0.28
Mean (phi):	1.83	Median (phi):	1.86
Sorting:	0.33	Skewness:	-0.17

Grain Size Classification after Wentworth (1922)
All formulas used to calculate settling velocities and grain size radii after Gibbs (1971)

COUNCIL FOR GEOSCIENCE SETTLING TUBE ANALYSIS

Council for Geoscience

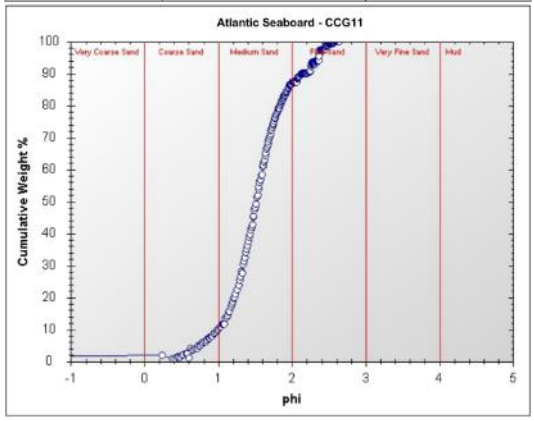

Project and Sample Details:			
Sample Number:	CCG11	Client:	University of Cape Town
Analysis By:	Leslee Salzmann	Project Name:	Atlantic Seaboard
Date Analysed:	24/02/2017	Project Location:	Camps Bay

Sediment Statistics:			
Mean (mm):	0.35	Median (mm):	0.35
Mean (phi):	1.53	Median (phi):	1.52
Sorting:	0.43	Skewness:	0.09

Grain Size Classification after Wentworth (1922)
All formulas used to calculate settling velocities and grain size radii after Gibbs (1971)

COUNCIL FOR GEOSCIENCE SETTLING TUBE ANALYSIS

Council for Geoscience

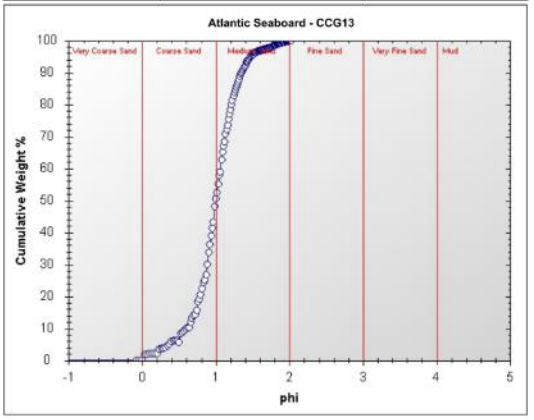

Project and Sample Details:			
Sample Number:	CCG13b	Client:	University of Cape Town
Analysis By:	W. van Zyl	Project Name:	Atlantic Seaboard Sediment Dynamics
Date Analysed:	2014/03/17	Project Location:	Camps Bay, South Africa

Sediment Statistics:			
Mean (mm):	0.51	Median (mm):	0.50
Mean (phi):	1.00	Median (phi):	1.00
Sorting:	0.30	Skewness:	-0.08

Grain Size Classification after Wentworth (1922)
All formulas used to calculate settling velocities and grain size radii after Gibbs (1971)

COUNCIL FOR GEOSCIENCE SETTLING TUBE ANALYSIS

Council for Geoscience

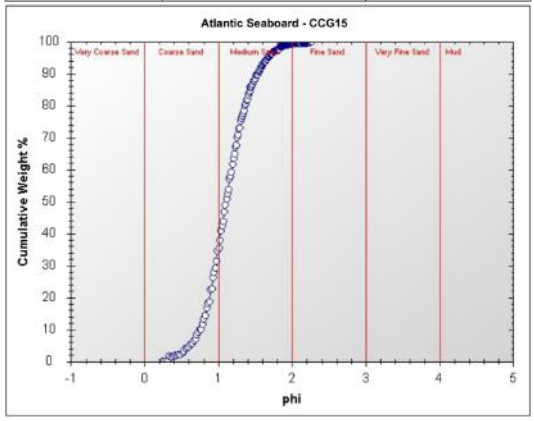

Project and Sample Details:			
Sample Number:	CCG15c	Client:	University of Cape Town
Analysis By:	Wilhelm van Zyl	Project Name:	Atlantic Seaboard Sediment Dynamics
Date Analysed:	2016/09/22	Project Location:	Atlantic Seaboard

Sediment Statistics:			
Mean (mm):	0.47	Median (mm):	0.46
Mean (phi):	1.12	Median (phi):	1.10
Sorting:	0.31	Skewness:	0.05

Grain Size Classification after Wentworth (1922)
All formulas used to calculate settling velocities and grain size radii after Gibbs (1971)

COUNCIL FOR GEOSCIENCE SETTLING TUBE ANALYSIS

Council for Geoscience

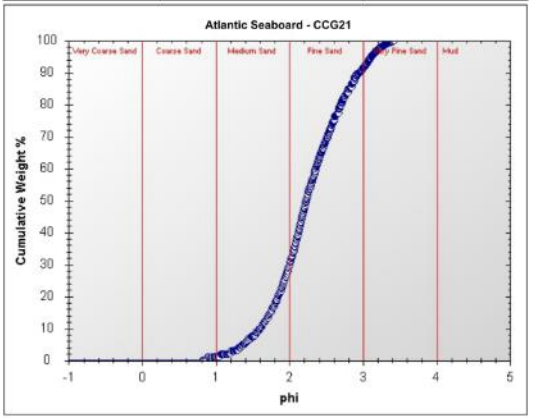

Project and Sample Details:			
Sample Number:	CCG21c	Client:	University of Cape Town
Analysis By:	Wilhelm van Zyl	Project Name:	Atlantic Seaboard Sediment Dynamics
Date Analysed:	2016/09/23	Project Location:	Atlantic Seaboard

Sediment Statistics:			
Mean (mm):	0.22	Median (mm):	0.21
Mean (phi):	2.26	Median (phi):	2.23
Sorting:	0.52	Skewness:	0.08

Grain Size Classification after Wentworth (1922)
All formulas used to calculate settling velocities and grain size radii after Gibbs (1971)

COUNCIL FOR GEOSCIENCE SETTLING TUBE ANALYSIS

Council for Geoscience

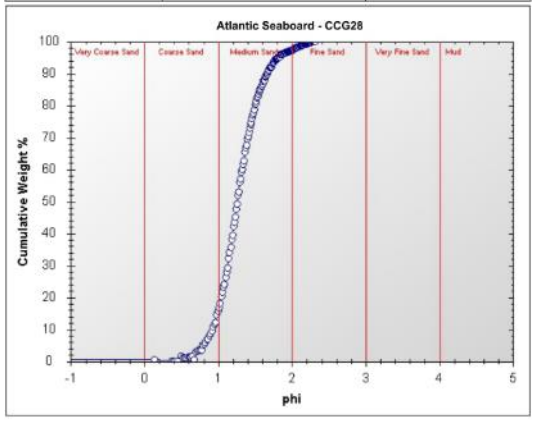

Project and Sample Details:			
Sample Number:	CCG28c	Client:	University of Cape Town
Analysis By:	Wilhelm van Zyl	Project Name:	Atlantic Seaboard Sediment Dynamics
Date Analysed:	2016/09/22	Project Location:	Atlantic Seaboard

Sediment Statistics:			
Mean (mm):	0.42	Median (mm):	0.42
Mean (phi):	1.27	Median (phi):	1.26
Sorting:	0.30	Skewness:	0.05

Grain Size Classification after Wentworth (1922)
All formulas used to calculate settling velocities and grain size radii after Gibbs (1971)

COUNCIL FOR GEOSCIENCE SETTLING TUBE ANALYSIS

Council for Geoscience

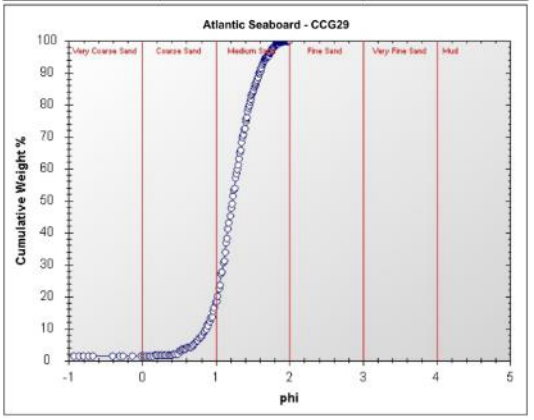

Project and Sample Details:			
Sample Number:	CCG29	Client:	University of Cape Town
Analysis By:	Wilhelm van Zyl	Project Name:	Atlantic Seaboard
Date Analysed:	2016/06/23	Project Location:	Camps Bay

Sediment Statistics:			
Mean (mm):	0.43	Median (mm):	0.43
Mean (phi):	1.23	Median (phi):	1.22
Sorting:	0.90	Skewness:	-10.42

Grain Size Classification after Wentworth (1922)
All formulas used to calculate settling velocities and grain size radii after Gibbs (1971)

COUNCIL FOR GEOSCIENCE SETTLING TUBE ANALYSIS

Council for Geoscience

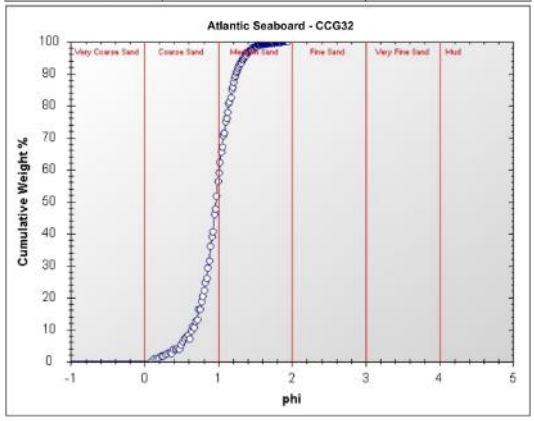

Project and Sample Details:			
Sample Number:	CCG32b	Client:	University of Cape Town
Analysis By:	Leslee Salzmann	Project Name:	Atlantic Seaboard
Date Analysed:	09/06/2017	Project Location:	Camps Bay

Sediment Statistics:			
Mean (mm):	0.52	Median (mm):	0.51
Mean (phi):	0.96	Median (phi):	0.97
Sorting:	0.24	Skewness:	-0.05

Grain Size Classification after Wentworth (1922)
All formulas used to calculate settling velocities and grain size radii after Gibbs (1971)

COUNCIL FOR GEOSCIENCE SETTLING TUBE ANALYSIS

Council for Geoscience

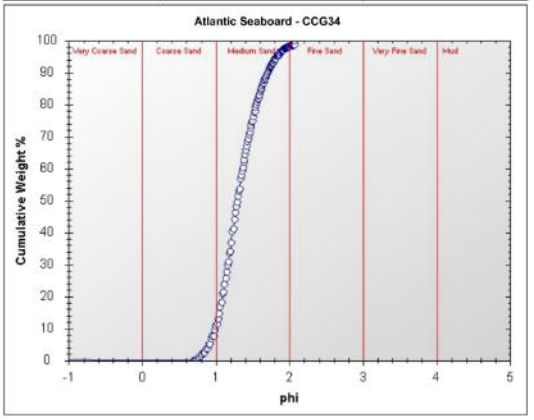

Project and Sample Details:			
Sample Number:	CCG34	Client:	University of Cape Town
Analysis By:	Leslee Salzmann	Project Name:	Atlantic Seaboard
Date Analysed:	12/06/2017	Project Location:	Camps Bay

Sediment Statistics:			
Mean (mm):	0.41	Median (mm):	0.41
Mean (phi):	1.32	Median (phi):	1.29
Sorting:	0.27	Skewness:	0.09

Grain Size Classification after Wentworth (1922)
All formulas used to calculate settling velocities and grain size radii after Gibbs (1971)

Council for Geoscience
Leaders in Applied Geoscience Solutions

COUNCIL FOR GEOSCIENCE SETTLING TUBE ANALYSIS

Council for Geoscience

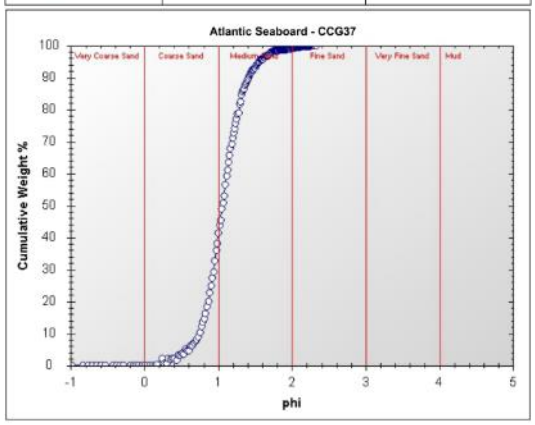

Project and Sample Details:			
Sample Number:	CCG37	Client:	University of Cape Town
Analysis By:	Leslee Salzmann	Project Name:	Atlantic Seaboard
Date Analysed:	24/02/2017	Project Location:	Camps Bay

Sediment Statistics:			
Mean (mm):	0.48	Median (mm):	0.48
Mean (phi):	1.06	Median (phi):	1.06
Sorting:	0.27	Skewness:	0.00

Grain Size Classification after Wentworth (1922)
All formulas used to calculate settling velocities and grain size radii after Gibbs (1971)

COUNCIL FOR GEOSCIENCE SETTLING TUBE ANALYSIS

Council for Geoscience

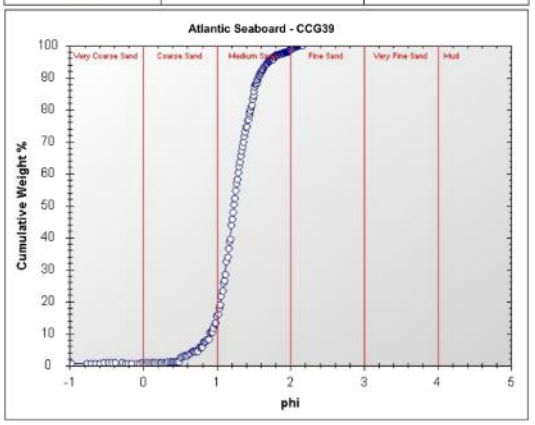

Project and Sample Details:			
Sample Number:	CCG39	Client:	University of Cape Town
Analysis By:	Wilhelm van Zyl	Project Name:	Atlantic Seaboard
Date Analysed:	2016/06/23	Project Location:	Camps Bay

Sediment Statistics:			
Mean (mm):	0.43	Median (mm):	0.43
Mean (phi):	1.25	Median (phi):	1.23
Sorting:	0.26	Skewness:	0.00

Grain Size Classification after Wentworth (1922)
All formulas used to calculate settling velocities and grain size radii after Gibbs (1971)

COUNCIL FOR GEOSCIENCE SETTLING TUBE ANALYSIS

Council for Geoscience

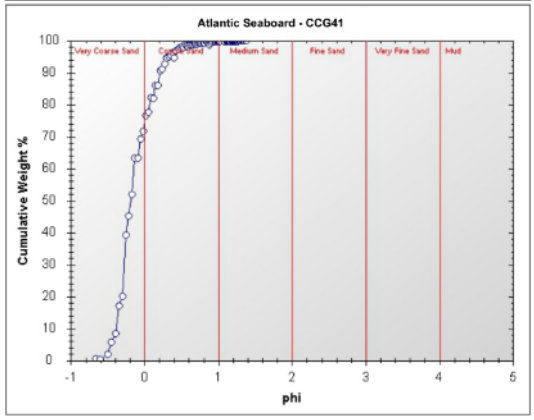

Project and Sample Details:			
Sample Number:	CCG41	Client:	University of Cape Town
Analysis By:	Wilhelm van Zyl	Project Name:	Atlantic Seaboard
Date Analysed:	2016/06/23	Project Location:	Camps Bay

Sediment Statistics:			
Mean (mm):	1.11	Median (mm):	1.14
Mean (phi):	-0.13	Median (phi):	-0.18
Sorting:	0.24	Skewness:	0.13

Grain Size Classification after Wentworth (1922)
All formulas used to calculate settling velocities and grain size radii after Gibbs (1971)

COUNCIL FOR GEOSCIENCE SETTLING TUBE ANALYSIS

Council for Geoscience

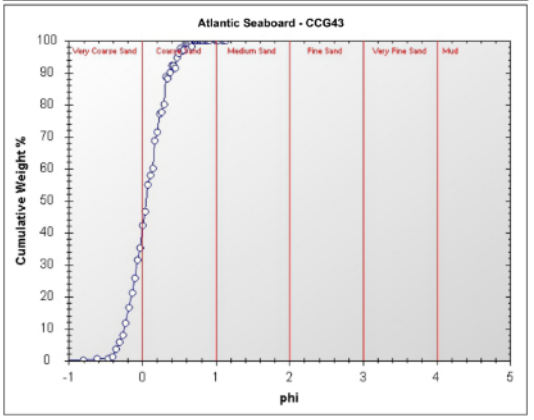

Project and Sample Details:			
Sample Number:	CCG43	Client:	University of Cape Town
Analysis By:	Wilhelm van Zyl	Project Name:	Atlantic Seaboard
Date Analysed:	2016/06/23	Project Location:	Camps Bay

Sediment Statistics:			
Mean (mm):	0.97	Median (mm):	0.96
Mean (phi):	0.06	Median (phi):	0.06
Sorting:	0.24	Skewness:	0.02

Grain Size Classification after Wentworth (1922)
All formulas used to calculate settling velocities and grain size radii after Gibbs (1971)

COUNCIL FOR GEOSCIENCE SETTLING TUBE ANALYSIS

Council for Geoscience

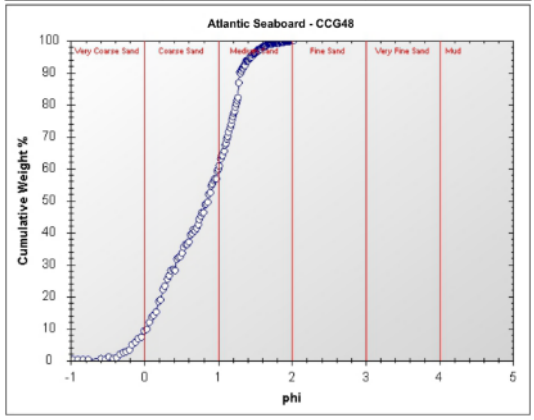

Project and Sample Details:			
Sample Number:	CCG48	Client:	University of Cape Town
Analysis By:	Wilhelm van Zyl	Project Name:	Atlantic Seaboard
Date Analysed:	2016/06/23	Project Location:	Camps Bay

Sediment Statistics:			
Mean (mm):	0.62	Median (mm):	0.55
Mean (phi):	0.77	Median (phi):	0.86
Sorting:	0.52	Skewness:	-0.49

Grain Size Classification after Wentworth (1922)
All formulas used to calculate settling velocities and grain size radii after Gibbs (1971)

COUNCIL FOR GEOSCIENCE SETTLING TUBE ANALYSIS

Council for Geoscience

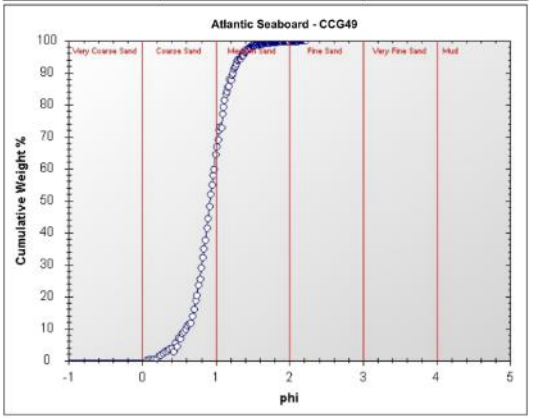

Project and Sample Details:			
Sample Number:	CCG49	Client:	University of Cape Town
Analysis By:	Leslee Salzmann	Project Name:	Atlantic Seaboard
Date Analysed:	24/02/2017	Project Location:	Camps Bay

Sediment Statistics:			
Mean (mm):	0.53	Median (mm):	0.53
Mean (phi):	0.92	Median (phi):	0.92
Sorting:	0.25	Skewness:	-0.02

Grain Size Classification after Wentworth (1922)
All formulas used to calculate settling velocities and grain size radii after Gibbs (1971)

COUNCIL FOR GEOSCIENCE SETTLING TUBE ANALYSIS

Council for Geoscience

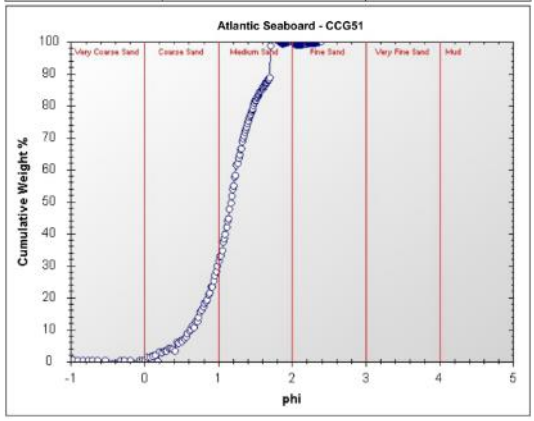

Project and Sample Details:			
Sample Number:	CCG51	Client:	University of Cape Town
Analysis By:	Leslee Salzmann	Project Name:	Atlantic Seaboard
Date Analysed:	24/02/2017	Project Location:	Camps Bay

Sediment Statistics:			
Mean (mm):	0.46	Median (mm):	0.44
Mean (phi):	1.17	Median (phi):	1.17
Sorting:	0.39	Skewness:	-0.14

Grain Size Classification after Wentworth (1922)
All formulas used to calculate settling velocities and grain size radii after Gibbs (1971)

COUNCIL FOR GEOSCIENCE SETTLING TUBE ANALYSIS

Council for Geoscience

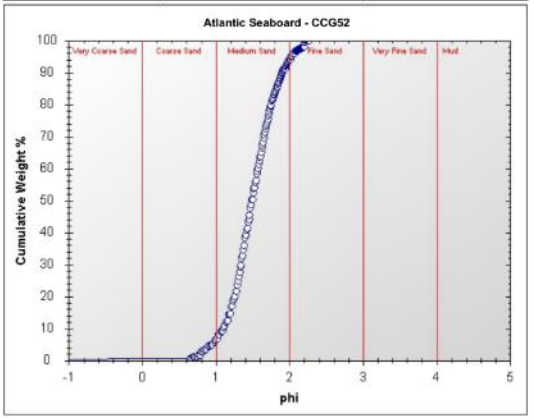

Project and Sample Details:			
Sample Number:	CCG52	Client:	University of Cape Town
Analysis By:	Wilhelm van Zyl	Project Name:	Atlantic Seaboard
Date Analysed:	2016/06/24	Project Location:	Camps Bay

Sediment Statistics:			
Mean (mm):	0.36	Median (mm):	0.36
Mean (phi):	1.50	Median (phi):	1.49
Sorting:	0.31	Skewness:	0.01

Grain Size Classification after Wentworth (1922)
All formulas used to calculate settling velocities and grain size radii after Gibbs (1971)

COUNCIL FOR GEOSCIENCE SETTLING TUBE ANALYSIS

Council for Geoscience

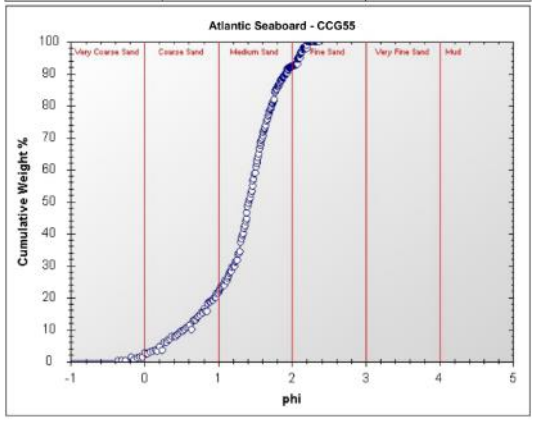

Project and Sample Details:			
Sample Number:	CCG55	Client:	University of Cape Town
Analysis By:	Wilhelm van Zyl	Project Name:	Atlantic Seaboard
Date Analysed:	2016/06/24	Project Location:	Camps Bay

Sediment Statistics:			
Mean (mm):	0.41	Median (mm):	0.38
Mean (phi):	1.33	Median (phi):	1.42
Sorting:	0.52	Skewness:	-0.56

Grain Size Classification after Wentworth (1922)
All formulas used to calculate settling velocities and grain size radii after Gibbs (1971)

COUNCIL FOR GEOSCIENCE SETTLING TUBE ANALYSIS

Council for Geoscience

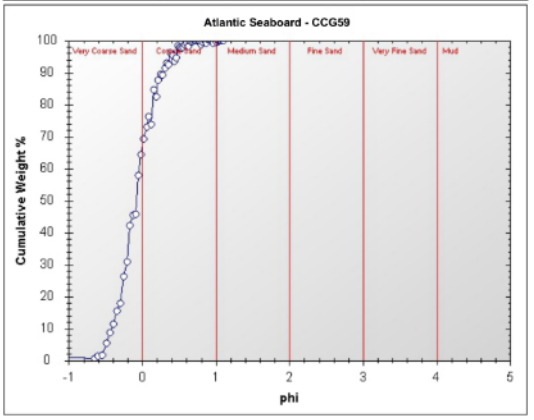

Project and Sample Details:			
Sample Number:	CCG59	Client:	University of Cape Town
Analysis By:	Wilhelm van Zyl	Project Name:	Atlantic Seaboard
Date Analysed:	2016/06/24	Project Location:	Camps Bay

Sediment Statistics:			
Mean (mm):	1.07	Median (mm):	1.05
Mean (phi):	-0.08	Median (phi):	-0.07
Sorting:	0.25	Skewness:	0.01

Grain Size Classification after Wentworth (1922)
All formulas used to calculate settling velocities and grain size radii after Gibbs (1971)

COUNCIL FOR GEOSCIENCE SETTLING TUBE ANALYSIS

Council for Geoscience

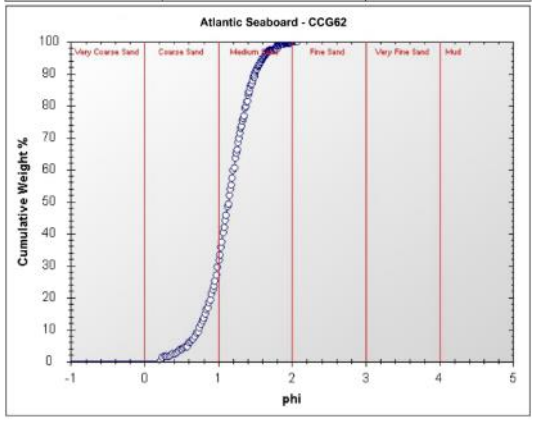

Project and Sample Details:			
Sample Number:	CCG62b	Client:	University of Cape Town
Analysis By:	Wilhelm van Zyl	Project Name:	Atlantic Seaboard Sediment Dynamics
Date Analysed:	2016/09/23	Project Location:	Atlantic Seaboard

Sediment Statistics:			
Mean (mm):	0.46	Median (mm):	0.45
Mean (phi):	1.13	Median (phi):	1.14
Sorting:	0.30	Skewness:	-0.06

Grain Size Classification after Wentworth (1922)
All formulas used to calculate settling velocities and grain size radii after Gibbs (1971)

COUNCIL FOR GEOSCIENCE SETTLING TUBE ANALYSIS

Council for Geoscience

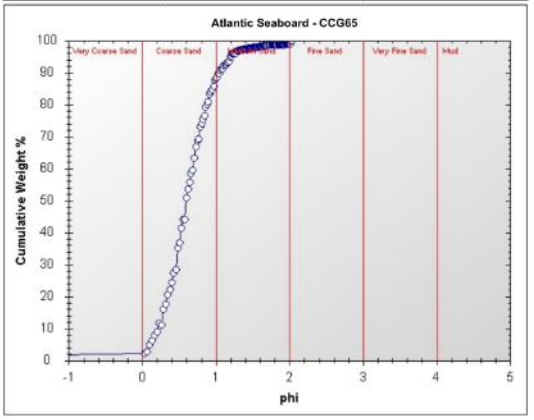

Project and Sample Details:			
Sample Number:	CCG65	Client:	University of Cape Town
Analysis By:	Leslee Salzmann	Project Name:	Atlantic Seaboard
Date Analysed:	24/02/2017	Project Location:	Camps Bay

Sediment Statistics:			
Mean (mm):	0.67	Median (mm):	0.66
Mean (phi):	0.61	Median (phi):	0.60
Sorting:	0.33	Skewness:	0.07

Grain Size Classification after Wentworth (1922)
All formulas used to calculate settling velocities and grain size radii after Gibbs (1971)

COUNCIL FOR GEOSCIENCE SETTLING TUBE ANALYSIS

Council for Geoscience

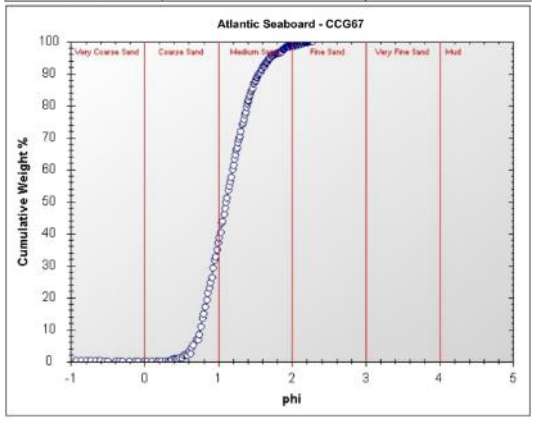

Project and Sample Details:			
Sample Number:	CCG67	Client:	University of Cape Town
Analysis By:	Leslee Salzmann	Project Name:	Atlantic Seaboard
Date Analysed:	24/02/2017	Project Location:	Camps Bay

Sediment Statistics:			
Mean (mm):	0.47	Median (mm):	0.46
Mean (phi):	1.12	Median (phi):	1.11
Sorting:	0.32	Skewness:	0.09

Grain Size Classification after Wentworth (1922)
All formulas used to calculate settling velocities and grain size radii after Gibbs (1971)

COUNCIL FOR GEOSCIENCE SETTLING TUBE ANALYSIS

Council for Geoscience

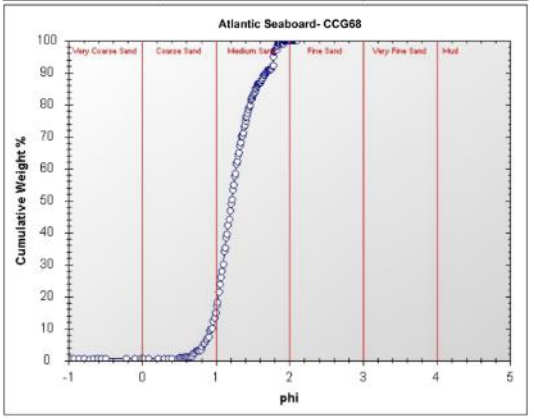

Project and Sample Details:			
Sample Number:	CCG68b	Client:	University of Cape Town
Analysis By:	Wilhelm van Zyl	Project Name:	Atlantic Seaboard
Date Analysed:	2016/06/24	Project Location:	Camps Bay

Sediment Statistics:			
Mean (mm):	0.43	Median (mm):	0.43
Mean (phi):	1.25	Median (phi):	1.21
Sorting:	0.28	Skewness:	0.11

Grain Size Classification after Wentworth (1922)
All formulas used to calculate settling velocities and grain size radii after Gibbs (1971)

COUNCIL FOR GEOSCIENCE SETTLING TUBE ANALYSIS

Council for Geoscience

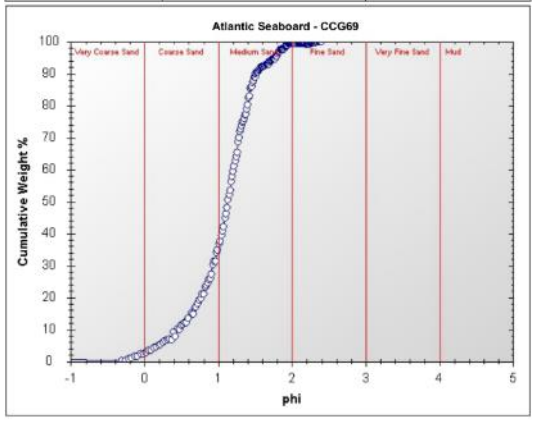

Project and Sample Details:			
Sample Number:	CCG69	Client:	University of Cape Town
Analysis By:	Leslee Salzmann	Project Name:	Atlantic Seaboard
Date Analysed:	24/02/2017	Project Location:	Camps Bay

Sediment Statistics:			
Mean (mm):	0.49	Median (mm):	0.46
Mean (phi):	1.07	Median (phi):	1.13
Sorting:	0.43	Skewness:	-0.29

Grain Size Classification after Wentworth (1922)
All formulas used to calculate settling velocities and grain size radii after Gibbs (1971)

COUNCIL FOR GEOSCIENCE SETTLING TUBE ANALYSIS

Council for Geoscience

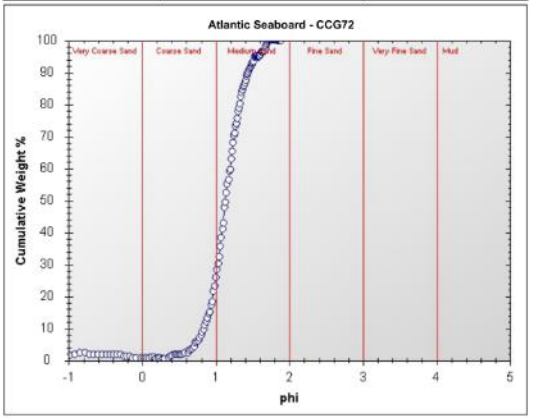

Project and Sample Details:			
Sample Number:	CCG72	Client:	University of Cape Town
Analysis By:	Wilhelm van Zyl	Project Name:	Atlantic Seaboard
Date Analysed:	2016/06/24	Project Location:	Camps Bay

Sediment Statistics:			
Mean (mm):	0.46	Median (mm):	0.46
Mean (phi):	1.14	Median (phi):	1.13
Sorting:	0.23	Skewness:	-0.01

Grain Size Classification after Wentworth (1922)
All formulas used to calculate settling velocities and grain size radii after Gibbs (1971)

COUNCIL FOR GEOSCIENCE SETTLING TUBE ANALYSIS

Council for Geoscience

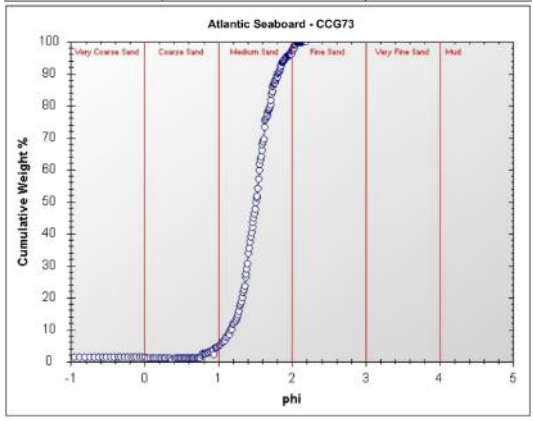

Project and Sample Details:			
Sample Number:	CCG73	Client:	University of Cape Town
Analysis By:	Wilhelm van Zyl	Project Name:	Atlantic Seaboard
Date Analysed:	2016/06/23	Project Location:	Camps Bay

Sediment Statistics:			
Mean (mm):	0.36	Median (mm):	0.35
Mean (phi):	1.50	Median (phi):	1.51
Sorting:	0.25	Skewness:	-0.04

Grain Size Classification after Wentworth (1922)
All formulas used to calculate settling velocities and grain size radii after Gibbs (1971)

COUNCIL FOR GEOSCIENCE SETTLING TUBE ANALYSIS

Council for Geoscience

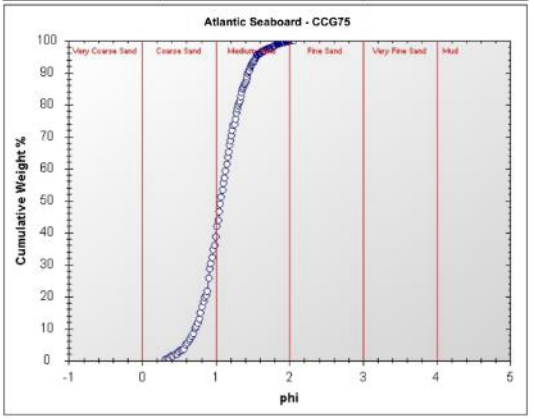

Project and Sample Details:			
Sample Number:	CCG75b	Client:	University of Cape Town
Analysis By:	W. van Zyl	Project Name:	Atlantic Seaboard Sediment Dynamics
Date Analysed:	2014/03/17	Project Location:	Camps Bay, South Africa

Sediment Statistics:			
Mean (mm):	0.48	Median (mm):	0.48
Mean (phi):	1.07	Median (phi):	1.07
Sorting:	0.28	Skewness:	0.01

Grain Size Classification after Wentworth (1922)
All formulas used to calculate settling velocities and grain size radii after Gibbs (1971)

COUNCIL FOR GEOSCIENCE SETTLING TUBE ANALYSIS

Council for Geoscience

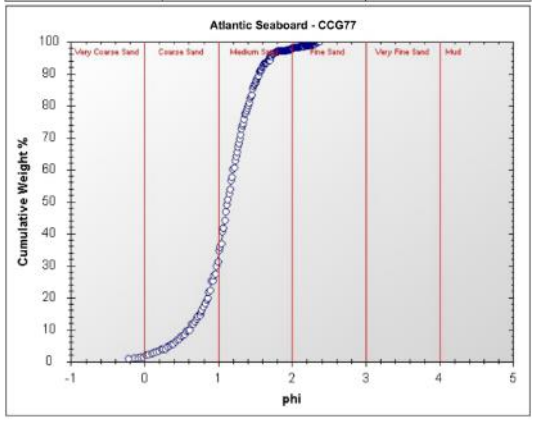

Project and Sample Details:			
Sample Number:	CCG77	Client:	University of Cape Town
Analysis By:	Leslee Salzmann	Project Name:	Atlantic Seaboard
Date Analysed:	24/02/2017	Project Location:	Camps Bay

Sediment Statistics:			
Mean (mm):	0.47	Median (mm):	0.46
Mean (phi):	1.12	Median (phi):	1.13
Sorting:	0.37	Skewness:	-0.14

Grain Size Classification after Wentworth (1922)
All formulas used to calculate settling velocities and grain size radii after Gibbs (1971)

COUNCIL FOR GEOSCIENCE SETTLING TUBE ANALYSIS

Council for Geoscience

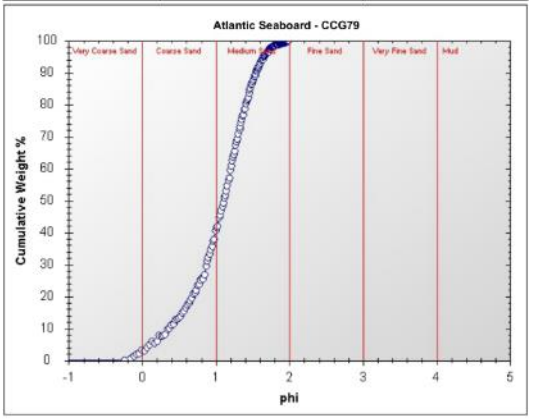

Project and Sample Details:			
Sample Number:	CCG79	Client:	University of Cape Town
Analysis By:	Leslee Salzmann	Project Name:	Atlantic Seaboard
Date Analysed:	12/06/2017	Project Location:	Camps Bay

Sediment Statistics:			
Mean (mm):	0.50	Median (mm):	0.46
Mean (phi):	1.05	Median (phi):	1.11
Sorting:	0.45	Skewness:	-0.43

Grain Size Classification after Wentworth (1922)
All formulas used to calculate settling velocities and grain size radii after Gibbs (1971)

COUNCIL FOR GEOSCIENCE SETTLING TUBE ANALYSIS

Council for Geoscience

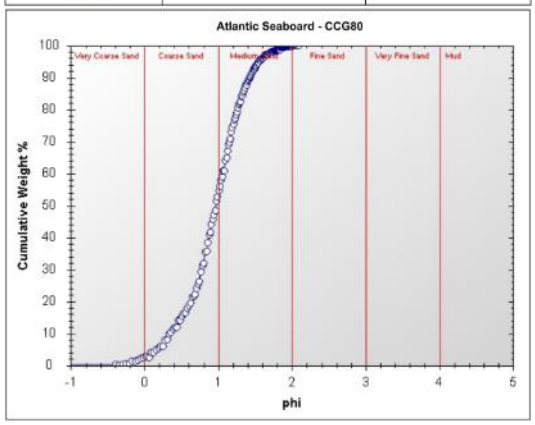

Project and Sample Details:			
Sample Number:	CCG80c	Client:	University of Cape Town
Analysis By:	Wilhelm van Zyl	Project Name:	Atlantic Seaboard Sediment Dynamics
Date Analysed:	2016/09/23	Project Location:	Camps Bay

Sediment Statistics:			
Mean (mm):	0.54	Median (mm):	0.51
Mean (phi):	0.94	Median (phi):	0.97
Sorting:	0.41	Skewness:	-0.18

Grain Size Classification after Wentworth (1922)
All formulas used to calculate settling velocities and grain size radii after Gibbs (1971)

COUNCIL FOR GEOSCIENCE SETTLING TUBE ANALYSIS

Council for Geoscience

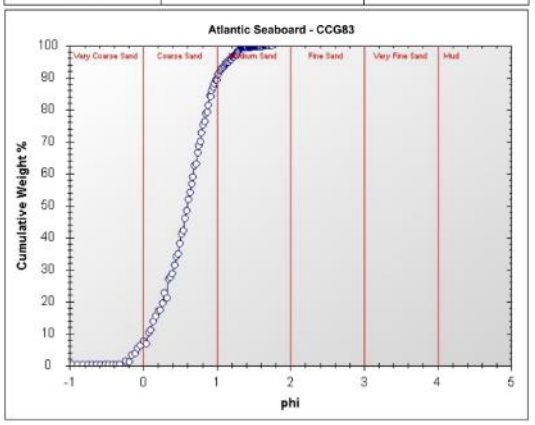

Project and Sample Details:			
Sample Number:	CCG83b	Client:	University of Cape Town
Analysis By:	Wilhelm van Zyl	Project Name:	Atlantic Seaboard Sediment Dynamics
Date Analysed:	2016/09/23	Project Location:	Camps Bay

Sediment Statistics:			
Mean (mm):	0.69	Median (mm):	0.66
Mean (phi):	0.56	Median (phi):	0.60
Sorting:	1.73	Skewness:	-46.82

Grain Size Classification after Wentworth (1922)
All formulas used to calculate settling velocities and grain size radii after Gibbs (1971)

COUNCIL FOR GEOSCIENCE SETTLING TUBE ANALYSIS

Council for Geoscience

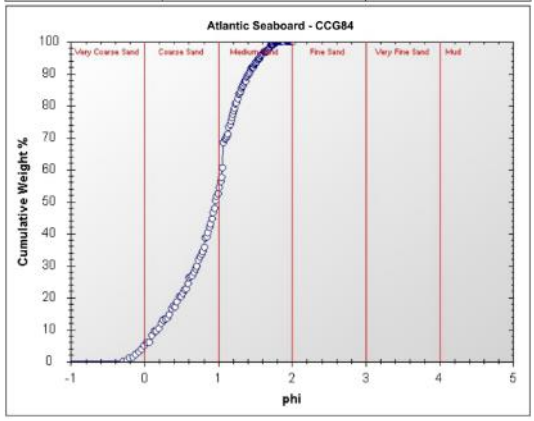

Project and Sample Details:			
Sample Number:	CCG84c	Client:	University of Cape Town
Analysis By:	W. van Zyl	Project Name:	Atlantic Seaboard Sediment Dynamics
Date Analysed:	2014/03/18	Project Location:	Camps Bay, South Africa

Sediment Statistics:			
Mean (mm):	0.57	Median (mm):	0.51
Mean (phi):	0.87	Median (phi):	0.96
Sorting:	0.47	Skewness:	-0.41

Grain Size Classification after Wentworth (1922)
All formulas used to calculate settling velocities and grain size radii after Gibbs (1971)

COUNCIL FOR GEOSCIENCE SETTLING TUBE ANALYSIS

Council for Geoscience

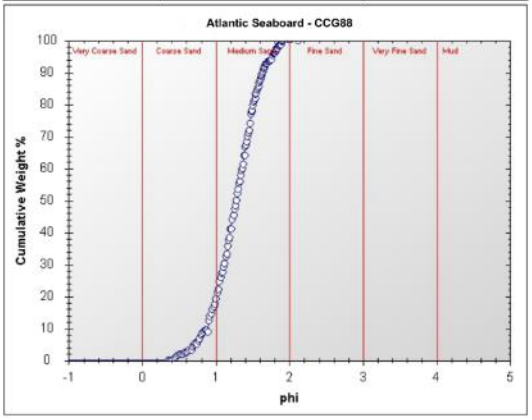

Project and Sample Details:			
Sample Number:	CCG88b	Client:	University of Cape Town
Analysis By:	Leslee Salzmann	Project Name:	Atlantic Seaboard
Date Analysed:	09/06/2017	Project Location:	Camps Bay

Sediment Statistics:			
Mean (mm):	0.42	Median (mm):	0.41
Mean (phi):	1.26	Median (phi):	1.27
Sorting:	0.31	Skewness:	-0.05

Grain Size Classification after Wentworth (1922)
All formulas used to calculate settling velocities and grain size radii after Gibbs (1971)

COUNCIL FOR GEOSCIENCE SETTLING TUBE ANALYSIS

Council for Geoscience

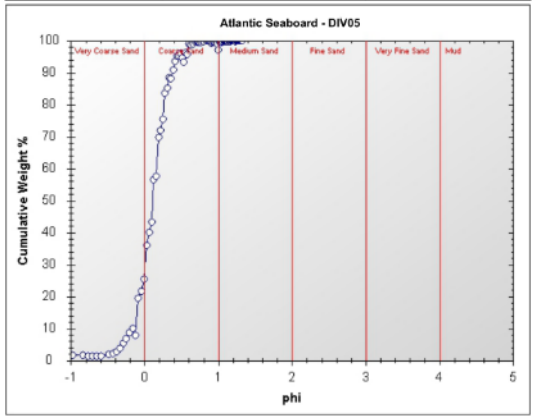

Project and Sample Details:			
Sample Number:	DIV05	Client:	University of Cape Town
Analysis By:	Wilhelm van Zyl	Project Name:	Atlantic Seaboard
Date Analysed:	2016/06/23	Project Location:	13 Apostle

Sediment Statistics:			
Mean (mm):	0.94	Median (mm):	0.93
Mean (phi):	0.10	Median (phi):	0.11
Sorting:	0.21	Skewness:	-0.04

Grain Size Classification after Wentworth (1922)
All formulas used to calculate settling velocities and grain size radii after Gibbs (1971)

COUNCIL FOR GEOSCIENCE SETTLING TUBE ANALYSIS

Council for Geoscience

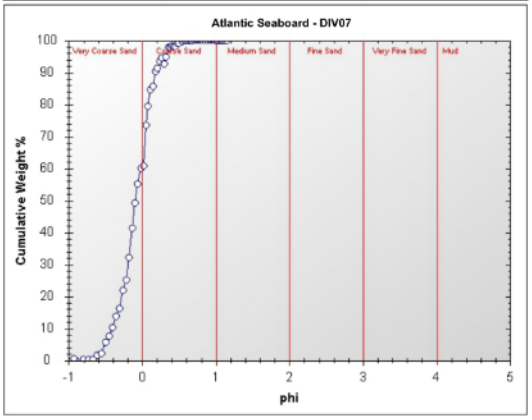

Project and Sample Details:			
Sample Number:	DIV07	Client:	University of Cape Town
Analysis By:	Wilhelm van Zyl	Project Name:	Atlantic Seaboard
Date Analysed:	2016/06/23	Project Location:	13 Apostle

Sediment Statistics:			
Mean (mm):	1.08	Median (mm):	1.07
Mean (phi):	-0.10	Median (phi):	-0.09
Sorting:	0.23	Skewness:	0.00

Grain Size Classification after Wentworth (1922)
All formulas used to calculate settling velocities and grain size radii after Gibbs (1971)

COUNCIL FOR GEOSCIENCE
SETTLING TUBE ANALYSIS

Council for Geoscience

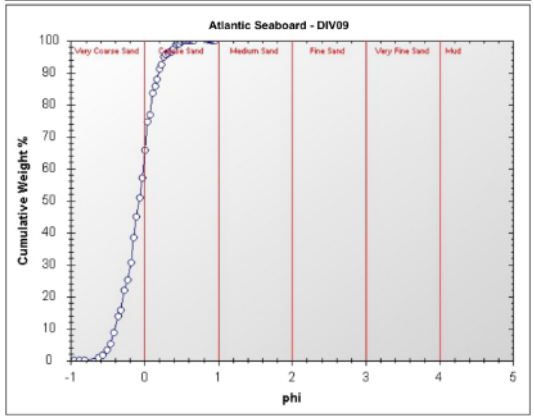

Project and Sample Details:			
Sample Number:	DIV09	Client:	University of Cape Town
Analysis By:	Wilhelm van Zyl	Project Name:	Atlantic Seaboard
Date Analysed:	2016/06/23	Project Location:	13 Apostle

Sediment Statistics:			
Mean (mm):	1.07	Median (mm):	1.05
Mean (phi):	-0.09	Median (phi):	-0.07
Sorting:	0.22	Skewness:	-0.03

Grain Size Classification after Wentworth (1922)
All formulas used to calculate settling velocities and grain size radii after Gibbs (1971)

COUNCIL FOR GEOSCIENCE
SETTLING TUBE ANALYSIS

Council for Geoscience

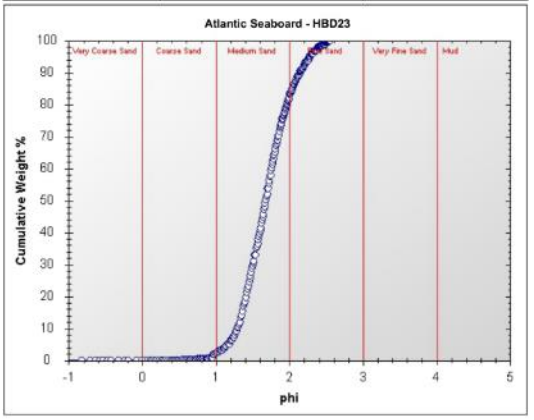

Project and Sample Details:			
Sample Number:	HBD23	Client:	University of Cape Town
Analysis By:	Leslee Salzmann	Project Name:	Atlantic Seaboard
Date Analysed:	09/06/2017	Project Location:	Hout Bay Dune

Sediment Statistics:			
Mean (mm):	0.32	Median (mm):	0.31
Mean (phi):	1.69	Median (phi):	1.68
Sorting:	0.33	Skewness:	0.05

Grain Size Classification after Wentworth (1922)
All formulas used to calculate settling velocities and grain size radii after Gibbs (1971)

COUNCIL FOR GEOSCIENCE
SETTLING TUBE ANALYSIS

Council for Geoscience

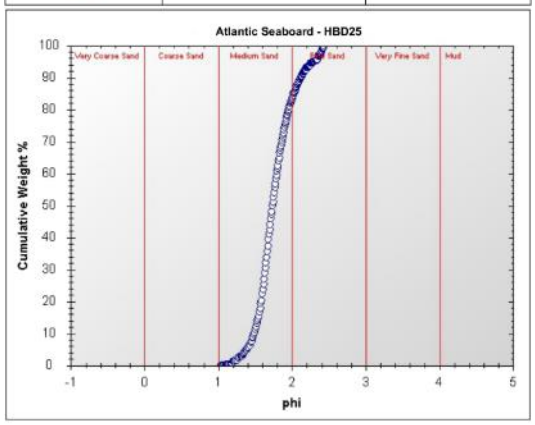

Project and Sample Details:			
Sample Number:	HBD25c	Client:	University of Cape Town
Analysis By:	Leslee Salzmann	Project Name:	Atlantic Seaboard
Date Analysed:	12/06/2017	Project Location:	Hout Bay Dune

Sediment Statistics:			
Mean (mm):	0.30	Median (mm):	0.30
Mean (phi):	1.76	Median (phi):	1.73
Sorting:	0.25	Skewness:	0.11

Grain Size Classification after Wentworth (1922)
All formulas used to calculate settling velocities and grain size radii after Gibbs (1971)

COUNCIL FOR GEOSCIENCE
SETTLING TUBE ANALYSIS

Council for Geoscience

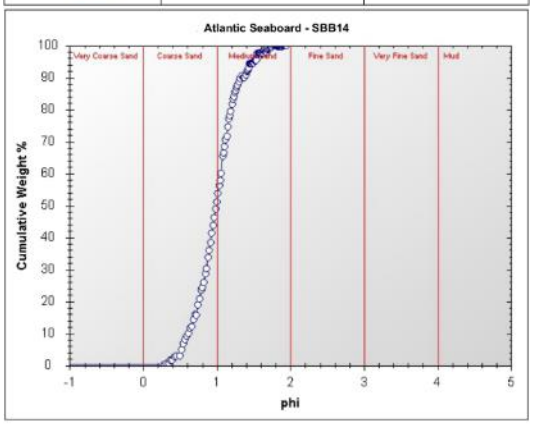

Project and Sample Details:			
Sample Number:	SBB14	Client:	University of Cape Town
Analysis By:	Leslee Salzmann	Project Name:	Atlantic Seaboard
Date Analysed:	23/02/2017	Project Location:	Sandy Bay Beach

Sediment Statistics:			
Mean (mm):	0.51	Median (mm):	0.50
Mean (phi):	0.98	Median (phi):	0.99
Sorting:	0.27	Skewness:	0.02

Grain Size Classification after Wentworth (1922)
All formulas used to calculate settling velocities and grain size radii after Gibbs (1971)

COUNCIL FOR GEOSCIENCE
SETTLING TUBE ANALYSIS

Council for Geoscience

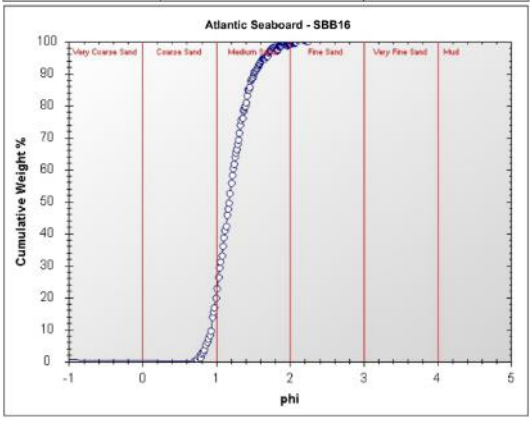

Project and Sample Details:			
Sample Number:	SBB16	Client:	University of Cape Town
Analysis By:	Leslee Salzmann	Project Name:	Atlantic Seaboard
Date Analysed:	23/02/2017	Project Location:	Sandy Bay Beach

Sediment Statistics:			
Mean (mm):	0.44	Median (mm):	0.44
Mean (phi):	1.19	Median (phi):	1.18
Sorting:	0.24	Skewness:	0.08

Grain Size Classification after Wentworth (1922)
All formulas used to calculate settling velocities and grain size radii after Gibbs (1971)

COUNCIL FOR GEOSCIENCE
SETTLING TUBE ANALYSIS

Council for Geoscience

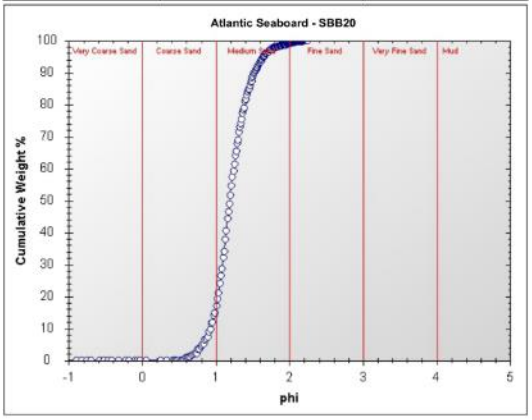

Project and Sample Details:			
Sample Number:	SBB20	Client:	University of Cape Town
Analysis By:	Leslee Salzmann	Project Name:	Atlantic Seaboard
Date Analysed:	23/02/2017	Project Location:	Sandy Bay Beach

Sediment Statistics:			
Mean (mm):	0.44	Median (mm):	0.44
Mean (phi):	1.21	Median (phi):	1.19
Sorting:	0.23	Skewness:	0.05

Grain Size Classification after Wentworth (1922)
All formulas used to calculate settling velocities and grain size radii after Gibbs (1971)

Appendix C – Multibeam Bathymetry of the Atlantic Seaboard

Appendix D – Seafloor Facies of the Atlantic Seaboard

Appendix E – Geology of the Atlantic Seaboard

18°16'0"E
18°18'0"E
18°20'0"E
18°22'0"E
18°24'0"E
33°54'0"S
33°56'0"S
33°58'0"S
34°0'0"S
34°2'0"S
6246000
6244000
6242000
6240000
6238000
6236000
6234000
6232000
6230000
6228000
248000
250000
252000
254000
256000
258000
260000

Scale: 1:10 000
0 250 500 750 1 000 Metres

Scale: 1:10 000
0 250 500 750 1 000 Metres

Scale: 1:10 000
0 250 500 750 1 000 Metres

Mouille Point
Sea Point
Clifton Beach
Camps Bay
Oudekraal
Llandudno
Sandy Bay
Karbonkelberg Dune
Maori Bay
Hout Bay

Multibeam Bathymetry of the Atlantic Seaboard

Wilhelm van Zyl
2018

SANAP — South African Nearshore Mapping Programme
Council for Geoscience
University of Cape Town · Universiteit van Kaapstad · iYunivesithi yaseKapa

Depth in Chart datum

-5 m
-15 m
-25 m
-35 m
-45 m
-55 m
-65 m
-75 m

Co-ordinate system
WGS_1984_UTM_Zone_34S
Projection: Transverse_Mercator
False_Easting: 500000.00
False_Northing: 10000000.00
Central_Meridian: 21.000000
Scale_Factor: 0.999600
Latitude_Of_Origin: 0.00
Linear Unit: Metre

GCS_WGS_1984
Datum: D_WGS_1984

Notes
Aerial Photos from the
City of Cape Town 2008
Survey Dates 2012 - 2014

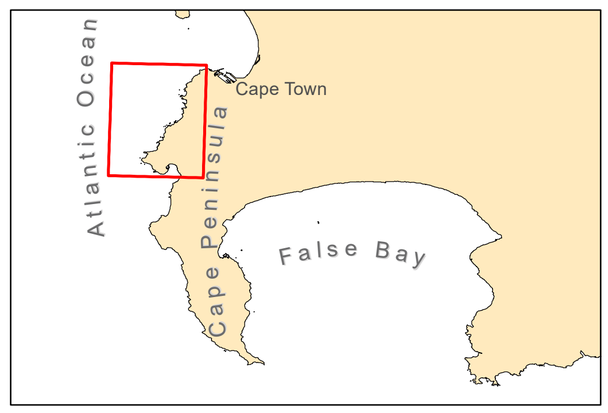

N
W E
S

Scale: 1:25 000
0 500 1 000 1 500 2 000 Metres

Seafloor Facies of the Atlantic Seaboard

Wilhelm van Zyl
2018

Council for Geoscience

Legend

Wrecks

Atlantic Seafloor Geology

Facies

- Anthropogenic
- Scree
- Boulder Beach
- Bioclastic Gravel
- Sand
- Scattered Reef
- Low Relief Reef
- Prominent Reef
- Striated Reef
- Dykes

Co-ordinate system
WGS_1984_UTM_Zone_34S
Projection: Transverse_Mercator
False_Easting: 500000.00
False_Northing: 10000000.00
Central_Meridian: 21.000000
Scale_Factor: 0.999600
Latitude_Of_Origin: 0.00
Linear Unit: Metre

GCS_WGS_1984
Datum: D_WGS_1984

Notes
Aerial Photos from the City of Cape Town 2008
Survey Dates 2012 - 2014

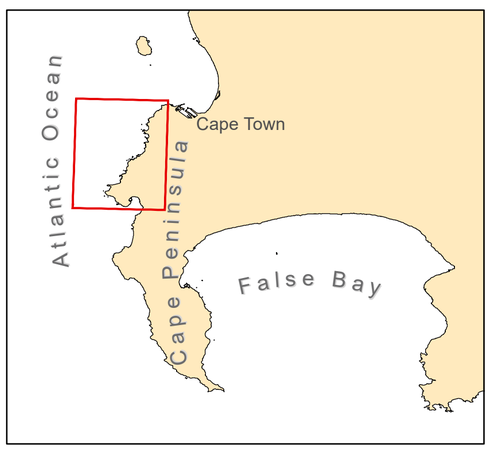

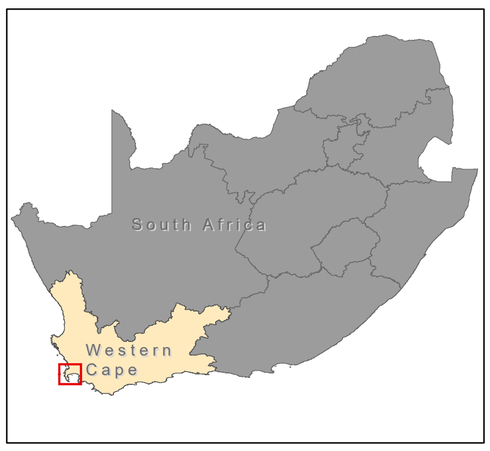

Mouille Point
Sea Point
Clifton Beach
Camps Bay
Oudekraal
HET HUIS DE KRAAISTEEN
ANTIPOLIS
Llandudno
ROMELIA
Sandy Bay
Karbonkelberg Dune
Maori Bay
S.A.S. GELDERLAND
MAORI
BOS 400
OAKBURN
Hout Bay

18°16'0"E 18°18'0"E 18°20'0"E 18°22'0"E 18°24'0"E
33°54'0"S 33°56'0"S 33°58'0"S 34°0'0"S 34°2'0"S
6246000 6244000 6242000 6240000 6238000 6236000 6234000 6232000 6230000 6228000
248000 250000 252000 254000 256000 258000 260000

N W E S

Scale: 1:25,000

0 500 1,000 1,500 2,000 Metres

Geological Legend

Sedimentary and Volcanic Rocks

Group	Formation	Lithology
Quaternary		Qd Fill, reclaimed area
		Alluvium
		Scree
		Qt Gritty sand
	Witzand	Snd Fine to medium marine sand
		Sg Shelly gravel
		Qsr Generally unconsolidated, calcareous dune sand
SANDVELD	Springfontein	Qg Light-grey to pale red sandy soil
		Qb Brackish calcareous soil
		Boulder Beach
	Langebaan	Qss Partly cemented calcareous sand with shells and tree roots
Carboniferous to Jurassic		
Ordovician	Pakhuis	Oa Mudstone (diamictite) or sandstone containing scattered pebbles, cobbles and boulders
TABLE MOUNTAIN	Peninsula	Op Quartzitic sandstone, minor conglomerate and shale
	Graafwater	Og Thin-bedded sandstone, reddish siltstone and shale
Cambrian		
Namibian	MALMESBURY Tygerberg	Nt Phyllite and greywacke sandstone

Intrusive Rocks

Suite		
FALSE BAY	Jd	Network of dolerite dykes
CAPE GRANITE (Cape Peninsula Pluton)	Cc-p	Coarse-porphyritic granite Cc-p
	Cc-t	Contact zone of hybridic granite and hornfels xenoliths Cc-t
	Cc-m	Microgranite and hybridic microgranite Cc-m

Structures

- Fold Axis Synclinal
- Fold Axis Anticlinal
- Fold Axis Anticlinal Infered
- Fold Axis Synclinal Infered
- Fault Observed
- Fault Infered
- Thrust Fault Observed
- Thrust Fault Infered
- Aeromagnetic Lineament
- Bedding Trace
- Joint
- Lineament Undifferenciated
- Coastline
- Water

Geology of the Atlantic Seaboard

Wilhelm van Zyl
2018

Council for Geoscience

Co-ordinate system
WGS_1984_UTM_Zone_34S
Projection: Transverse_Mercator
False_Easting: 500000.00
False_Northing: 10000000.00
Central_Meridian: 21.000000
Scale_Factor: 0.999600
Latitude_Of_Origin: 0.00
Linear Unit: Metre

GCS_WGS_1984
Datum: D_WGS_1984

Notes
Onshore Geology from CGS 1:50 000 map series
Survey Dates 2012 - 2014

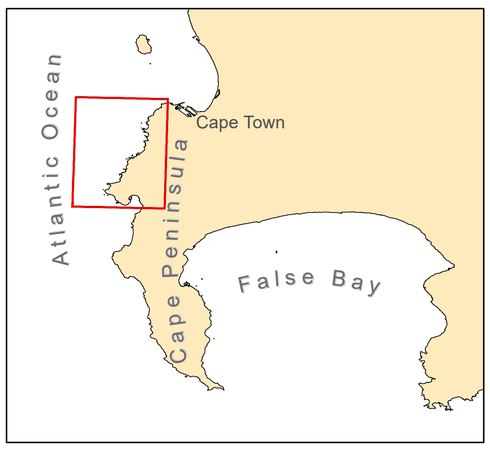

Scale: 1:25 000

0 500 1 000 1 500 2 000 Metres

18°16'0"E 18°18'0"E 18°20'0"E 18°22'0"E 18°24'0"E
33°54'0"S 33°56'0"S 33°58'0"S 34°0'0"S 34°2'0"S
248000 250000 252000 254000 256000 258000 260000
6246000 6244000 6242000 6240000 6238000 6236000 6234000 6232000 6230000 6228000

Mouille Point
Sea Point
Clifton Beach
Camps Bay
Oudekraal
Llandudno
Sandy Bay
Karbonkelberg Dune
Maori Bay
Hout Bay